URBAN ONTARIO RIVER REGIMES: AN ANALYSIS OF FOUR MAJOR WATERSHEDS

URBAN ONTARIO RIVER REGIMES: AN ANALYSIS OF FOUR MAJOR WATERSHEDS

By SHELBY GROHN, BES

A thesis submitted to the School of Graduate Studies in Partial Fulfilment of the Requirements for the Degree Master of Earth and Environmental Science

MASTER OF EARTH AND ENVIRONMENTAL SCIENCE (2024)

McMaster University, Hamilton, Ontario, Canada

TITLE: Urban Ontario River Regimes: An Analysis of Four Major Watersheds

AUTHOR: Shelby Grohn, BES (University of Waterloo, 2014)

SUPERVISOR: Professor Elli Papangelakis

NUMBER OF PAGES: iii, 65

LAY ABSTRACT

The effects of urbanization on river systems are not well understood as appropriate field parameters for representing such changes require years of consistent data for an accurate comparison which is not typically available in Ontario due to budget and personnel constraints. To direct monitoring and management efforts more effectively, a comparative aerial imagery analysis, field study, and statistical analysis comprised of a Pearson correlation coefficient analysis and stepwise regression were undertaken for twenty sites across four major watersheds in the Greater Toronto Area (GTA). Values obtained through the Stream Power Index for Networks (SPIN) tool and manual calculations of entrenchment and three ratios from *Wood-Smith & Buffington (1996)* were utilized. Results indicate that statistical parameters such as the ability for specific stream power and imperviousness to predict the shear stress ratio can be considered applicable initial estimates of river patterns but are not strong enough for design purposes.

ABSTRACT

The effects of urbanization on river systems are not well understood as appropriate field parameters for representing such changes require years of consistent monitoring data for an accurate comparison. Furthermore, due to their varying degrees of urbanization and management efforts, conditions are not consistent even within the same watersheds so representative sites are difficult to distinguish. This level of data is not typically available for watersheds in Ontario due to budget and personnel constraints of organizations undertaking such monitoring activities. To direct monitoring and management efforts more effectively, a comparative aerial imagery analysis was undertaken for a ~50-year timeline for twenty study sites across the Mimico Creek, Etobicoke Creek, Highland Creek, and Duffins Creek watersheds as well as a comprehensive field analysis to characterize current conditions. A statistical analysis that included a Pearson correlation coefficient analysis and stepwise regression utilizing values obtained through the Stream Power Index for Networks (SPIN) tool and manual calculations including three ratios from *Wood-Smith & Buffington (1996)* was also completed. These ratios included: bankfull width (W_{bf})/bankfull depth (h_{bf}), D_{50}/bankfull depth (h_{bf}), and critical shear stress (τ_{c50})/bankfull shear stress (τ_{bf}). Results indicated a strongly negative correlation between entrenchment and the W_{bf}/h_{bf} ratio and positive correlations of varying strengths between the τ_{c50}/τ_{bf} ratio and both the W_{bf}/h_{bf} and D_{50}/h_{bf} ratios. Though weak, percent imperviousness and specific stream power were able to predict the τ_{c50}/τ_{bf} ratio. Finally, t-tests between sites categorized as “rural” (≤30% imperviousness) and “urban” (>30% imperviousness) revealed when a control is placed on drainage area, increases in specific stream power, D_{50}, bankfull width, bankfull depth, and slope is observed in “urban” areas. It is believed that such statistical parameters could be considered applicable as a first order estimate of further stream pattern analyses but are not strong enough correlations to be utilized for design purposes.

ACKNOWLEDGEMENTS

These acknowledgements begin with Dr. Elli Papangelakis, who acted as advisor and for whom her contributions of feedback and the specialized R code utilized in the statistical analysis component of this research were integral to its completion and quality. As well, the contributions of committee members Dr. James Michael Waddington and Dr. Altaf Arain are acknowledged and appreciated, as are those from Lily Charles and Nicholas Schmitz-Dasilva for their participation in the field component of this research. Finally, the assistance with the calibration and trouble shooting of the SPIN software from Priyanka Hire is greatly appreciated. Financial support for field personnel costs were reimbursed through research funds from Dr. Elli Papangelakis via the Natural Sciences and Engineering Research Council of Canada (NSERC). The mention of trade names or commercial products does not constitute an endorsement or a recommendation for use.

TABLE OF CONTENTS

LIST OF TABLES

LIST OF FIGURES

LIST OF ABBREVIATIONS AND SYMBOLS

CEM	Channel Evolution Model
DEM	Digital Elevation Model
FVC	Flood Vulnerable Cluster
GPS	Global Positioning System
GTA	Greater Toronto Area
LID	Low Impact Development
NCD	Natural Channel Design
RGA	Rapid Geomorphic Assessment
RSA	Rapid Stream Assessment
RTK	Real-Time Kinematic
SPIN	Stream Power Index for Networks
SWM	Stormwater Management
TRCA	Toronto and Region Conservation Authority
D_{50}	The median grain size on the channel bed
D_{84}	The particle size in which 84% of the sample is smaller than
h_{bf}	Bankfull depth
τ^*	Shields parameter
τ_{bf}	Bankfull shear stress
τ_{c50}	Critical shear stress
W_{bf}	Bankfull width
Ω	Total stream power

DECLARATION OF ACADEMIC ACHIEVEMENT

I, Shelby Grohn, declare that I conceptualized, designed, and implemented the research contained in this dissertation with guidance and input from my program supervisor, Dr. Elli Papangelakis. My thesis committee, including Dr. James Michael Waddington and Dr. Altaf Arain, provided comments on the thesis proposal, study protocols, and research methodologies and instruments. In the School of Earth, Environment and Society, two forms of presentation of the master's dissertation are permitted: (i) a standard dissertation monograph, and (ii) a sandwich thesis option. This dissertation is a standard dissertation monograph. I confirm that I am the primary author of the content in my dissertation, and that the work was dominated by my intellectual efforts.

SHELBY GROHN (Master's Student)

CHAPTER 1: Introduction

Over the past few decades, much research has been conducted regarding the effects of different disturbances on stream morphology and their capacity to maintain essential functions such as sediment transport and flood conveyance. The effects of urbanization on river systems have become a popular research focus in recent years due to ongoing residential and commercial expansion in response to a predicted increase in urban populations of 1.5 times by 2045 (*The World Bank, 2023*). Research such as that from *Boggs & Sun (2011)* has found that urbanization intensifies natural hydrological cycles, increasing stormflows by 75% in areas with at least 44% impervious surface cover when compared to those dominated by natural cover. In response to these intensified flows, urban rivers undergo geomorphic adjustments such as channel enlargement, incision (*Papangelakis et al., 2022*[b]), and bed coarsening (*Hawley et al., 2013*). The typical timespan for natural watercourses to undergo these adjustments can be decades to millennia depending on the process, however, degradation processes have been observed in as little as 10-100 years in urbanized watersheds (*Simon & Rinaldi, 2006*). To describe these effects of urbanization on stream systems in addition to increased stream erosion, changes in alluvial materials, flashy hydrology, and degradation of water quality and aquatic habitat, the term "urban stream syndrome" has been coined (*Mackenzie et al., 2022*[a]; *Mackenzie et al., 2022*[b]). Unfortunately, due to the highly variable nature of land use change, channel evolution, and anthropogenic influences, indicators of change vary between streams (*Ashmore et al., 2023*), making it challenging to identify early indicators of geomorphic instability, which is an ongoing challenge for successful river management.

The sediment regime is of major importance when attempting to determine the historical, present, and future condition of a channel. Urbanization disturbs the natural sediment regime (*Wohl et al., 2015*), with literature supporting an increase of the D_{84} (i.e., the particle size in which 84% of the sample is smaller than) (*Bunte & Abt, 2001*) by approximately 4 times in urban streams versus rural streams (*Robinson, 1976*). This is a result of excess sediment transport capacity, which *Gregory (2011)* noted correlated to an increase in sediment yield of ~160 times from rural areas (i.e., agricultural lands) and artificial areas (i.e., exposed construction sites). In addition, eroding outer meander bend banks are typical in pool-riffle channels (*Montgomery & MacDonald, 2002*) and a corresponding width-to-depth ratio would be deeper in these areas and perhaps wider to accommodate the discharge energy. However, not all literature is consistent, with studies such as that from *Annable et al. (2012)* finding contradictory information that with increasing urbanization, bed material supply tends to decrease which is offset by a smaller bankfull channel width, depth, and access to floodplains during major events. This inconsistency in channel response leads to difficulties when developing effective management and restoration techniques.

In response to urban river degradation, stream restoration has become a multi-billion-dollar effort globally (*Palmer et al., 2007*). However, the responsibility for watercourse management tends to be allocated to municipalities or local watershed management authorities (e.g., conservation authorities) who typically do not have the budget and resources to accommodate upkeep and restoration for all areas of concern. As a result, conventional approaches to mitigating the effects of urban hydrology such as centralized SWM and channel hardening (e.g., armourstone) have long been preferred due to upfront cost and technique familiarity (*Papangelakis et al., 2022*[a]). Unfortunately, these traditional methods have revealed a high rate of failure from which the necessity for alternative approaches such as adaptive management have stemmed. The high failure rate is, in part, due to a persistent gap in understanding of geomorphic responses to urbanization and the ability to predict them. Most of the previous literature related to geomorphic responses in urban watersheds has focused on individual river systems (e.g., *Ashmore et al., 2023*), and whether signals of geomorphic adjustments are consistent between different watersheds remains unanswered, presenting a significant challenge for developing effective monitoring and management plans.

1.1 Research Aim and Objectives

The aim of this research is to better understand the trajectories of fluvial responses to urbanization in the GTA. Specific objectives are to:

1. Provide a baseline historical geomorphic analysis of urbanizing watersheds in the GTA
2. Present a current geomorphic condition snapshot of watersheds to assess fluvial responses to urbanization in the GTA
3. Identify the most sensitive geomorphic indicators of urbanization that can be used as predictive tools to guide watershed monitoring and management priorities

The overarching goal is that this research may be utilized for education and decision-making purposes on a municipal and provincial level with respect to watershed management and development. This thesis is organized as follows. *CHAPTER 2* presents a summary of a literature review discussing the findings and perspectives of recent and historical publications with relation to fluvial geomorphological concepts such as sediment transport and stream morphology. It also includes a review of literature used to formulate hypotheses and methodology for each of the main three methodological components of this thesis: 1) aerial imagery analysis, 2) field analysis, and 3) statistical analysis. *CHAPTER 3* describes the watersheds studied and the methodology used for analysis. *CHAPTER 4* presents the results of all analyses conducted as well as a discussion relating to management implications, limitations, and future research recommendations. Finally, CHAPTER 5 provides a conclusion, summarizing the main points of this study.

CHAPTER 2: Literature Review

2.1 River Responses to Urbanization

Multiple studies have been conducted to quantify the effects of urbanization on channel processes. Urbanization initiates morphological adjustments in response to changes to the hydrology and sediment regime of channels. The conversion of natural cover to impervious cover that occurs during urbanization intensifies natural hydrological cycles by increasing surface runoff and therefore stream discharges (*Papangelakis et al., 2022*[b]). For instance, *Arnold & Gibbons (1996)* found that when impervious surfaces in a watershed accounted for 10-20% of ground cover, runoff doubled, and when it accounted for 35-50% of ground cover, it tripled. Adaptations in response to increased streamflows initiate morphologic responses such as increased channel width and incision which are an endemic problem in urban channels (*Papangelakis et al., 2022*[b]). The rapid response of rivers to urbanization can be seen when reviewing sediment budgets and transport capabilities and can be further intensified when reaches are straightened as is often the case in urbanized areas to accommodate linear infrastructure. In urban watersheds, mid-watershed reaches no longer function as temporary storage for coarse sands and gravels (as is expected in natural watersheds), leading to an erosion-dominant condition in the channel through the disruption of the sediment cascade process (*Wohl & Merritts, 2007*). Natural degradational processes are escalated in urbanized watersheds to as little as 10-100 years compared to the typical timespan for natural watercourses of decades to millennia (*Simon & Rinaldi, 2006*). Alternatively, urbanization may also result in continuous changes with no perceived end as the intensity and type of urbanization activities keep the stream in a constant state of stress and adaptation (*Ashmore, 2015*).

Urbanization-induced disturbances to fluvial systems can be visible when analyzing the natural sediment regime (*Wohl et al., 2015*) through alterations to bed particle size and location along the channel. For instance, bed coarsening in urban rivers has been observed by *Robinson (1976)* who discovered that the D_{84} in urban streams was ~4 times greater than that in rural streams, and further supported by a regression analysis conducted by *Hawley et al. (2013)*, especially in early development streams. Bed coarsening is due to excess sediment transport capacity, typically initiated by headcuts migrating upstream causing channel incision, therefore increasing the bank height, and consequently, the concentration of erosive energy in the channel. Shear stress is also directly correlated with transport capacity as the higher the shear stress exerted on the bed, the larger the particle size that can be moved in the water column (*Wilzbach & Cummins, 2018*).

Increases in not only sediment size, but sediment yield, are an important response to consider when discussing urbanized areas. *Wolman (1967)* noted an increase in suspended sediment yield of ~160 times from rural areas (i.e., agricultural lands) to artificial areas (i.e., exposed construction sites) in a Maryland, USA case study. *Smith & Wilcock (2015)* quantified this difference further by determining that suspended sediment yields from urban watersheds were 2-70 times higher than background levels, with a median increase of ~6 times from forested areas and ~3 times from agricultural areas. Furthermore, the time for excess sediment to be flushed from the system is highly variable, ranging from just 5 years to 50 years (*Chin, 2006*), depending on a multitude of factors such as geology and climate, resulting in observed sediment impacts beyond initial urban development. A case study in Maryland, USA found that coarse-grained sediment load was averaging 90 t/km^2/year in a full suburban basin compared to a yield of 5-22 t/km^2/year in forested basins. *Russell et al. (2017)* found the increase in sediment yields is at least in part due to the surrounding activity (e.g., construction) allowing for riprap, concrete, brick, and other anthropogenic materials to supplement coarse sediment loading, making up 2-21% of bed particles alone. These changes in sediment supply alter the state of the channel beyond hardening and straightening as the natural progression of larger particles near the headwaters where flow is slowest and reduced particle size downstream where flow is more intense is interrupted, leading to unintended consequences such as erosion. Furthermore, pool-riffle channels have been found to display the greatest sensitivity to increases in sediment supply and/or peak flows (*Montgomery & MacDonald, 2002*) which would encompass most channel types in Southern Ontario, especially in urban areas. *Papangelakis et al. (2019)* found an increase in transport distances of coarse particles (>D_{50}) in urban channels. Since many of the channels studied in urban environments have been straightened to some degree, this would result in a more consistent display of sediment size between sites at different points along the channel as there are less local sorting points.

Contradictory to prior studies at the time, *Annable et al. (2012)* found that there was no increase in observed bankfull width and depth versus bankfull discharge as a function of urbanization. The authors also discovered that with increasing urbanization, bed material supply tends to decrease which is offset by a smaller bankfull channel width, depth, and access to floodplains during major events. This observation was further supported in their study by measurements of decreased sinuosity and bed material transport and thus, channel degradation, with increasing urbanization in sites where artificial structures (e.g., armourstone) were installed. These findings are consistent with previous studies conducted by *Bravard & Petit (2009)* especially with regards to observed slope alterations. Slope decreases downstream via lateral migration extension which *Bravard & Petit (2009)* explains by the correlation of river slope to bedload size. Bedload size decreases downstream through sorting, attrition, and dissolution in circumstances of materials such as limestone. Unfortunately, due to the highly variable effects of urbanization, each stream indicates changes differently and in such a complex manner that it is difficult to disentangle the influences of disturbances to the flow regime from those of the sediment regime (*Russell et al., 2017*). Such contradictions in findings reinforce the inconsistent nature of river science research, the validity of patterns, and the need for continuous comprehensive research.

2.2 Adaptive Management

The necessity for continuous comprehensive research is highlighted by the establishment of the term "urban stream syndrome" which describes the effects of unmanaged and significant urbanization on stream systems such as increased channel dimensions (*Booth et al., 2016*), changes in alluvial materials, flashy hydrology, and degradation of water quality and aquatic habitat (*Mackenzie et al., 2022*[a]*; Mackenzie et al., 2022*[b]). *Meyer et al. (2005)* found that this level of degradation was observed most often in urban environments where channel morphologies are simplified (i.e., straightened). Such alterations were common in the 1970s and 1980s and accompanied surrounding land use changes such as agricultural and urban development (*Padovan, 2016*).

There are three prevailing approaches to traditional urban river management:

1. Manage the flow regime (e.g., SWM, LID)
2. Manage the transport capacity of the channel (i.e., restoration)
3. Manage the sediment regime (e.g., sediment augmentation)

Examples of conventional activities include centralized SWM and channel hardening such as gabion baskets, armourstone, and complete concrete channelization (*Papangelakis et al., 2022*[a]). SWM and restoration are very prevalent in urban areas and are often driven by policy and/or the need to protect infrastructure. A process that has primarily been used downstream of dams (e.g., *Sumi et al., 2017*) but remains experimental for urban applications is sediment augmentation. Sediment augmentation involves the artificial supply of sediment to a channel with the intent to offset the effects of sediment deficits such as decreased riverbank stability and local scour (*Mörtl & De Cesare, 2021*).

Conventional SWM practices that focus on peak discharge control are the most popular strategy due to familiarity and upfront cost. This type of SWM relies on runoff retention ponds and results in lowered peak discharges but often prolonged duration of erosive discharges, which in turn negatively affect receiving stream networks (*Bledsoe & Watson, 2001; Bledsoe, 2002; Nehrke & Roesner, 2004; Rohrer & Roesner, 2006; Hawley et al., 2013; Papangelakis et al., 2019*). The consequences can be seen in the larger cross-sectional dimensions in areas where these practices are implemented when compared to forested areas as channel geometry is typically not a management priority (*Hawley et al., 2013*). An example of this effect was captured by *Papangelakis et al. (2022*[b]*)*, who measured stream flows in neighbouring urban watersheds with (i.e., Morningside Creek) and without (i.e., Wilket Creek) traditional SWM ponds. The channel with SWM had a smaller peak flow than the urban channel with no SWM but the flows capable of transporting sediment (i.e., "erosive" flows) lasted significantly longer (*Figure 1*).

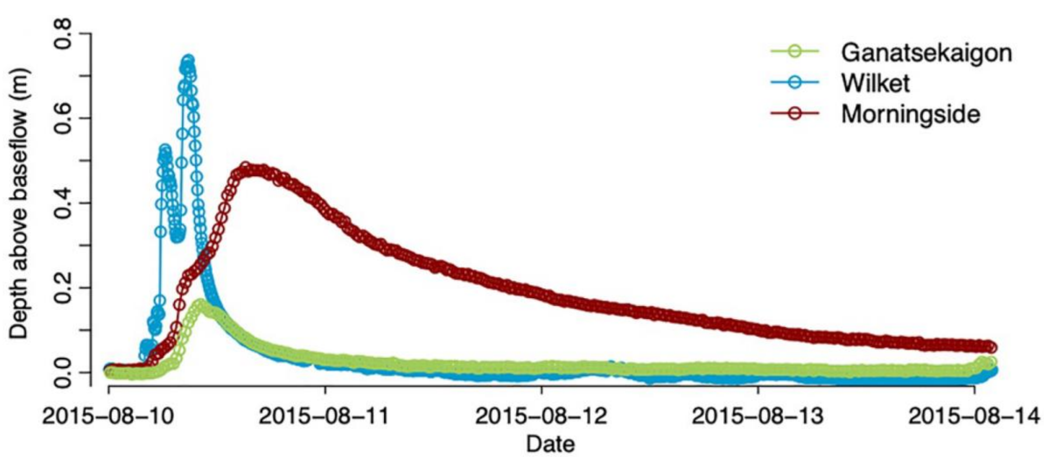

Figure 1. Stormflow characteristics for three study sites (*Papangelakis et al., 2022*[b])

As urban populations continue to grow at a rate of 1.5 times by 2045 (*The World Bank, 2023*), the observed degradation of waterways remains a pressing issue. Stream restoration has become a multi-billion-dollar effort globally (*Palmer et al., 2007*), which has led to the need for the development of more effective solutions. Current methods range from local hardening to complete channel reconstruction, most based around pool-riffle designs. Pool-riffle sequences are considered the foundation for rivers due to their influence on channel morphology (*Thompson, 1986; Kleinhans & van den Berg, 2011*) and are typically identified visually from aerial imagery or 1D plots of thalweg elevations (*Richards, 1976; O'Neill & Abrahams, 1984; Lisle & Hilton, 1992*). Designs based on pool-riffle sequences are popular due to their perceived benefits for channel stability (*Obach, 2011*) and habitat availability (*Wade et al., 2002*). However, not all initiatives that have implemented pool-riffle bedforms have been successful as some have become eroded or filled in with sediment, resulting in increased flooding and failed channel stabilization (*Walker et al., 2004*). The use of traditional SWM and restoration methods remain an issue as the lack of consideration for channel adjustments and the dynamic nature of geomorphic processes (including sediment transport), has led to high failure rates, and a need for more financial investment and continuously updated management plans (*Papangelakis et al., 2022*[a]). This responsibility tends to be allocated to municipalities or local watershed management authorities (e.g., conservation authorities) who typically do not have the budget to adequately respond to all areas of concern.

The past decade has seen a shift towards acknowledging the need for unique hybrid approaches to urban development and restoration that accommodate urban constraints while focusing on re-establishing fluvial and sedimentary processes that mimic the natural evolutionary progression of the channel (*Padovan, 2016; Wohl et al., 2015*). Adaptive management is an approach that has become of interest for urban systems in recent years that treats policies and management practices as experiments from which to learn (*Levine, 2004*) and often involves non-traditional methods. More holistic approaches to urban watershed management such as the implementation of LID (*Mackenzie et al., 2022*[a]*; Fletcher et al., 2015*) have been of interest. However, for these approaches to be successful, it is necessary to derive tools that identify areas within watersheds most at risk for channel degradation to help facilitate effective watershed management efforts. Regime requirements as defined by *Mackenzie et al. (2022*[a]*)* refer to "…a dynamically stable state of existence for a watercourse, for which the rate of energy expenditure approaches a minimum, and the rate of sediment transport into and out of the regime reach is approximately equal over time." Early identification of the potential for a stream to exhibit a shift away from "in regime" conditions has become essential for the management of urban watersheds.

Several approaches have been developed to identify areas at risk of current and future channel erosion and morphological adjustments to guide more accurate analyses of conservation methods for infrastructure and critical habitats (*Howett, 2017*). Given the fundamental control of geology and climate on geomorphic processes, approaches to identify sensitive areas are necessarily regionally specific (*Table 1*). In Southern Ontario, the meander belt concept by *Parish Geomorphic (2004)* tends to be the most cited. The goal of river corridor management should be to promote ecological resilience which is "…the ability to absorb disturbance without exhibiting permanent detrimental effects" (*Padovan, 2016*) and can be achieved through establishing stable geomorphic planforms that account for all factors (i.e., flow, sediment, surrounding land use, stormwater systems, long-term area needs, etc.).

Table 1. Summary of concepts of river corridor management (*Howett*, *2017*)

Concept	Region of Application	Source
River corridor	Vermont	(Kline & Dolan, 2008)
Channel migration zone	Washington	(Rapp & Abbe, 2003)
Area of fluvial freedom	Spain	(Ollero, 2010)
Erodible corridor concept	(n/a)	(Piegay H., Darby, Mosselman, & Surian, 2005)
Freedom space	Quebec	(Biron, et al., 2014)
Streamway	Oregon & Washington	(Palmer, 1976)
Stream corridor	U.S.A.	(FISRWG, 1998)
Inner river zone	California	(Department of Water Resources (state of California), 1998)
Riparian corridor	United Kingdom	(Thorne, Masterman, & Darby, 1992)
Meander belt	Ontario	(Parish Geomorphic, 2004)

To best predict which watershed segments are most in need of management interventions, it is often beneficial to reference the basics. The natural evolution of a channel was described by *Schumm et al. (1984)* through a model outlining the several stages of such a progression as stream networks react to disturbances, particularly those related to urbanization such as channelization and dredging. This model (*Figure 2*) displays five stages in which the channel begins in equilibrium followed by cycles of incision, widening, and aggradation, before coming full circle back to a state of quasi-equilibrium (*Hawley et al., 2013*). Quasi-equilibrium as defined by *Annable (2012)* is “a river reach which maintains flow and sediment transport continuity and geotechnical stability over a significant period of time during which there is no net intermediate to long-term aggradation or degradation of the channel form.” In other words, it is considered “in-regime”. The phase in this model of particular interest to this study is phase four because as the channel adjusts towards a new equilibrium in response to the increased erosive conditions, the channel’s susceptibility to erosion intrinsically decreases due to a reduction in slope, increased widening, and therefore reduced specific stream power (*Hawley et al., 2013*). This process is self-limiting as the increased erosive forces lead to the observed channel adjustments until the river reaches a new condition that accommodates this new flow.

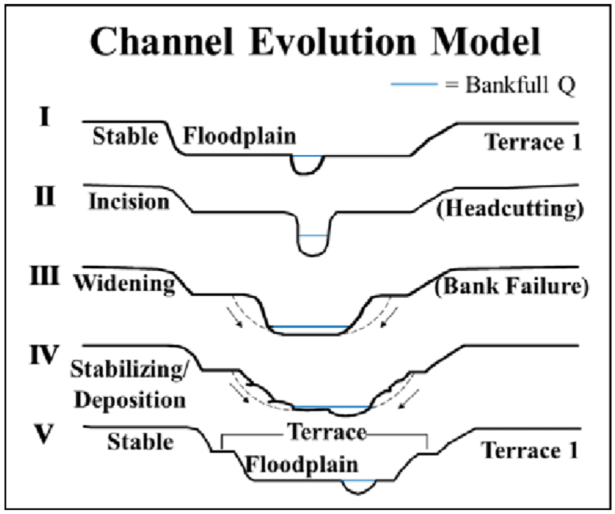

Figure 2. Channel Evolution Model (CEM) (*Maestas et al., 2018*)

Despite attempts to identify patterns in urban river change, there are several complicating factors that have precluded the development of a universal model of urban river adjustment. Though urban transformation of rivers can be partially predicted through physical attributes related to fluvial geomorphology, they are also path dependent. Thus, anthropogenic interventions also play into the predictability of a watershed as they will make some adjustment pathways unavailable (*Ashmore et al., 2023*), even if it seems feasible at the time of the assessment. For example, the presence of bedrock, vegetation, and urban constraints such as infrastructure will impede the progression of channel evolution in the expected CEM path and may open different pathways of adjustment (*Booth & Fischenich, 2015*). Additionally, most detailed reach-scale assessments used today rely on repeated measurements of channel dimensions and identification of erosion indicators to monitor channel geomorphology along a reach of 100-300 m (*Papangelakis et al., 2022*[a]) which may misrepresent key information about a channel's adjustment process as results are subjective based on individual observations (*Gazendam et al., 2016*) and site-specific conditions (*Padovan, 2016*).

An increasingly common method for assessing geomorphic sensitivity and predicting morphologic adjustments at the watershed scale is to utilize stream power (i.e., energy expenditure of flow per unit downstream length):

$$\Omega = \rho g S Q \qquad \textit{(Equation 1)}$$

where ρ = density of water (~ 1000 kg/m^3), g = acceleration due to gravity (9.8 m/s^2), S = channel slope, and Q = discharge (m^3/s). Due to its dependence on channel slope and discharge, stream power is sensitive to changes in hydrology (i.e., urbanization and SWM interventions) and channel straightening (*Papangelakis et al., 2022*[a]). Specific stream power, equal to the total stream power divided by the channel width, is a measure of energy expenditure per unit area (W/m^2), which can be used as a predictor of sediment entrainment thresholds (*Bagnold, 1966; Ferguson, 2005*). Due to its link with sediment entrainment, specific stream power is a powerful metric that has been used to estimate sediment transport rates (e.g., *Parker et al., 2011*), discriminate between channels of different morphology (e.g., *Candel et al., 2021; Phillips & Desloges, 2015*), and predict areas of aggradation and degradation (e.g., *Yochum et al., 2017*). The significance of this metric cannot be understated as it has been used to identify areas of susceptibility to morphology change and instability, especially in urban systems (*Bizzi & Lerner, 2015; Mackenzie et al., 2022[a]*).

Several studies have applied a stream power-based approach to assess the potential for channel morphologic adjustments in urban watersheds such as *Vocal Ferencevic & Ashmore (2011)*. *Mackenzie et al. (2022[a])* developed the Group Method of Data Handling (GMDH) model to predict specific stream power with the aim of determining whether a channel is in or out of regime based on a comparison with observed values. The authors found that changes in specific stream power are "a reliable early detection metric for the occurrence of the urban stream syndrome." In addition, *Ashmore et al. (2023)* supports the commonly cited value of 300 W/m^2 as the threshold specific stream power for substantial erosion and widening onset as well as observed channel pattern change stemming from high-magnitude flooding events. They also note that changes in channel width are correlated with total stream power rather than discharge for given bed material particle sizes (*Ashmore et al., 2023*).

Building upon years of foundation surrounding stream power, the Stream Power Index for Networks (SPIN) tool was created by *Ghunowa et al. (2021)*. SPIN is a GIS-based toolbox that utilizes a watershed DEM and either land-use information or existing hydraulic models to calculate a variety of variables including total stream power, specific stream power, and their changes though historical, current, and future land-use conditions. Where existing hydrologic data does not exist, SPIN relies on empirical relations between drainage area, channel width, percent imperviousness, and discharge (typically the two-year return) to calculate stream power metrics (*Ghunowa et al., 2021*). Research conducted by *Papangelakis et al. (2022[a])* tested the effectiveness and reliability of the SPIN tool on the Etobicoke Creek watershed in Toronto, Ontario and confirmed that the calculated metrics matched measured values, including channel slope and threshold substrate size. Furthermore, they determined that both total and specific stream power displayed an increase when comparing pre-urban to urban land-use conditions. Overall, they found that SPIN offers a quick alternative for visualizing trends in stream power indices at the watershed scale which has very applicable benefits for watershed managers and city planners during the initial analysis stage. More specifically, it can aid in identifying areas requiring intervention based on where the increase in stream power is predicted to exceed thresholds.

2.3 The Greater Toronto Area (GTA)

The Greater Toronto Area (GTA) is Canada's most populus urban area, with a population of ~6.5 million residents as of 2022 (*City of Toronto, n.d.[b]*). Since its founding in 1934 (*Careless, 2022*), the GTA has experienced continuous rapid growth, with an increase in population of ~10% from 1931 to 1941 alone, and a 300% increase from 1941 to 2021 (*Statistics Canada, 2009; Statistics Canada, 2023*). In response to growing infrastructure needs and severe flooding caused by Hurricane Hazel in 1954, the Toronto and Region Conservation Authority (TRCA) was established in 1957 (*Ashmore, 2018*). The TRCA is responsible for the management of the region's nine watersheds: Carruthers Creek, Don River, Duffins Creek, Etobicoke Creek, Highland Creek, Humber River, Mimico Creek, Petticoat Creek, and Rouge River (*TRCA, n.d.[a]*). The establishment of the TRCA was necessary to facilitate the growing infrastructure needs that came with an increasing population.

A study by *Aquafor Beech Limited (2006)* found that even at 30% watershed impervious cover, peak flows associated with 1, 2, and 100-year storms in the GTA become more frequent by 10.6, 3.3, and 1.5-fold, respectively. To put that into perspective, that would equate to an annual storm peak occurring more than 10 times per year. Similarly, *Papangelakis et al. (2019)* found that urban watersheds in the GTA had more sediment mobilizing events than rural watersheds, with 81 events recorded in an urban watershed and only 18 recorded in a neighbouring rural watershed over the same 3-year study period. The effects of urban land use on event-scale hydrologic characteristics in the GTA (e.g., increase in flood frequency, magnitude, and flashiness) have also been noted by *Trudeau & Richardson (2016)*. As urbanization has continued to intensify, the human consequences of altered watershed hydrology have become evident as the rate of displacement has risen (19,000 Canadians in 2018) due to climate change related events exacerbated by inadequately managed urbanization (*Library of Parliament, 2020*).

Much of the GTA (65-70%) was constructed prior to when the implementation of SWM was mandated and areas where traditional SWM was implemented still experience flooding and erosion due to a lack of adequate research at the time (*STEP, n.d.*). Traditional strategies included peak-shaving SWM ponds and significant channel realignment (*Ashmore, 2018; MTO, 1997*) to facilitate housing needs. Consequently, many older developments lack any SWM at all and for many others that do have SWM in place, it is not adequate as it only supports a fraction of the watershed. A study by the *TRCA (2021)* concluded that only a small fraction of land in the GTA has adequate SWM for both flood management and erosion control. A prominent example of failed urban watershed management strategies was the significant rain event which occurred on July 8, 2013, that broke the rainfall record set 60 years prior. Due to the severity of the storm, there was widespread flooding on major highways and the city's transit system was significantly disrupted (*Tillekeratne, 2024*). More instances such as these are now occurring as outdated infrastructure continues to fail at an increasing pace due to climate change and intensifying urbanization.

Studies conducted in the GTA have documented anthropogenic-induced channel alterations such as widening, incision, and instability (e.g., *Padovan, 2016; Bevan et al., 2018; Mackenzie et al., 2022[a]; Mackenzie et al., 2022[b]*). In response to such research and the ineffectiveness of traditional watershed management approaches in the GTA, the TRCA has adopted new tactics that aim to restore the geomorphic and ecological processes of channels via "natural channel design" (NCD). NCD is defined as "restoring streams to mimic the natural form, flow and movement of streams unaffected by human influence" (*TRCA, 2021*). These projects typically rely on designing channel dimensions and building geomorphic units such as pools and riffles using reference reaches with the goal of replicating channel conditions and re-establishing ecological processes (*Padovan, 2016*). However, these methods are still not very well defined due to a lack of adequate monitoring and a focus on short-term (e.g., 5-10 year) outcomes, as is common when the requirement for justification to government bodies exists. Therefore, an understanding of how effective different strategies are is still lacking which has led to many project failures and high maintenance costs. Thus, efforts would best be spent on the initial stages of projects to predict which areas are most at risk of failure and/or highest priority for restoration and monitoring.

As the effects of poor management methods and the reality of climate change continue, it is more important than ever to develop effective tools for identifying and monitoring sensitive river reaches.

This can be achieved through analysis of the previous methods and their points of failure, as well as modelling the trajectory of the watersheds utilizing verified scientific research methods.

2.4 Geomorphic Assessment Methods

2.4.1 Historical Analysis

Historical analyses of river morphology are a critical component of river characterization and form the basis of understanding for how a system has changed over time (*Padovan, 2016*). Most commonly, the use of historical data such as topographic maps, flow records, aerial photographs, and floodplain stratigraphy. Historical analyses provide context for how a system may look and function today and is especially important in rapidly changing environments such as urban watersheds. Furthermore, historical analyses can be used to predict the future behaviour of a river system (*Papangelakis et al., 2023*), which, as climate change continues to alter what are considered “normal” conditions (*Papangelakis et al., 2022*[b]), is becoming more and more essential.

Two important morphological characteristics that are most often measured from historical and current aerial imagery are sinuosity and thread (e.g., single vs. braided) which describe the pattern of a channel (*Wilzbach & Cummins, 2018*). Calculating the sinuosity index for a channel consists of measuring channel length along the thalweg (i.e., drawing a line through the deepest points of successive cross-sections for the length of the channel chosen) and dividing by the valley length (i.e., a straight line drawn beside the river for the same length of channel as the valley length was measured for). To be considered meandering, channels must have a sinuosity index value exceeding 1.5 (*Wilzbach & Cummins, 2018*). Unfortunately, locating the true thalweg from aerial imagery alone is often difficult, and as such, the centreline of the channel is sometimes used in lieu to achieve greater accuracy (e.g., *Clerici & Perego, 2016*). Furthermore, as the process for delineating sinuosity is subjective based on individual linework techniques, the margin for error should be a consideration (*Limaye et al., 2021*). To attempt to improve consistency, computer programs such as the QGIS plugin “RiverMetrics” have been introduced in recent years which calculate sinuosity with minimal human input (*De Rosa et al., 2017*).

2.4.2 Field Analysis

Though desktop-based historical analyses of channel pattern provide a basis for understanding watershed trajectories, they do not provide a complete picture. As such, they are often supplemented by data collected in-field regarding channel dimensions, substrate characteristics, morphology, and flow regime. Methods for data collection include Wolman pebble counts, cross-section surveys (e.g., total station, GPS), photographs, drone imagery, and flow measurements (*Papangelakis et al., 2023*). In-field data provides information that, when analyzed against historical data, can provide a fuller picture of the current geomorphic condition of a watershed. For instance, an indicator of stream channel condition can be indicative of different influences depending on local geomorphic context and history of the watershed (*Montgomery & MacDonald, 2002; Hazbavi, 2018*).

Though predictions can be made to establish general hypotheses and guidance for channel assessment and monitoring across varying locations, the implications of the variability of each watershed, even within the same region (e.g., province), are too great to rely on pre-prescribed guidelines alone (*Papangelakis et al., 2023*). The formulation of diagnostic criteria and protocols tailored to specific geographic areas is essential for the most effective planning (*Montgomery & MacDonald, 2002; Conservation Ontario, 2010*). For example, utilizing a single parameter such as a 2-year storm flow for all of Southern Ontario could lead to over-mitigation in some areas and under-mitigation in others (*Papangelakis et al., 2023*). Additionally, bank erosion is a natural process with some benefits such as promoting riparian vegetation succession and creating dynamic habitats for aquatic animals, and thus, erosion rates must be placed in context of historical values (*Florsheim et al., 2008*). For example, eroding banks might be typical for channels in arid to semi-arid areas but an indicator of severe disturbance in meadows so the same management efforts would not be applicable to both environments (*Montgomery & MacDonald, 2002*). The effects of sediment regime changes are further complicated by effects stemming from the degree/time persistence of anthropogenic influences such as urbanization. For example, a pulse of fine sediment into a steep portion of the uppermost channel from a construction zone may be rapidly transported downstream but persist in the low-gradient portion of the channel which can have implications for aquatic ecosystems and their inhabitants (*Montgomery & MacDonald, 2002*).

Over 100 different river assessment frameworks have been developed since the 1970s with a large diversity of geographic focus and approaches, including the Natural Character index (*Fuller et al., 2021*), The River Styles Framework (*Fryirs et al., 2019*), and Process-Based Restoration (*Beechie et al., 2010*). Popular baseline inventory assessments which consider a variety of geomorphic parameters include Rapid Geomorphic Assessments (RGAs) and Rapid Stream Assessments (RSAs). These assessments are beneficial as they do not require a large time commitment to complete and provide a relatively accurate snapshot of the dominant channel processes at the time (*Padovan, 2016*). Furthermore, when monitoring the same locations over consecutive years, the observed changes can provide insight into the reasons for such channel adjustment and aid in predicting future alterations. However, they also have limitations such as subjectivity due to the qualitative nature of the assessments (*Habberfield et al., 2014; Lisle et al., 2015*).

Montgomery & MacDonald (2002) provide a basic conceptual framework for channel assessment and monitoring which has become the basis for most subsequent research regarding watershed condition. In their paper, they determined three principles:

1. Stream channel condition reflects the capability of the channel to accommodate, or resist change due to inputs of sediment, water, organic matter, or alterations of the riparian vegetation
2. Different channel types vary in their sensitivity and response to changes in inputs or local controls
3. Catchment and local scale differences in channel processes, historical disturbance, topography, lithology, structural controls, and geomorphic history result in a variety of channel types throughout a watershed (p. 1)

Utilizing these three principles, channel assessment and monitoring procedures must consider the following parameters:

a) Differences in sensitivity and response due to channel type

b) Spatial and temporal variability in the input parameters in different portions of a watershed
c) The effects of other controls at both reach and watershed scales (p. 2)

To put these ideas into practice, *Montgomery & MacDonald (2002)* proposed a diagnostic approach which incorporates at minimum the following phases (*Figure 3*):

Phase 1: Define the system of interest and the controlling variables
Phase 2: Use qualitative and quantitative observations to characterize the current state of the system
Phase 3: Evaluate the controlling variables and current symptoms to infer both relative condition and the causal mechanisms producing this condition (p. 2-3)

With relation to stream channel assessments, phase 1 includes steps such as an evaluation of the location within the channel network (e.g., upper reach vs. lower reach), channel type (i.e., braided, meandering, straight), associated controlling influences (e.g., dams), temporal variability in inputs, and historical conditions (*Montgomery & MacDonald, 2002*). Once these parameters have been established, phase 2 utilizes field observations to evaluate indicators of channel condition which, if the indicators are proven consistent, can lead to a confident diagnosis. However, as with most diagnoses, they are complicated by the interactions among causal factors and conflicting or ambiguous indicators. The most effective remedy for such a situation involves a combination of judgement and additional observations/data (*Montgomery & MacDonald, 2002*).

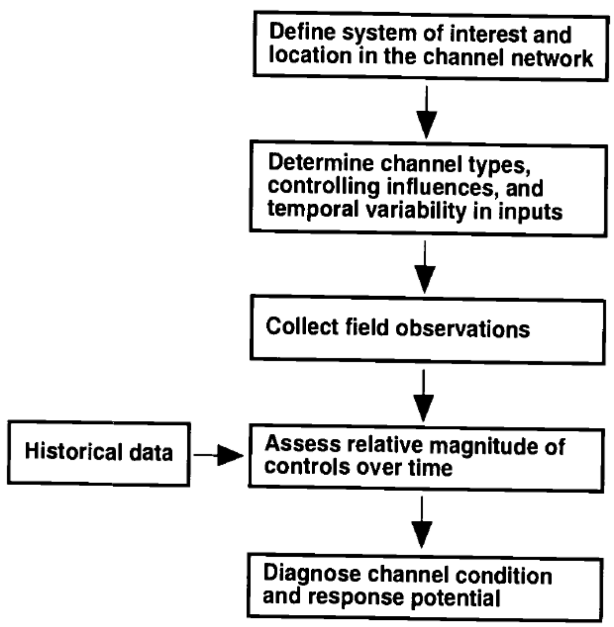

Figure 3. Suggested steps in the channel diagnostic procedure (*Montgomery & MacDonald, 2002*)

Several primary geomorphic field indicators discussed by *Montgomery & MacDonald (2002)* are common among most river assessment frameworks due to their importance in characterizing geomorphic processes (*Papangelakis et al., 2023*). These indicators include slope, confinement, entrenchment, riparian vegetation, overbank deposits, channel pattern, bank conditions, gravel bars, pool characteristics, and bed material (*Table 2*). While both valley bottom and active channel characteristics are important for developing a full understanding of a channel, most investigations that attempt to infer relationships among sediment supply and transport capacity typically focus on slope, confinement, channel pattern, bank conditions, and bed material (*Papangelakis et al., 2023*). The commonality of these geomorphic indicators in river assessment procedures likely stems from their economical effectiveness in describing channel conditions as much of the research being conducted is by government on limited resources (e.g., conservation authorities in Southern Ontario).

Table 2. Role of the primary field indicators in diagnosing channel condition (*Montgomery & MacDonald, 2002*)

Field Indicators	Role
Valley Bottom Characteristics	
Slope	Primary control on channel type and style of energy dissipation.
Confinement	Primary control on possible planform channel patterns.
Entrenchment	Indicates longer-term balance between runoff and sediment loads, and likely range of responses to high flows.
Riparian Vegetation	Primary control on channel characteristics.
Overbank Deposits	Indicates type and magnitude of recent deposits.
Active Channel Characteristics	
Channel Pattern	Braided channels imply high sediment loads, non-cohesive banks, or steep slopes. Large amounts of LWD can also generate anastomosing channel form in lower-gradient channels.
Bank Conditions	Location and extent of eroding bank relative to stream type can indicate level of recent disturbance.
Gravel Bars	Number, locations, extent, and condition related to sediment supply.
Pool Characteristics	Distribution and amount of fine sediment deposition can indicate role of flow obstructions and whether sediment loads are high for a given channel type.
Bed Material	Size and distribution of surface and subsurface bed material can indicate relative balance between recent discharge and sediment supply.

Slope is considered a key parameter for interpreting channel condition because of its control on stream power and the expected channel types (*Montgomery & MacDonald, 2002*), which is especially important in urban channels as they tend to change rapidly compared to rural channels (*Papangelakis et al., 2022*[a]). This can be seen in research conducted by *Vocal Ferencevic & Ashmore (2011)* as they noted an increase in channel slope due to anthropogenic interventions such as channelization or artificial straightening led to an increase in stream power.

Confinement is characterized by “the ratio of the valley bottom width to the bankfull channel width” (*Montgomery & MacDonald, 2002*). This ratio is important when considering controls on channel response because it determines the space available to the channel for lateral adjustments and the resulting changes in sinuosity and/or planform. Confinement may also influence how easily sediment is delivered to the stream, thereby affecting the sediment supply. On the other hand, it is important to note channels that are confined by valley walls as they do not experience this type of freedom and therefore are limited in their disturbance response potential. For example, many urban channels in Southern Ontario that are positioned within deep glacial valleys are more likely to respond to avulsions when they can no longer adjust laterally (*Bevan et al., 2018*). Together, valley bottom slope and confinement can be used to predict probable channel form and overall response potential for various disturbances (*Montgomery & MacDonald, 2002*).

Channel pattern (e.g., meandering, straight) is closely associated with the volume and sizing of available sediment supply in conjunction with transport capacity. This means that one would be able to infer a change in these factors from observing a change in channel type or sinuosity using resources such as aerial imagery (*Montgomery & MacDonald, 2002*). For example, Highland Creek in Toronto has a history of flow regime transformation, including channel straightening and steepening which has led to significant increases in specific and total stream power (*Vocal Ferencevic & Ashmore, 2011; Ashmore et al., 2023*).

Bank conditions refer to characteristics of the bank that influence the channel morphology, such as the bank height and angle, dominant material, presence of vegetation, and indications of erosion. Channel dimensions such as the bankfull width, bankfull depth, and the width-to-depth ratio act as a complimentary response variable when characterizing a channel (*Montgomery & MacDonald, 2002*) with bankfull stage considered to represent the dominant discharge associated with channel-forming events (*Wolman & Leopold, 1957*). This means that both the channel dimensions and bank conditions are linked in that an exhibit in one, is indicative of a response in the other. For instance, eroding outer meander bend banks are typical in pool-riffle channels (*Montgomery & MacDonald, 2002*) and a corresponding width-to-depth ratio would present as being deeper in such areas and perhaps wider to accommodate the discharge energy. This type of information is indicative of what stage of the CEM the channel is in, which can inform decisions for its management as it places the channel in the timeline of adjustment and can predict its future behaviour.

Bed material is most often characterized by the D_{50} which is the median grain size on the channel bed (*Montgomery & MacDonald, 2002*) and is one of the most important factors to consider when completing a channel characterization as it is an indicator of several factors such as discharge, sediment supply, and obstruction roughness (including channel walls). An increase in shear stress coupled with a reduction in sediment supply will coarsen the bed surface, while a decrease in flow amplitude in tandem with an increase in fine sediment supply will lead to a finer bed surface (*Montgomery & MacDonald, 2002*). The size of available sediment in the channel is important because sediment transport is the process that mediates morphologic adjustments which most assessments fail to consider adequately (*Papangelakis et al., 2023*).

2.4.3 Statistical Analysis

Statistical analyses have provided a basis for predicting changes in river systems in response to anthropogenic stressors for decades. Research from *Wood-Smith & Buffington (1996)* consisted of a discriminant function analysis which indicated a three-variable model is the most successful (~90% success rate) in distinguishing between channel reaches that were disturbed by logging and those that were undisturbed. These variables included: a) total number of pools per reach, b) mean pool depth to mean bankfull depth, and c) the ratio between the critical shear stress needed to mobilize the D_{50} and the bankfull shear stress. The proposed application of these functions to other sites was to facilitate identification of those in need of restoration and most at risk of being degraded. Similarly, *Chen & Wei (2008)* conducted a Pearson correlation analysis, where they found that relative width (ratio of the b-axis diameter of the largest substrate particle found in the reach (*D*) to bankfull width), relative roughness (ratio of *D* to bankfull depth), pool frequency, and per piece large woody debris volume are sensitive to percent equivalent clear-cut area (ECA) but independent of influence from non-logging activity.

Hawley et al. (2013) also conducted a study in which they attempted to isolate the effects of disturbance on a watershed, though their focus was on the effects of urbanization in-lieu of forest logging. To attempt to isolate the effects of disturbance, as was consistent with precedents in prior literature at the time, they utilized total impervious area as a surrogate for urbanization and conducted a Pearson correlation analysis. They found that in stream channels where sediment/siltation was listed as the prominent cause for water quality decline, stream bank instability was the dominant source of fine sediment even at low levels of imperviousness. These findings were able to support their hypothesis that the excess energy of the urban flow regime caused excess bed material transport and led to a series of complex responses in channels. Commonly, stream degradation effects begin to manifest when impervious cover exceeds 10% (*Mackenzie et al., 2022*[b]) as it increases stormwater runoff, the rate of which has been found by *Jang et al. (2021)* to be an effective indicator of land development impact on stream water quality.

The dimensionless shear stress, also known as the Shields parameter (τ^*), has been shown to be an influential factor when determining the level of channel stability as it has a significant impact on depth and slope prediction accuracy (*Afzalimehr et al., 2009*) as a criterion for incipient motion of sediment (*Cao et al., 2006*). Further, it has been found that width and D_{50} would most often be the first to adjust in response to a change in discharge. The D_{50} itself is quite important, serving as both an indicator of substrate erosion resistance and a simple quantification of flow resistance (*Mackenzie et al., 2022*[a]).

Despite the growing literature employing statistical methods to understand trends in channel adjustments in response to disturbances, there remains a need to identify parameters that best indicate channel reaches at most risk for geomorphic adjustments in response to urbanization. In other words, whether there are parameters that best distinguish between urban and non-urban reaches analogous to the results by *Wood-Smith & Buffington (1996)* and *Chen & Wei (2008)* in response to logging disturbances remains an open question. This question formed the basis for the research questions and statistical analysis performed in this thesis, as is explained in more detail in *CHAPTER 3*.

CHAPTER 3: Methodology

3.1 Study Sites

Four watersheds in the GTA were chosen for this study: Mimico Creek, Etobicoke Creek, Highland Creek, and Duffins Creek. These watersheds were chosen for their similar climate, vegetation, and underlying geology conditions as well as their range of urbanization, with Duffins Creek having the lowest fraction of impervious area and Mimico Creek displaying the most (*TRCA, 2018[a]; TRCA, 2018[d]*) (*Table 3*). Five sites were chosen within each watershed for a total of twenty study sites (*Figure 4*). Larger scale maps of each watershed are shown in *APPENDIX A*.

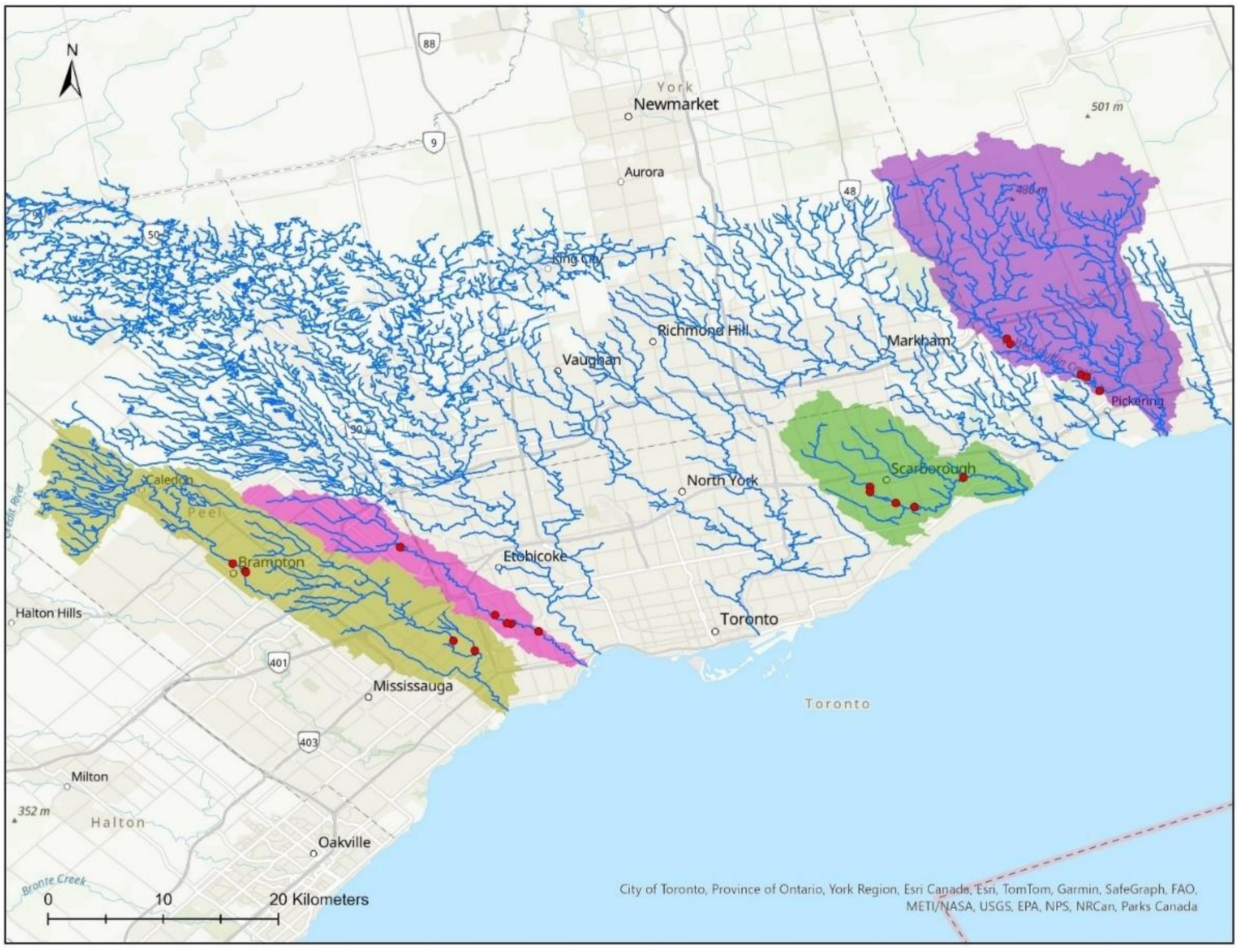

Figure 4. Study area map displaying the twenty study sites (red circles) and Mimico Creek (pink), Etobicoke Creek (yellow), Highland Creek (green), and Duffins Creek (purple) watershed boundaries.

Table 3. Summary of watershed characteristics

Watershed	Total Area	Land Use (2018)	Imperviousness
Mimico Creek[1, 2, 3]	~7,370 ha	Urban = 90% Rural = 0% Natural Cover = 10%	63%
Etobicoke Creek[1, 4, 3]	~22,405 ha	Urban = 67% Rural = 19% Natural Cover = 14%	33%
Highland Creek[1, 5, 3]	~10,583 ha	Urban = 89% Rural = 0% Natural Cover = 11%	57%
Duffins Creek[1, 6, 7, 3]	~28,216 ha	Urban = 18% Rural = 71% Natural Cover = 42%	5%

[1](*Tam, 2023*), [2](*TRCA, 2018[d]*), [3]Derived from the SPIN tool, [4](*TRCA, 2018[b]*), [5](*TRCA, 2018[c]*), [6](*TRCA, 2018[a]*), [7](*TRCA, n.d.[b]*)

3.1.1 Mimico Creek Watershed

The Mimico Creek watershed (~74 km^2) (*Tam, 2023*) is heavily urbanized, with the highest proportion of urban area (90%) and the lowest proportion of natural cover (10%) in the TRCA jurisdiction (*TRCA, 2018[d]*). Of that natural cover, approximately 2% is forest cover, with less than 1% being interior forest cover, and 19% is streamside cover as of the 2018 Watershed Report Card (*TRCA, 2018[d]*). Streamside cover has seen an increase of nearly 5% since the previous Watershed Report Card in 2013 (*TRCA, 2013[d]*), which can be attributed to the various restoration initiatives that have taken place such as the "DePave" project. This project converted an under-utilized paved surface to a recreational space for residents of a nearby housing co-op that includes a garden and seating area (*TRCA, 2018[d]*). Another notable project was the streambank stabilization measures undertaken within Malton Greenway, which aimed to protect the sanitary sewer running parallel to the East Branch of Mimico Creek and consisted primarily of the planting of a variety of native vegetative species to stabilize the stream bank (*TRCA, 2018[d]*).

In addition to the high proportion of urban area, the Mimico Creek watershed also has limited and outdated stormwater management systems (*TRCA, 2018[d]*). Historically, many kilometers of stream have been straightened to accommodate an increase in urbanization activities, including being lined with concrete in some areas to facilitate rapid stormwater drainage. Unfortunately, many of these projects are now failing due to age and more frequent intense storm events that exceed their design capacity (*TRCA, 2018[d]*). The failure of river management projects has resulted in increased flooding risk by preventing floodplain access and permeability of stormflow (e.g., through concrete lined channels), increased erosion rates, and failed works contributing excess sediment to the stream (e.g., broken gabion baskets) (*Papangelakis et al., 2022[a]*).

3.1.2 Etobicoke Creek Watershed

The Etobicoke Creek watershed is a large and heavily urbanized area (~224 km^2) (*Tam, 2023*) with a ratio of ~60% urban area to only ~12% natural cover as of 2021 (*TRCA, 2021*). The dominant surficial geology within the watershed is Halton Till. The dominant sediment materials in the upper sections of the channel are relatively fine (e.g., sand/clay) while the lower portions are dominated by coarser sediment such as gravel. The primary source of sediment in the lower sections is direct erosion of the bed and banks (*Papangelakis et al., 2022*[a]). The watershed is home to the Brampton Esker, a long, winding ridge of sand and gravel deposited by glacial meltwaters and the only esker in the TRCA's jurisdiction. Its sediments hold and purify water as it percolates, making it an important groundwater resource (*TRCA, 2021*). Unfortunately, even with this capacity for water retention, among larger watersheds in the TRCA jurisdiction, Etobicoke Creek displays the highest annual runoff, second only to the Don River, with 402 mm/year. This is indicative of an increase of 28% compared to baseline (2002-2010) measurements of 314 mm/year and has led to the designation of six Flood Vulnerable Clusters (FVC) in the watershed with a total area of 508 hectares (*TRCA, 2021*). An FVC is "an area within the flood plain where there is a higher concentration of roads and structures at risk of flooding" (*TRCA, n.d.*[c]).

More detail of the spatial patterns of urban development can be observed by evaluating the imperviousness of each of the eight Etobicoke Creek subwatersheds. With the exception of the Headwaters, all subwatersheds display impervious cover >50% as of 2019 (*Table 4*). The highest percentage is linked to the Little Etobicoke Creek subwatershed with a nearly 70% imperviousness cover, while the Headwaters show the least with just above 14%. The proportion of natural cover is consequently low across the entire watershed, with the Tributary 4 subwatershed displaying around only 7% as of 2019. Though these values are low, the overall watershed natural cover percentage is similar to other heavily urbanized watersheds at just under 12% (*TRCA, 2021*). The low natural cover can be attributed to this watershed containing a large amount of industrial and commercial land uses such as hosting the majority of the Lester B. Pearson International Airport.

Table 4. Percent impervious cover for Etobicoke Creek (*TRCA, 2021*)

Watershed	**2002**	**2012**	**2019**
	42.9	***45.6***	***47.9***
Headwaters	10.0	11.9	14.2
Spring Creek	46.6	50.3	54.1
West Branch	57.2	60.0	61.2
Tributary 3	57.1	65.1	66.8
Tributary 4	48.4	50.4	51.4
Main Branch	57.5	59.5	61.9
Little Etobicoke	64.5	66.8	68.7
Lower Etobicoke	65.0	64.9	65.7

The Etobicoke Creek watershed has limited and outdated SWM systems in place, resulting in issues related to flooding, erosion, water quality, and poor habitat quality (*TRCA, 2018*[b]). Only about

36% of the urbanized area had some form of SWM as of 2021, including 77 stormwater retention ponds. Of that 36%, only about 19% of the area had been determined to have adequate SWM capabilities to reduce peak flood flows, improve water quality, and mitigate erosion (*TRCA, 2021*). The inadequacy of SWM in the watershed is demonstrated by the results from the TRCA analysis which confirmed that flow tends to correspond directly to measured changes in the watershed's total imperviousness. Specifically, baseflows displayed an increase of 15% from historical conditions (i.e., 1960-1990) which is theorized to be caused by groundwater being intercepted by underground infrastructure (*TRCA, 2021*). However, average total flow increased by 44% between 1970 and 2010, with an additional 28% increase in average streamflow specifically between monitoring periods (i.e., 2002-2010 and 2010-2020) (*Papangelakis et al., 2022[a]*). Due to inadequate SWM, most of the watershed can be categorized as having the potential for and/or currently exhibiting moderate to high erosion sensitivity (*TRCA, 2021*).

Recent research has confirmed that the channels in the Etobicoke Creek watershed have responded to the hydrologic changes caused by urbanization. A study conducted by *Papangelakis et al. (2022[a])* found that the channels in the Etobicoke Creek watershed have coarsened from modelled pre-urban conditions to match the increased urban stream power conditions, the results of which were found to be consistent with the range expected in Southern Ontario based on previous studies of both urban and rural conditions. In addition to coarsening, the channels in the Etobicoke Creek watershed have also been observed to have enlarged by nearly 40% compared to pre-urban conditions (*Papangelakis et al., 2022[a]*).

The Etobicoke Creek watershed has a long history of urban development and management. Historically, the outlet of Etobicoke Creek into Lake Ontario was a wetland. The first engineered alteration was completed in 1929 to reinforce the sandbar across the outlet to allow for a road extension. Hurricane Hazel in 1954 was a large catalyst for water management in the watershed and in the years that followed, provincial and municipal governments purchased the land that was impacted, along with 164 properties in the floodplain, and converted them into the Marie Curtis Park. By 1959, the original creek mouth was unrecognizable (*TRCA, 2021*). In the following years, urban development in the watershed occurred rapidly, especially during the 1980s and 1990s, resulting in urban land use increasing from only 21% in 1978 to 53% by 1998. Today, the urban landscape is comprised of a mixture of industrial, commercial, residential, and park area (*Table 5*). By 2002, Etobicoke Creek was identified as one the most degraded watersheds within the TRCA jurisdiction, and unfortunately not much improvement has been made since (*Papangelakis et al., 2022[a]*). The number of erosion control structures within the watershed highlights the persistent erosion problems faced along Etobicoke Creek; as of 2019, the watershed contains (*TRCA, 2021*):

- 3,550 inventoried erosion control structures (2009-2017)
- 675 infrastructure hazard monitoring sites (within the Region of Peel)
- 138 TRCA-owned or managed erosion control structures; and
- 29 erosion hazard sites on private or public property

Table 5. Overview of land use change in Etobicoke Creek (*TRCA, 2021*)

	2002 (area %)	**2012 (area %)**	**% change from 2002-2012 (+ or -)**	**2019 (area %)**	**% change from 2012 to 2019 (+ or -)**
Urban	53.4%	56.4%	5.6%	59.5%	5.4%
Rural*	32.5%	30.9%	-5.0%	28.2%	-8.5%
Natural	14.1%	12.7%	-9.6%	12.3%	-3.4%
Impervious Cover	42.9%	45.6%	6.3%	47.9%	4.9%

*Rural includes land use such as agriculture, golf courses, open space, hydro corridors, etc.

In response to flooding and erosion problems, several river restoration efforts have been implemented in the Etobicoke Creek watershed. In total, 111 restoration projects were completed in the watershed between 2002 and 2019 (*Papangelakis et al., 2022*[a]). A study by the TRCA found that wetland habitat improved, and streamside cover increased by nearly 4% between 2013 and 2018 (*TRCA, 2018*[b]). This improvement is directly attributed to restoration efforts such as the removal and re-naturalization of a 400 m stretch of channel which had been previously straightened and lined with concrete. The channel was reconnected to the floodplain and riparian habitat was substantially increased through the implementation of riffles, pools, and riparian vegetation. This project also created wetland habitat and provided flood relief to areas downstream of the site (*TRCA, 2018*[b]). Despite these recent improvements, the watershed continues to experience challenges related to river adjustment.

3.1.3 Highland Creek Watershed

The Highland Creek watershed covers ~106 km^2 (*Tam, 2023*). The surficial geology of the watershed is dominated by glacial sediments originating from the Laurentide Ice Sheet which includes a mixture of till, sands, gravels, clay, and lacustrine silt (*Ashmore et al., 2023*). The terrain is very low relief, with the channels in narrow valleys being incised locally into glacial sediments. As such, bed material is primarily gravel-cobble with some sand and fine gravel, with particle sizes for D_{50} ranging from 35-65 mm typically, fining downstream towards the outlet at Lake Ontario (*Ashmore et al., 2023*).

Like most watersheds in the TRCA jurisdiction, the Highland Creek watershed has undergone a significant land cover change from agricultural to completely urban (>85% excluding valley lands) between the 1950s and 2000s and displays a high imperviousness value of 57% (*Table 3*). Of the observed 11% natural cover remaining in the watershed, most is forest (6%) with the remaining 5% attributed to meadow (*Padovan, 2016*). In response to the high proportion of impervious surfaces, flood peaks have increased by up to 5-fold in some areas, with total annual flow for the creek nearly doubling between the 1960s and 1990s alone, increasing from 20 million m^3 to 40 million m^3, respectively. The ratio of annual maximum instantaneous versus annual maximum mean daily discharge has also increased from <2 to 5-10 once full urbanization was achieved (*Ashmore et al., 2023*). The progressive reduction in sinuosity and increase in imperviousness has played a significant role in the observed flood and discharge values. Local channel slopes have increased by as much as 15% in some places since the 1960s and the total channel length was reduced from 104 km to just 74 km, resulting in increased stream power and consequent potential for erosion and flooding (*Ashmore et al., 2023; Vocal Ferencevic &*

Ashmore, 2011). The complete transformation of the flow regime in tandem with channel straightening and steepening has resulted in stream power values increasing by an order of up to ten times. In response to these changes, the channel has undergone significant channel widening by factors of up to five in some areas, which has led to anthropogenic interventions such as channelization and hardening in an attempt to mitigate erosion and protect local infrastructure (*Ashmore et al., 2023*). Due to the complexity of its response to urbanization and long history of management, the Highland Creek watershed has been the subject of many studies that have described and analyzed the factors contributing to its significantly degraded state and active erosion along both its bed and banks (e.g., *Vocal Ferencevic & Ashmore, 2011; Ashmore, 2015; Mackenzie et al., 2022*[b]*; Ashmore et al., 2023*).

The beginning of watershed management efforts can be traced back to the Hurricane Hazel flood in 1954 which, as in the case of Etobicoke Creek, resulted in significant anthropogenic alterations to the affected areas. Several reaches of the Highland Creek were engineered and narrowed after the flood (*Ashmore et al., 2023*). In the headwater tributaries, complete hardening can be seen, while the main branches experience about 50% hardening. These factors make determining the effects of urbanization on channel width quite difficult (*Ashmore et al., 2023*). The TRCA in coordination with the City of Toronto, aim to develop the Highland Greening Strategy, which would prioritize projects with goals that aim to restore the watershed, resulting in a higher level of climate change preparedness for residents (*TRCA, 2018*[c]). Such projects have included the “Highland Creek Rehabilitation Project - Markham Branch” which aimed to restore 1.5 km of channelized stream into a natural watercourse by applying natural channel design techniques (*City of Toronto, n.d.*[a]). The project was completed in 1998 and included the implementation of fascines, brush layering, and live crib walls to promote slope stability. In addition, floodplain wetlands were created to treat stormwater and provide habitat (*City of Toronto, n.d.*[a]).

3.1.4 Duffins Creek Watershed

The Duffins Creek watershed is ~282 km^2 (*Tam, 2023*) and has a higher fraction of rural land use (71%) (*TRCA, n.d.*[b]) compared to the other watersheds studied. With 42% natural cover as of 2018, it boasts the highest proportion of natural cover in the TRCA jurisdiction (*TRCA, 2018*[a]). The watershed has also seen an increase of nearly 3% in forest cover since the last Watershed Report Card in 2013 (*TRCA, 2013*[a]), resulting in it also holding the title for the watershed with the highest proportion of forest cover in the TRCA jurisdiction (*TRCA, 2018*[a]). The watershed encompasses a portion of the Oak Ridges Moraine (ORM) (*Simic et al., 2014*), an ~80 km^3 area of stratified meltwater deposits (*Sharpe & Russell, 2023*). The watershed’s geologic setting therefore consists of a series of alternating till and lake (silt and clay) and river (sand or gravel) deposits overlying bedrock, ranging in thickness from 0 to 200 m (*Simic et al., 2014*).

The increase in forest cover can be partially attributed to restoration projects such as the 2008 Lake Ontario Atlantic Salmon Restoration Program undertaken by the provincial government that involved streamside plantings, stream-bank stabilization, and construction of cattle crossings and fish by-pass channels (*Government of Ontario, 2008*). In addition, due to the level of naturalization in the watershed, aquatic habitat is a high priority and as such, the TRCA is a partner in the Bring Back the

Salmon program. This program aims to re-establish the native Atlantic Salmon population in the creek through fish stocking and habitat restoration (such as increasing canopy cover) (*TRCA, 2018[a]*).

Although the Duffins Creek watershed is the least urban of the watersheds studied, it is facing continual development pressures. The most notable current development is through the Seaton Lands project, which aims to convert 7,000 acres of undeveloped land into areas for residential, commercial, and institutional uses (3,064 acres) as well as employment (815 acres) (*City of Pickering, n.d.*). Though the remaining 3,121 acres of land are to be preserved as open space lands (*City of Pickering, n.d.*), that is still less than half of the total watershed area, reinforcing the trend of urbanization in the GTA and emphasizing the importance of early and continuous monitoring of its effects.

3.2 Methodology

Background information pertaining to the methodology for this study was collected through a literature review as discussed in *CHAPTER 2*. Chosen methods were scaled according to available resources (i.e., scheduling constraints and data availability). Four categories of geomorphic parameters were collected: 1) watershed characteristics (percent imperviousness, drainage area), 2) flow characteristics (discharge, specific stream power), 3) reach scale parameters (slope, sinuosity, entrenchment ratio, bankfull width (W_{bf}), bankfull depth (h_{bf}), particle size), and 4) geomorphic ratios (width to depth (W_{bf}/h_{bf}), relative roughness (D_{50}/h_{bf}), shear stress (τ_{c50}/τ_{bf})). Utilizing the calculated parameters, two analyses were conducted: 1) historical change in sinuosity, and 2) statistical analysis of the relationships between the watershed characteristics, flow characteristics, reach scale parameters, and geomorphic ratios. Each component of the methodology is outlined in their own subsections below.

3.2.1 Watershed Characteristics

To explore relationships between the measured watershed characteristics and the reach-scale parameters, the following were calculated for each field site: percent imperviousness, drainage area, discharge, slope, and specific stream power. These parameters were calculated using the Stream Power Index for Networks (SPIN) version 2.0 toolbox for ArcGIS developed by *Ghunowa et al. (2021)* (available open source at https://github.com/macvicab/SPIN). Layers required by the SPIN tool to perform its functions were created in ArcGIS pro from the DEM and imperviousness layers outlined in *Table 6*. The watershed-specific clippings of each of these layers were input into SPIN. The first step of the SPIN tool is to use the DEM to delineate the channel network that is then split into 30-40 m segments. SPIN then calculates the weighted total percent imperviousness, drainage area, discharge, slope, channel width, and total stream power for each channel segment and stores them as attributes. A detailed description of how the tool operates is presented in *Ghunowa et al. (2021).*

Table 6. Input layers for the SPIN tool analysis

Layer Description	**Source**
Shapefile of the 2017 land-use polygon layer for the TRCA jurisdiction with an assigned total impervious value for each polygon from 0 (least impervious) to 100 (most impervious)	TRCA
Shapefile of watershed boundaries	TRCA
Hydrologically enforced Digital Elevation Model (DEM) layer for Ontario	Government of Ontario

The SPIN tool calculates the 2-year urban flood discharge (Q_{2u}) at each stream segment using the following empirical equation:

$$Q_{2u} = aA^bI^c \qquad \textit{(Equation 2)}$$

where A is the drainage area (m^2), I is the weighted total percent imperviousness for the area draining to the given segment calculated from the TRCA land-use layer (*Table 6*), and a, b, and c are empirical coefficients. The values of a = 0.248 and b = 0.910 were used based on data from 210 watersheds in Southern Ontario by *Phillips & Desloges (2014)*. The coefficient c = 0.3 was calculated by *Bledsoe & Watson (2001)*. Since the SPIN tool calculates these parameters for each 30-40 m channel segment, the segments corresponding to each study site were located and the applicable parameters extracted from the resulting SPIN layer. The specific stream power at each site was calculated by dividing the SPIN calculated total stream power value by the measured bankfull width (W_{bf}). This was done as it was determined to be more accurate than the SPIN calculation for specific stream power that utilizes a rural (non-urban) reference value for channel width. The average value for each parameter across each site was calculated and is referred to as the "site average". The average for all segments within each watershed was calculated as well and is referred to as the "watershed average".

3.2.2 Reach Scale Parameters

3.2.2.1 Sinuosity Analysis

The sinuosity analysis consisted of the collection of current and historical aerial imagery provided by the City of Toronto Archives (TA), the City of Toronto Geospatial Competency Centre (TGCC), The City of Brampton (CB), and The Regional Municipality of Durham (RMD). The aerial imagery for 2021 was used to represent current conditions as it was the most recent imagery that was available for all sites. The historical imagery varied between 1973, 1977, and 1978 for each site depending on availability and clarity of the imagery for optimum comparison (*Table 7*). The images were used to calculate sinuosity (channel length divided by valley length) in ArcGIS Pro 3.0 for the current (2021) and historical (1973-1978) conditions. The channel length was determined by tracing the centreline of the river over a 500 m reach (250 m upstream and 250 m downstream of the study site where possible), which is consistent with the standard reach length (200 m to 2 km) from the *Parish Geomorphic (2004)* outline for meander belt width delineation in Southern Ontario. The chosen valley length was also 500 m for ease of comparison. The sinuosity calculations for both years for each site were combined to yield a change value (+/-) for comparison.

Table 7. Aerial imagery specifications summary

Site	**Recent Imagery (2021)**		**Historical Imagery (1973/1977/1978)**		
	Required Georeferencing?	*Source*	*Required Georeferencing?*	*Source*	*Year of Data*
Mimico					
MCAI	No	TGCC	No	TGCC	1978
RAVP	No	TGCC	No	TGCC	1978
MATC	No	TGCC	No	TGCC	1978
EVAP-A	No	TGCC	No	TGCC	1978
EVAP-B	No	TGCC	No	TGCC	1978
Etobicoke					
ECT-A	No	TGCC	No	TGCC	1978
GET-6	No	CB	Yes	TA	1973
CENP	No	CB	Yes	TA	1973
ECAB	No	CB	Yes	TA	1973
GET-2	No	TGCC	No	TGCC	1978
Highland					
BDR-B	No	TGCC	No	TGCC	1978
BDR-A	No	TGCC	No	TGCC	1978
BENP	No	TGCC	No	TGCC	1978
MSPT	No	TGCC	No	TGCC	1978
CDBP	No	TGCC	No	TGCC	1978
Duffins					
SHT-A	No	RMD	Yes	TA	1977
SHT-B	No	RMD	Yes	TA	1977
SHT-E	No	RMD	Yes	TA	1973
SHT-D	No	RMD	Yes	TA	1973
RIVT	No	RMD	Yes	TA	1973

3.2.2.2 Field Analysis

The field analysis involved the establishment of monitoring sites for which various methods were employed to capture data to characterize the dimensions and substrate. Initially, ten potential sites per watershed were identified via aerial imagery obtained from Google Maps. The criteria for the chosen sites were: 1) had no significant anthropogenic reinforcement along the established cross section where possible (e.g., bank armourstone), and 2) were accessible through public trails/lands. Following ground-truthing, many identified sites were found to be inaccessible (e.g., due to construction) or not appropriate (e.g., unsafe flow conditions). Thus, a total five per sites per watershed were identified for a total of twenty study sites.

Cross-sectional surveys and substrate particle size data were collected between September and October 2023. One representative cross-section was surveyed at each site using a Benchmark Hemisphere 631 GPS with Real-Time Kinematic (RTK) and positioning engine. Representative cross-sections were chosen where riffle characteristics were dominant as they are considered stable/static at low flows and thus representative of bankfull conditions. Due to local in-channel effects such as obstructions and bank erosion, the top of bank at each cross-section was established visually as the breakpoint along the bank beyond which the bank slope remained relatively constant. Using the cross-section surveys, bankfull width (W_{bf}) and bankfull depth (h_{bf}) were measured.

To characterize the substrate particle size distribution at each site, a modified 100-particle Wolman pebble count was conducted along the established cross section for each site. Though this method involves multiple transects and a non-discriminate picking method, the method was modified for this research in the following ways:

a) Only one transect was surveyed, the same one where the cross-section data was collected with the GPS unit.
b) Pebble particles were hand selected to ensure that the full range of particle sizing was captured.
c) A size value of 0.1 cm was assigned to pebble particles measuring <0.5 cm

These changes were implemented based on the effectiveness displayed through personal industry experience of this method and an attempt to offer an alternative for practical field and research use. Though the traditional method was developed to be non-discriminate, knowledge gained through industry experience highlighted the potential opportunity for misrepresentation of the accurate quantity of certain particle sizes. However, the industry standard of measuring particles along the b-axis was still adhered to. In addition to these data collection methods, site photos were taken at each site facing upstream, downstream, the left bank (facing upstream), the right bank (facing upstream), and the bed (see *APPENDIX B)*.

3.2.3 Geomorphic Ratios

Using previous literature, three geomorphic ratios for quantifying morphologic adjustments were chosen: the width to depth ratio, the relative roughness, and the shear stress ratio (*Table 8*). *Wood-Smith & Buffington (1996)* used the active channel width (W_{ac}) (i.e., where a sharp change from unvegetated to vegetated banks occurs in the channel) for their calculations whereas this research utilized the bankfull channel width (W_{bf}) (i.e., channel width at bankfull discharge) (*USACE, 2013*) for ease of comparability with previous literature on urbanizing watersheds.

Table 8. Ratio equations and contributing parameters

Ratios	**Equation**
Width to depth ratio	W_{bf}/h_{bf}
Relative roughness	D_{50}/h_{bf}
Shear stress ratio	τ_{c50}/τ_{bf}

The ratio of the critical shear stress (τ_{c50}) to the bankfull shear stress (τ_{bf}) is of particular interest as it is a measure of the shear stress theoretically required to mobilize the observed D_{50} scaled by the total boundary shear stress at bankfull discharge (*Wood-Smith & Buffington, 1996*). This ratio is interpreted as a measure of bed surface mobility where a fixed discharge transport threshold is not assumed.

The τ_{bf} was calculated as:

$$\tau_{bf} = \rho g S h_{bf} \qquad \textit{(Equation 3)}$$

and the τ_{c50} was calculated as:

$$\tau_{c50} = \tau_c^*(\rho_s - \rho) g D_{50} \qquad \textit{(Equation 4)}$$

where ρ_s= the density of quartz (2650 kg/m^3) and τ_c^* = the dimensionless critical shear stress of gravel. As per *Wood-Smith & Buffington (1996)* a τ_c^* value of 0.05 was employed in this research. In addition to these three ratios, the entrenchment ratio was calculated by multiplying the bankfull depth (h_{bf}) by two and dividing that value by the bankfull width (W_{bf}) value.

3.2.4 Statistical Analysis

To investigate relationships between watershed characteristics and reach scale parameters, statistical analyses were performed. The aim of this component was to determine which parameters were most strongly correlated to one another and if these relationships were consistent between watersheds. Underlying assumptions were made for certain relationships based on previous literature.

The statistical analysis involved three parts. The first part involved separating the study sites into "rural" and "urban" based on their percent imperviousness. As previously outlined in *CHAPTER 2*, *Aquafor Beech Limited (2006)* found that even at 30% imperviousness cover significant changes began to occur. Based on this, 30% imperviousness was the threshold to divide reaches into "urban" and "rural" for this analysis. Boxplots were plotted and t-tests were employed to compare the distribution of values between the two groups of sites for the specific stream power, D_{50}, bankfull width (W_{bf}), bankfull depth (h_{bf}), slope, the entrenchment ratio, and the three geomorphic ratios (W_{bf}/h_{bf}, D_{50}/h_{bf}, τ_{c50}/τ_{bf}). As well, a control on drainage area was applied for specific stream power, D_{50}, bankfull width (W_{bf}), and bankfull depth (h_{bf}) with corresponding t-tests conducted and boxplots produced. The interpretation of the t-tests was as follows:

If the p-value <0.05, then they are statistically different at 95% confidence

If the p-value <0.1, then they are statistically different at 90% confidence

If the p-value >0.1, then they are not statistically different

The second part of the statistical analysis was a Pearson correlation coefficient analysis that investigated the correlation between the calculated channel and watershed parameters of percent imperviousness, drainage area, specific stream power, the entrenchment ratio, and the three geomorphic ratios. *Table 10* below provides the thresholds for such categorizations as well as a legend of colours to correspond to each degree of correlation that was used for the interpretation of the results.

Table 9. Pearson correlation coefficient strength indication chart (*Ratnasari et al., 2016*)

Correlation Coefficient Value (*r*)	**Direction and Strength of Correlation**	**Corresponding Colour**
-1	Perfectly negative	
-0.8	Strongly negative	
-0.5	Moderately negative	
-0.2	Weakly negative	
0	No association	
0.2	Weakly positive	
0.5	Moderately positive	
0.8	Strongly positive	
1	Perfectly positive	

Finally, the third statistical analysis component was a stepwise regression that attempted to determine the combination of watershed parameters (percent imperviousness, drainage area, and specific stream power) that best predicts the channel parameters (width to depth ratio, entrenchment ratio, relative roughness, and the shear stress ratio). The regression was completed through a specialized R code that provided the following test statistics: F-statistic, R^2, and p-value. The stepwise regression was performed in three directions: forward selection, backward elimination, and bidirectional elimination, to ensure the highest confidence in the results. A description of each is provided below (*Hayes, 2022*):

1. *Forward Selection:* begins with no variables in the model, tests each variable as it is added to the model, then keeps those that are deemed most statistically significant.
2. *Backward Elimination:* starts with a set of independent variables, deleting one at a time, then testing to see if the removed variable is statistically significant.
3. *Bidirectional Elimination:* a combination of the first two methods that test which variables should be included or excluded.

CHAPTER 4: Results and Discussion

4.1 Results

Table 10 below summarizes the results of the linework, fieldwork, and calculated SPIN-parameters, while detailed results are presented in Appendices *C – G*.

Table 10. Summary of site characteristics

Mimico Creek Watershed Parameters	**Site**				
	MCAI	*RAVP*	*MATC*	*EVAP-A*	*EVAP-B*
Watershed Characteristics					
Drainage area (km^2)	59.52	51.46	31.19	52.15	52.08
Imperviousness (%)	61	63	64	63	63
Flow Characteristics					
Discharge (m^3/s)	10.22	8.95	5.68	9.06	9.05
Specific stream power (W/m^2)	109.69	28.62	77.55	1.70	20.65
Reach Scale Parameters					
Sinuosity (1970s)	1.065	1.499	1.451	2.128	1.014
Sinuosity (2021)	1.038	1.530	1.419	2.169	1.004
D_{50} (mm)	28	25	25	38	40
Bankfull width (m)	15.85	14.73	10.18	13.12	21.61
Bankfull depth (m)	1.55	1.98	1.21	1.08	1.75
Slope	0.07216	0.04433	0.04142	0.02846	0.04225
Entrenchment ratio	0.20	0.27	0.24	0.16	0.16
Geomorphic Ratios					
Bankfull width to depth ratio (W_{bf}/h_{bf})	10.21	7.44	8.43	12.18	12.34
Relative roughness (D_{50}/h_{bf})	0.018	0.013	0.021	0.035	0.023
Shear stress ratio (τ_{c50}/τ_{bf})	0.02	0.02	0.04	0.10	0.04
Etobicoke Creek Watershed Parameters	**Site**				
	ECT-A	*GET-6*	*CENP*	*ECAB*	*GET-2*
Watershed Characteristics					
Drainage area (km^2)	164.74	67.98	67.92	65.62	4.73
Imperviousness (%)	41	18	18	17	44
Flow Characteristics					
Discharge (m^3/s)	25.81	11.53	11.52	11.17	1.02
Specific stream power (W/m^2)	205.01	91.92	114.32	12.36	43.14
Reach Scale Parameters					
Sinuosity (1970s)	1.321	1.611	1.086	1.010	1.854
Sinuosity (2021)	1.328	1.594	1.100	1.016	1.859
D_{50} (mm)	51	35	45	38	64
Bankfull width (m)	25.27	15.60	14.60	12.66	8.79
Bankfull depth (m)	2.54	1.46	1.54	1.01	1.96
Slope	0.06263	0.02491	0.04154	0.00357	0.00855
Entrenchment ratio	0.20	0.19	0.21	0.16	0.45

Geomorphic Ratios					
Bankfull width to depth ratio (W_{bf}/h_{bf})	9.95	10.69	9.46	12.50	4.48
Relative roughness (D_{50}/h_{bf})	0.020	0.024	0.029	0.038	0.033
Shear stress ratio (τ_{c50}/τ_{bf})	0.03	0.10	0.06	3.14	0.32
Highland Creek Watershed Parameters	**Site**				
	BDR-B	*BDR-A*	*BENP*	*MSPT*	*CDBP*
Watershed Characteristics					
Drainage area (km^2)	20.60	20.25	23.50	84.26	39.62
Imperviousness (%)	55	56	54	57	56
Flow Characteristics					
Discharge (m^3/s)	3.89	3.83	4.39	14.02	7.06
Specific stream power (W/m^2)	20.68	92.51	44.12	1.22	48.55
Reach Scale Parameters					
Sinuosity (1970s)	1.688	1.313	1.036	1.245	1.516
Sinuosity (2021)	1.672	1.353	1.080	1.191	1.396
D_{50} (mm)	26	70	25	41	55
Bankfull width (m)	13.04	11.83	12.91	26.94	14.26
Bankfull depth (m)	2.23	1.11	1.93	3.84	1.26
Slope	0.02763	0.01825	0.01576	0.01876	0.06525
Entrenchment ratio	0.34	0.19	0.30	0.29	0.18
Geomorphic Ratios					
Bankfull width to depth ratio (W_{bf}/h_{bf})	5.85	10.65	6.69	7.01	11.29
Relative roughness (D_{50}/h_{bf})	0.012	0.063	0.013	0.011	0.044
Shear stress ratio (τ_{c50}/τ_{bf})	0.03	0.28	0.07	0.05	0.06
Duffins Creek Watershed Parameters	**Site**				
	SHT-A	*SHT-B*	*SHT-E*	*SHT-D*	*RIVT*
Watershed Characteristics					
Drainage area (km^2)	112.91	113.81	129.13	127.86	130.46
Imperviousness (%)	5.1	5.1	4.7	4.7	4.8
Flow Characteristics					
Discharge (m^3/s)	18.30	18.43	20.68	20.49	20.87
Specific stream power (W/m^2)	173.30	134.09	241.82	204.00	110.63
Reach Scale Parameters					
Sinuosity (1970s)	1.560	1.156	1.362	1.287	1.102
Sinuosity (2021)	1.689	1.123	1.547	1.585	1.298
D_{50} (mm)	67	50	24	62	67
Bankfull width (m)	12.96	20.48	11.29	11.91	11.51
Bankfull depth (m)	0.43	3.48	1.87	2.18	0.89
Slope	0.01292	0.00706	0.00284	0.00567	0.00717
Entrenchment ratio	0.07	0.34	0.33	0.37	0.16

Geomorphic Ratios					
Bankfull width to depth ratio (W_{bf}/h_{bf})	29.99	5.89	6.04	5.46	12.89
Relative roughness (D_{50}/h_{bf})	0.155	0.014	0.013	0.028	0.075
Shear stress ratio (τ_{c50}/τ_{bf})	0.99	0.17	0.37	0.41	0.86

4.1.1 Watershed Characteristics

4.1.1.1 Drainage Area

The results from the study sites captured a range of drainage areas (*Table 10)*. On average, the sites in the Duffins Creek watershed displayed the highest drainage areas, ranging from 112.91 km^2 for SHT-A to 130.46 km^2 for RIVT. Conversely, the average drainage area for the sites in the Highland Creek watershed was the lowest, ranging from only 20.60 km^2 for BDR-B to 84.26 km^2 for MSPT. This is reflective of their positions within the watershed with BDR-B being the second most upstream while MSPT is the furthest downstream. Furthermore, when compared against the other watersheds, as Highland Creek has the second highest imperviousness of the four, this result is also to be expected.

4.1.1.2 Imperviousness

The calculated imperviousness values for all study sites ranged from 4.7% to 64%, confirming that a range of urbanization was captured (*Table 10*). The sites show that on a watershed level, Mimico Creek has the highest percent impervious cover, while Etobicoke Creek has the lowest. These values are relatively consistent with the site average imperviousness for the Mimico, Etobicoke, and Highland Creek watersheds, with only a <20% difference (*Table 11*). Duffins Creek however, experienced a very large discrepancy between the site average imperviousness and the watershed average of an order of 1.67. Most sites for the Duffins Creek watershed were surveyed in the upper parts of the watershed due to several logistical constraints (see *CHAPTER 4.2.2* for details on site selection), which has likely resulted in this discrepancy as they were not truly representative of the variation within the watershed. The location of the Duffins Creek sites also led to a small range of imperviousness values (4.71% to 5.07%) (*Table 10*) which, with a site-to-site standard deviation of only 0.002, represents the least variability between site values.

Table 11. Summary of imperviousness results

Watershed	**Site Average Imperviousness (%)**	**Site Standard Deviation**	**Watershed Average Imperviousness (%)**	**Site Average vs. Watershed Average Difference**
Mimico	63	0.011	63	0%
Etobicoke	27	0.136	33	20%
Highland	56	0.011	57	1.8%
Duffins	4.9	0.002	54	167%

4.1.2 Flow Characteristics

4.1.2.1 Discharge

The chosen study sites captured a range of 2-year discharges (*Table 10*). The Duffins Creek watershed sites exhibited the lowest variance, with values ranging between 18.30 m^3/s (site SHT-A) and 20.87 m^3/s (site RIVT), and an average standard deviation of 2-year discharge values of 8.7. The Etobicoke Creek watershed displayed the largest standard deviation between sites of 57.4, with a discharge for ECT-A of 25.81 m^3/s and only 1.02 m^3/s for GET-2. These results confirm that the Etobicoke Creek sites most closely follow the pattern of imperviousness.

4.1.2.2 Specific Stream Power

A range of specific stream power conditions were captured which is reflective of the range of discharge and imperviousness values (*Table 10*). Though each watershed displayed a large range of specific stream power values, the Etobicoke Creek watershed showed the highest standard deviation between sites, with individual values ranging from 2205.01 W/m^2 for ECT-A to 43.14 W/m^2 for GET-2. Conversely, the Highland Creek watershed displayed the lowest standard deviation of 34.3, with site values ranging from 92.51 W/m^2 for BDR-A to 1.22 W/m^2 for MSPT. As expected, the rivers with higher percent imperviousness also tend to display a higher specific stream power (for the same drainage area); a result the confirms the effect of urbanization on the flow regime.

Comparison of the specific stream power values between the sites categorized as “rural” (<30% imperviousness) and “urban” (>30% imperviousness) reveals that “rural” streams display both a higher mean and larger range in excess of 225 W/m^2, whereas the range for “urban” streams levels out between 100-150 W/m^2 (*Figure 5-A*). This significant difference is further underscored by its t-test p-value of 0.02352, rendering this parameter statistically different enough for inclusion at 95% confidence.

Unfortunately, directly comparing specific stream power values between the study sites is complicated by the control of site location on discharge; sites with larger drainage area have higher discharge values, and therefore higher specific stream power, which may obscure the effect of urbanization. To remove the effect of drainage area, specific stream power was divided by drainage area for each site and the boxplot of values plotted in *Figure 5-B*. The range of values for the “urban” sites is now displayed as being larger than that for the “rural” sites, confirming that specific stream power is higher in urban areas compared to rural areas when a control on drainage area is applied. Despite this finding however, the t-test p-value of 0.3453 revealed there is not a significant statistical difference.

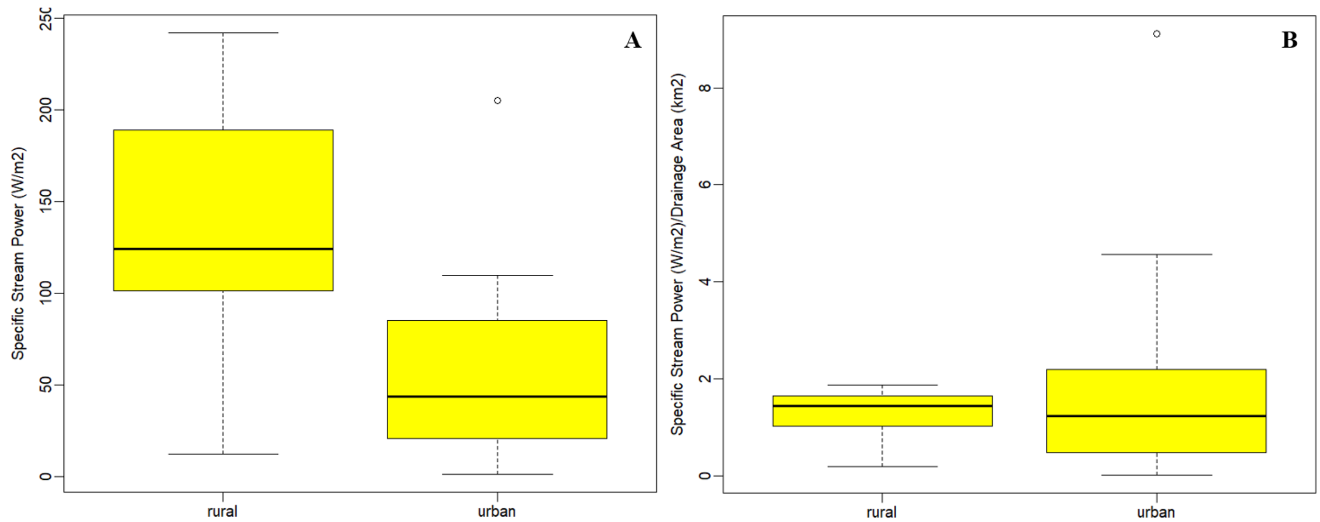

Figure 5. Boxplots of (A) specific stream power, (B) specific stream power/drainage area

4.1.3 Reach Scale Parameters

4.1.3.1 Sinuosity

A summary of the average calculated sinuosity index for each watershed is shown in *Table 12* and the sinuosity index of each study site is tabulated in *APPENDIX D*. The average sinuosity across all sites increased from historical values (1973/1977/1978) of 1.365 to 1.400 in 2021 for all watersheds despite 40% of individual sites decreasing in sinuosity. Between the two comparison years, Etobicoke Creek saw the smallest change in average sinuosity of 0.010, whereas Duffins Creek saw the largest change of 0.168. The linework analysis (*APPENDIX C*) visually supports these results as most thalweg paths look nearly identical, with those in Duffins Creek watershed displaying the largest difference of up to 0.298 for site SHT-D. By contrast, the sites in Etobicoke Creek watershed displayed the smallest changes, the lowest being 0.005 for site GET-2. These findings are further verified by the standard deviations for both the 1970s aerial imagery and 2021 imagery being very comparable, with the largest difference displayed in the Duffins Creek watershed of 0.051.

The patterns of sinuosity change in the study watersheds are congruent with earlier descriptions of most of the channels not experiencing much change between the comparison years. These minimal changes can likely be attributed to the major channel alterations (e.g., straightening) having taken place prior to the initial study year (1973/1977/1978). For instance, the shortening and elimination of any natural bend and bar development in the Etobicoke, Mimico, and Highland watersheds was mostly completed by the early 1970s, which is why the degree of sinuosity adjustment since then has been minimal. By comparison, the Duffins Creek watershed began urbanizing later and is still undergoing that process and is showing greater adjustments in sinuosity. These results support previous literature that sinuosity adjusts relatively quickly to urbanization.

Table 12. Summary of sinuosity index results

Watershed	Average Sinuosity (1970s)	Site Standard Deviation (1970s)	Average Sinuosity (2021)	Site Standard Deviation (2021)	Average Change in Sinuosity
Mimico	1.431	0.447	1.432	0.472	0.026
Etobicoke	1.376	0.355	1.379	0.350	0.010
Highland	1.360	0.251	1.338	0.225	-0.055
Duffins	1.293	0.181	1.448	0.232	0.168
Overall Average	***1.365***		***1.400***		***0.065***

Meandering is a fundamental characteristic of stable channels as by increasing the distance that water travels, the risk for bed and bank erosion is limited through the reduction in slope, lending to the easing of water velocity (*Minnesota DNR, 2006*). The results from the GTA study sites indicates that according to *Table 13* below, all four watersheds are considered "sinuous" overall, but none reach "meandering" state. Unfortunately, reaching such a state is no longer an option for most of the sites studied as they are confined by urban infrastructure such as residential neighbourhoods.

Table 13. Sinuosity ratio categorization (*Kusratmoko et al., 2019*)

Sinuosity Ratio	Channel Type
<1.1	Straight
1.1-1.5	Sinuous
>1.5	Meandering

4.1.3.2 Grain Size

The Duffins Creek watershed displays the largest average D_{50} (54 mm) (*Table 14*). As discussed in *CHAPTER 1*, urban streams tend to be coarser as urbanization-promoted sediment starvation (i.e., a decrease in sediment supply) combined with an increase in discharge and stream power leads to all the finer material washing out, leaving behind a coarser bed. However, despite this trend, the sediment observed in the Duffins Creek sites were on average larger than that in the more urbanized watersheds. This is likely due to the location of the study sites for Duffins Creek being located further upstream than those in the other watersheds, which is where coarser sediment is expected to be found, therefore skewing the comparison between watersheds with respect to average particle size.

Table 14. Summary of D_{50} results

Parameter	Watershed			
	Mimico	*Etobicoke*	*Highland*	*Duffins*
Average D_{50} (mm)	31	47	43	54

Based on the size classes laid out by *Wilzbach & Cummins (2018)* (*Table 15*), the average D_{50} for all watersheds falls within the category of "Large Pebble" except for the sites within the Mimico

Creek watershed which are finer and fall within the "Small Pebble" category. However, the range for each site defies these general characterizations. For instance, Mimico Creek sites ranged from 13.86 mm (EVAP-A) to 36.35 mm (EVAP-B), placing them between "Coarse Gravel" and "Large Pebble". The Etobicoke Creek sites ranged from 26.69 mm (ECAB) to 53.56 mm (GET-2), placing them between "Small Pebble" and "Large Pebble". The Highland Creek sites followed the same suite as Etobicoke Creek, with D_{50} particle sizes for sites ranging from 23.82 mm (BDR-B) to 52.78 mm (BDR-A), as well as the Duffins Creek sites with a range of 31.88 mm (SHT-E) to 60.11 mm (RIVT). This additional context speaks to the complexity of characterizing sites based on average values only as the level of variation within one reach alone can be high.

Table 15. Particle size categories based on the Wentworth grain size scale (*Wilzbach & Cummins, 2018*)

Size Category	**Particle Diameter (range in mm)**
Boulder	>256
Cobble	
Large	128-256
Small	64-128
Pebble	
Large	32-64
Small	16-32
Gravel	
Coarse	8-16
Medium	4-8
Fine	2-4
Sand	
Very Coarse	1-2
Coarse	0.5-1
Medium	0.25-0.5
Fine	0.125-0.25
Very Fine	0.063-0.125
Silt	<0.063

The difference between "rural" and "urban" sites with regards to the D_{50} is reflected in the plotted boxplots (*Figure 6-A*). Not much difference is indicated, with both "urban" and "rural" ranges beginning around 20 mm and ending around 70 mm. The most distinct difference is in their mean values, with that for "rural" between 45-50 mm and ~40 mm for "urban". Despite this, however, the t-test p-value for the relationship is not statistically different enough for inclusion at 0.2994. These findings are opposite to what previous literature suggests, as studies such as *Finkenbine et al. (2000)* and *Papangelakis et al. (2019)* report an increased coarseness in sediment in urbanized systems.

As position within the drainage area is key to the D_{50} results, a control was implemented to remove this data influence by dividing the D_{50} by the drainage area for the site as seen in *Figure 6-B*. The results from this are more consistent with previous literature as the range and average particle size of the D_{50} for the "urban" sites is larger than that of the "rural" sites. Despite these results however, the t-test p-value of 0.1717 revealed there is not a significant statistical difference. This may be due to the fact that rivers in Southern Ontario have highly variable sediment source material size even within the same watershed (*Phillips & Desloges, 2015*)

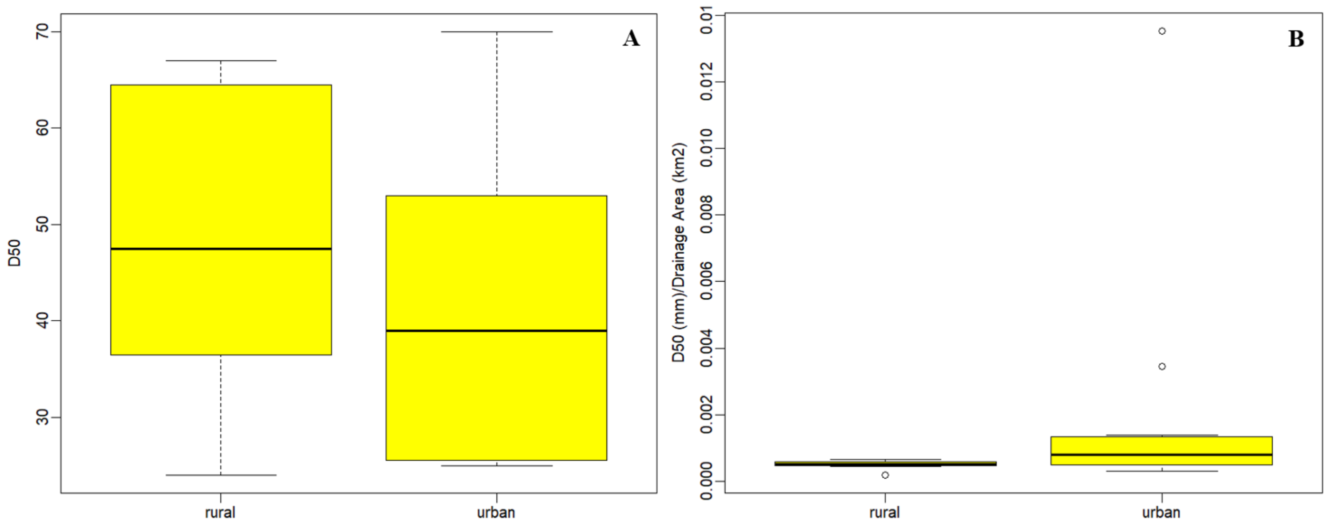

Figure 6. Boxplots of (A) D_{50}, (B) D_{50}/drainage area

4.1.3.3 Bankfull Dimensions

Despite having the largest drainage areas, the Duffins Creek watershed sites have the smallest average cross section width for both top of bank and bottom of bank (*Table 16*). By comparison, the average top of bank cross section width for Mimico, Etobicoke, and Highland Creek watersheds are all similar falling between 15.10 m and 15.80 m. As well, all four watersheds display only an 8 to 10% difference in bottom of bank width with Duffins Creek showing the smallest (8.47 m) and Highland Creek with the largest (11.22 m).

Table 16. Summary of average cross section width

Parameter	**Watershed**			
	Mimico	*Etobicoke*	*Highland*	*Duffins*
Average cross section width (m) – bottom of bank	10.32	9.50	11.22	8.47
Average cross section width (m) – top of bank	15.10	15.39	15.80	13.63

The difference between “rural” and “urban” sites with regards to the bankfull width are shown in the boxplots in *Figure 7-A*. Though the lower ranges are the same, around 1.0 m, the upper range for the “rural” sites ends lower, around 1.6 m, while that for “urban” sites extends to >2.0 m. Despite this, however, their mean values are comparable, with that for “rural” sites ~1.2 m and for “urban” sites ~1.4

m. These minimal differences are reflected in their accompanying t-test p-value of 0.3703, indicating such a difference is not significant enough for inclusion.

The comparison of bankfull widths does not account for the complicating effect of sites being located in different points within the watershed. To investigate whether the differences noted are due to degree of urbanization or the position along the channel, the bankfull width was divided by the site drainage area (*Figure 7-B)*. Previous literature supports that the bankfull width increases downstream as well as with urbanization due to the excess stream power. With the control on drainage area, the findings in *Figure 7-B* are more consistent with such findings and with a t-test p-value of 0.02174, there is a significant difference at 95% confidence.

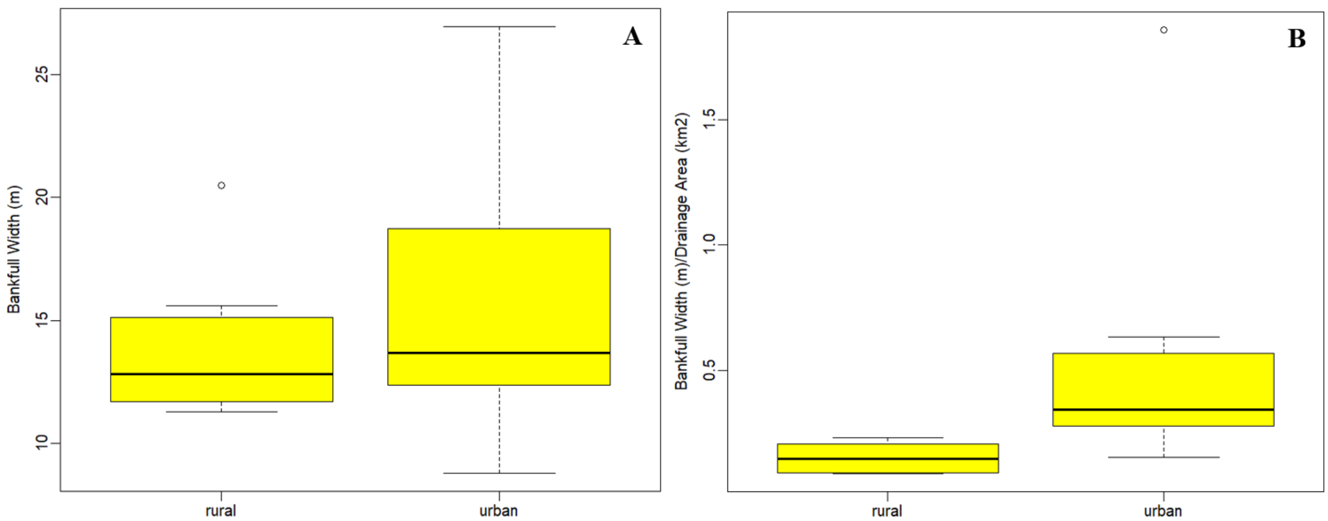

Figure 7. Boxplots of (A) bankfull width (W_{bf}), (B) bankfull width (W_{bf})/drainage area

The boxplots of the site bankfull depths (*Figure 8-A*) reveal that "rural" sites have a larger range (from 0.5 m to ~3.5 m) compared to the "urban" sites (from 1.0 m to ~2.5 m). However, the mean of the two groups is similar at 1.5-2.0 m. These differences are reflected in their t-test p-value of 0.5238, rendering the comparison not statistically different enough for inclusion.

As with bankfull width, bankfull depth is also influenced by degree of urbanization and position along the channel. To account for this, bankfull depth was also divided by drainage area as shown in *Figure 8-B*. Previous literature supports the idea that bankfull depth increases with position along the channel but also with degree of urbanization, which is consistent with the normalized values of the studied site (*Figure 8-B);* the "urban" sites' average and range are both larger than that for the "rural" sites. This difference is further underscored by its t-test p-value of 0.08893 which is statistically different at 90% confidence. These results therefore confirm the expected increase in channel dimensions with urbanization that is seen in previous literature.

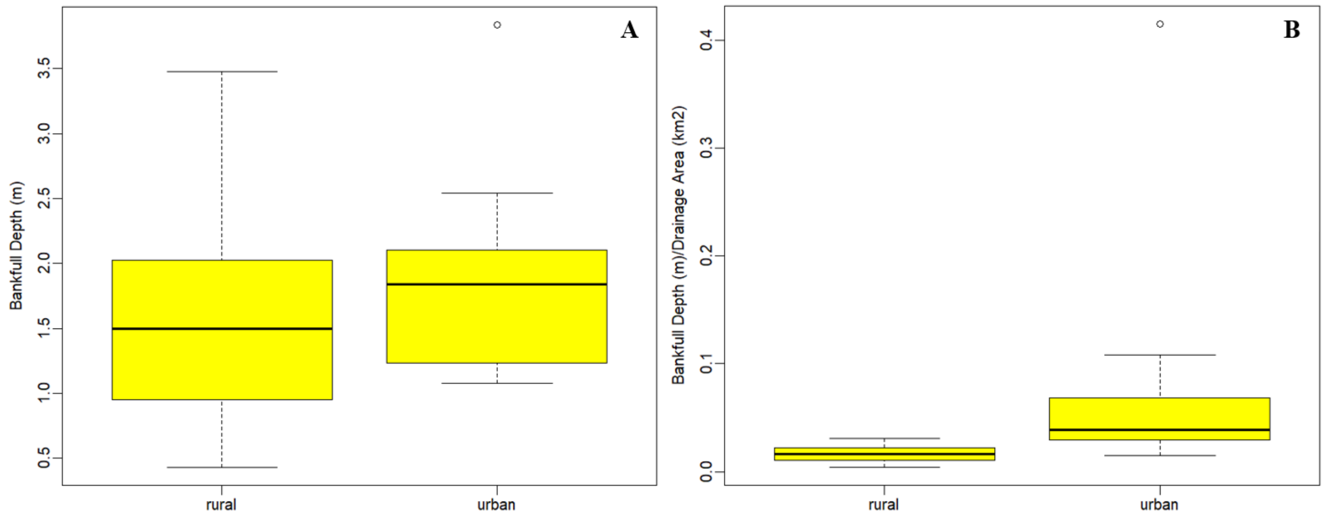

Figure 8. Boxplots of (A) bankfull depth (h_{bf}), (B) bankfull depth (h_{bf})/drainage area

4.1.3.4 Slope

The results for the slope calculations derived from the SPIN tool are displayed in *Table 17* below. What is evident is the watershed average slope is quite lower than its site average counterpart for Mimico, Etobicoke, and Highland Creek watersheds, but unsurprisingly, higher for Duffins Creek watershed. For instance, the Etobicoke Creek watershed site values ranged from 0.06263 for ECT-A to 0.00357 for ECAB, the largest site to site difference with a standard deviation of 0.024, and a site average versus watershed average difference by a factor of 1.3. Conversely, for the Duffins Creek watershed, slope values ranged from 0.01292 for SHT-A to 0.00284 for SHT-E, the lowest site to site difference with a standard deviation of only 0.004 as well as the smallest site average to watershed average difference of only 45%. Again, as with previous parameters discussed, this is likely due to its percentage of urbanization compared to the other watersheds, so consistency would be more probable between the two averages.

Table 17. Summary of slope results

Watershed	Site Average Slope	Site Standard Deviation	Watershed Average Slope	Site Average vs. Watershed Average Difference
Mimico	0.0457	0.016	0.0065	150%
Etobicoke	0.0282	0.024	0.0057	133%
Highland	0.0291	0.021	0.0092	104%
Duffins	0.0071	0.004	0.0112	45%

As seen in *Figure 9* below, the "rural" sites display both a lower mean and smaller range with values up to ~0.025. Comparatively, "urban" sites have a higher average and larger range, reaching values as high as 0.07. This significant difference is further underscored by a t-test p-value of 0.00629, deeming this parameter applicable, as there was found to be a statistical difference between "urban" and "rural" sites at 95% confidence. This trend of urban rivers displaying a steeper slope is consistent with previous literature describing it as an adjustment to higher stream power values. As well, anthropogenic influences such as urbanization result in the establishment of linear infrastructure (e.g., roads, sewers, etc.) that often leads to channels being artificially straightened to accommodate this.

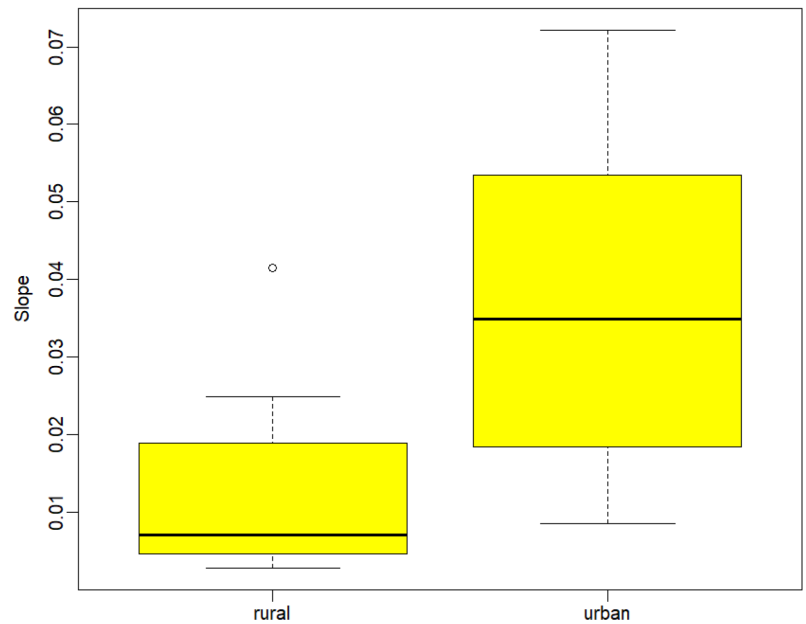

Figure 9. Slope boxplot

4.1.3.5 Entrenchment

The average entrenchment ratio amongst the sites for each watershed is presented in *Table 18*. Findings indicate that entrenchment values for all four watersheds are similar, which reflects the sites being chosen specifically to represent areas of the most minimal anthropogenic influence. On average, the Highland Creek watershed sites have experienced the most entrenchment, and while the Duffins Creek watershed sites were the least urbanized, they also had the least amount of erosion control. Furthermore, the Duffins Creek watershed sites experienced the largest site to site difference with a standard deviation of 0.132, while the values for the other four watersheds were more consistent, which could also be a contributing factor.

Table 18. Summary of entrenchment ratio results

Watershed	**Site Average Entrenchment**	**Site Standard Deviation**
Mimico	0.21	0.049
Etobicoke	0.24	0.118
Highland	0.26	0.071
Duffins	0.25	0.132

The difference between “rural” and “urban” streams with regards to entrenchment is reflected in their range of values (*Figure 10*). In contrast to the other geomorphic parameters investigated, the entrenchment ratios showed differences in both the upper and lower ranges of the two groups of sites, whereas the others had similar lower range cut offs. Specifically, the “rural” sites had a lower range of nearly 0.0, while “urban” sites had no values <0.15. As well, the upper range for the “rural” sites was <0.4, while several “urban” sites exceeded 0.4. Influences of urbanization such as property development along the stream banks tend to limit the entrenchment ratios of channels (due to the reduction in available flood plain width) (*Sen et al., 2008*). However, this effect leads to increased water depth, shear stress applied to the bed and toe bank, and runoff (*Sen et al., 2008*). These factors lead to increased instances and degrees of entrenchment, which can be seen in the high lower bound of values for the “urban” sites. Despite the observed differences in the range of values, the mean for each site type was very comparable, as reflected in the t-test p-value of 0.6714. The comparison of “urban” and “rural” sites indicates that entrenchment was not statistically different with enough confidence to be suitable for practical application.

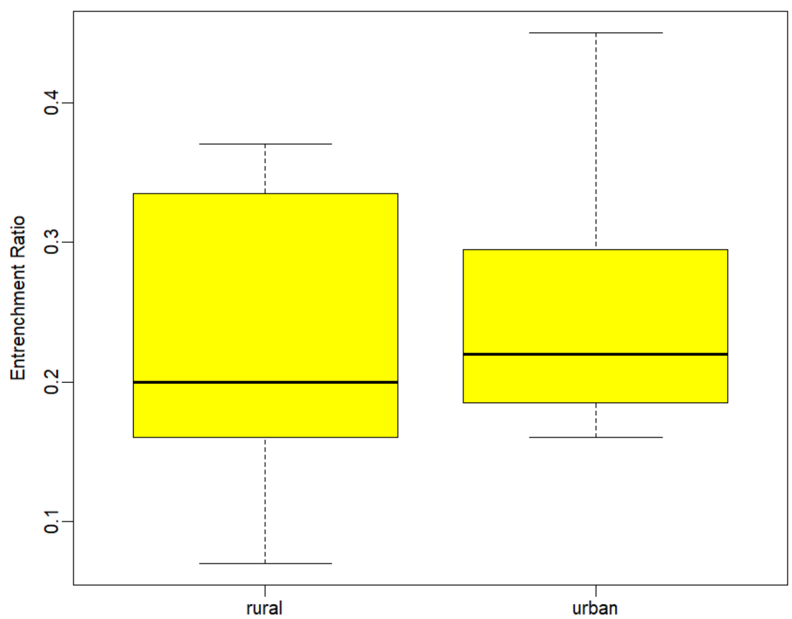

Figure 10. Entrenchment ratio boxplot

4.1.4 Geomorphic Ratios

As discussed in *CHAPTER 3.2.1* , the ratios for bankfull width (W_{bf}) to bankfull depth (h_{bf}), D_{50} to bankfull depth (h_{bf}), and critical shear stress (τ_{c50}) to bankfull shear stress (τ_{bf}) were calculated for each watershed. A summary of the results for the ratios are presented in *Table 19*.

Table 19. Summary of site average geomorphic ratio results

Watershed	**Bankfull width (W_{bf})/ Bankfull depth (h_{bf})**	**D_{50}/Bankfull depth (h_{bf})**	**Critical shear stress (τ_{c50})/ Bankfull shear stress (τ_{bf})**
Mimico	10.12	0.022	0.05
Etobicoke	9.42	0.029	0.73
Highland	8.30	0.028	0.10
Duffins	12.05	0.057	0.56

The difference between "rural" and "urban" sites with regards to the W_{bf}/h_{bf} ratio is reflected in their boxplots, particularly in the lower bound of values (*Figure 11*). The lowest values measured in the "rural" sites is ~5, whereas that of the "urban" sites is <5. Interestingly, however, the upper extent of values was nearly the same at ~13, save for one outlier among the "rural" sites that had an exceptionally high value of ~30. This similarity extends to the means of both stream types, as they are nearly the same as well. This minimal difference in the two is further reinforced by the t-test p-value of 0.3764.

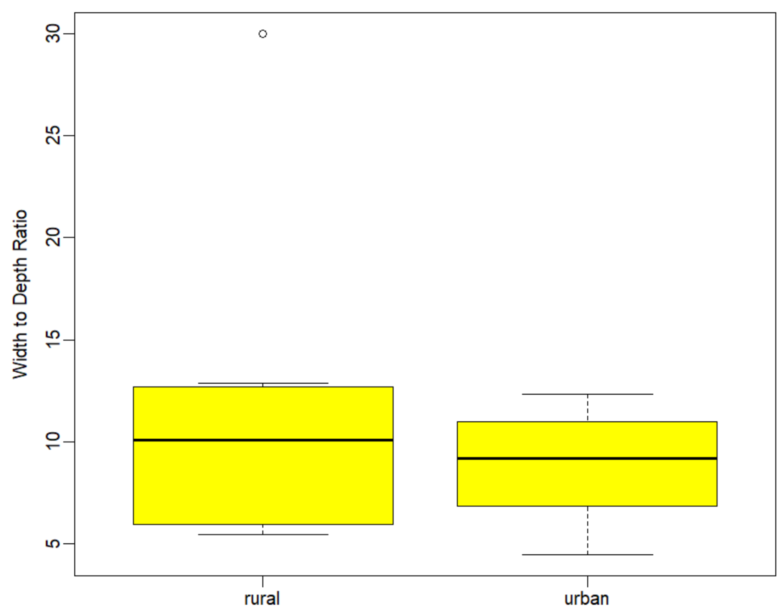

Figure 11. Width to depth (W_{bf}/h_{bf}) ratio boxplot

As seen in the boxplots of values (*Figure 12*), the difference between "rural" and "urban" sites with regards to the roughness ratio (D_{50}/h_{bf}) is reflected in their range discrepancies. Specifically, the "rural" sites have a larger range reaching values of up to 0.075, whereas the "urban" sites only reach values of up to around 0.05. Despite previous literature that notes an increase in roughness of urban streams through channelization and infrastructure such as road embankments (e.g., *Hung et al., 2018*), the roughness ratios of the sites measured in this thesis do not follow these trends. This is reflective of the comparative mean between the site types and the subsequent t-test p-value of 0.2424 not indicating a statistically significant difference.

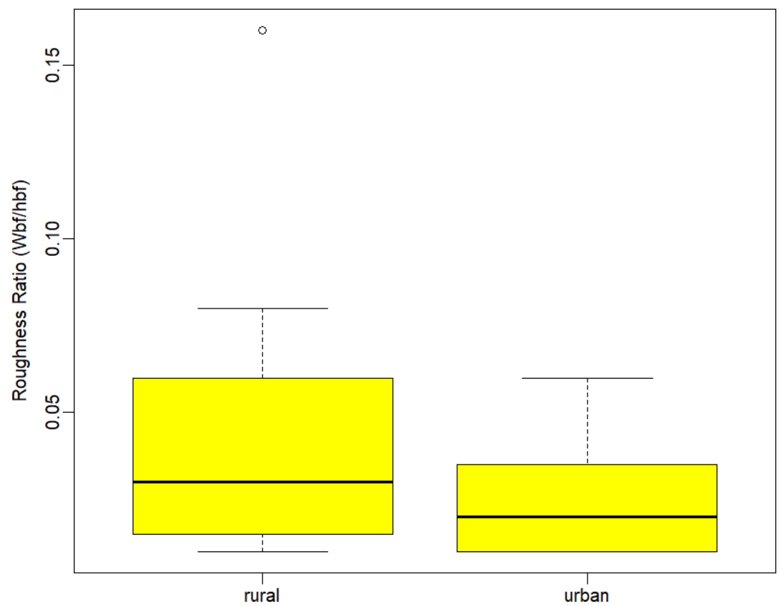

Figure 12. Roughness (D_{50}/h_{bf}) ratio boxplot

The "rural" and "urban" sites also show differences with regards to the distribution of shear stress (τ_{c50}/τ_{bf}) ratios, which is reflected in the boxplots in *Figure 13*. The "rural" sites display both a higher mean and larger range, with values up to 1.0, whereas the upper end of the range for the "urban" sites ends well below 0.5. This result was to be expected as previous literature supports that the potential for sediment transport increases with increasing urbanization/imperviousness (*Rohrer et al., 2004*). This is because a lower τ_{c50}/τ_{bf} ratio indicates that the bankfull width is close to the critical shear stress to mobilize sediment, especially in urban streams where bankfull occurs multiple times per year (*Padovan, 2016*). Interestingly, the t-test did not capture this significant difference, which further underscores the importance of a multi-component analysis of watersheds. However, the p-value it derived of 0.104 was right on the cut off threshold for 90% confidence and, as indicated previously, would likely be better understood with a larger sample size and further testing.

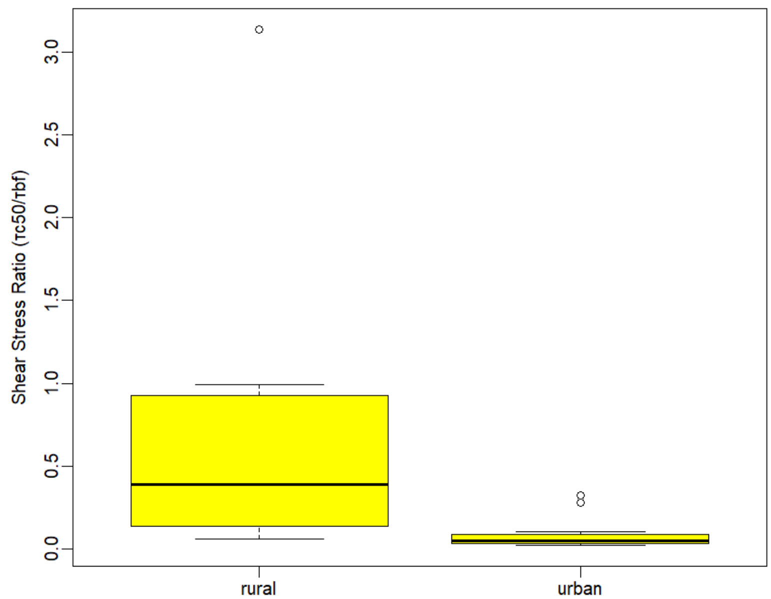

Figure 13. Shear stress (τ_{c50}/τ_{bf}) ratio boxplot

4.1.5 Statistical Analysis

4.1.5.1 Correlation Analysis

A Pearson correlation coefficient analysis was conducted to explore the relationship between the watershed parameters that were calculated by SPIN (i.e., percent imperviousness, drainage area, discharge, specific stream power) and the reach parameters (i.e., slope, entrenchment, and the three geomorphic ratios). The goal of the analysis was to determine which parameters are most strongly correlated in Southern Ontario watersheds with various levels of disturbance.

The strongest correlations amongst values measured in all four watersheds are the entrenchment to W_{bf}/h_{bf} and D_{50}/h_{bf} to W_{bf}/h_{bf} (*Table 20*). Of these, only entrenchment and W_{bf}/h_{bf} have a strong negative correlation, which indicates that with decreasing entrenchment there is an increasing W_{bf}/h_{bf} for the channel, a result that was to be expected. The D_{50}/h_{bf} to W_{bf}/h_{bf} ratio value is strongly positively correlated, indicating the opposite, that as one factor increases so does the other. This result has not been as commonly verified in previous literature but given the reliability of both ratio values of h_{bf}, their positive correlation is mathematically expected. The same can be said for the moderately negative correlation between D_{50}/h_{bf} and entrenchment. Finally, specific stream power is moderately positively correlated to drainage area, which was anticipated since a larger drainage area would yield higher discharges.

Table 20. Mimico Creek, Etobicoke Creek, Highland Creek, and Duffins Creek Pearson correlation coefficient comparison results

	Imp	***DA***	***SP***	***W/D***	***E***	***Rough***	***tau Ratio***
Imp	1.00						
DA	-0.67	1.00					
SP	-0.66	0.74	1.00				
W/D	-0.22	0.21	0.13	1.00			
E	-0.01	-0.15	0.05	-0.81	1.00		
Rough	-0.36	0.19	0.23	0.89	-0.58	1.00	
tau Ratio	-0.43	0.14	-0.06	0.34	-0.28	0.34	1.00

Imp = % Imperviousness, DA = Drainage Area, SP = Specific Stream Power, W/D = W_{bf}/h_{bf}, E = Entrenchment, Rough = D_{50}/h_{bf}, tau Ratio = τ_{c50}/τ_{bf}

The correlation analysis performed on each watershed separately revealed different results for each watershed. The strongest correlations amongst the sites in the Mimico Creek watershed are drainage area to percent imperviousness, entrenchment to W_{bf}/h_{bf}, and τ_{c50}/τ_{bf} to D_{50}/h_{bf} (*Table 21*). Of these, the drainage area to percent imperviousness and entrenchment to W_{bf}/h_{bf} correlations are strongly negative, indicating that as one parameter decreases, the other increases. Such findings were expected. Other findings that were anticipated were the negative association between specific stream power and percent imperviousness and specific stream power and drainage area. The values of τ_{c50}/τ_{bf} and D_{50}/h_{bf} have a strongly positive correlation, indicating that as one parameter increases so does the other. This finding is relatively new within literature, which provides the opportunity to enhance channel assessments by practitioners through replicating the methodology in this thesis to yield such parameters.

Table 21. Mimico Creek watershed Pearson correlation coefficient results

	Imp	***DA***	***SP***	***W/D***	***E***	***Rough***	***tau Ratio***
Imp	1.00						
DA	-0.83	1.00					
SP	-0.48	-0.08	1.00				
W/D	-0.19	0.40	-0.38	1.00			
E	0.22	-0.38	0.32	-1.00	1.00		
Rough	0.18	0.01	-0.49	0.76	-0.77	1.00	
tau Ratio	0.32	-0.05	-0.65	0.62	-0.62	0.96	1.00

Imp = % Imperviousness, DA = Drainage Area, SP = Specific Stream Power, W/D = W_{bf}/h_{bf}, E = Entrenchment, Rough = D_{50}/h_{bf}, tau Ratio = τ_{c50}/τ_{bf}

From *Table 22* below it can be inferred that the strongest correlations amongst the sites in the Etobicoke Creek watershed are between specific stream power and drainage area, entrenchment and W_{bf}/h_{bf}, and D_{50}/h_{bf} and specific stream power. Of these, specific stream power and drainage area are strongly positively correlated, while the entrenchment and W_{bf}/h_{bf} and D_{50}/h_{bf} are strongly negatively correlated.

Table 22. Etobicoke Creek watershed Pearson correlation coefficient results

	Imp	***DA***	***SP***	***W/D***	***E***	***Rough***	***tau Ratio***
Imp	1.00						
DA	0.09	1.00					
SP	0.33	0.83	1.00				
W/D	-0.73	0.52	0.06	1.00			
E	0.70	-0.63	-0.26	-0.97	1.00		
Rough	-0.28	-0.70	-0.91	-0.03	0.21	1.00	
tau Ratio	-0.40	-0.15	-0.66	0.51	-0.31	0.76	1.00

Imp = % Imperviousness, DA = Drainage Area, SP = Specific Stream Power,
W/D = W_{bf}/h_{bf}, E = Entrenchment, Rough = D_{50}/h_{bf}, tau Ratio = τ_{c50}/τ_{bf}

From *Table 23* below it can be inferred that the strongest correlations amongst the sites in the Highland Creek watershed are entrenchment and W_{bf}/h_{bf}, D_{50}/h_{bf} and specific stream power, D_{50}/h_{bf} and W_{bf}/h_{bf}, D_{50}/h_{bf} and entrenchment, τ_{c50}/τ_{bf} and specific stream power, and τ_{c50}/τ_{bf} and D_{50}/h_{bf}. Of these, D_{50}/h_{bf} and specific stream power, D_{50}/h_{bf} and W_{bf}/h_{bf}, τ_{c50}/τ_{bf} and specific stream power, and τ_{c50}/τ_{bf} and D_{50}/h_{bf} are all strongly positively correlated. Both, entrenchment and W_{bf}/h_{bf} and D_{50}/h_{bf} and entrenchment are strongly negatively correlated.

Table 23. Highland Creek watershed Pearson correlation coefficient results

	Imp	***DA***	***SP***	***W/D***	***E***	***Rough***	***tau Ratio***
Imp	1.00						
DA	0.74	1.00					
SP	-0.16	-0.65	1.00				
W/D	0.39	-0.11	0.70	1.00			
E	-0.40	0.07	-0.71	-0.99	1.00		
Rough	0.28	-0.35	0.89	0.91	-0.91	1.00	
tau Ratio	0.15	-0.37	0.87	0.55	-0.58	0.82	1.00

Imp = % Imperviousness, DA = Drainage Area, SP = Specific Stream Power,
W/D = W_{bf}/h_{bf}, E = Entrenchment, Rough = D_{50}/h_{bf}, tau Ratio = τ_{c50}/τ_{bf}

From *Table 24* below it can be inferred that the strongest correlations amongst the sites in the Duffins Creek watershed are drainage area and percent imperviousness, entrenchment and W_{bf}/h_{bf}, D_{50}/h_{bf} and W_{bf}/h_{bf}, D_{50}/h_{bf} and entrenchment, τ_{c50}/τ_{bf} and W_{bf}/h_{bf}, τ_{c50}/τ_{bf} and entrenchment, and τ_{c50}/τ_{bf} and D_{50}/h_{bf}. Of these, D_{50}/h_{bf} and W_{bf}/h_{bf}, τ_{c50}/τ_{bf} and W_{bf}/h_{bf}, and τ_{c50}/τ_{bf} and D_{50}/h_{bf} are strongly positively correlated. Conversely, the relationships of drainage area and percent imperviousness, entrenchment and W_{bf}/h_{bf}, D_{50}/h_{bf} and entrenchment, and τ_{c50}/τ_{bf} and entrenchment are all strongly negatively correlated.

Table 24. Duffins Creek watershed Pearson correlation coefficient results

	Imp	***DA***	***SP***	***W/D***	***E***	***Rough***	***tau Ratio***
Imp	1.00						
DA	-0.96	1.00					
SP	-0.48	0.25	1.00				
W/D	0.52	-0.51	0.19	1.00			
E	-0.41	0.30	0.41	-0.93	1.00		
Rough	0.45	-0.42	-0.26	0.99	-0.95	1.00	
tau Ratio	0.11	-0.03	-0.28	0.85	-0.94	0.91	1.00

Imp = % Imperviousness, DA = Drainage Area, SP = Specific Stream Power, W/D = W_{bf}/h_{bf}, E = Entrenchment, Rough = D_{50}/h_{bf}, tau Ratio = τ_{c50}/τ_{bf}

From analyses of *Table 20* through *Table 24*, it is noted that the correlation between entrenchment and W_{bf}/h_{bf} is the only one that is strongly correlated throughout all watersheds. This correlation was to be expected as previous literature (e.g., *Rosgen, 2001*) supports this. Another parameter that was consistently negatively correlated from weakly to strongly was τ_{c50}/τ_{bf} to entrenchment. This is a reasonable conclusion because as *Bowman (2019)* advises, "channelized flows attain greater flow depth and higher shear stress enabling more efficient sediment transport" and thus, an increase in entrenchment would be seen.

Though there was no parameter that was strongly positively correlated throughout all watersheds, the correlations between τ_{c50}/τ_{bf} and W_{bf}/h_{bf} and τ_{c50}/τ_{bf} and D_{50}/h_{bf} were consistently positive, ranging from weakly to strongly. The positive correlation between τ_{c50}/τ_{bf} and W_{bf}/h_{bf} is to be anticipated as *Phillips (2015)* found the same relationship. Furthermore, *Wang et al. (2023)* confirms through review of previous research that a positive relationship exists between shear stress and roughness, supporting this study's findings of the same. Overall, the result that the Duffins Creek watershed had the highest number of strongly correlated parameters is reflective of the geomorphic relationships expected in watersheds without human influence where rivers are able to adjust to their environment.

Furthermore, the correlation between τ_{c50}/τ_{bf} and drainage area is the weakest correlated, as the values for all tables were <0.20, with the value for Highland Creek being only exception of -0.37 (i.e., weakly negative). As well, the correlation of τ_{c50}/τ_{bf} and stream power is also weak, with only Mimico Creek and Highland Creek tables displaying values of -0.38 and 0.70, respectively, while the others were classified as "no association". This lack of correlation is an important result as it suggests that these parameters cannot be expected to have a significant relationship when measured for geomorphic assessments by future researchers and practitioners. For instance, the ratio of τ_{c50}/τ_{bf} indicates how prone sediment in a channel is to being transported (i.e., how close τ_{bf} is to inciting sediment movement) so with a higher drainage area (and consequently higher discharge) more particles would be expected to be in transit. However, the result that there is no correlation between τ_{c50}/τ_{bf} and drainage area advises the opposite: drainage area is not a reliable predictor of sediment mobility potential. What these results indicate is that there is no universal characterization that can be made for a watershed in

Southern Ontario based on one factor (e.g., percent imperviousness), which underscores the importance of a multi-factor analysis with regards to classification and management decisions.

4.1.5.2 Regression Analysis

The results from the stepwise regression analysis indicate that percent imperviousness, drainage area, nor specific stream power were able to reliably predict the W_{bf}/h_{bf} or entrenchment ratios as both tests returned a null hypothesis. However, percent imperviousness was able to predict D_{50}/h_{bf} using the following equation (*Equation 5*):

$$\frac{D_{50}}{h_{bf}} = -0.05I + 0.05 \quad \textit{(Equation 5)}$$

[R^2 = 0.1334, F = 2.772, p = 0.1132]

Unfortunately, this prediction yields a low R^2 and thus, is too weak to be useful for any practical purpose. Additionally, percent imperviousness and specific stream power together were able to predict τ_{c50}/τ_{bf} using the following equation (*Equation 6*):

$$\frac{\tau_{c50}}{\tau_{bf}} = -2.41I - 0.006\omega + 1.79 \quad \textit{(Equation 6)}$$

[R^2 = 0.3972, F = 5.6, p = 0.01354]

Though this prediction is also weak, it could be considered applicable as a first order estimate of what to expect when carrying out geomorphic assessments in urban watersheds. However, it is not strong enough of a relationship to be utilized for management or design purposes. Unfortunately, the lack of clear relationships between watershed and reach parameters in GTA streams and the lack of a set of useful predictor variables presents a challenge for watershed monitoring and management.

4.2 Discussion

4.2.1 Geomorphic Condition of GTA Rivers

Results from this work can be used to provide a snapshot of the current conditions in the study watersheds, as well as deduce trends in their responses to urbanization and their position within the channel evolution trajectory. Despite the constraints outlined in *CHAPTER 4.2.3.1*, trends in the measured parameters from previous literature were able to be compared and, in some cases, verified. For example, these results reveal that the study rivers are adjusting rapidly as differences in dimensions between "urban" and "rural" sites confirm channel enlargement is occurring when the data is normalized for drainage area. As well, sinuosity has shown to adjust rapidly, and increased stream power and coarsening has been observed.

The results from the t-tests between sites of ≤30% imperviousness ("rural") and >30% imperviousness ("urban") revealed that when a control is placed on drainage area, specific stream power is higher, the is D_{50} larger, bankfull width is wider, and bankfull depth is deeper in "urban" areas. As well, slope was found to be steeper in "urban" streams with a statistical difference at 95% confidence. Unfortunately, the other parameters of W_{bf}/h_{bf}, entrenchment, and D_{50}/h_{bf} ratios were not statistically different with enough confidence to consistently distinguish between "urban" and "rural" sites. The comparison for the τ_{c50}/τ_{bf} ratio was found to be on the cut off for applicability and it is believed that with a larger sample size and/or more testing, a definitive level of applicability would be able to be determined.

Duffins Creek watershed boasts the largest W_{bf}/h_{bf} ratio and D_{50} to h_{bf} ratio along with the second largest shear stress ratio. This signifies that the sites in the Duffins Creek watershed are not constrained in their enlargement within the floodplain and are shallow and wide, indicating they are in stage 3 of the CEM (see *Figure 14*). They also display higher average specific stream power values despite having the highest W_{bf}/h_{bf} ratio because they have a high average discharge of 19.75 m^3/s compared to the other watersheds that reach a maximum of 12.21 m^3/s. It is noted from such comparisons that the stream power order is following the discharge order, which can be seen in the sites for the Highland Creek watershed displaying the smallest specific stream power, discharge, and W_{bf}/h_{bf} ratio. This is to be expected as a lower specific stream power means the stream has less energy to erode.

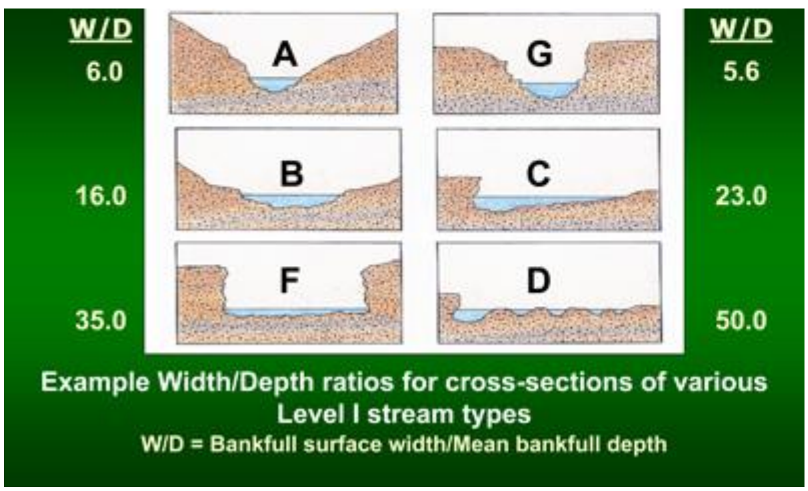

Figure 14. Examples of how different width (W_{bf}) to depth (h_{bf}) ratios present (*U.S. EPA, n.d.*)

Research from *Phillips & Desloges (2014)* indicates that based on stream power classifications, both Mimico Creek and Highland Creek watershed sites can be classified as M-type (20-50 W/m^2), corresponding to "gravel-dominated floodplains with mixed alluvial grain-size distributions". The Etobicoke Creek watershed sites can be classified as B-type (50-100 W/m^2), characterized by "cobble-bed channels with bimodal alluvial grain-size distributions". Finally, based on the results from *Papangelakis et al. (2022[a])*, the Duffins Creek watershed sites can be characterized as H-type, as their specific stream power exceeds 100 W/m^2. *Phillips & Desloges (2015)* further delineated bed substrate size ranges for each stream classification type corresponding to values from *Wilzbach & Cummins (2018)* (*Table 15*). Such classifications are cobble (~64-128 mm) for B-type, silt-clay (<0.063 mm) for C-type, sand-gravel (~0.25-8 mm) for M-type, and sand (0.063-2 mm) for S-type. When compared with the D_{50} for the watersheds studied in this thesis, it is noted that the measured sediment for Mimico and Highland Creek is larger than the range identified by *Phillips & Desloges (2015)* of ~68-80% for Mimico Creek sites and ~77-89% for Highland Creek when compared to the upper limit of 16 mm. Since the *Phillips & Desloges (2015)* framework was designed for rural streams and the Mimico Creek and Highland Creek watersheds are both very urbanized, this result indicates that these streams are coarsening in response; a conclusion that is in line with previous literature on the effects of urbanization on substrate characteristics. The opposite trend is observed for Etobicoke Creek however, with the largest site D_{50} (i.e., for GET-2) only reaching the bottom limit of the range of 64 mm. As the category of H-type was developed separately by *Papangelakis et al. (2022[a])* with no sediment size range, there is no comparison that can be made at this time for the Duffins Creek watershed sediment.

According to the Rosgen river classification key (*Figure 15*) using values calculated previously, the Mimico, Etobicoke, and Highland Creek sites most closely fit the “G” stream type (though slope values for Mimico Creek are consistent with stream type “A”) and Duffins Creek sites are type “F”. However, streams sometimes do not fit entirely into one category as they are constantly adjusting and even transitioning to other stream types. The type of analysis conducted for these watersheds was level II, which recognizes a continuum of river morphology that applies to cases such as that in Mimico Creek where values outside the typical range are present but do not warrant their own stream type (*Rosgen, 1994*). This is due to the understanding that general patterns of a stream don’t change with a minor value change such as that for slope in the case of Mimico Creek. Furthermore, the Rosgen river classification key is intended for “natural” rivers which none of the rivers studied can be classified as. Though the Duffins Creek watershed sites studied are predominantly “natural”, it is still worth considering the watershed overall is not.

Review of the classification based on specific stream power described in *CHAPTER 4.1* in addition to the particle size analysis can provide further context for the Rosgen classification. Though the particle size analysis did not yield the same results as the specific stream power classification of “gravel-bed dominated” or “cobble-bed dominated”, it is likely these classifications are more accurate as the particle size analysis completed was based only on a 100-particle modified Wolman pebble count, whereas the specific stream power method was much more robust.

Based on previous literature from *Ashmore et al. (2023)*, the classification of “G” for the Highland Creek watershed is consistent for certain branches. For instance, in *Ashmore et al. (2023)*, the authors noted a maximum slope of 0.0079 (Main Branch) to 0.016 (East Branch), which would be consistent with the “G” classification at the lower end but “C” on the larger end of the classification ranges. However, for Etobicoke Creek, values from *Cyples & Wojda (2020)* of 3.9 for entrenchment and 7.8 for the width/depth ratio, indicate a classification of “E”. Mimico Creek’s width/depth ratio ranges from ~4.4 to 7, indicating it could be classified as an “A”, “G”, or “E” type stream according to *Talpur & Bishop (2022)*. Finally, the classification of “F” for Duffins Creek follows a similar trend to that for Highland Creek in that some areas, an “F” classification may be appropriate but in others it may not as the width/depth ratio alone as per previous literature from the *City of Pickering (2008)* displays a range of ~7 to ~19. These conflicting results further underscore the complexity of watershed assessment and the need for frequent monitoring, particularly in urban watersheds where anthropogenic activities influence channel dimensions and substrate.

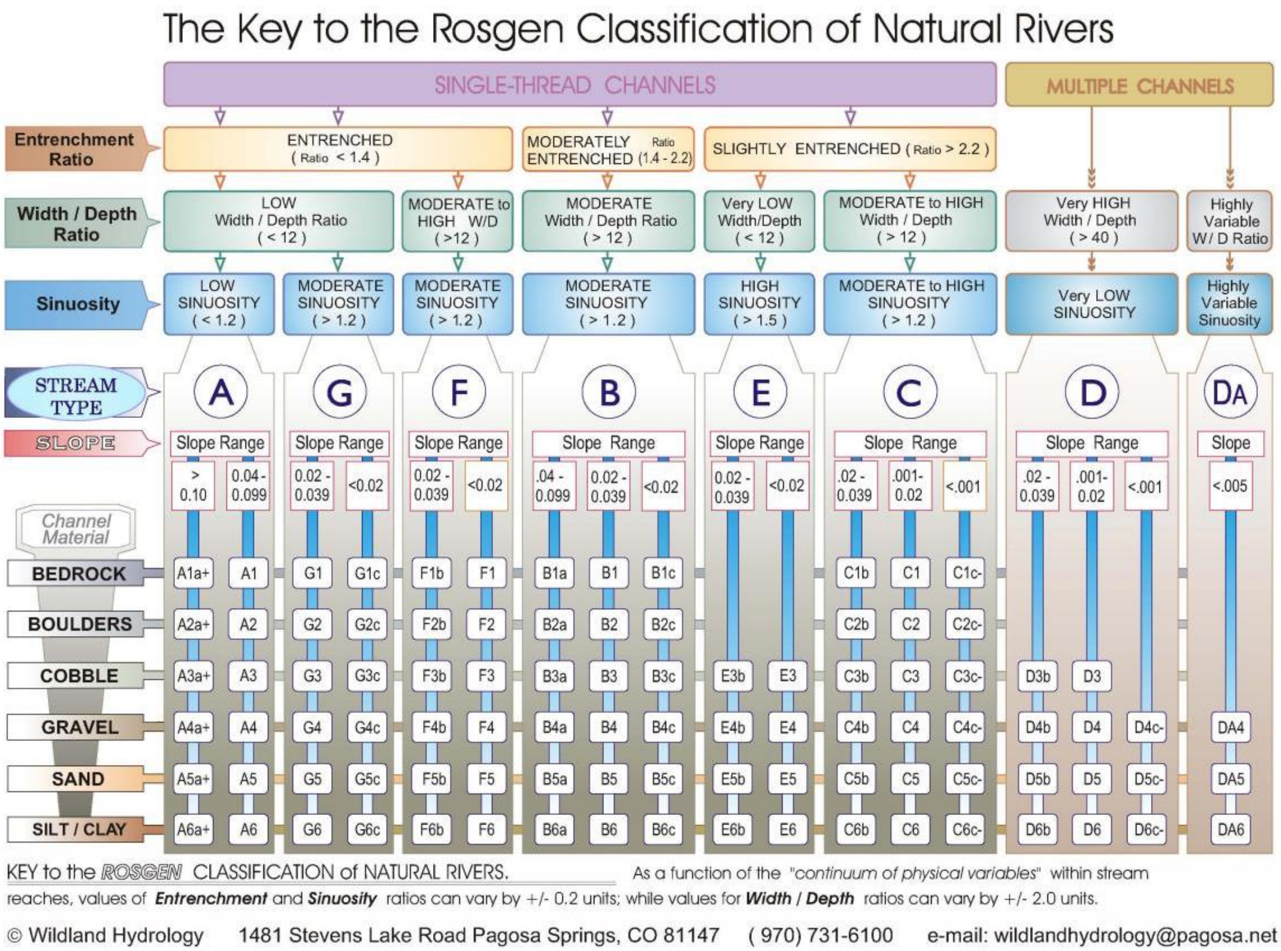

Figure 15. Rosgen river classification key (*NRCS, 2007*)

4.2.2 Management Implications

Results of the statistical analyses have some important implications for urban river management. The Pearson correlation coefficient test found a strongly negative correlation between entrenchment and the W_{bf}/h_{bf} ratio and a consistently positive (though varying in strength) correlation between the τ_{c50}/τ_{bf} ratio and both the W_{bf}/h_{bf} and D_{50}/h_{bf} ratios, all findings of which were consistent with previous literature. Additionally, the parameters which seemingly do not yield the expected correlation have important management implications. For instance, the lack of correlation between τ_{c50}/τ_{bf} and drainage area advises that these parameters are not anticipated to display a significant relationship. Since the ratio of τ_{c50}/τ_{bf} indicates how prone sediment in a channel is to being transported (i.e., how close τ_{bf} is to inciting sediment movement) more particles would be expected to be in transit with a higher drainage area (and subsequently higher discharge). The relationship of τ_{c50}/τ_{bf} to drainage area displaying a low association, however, advises the opposite: drainage area is not a reliable predictor of sediment mobility potential. Finally, the stepwise regression revealed that though weak, percent imperviousness and specific stream power were able to predict the τ_{c50}/τ_{bf} ratio. Overall, it is believed that such statistical parameters could be considered applicable as a first order estimate of further tests but unfortunately are not strong enough correlations to be utilized for design purposes. Taken together, the lack of consistently significant correlations between the watershed and reach parameters suggests that there is no universal geomorphic response to urbanization in the studied watersheds.

Though some parameters can be utilized across different watersheds as consistent indicators of geomorphic adjustment (specific stream power, D_{50}, normalized bankfull width and bankfull depth, and slope) others can not (W_{bf}/h_{bf}, entrenchment, and D_{50}/h_{bf} ratios). However, there does not appear to be a reliable set of indicator variables to predict geomorphic adjustments in the studied urban streams. This finding is in contrast to the case of watershed logging disturbances by *Wood-Smith & Buffington (1996)*, who found strong relationships between the parameters measured. In their study, the streams were located in areas without restrictions to geomorphic adjustments that are common in urban areas (e.g. infrastructure restraints or erosion control). The results from the GTA highlight the complexity of urban river responses and the role of human activities in restricting and altering the natural geomorphic response of rivers (*Ashmore, 2015*), as well as the need for watershed-specific approaches to monitoring and management.

Echoing *Hawley et al. (2013)*, this study demonstrates the importance of improving our understanding of the magnitude and rate of channel response in relation to the altered flow regime associated with urbanization. This understanding is crucial for stormwater management and stream restoration to inform the discovery of more suitable, cost-effective approaches which protect local infrastructure while also complying with anticipated water quality regulations. With regards to urban stormwater management, *Hawley et al. (2013)* found that such systems can effectively mitigate urbanization implications on streamflow and sediment regimes if they prioritize storage, infiltration, and evapotranspiration. As well, if implemented in tandem with streambed and bank stabilization measures designed to control large storm event peak flows, such an approach would prove to be the most beneficial.

As *Padovan (2016)* found, hybrid approaches to stream restoration tend to be used in urban settings as they consider environmental constraints that traditional methods do not leading to the integration of both naturalized and “harder” engineering elements. As outlined in *Schiff et al. (2007)*, such approaches use a semi-natural form design technique in conjunction with a partially constrained planform to limit channel migration, resulting in the elimination of channel evolution. *Houshmand et al. (2014)* demonstrated a reduction in maintenance costs and improvement of stream condition in systems by redirecting coarse-grained sediments currently being collected in stormwater control measures such as basins and wetlands back into the stream. Sediment replenishment downstream of dams has been trialed with promising results (*Zeug et al., 2013*) but *Ock et al. (2013)* found it important that the method of replenishment be tailored to the post-disturbance flow regime, especially in highly modified post-urban regimes.

To develop more innovative urban river management methods, improvements need to be made to how geomorphic monitoring is conducted. Current short-term monitoring practices rarely capture the full extend of the adjustment process as such changes could take decades to reveal themselves (*Padovan, 2016; Papangelakis et al., 2023*). Proposed improvements include standardizing the way in which studies on sediment yields are conducted as *Hawley et al. (2013)* found it would improve our understanding of a "common" response of sediment yields to urbanization. Some examples they provided included the addition of details regarding land cover, land use, and background factors such as slope, rainfall, and natural vegetation cover. As well, *Booth & Jackson (1997)* demonstrated that establishing a critical discharge for bed material mobility has the potential to lead to practical means of stormwater management in gravel/cobble streams. Such practical outputs include standard discharge duration ranges which exceed the critical discharge.

Furthermore, to enhance the current monitoring methods, implementation of GIS-based technologies such as the SPIN tool used in this study could provide beneficial initial assessments to aid in determining sensitive areas of the watershed to inform where best to allocate monitoring resources. As the toolbox requires minimal data inputs and required inputs such as DEMs and land-use maps are often readily available, it offers the opportunity for additional context particularly in data-scarce scenarios (*Papangelakis et al., 2022*[a]). Furthermore, it offers the capability of calculating erosion risk indices on a watershed level for past, present, and future land-use scenarios, so on the other end of the research it also could prove useful (*Papangelakis et al., 2022*[a]). Another useful method would be that outlined in *Bertalan et al. (2019)* which utilizes aerial imagery, topographical maps, and orthophotographs to classify reaches of a watershed into four degrees of modification (natural, slightly modified, modified, and intensely modified). As well, utilization of Google Earth Engine (GEE) as it offers open access to official Landsat imagery and a toolbox of options specifically designed for fluvial geomorphology such as those for analyzing wetted river channel planform, morphodynamics, and suspended sediment concentrations (*Boothroyd et al., 2020*).

4.2.3 Limitations and Future Research Recommendations

4.2.3.1 Limitations

The most significant limitation of this study was the urban conditions for which the study sites resided. Circumstances such as altered accessibility (e.g., emergent construction) and seasonal time constraints (e.g., unsafe water velocity) led to only five sites being surveyed per watershed. As only twenty sites were surveyed for all four watersheds and a limited selection of geomorphic parameters and ratios were analyzed, inferences of the overall watershed condition are limited and may not be truly reflective. Additionally, a complicating factor in the comparison of sites was that although the sites chosen themselves were free of anthropogenic structures (e.g., retaining features, bridges), in many cases such structures were located directly upstream and downstream of the sites, which may influence geomorphic responses of the studied sites. Further research is strongly recommended for confirmation as additional data points would allow for more robust results of the statistical analyses.

Another limitation was the availability of historical aerial imagery. Since the City of Toronto Geospatial Competency Centre did not have consistent historical aerial imagery of all the study sites, some site analyses had to be supplemented with individual aerial imagery photographs obtained through the City of Toronto Archives. Additionally, since the City of Toronto Geospatial Centre did not have consistent recent (i.e., within the last 5 years) aerial imagery, the 2021 aerial imagery for the affected sites had to be obtained through the City of Brampton and the Regional Municipality of Durham. This introduced some inconsistencies in the methodology of the linework as imagery quality varied.

With regards to the statistical analysis portion of the analysis, the use of a stepwise regression and correlation analysis were limiting in their capabilities compared to more advanced analyses. As well, the parameters for the classification of "rural" and "urban" sites could have had unintended influence on the results. Finally, should future researchers be interested in employing a higher resolution DEM such as that from LiDAR surveys in the SPIN tool to capture local changes to the bed slope, this may pose an issue as this tool uses the same slope values for all scenarios. This was not a limitation for this thesis however, as *Papangelakis et al. (2022[a])* found that "even a relatively coarse DEM was sufficient for calculating stream power indices at the watershed scale."

4.2.3.2 Future Research Recommendations

There are many opportunities to expand the scope of this work. For a more rigorous approach, additional statistical tests could be conducted to tease out more subtle relationships between parameters. As well, a more comprehensive in-field component could be considered that includes additional geomorphic parameters that are commonly measured in urban watersheds. For example, additional parameters included in Rapid Geomorphic Assessments (RGAs) and/or Rapid Stream Assessment Techniques (RSATs) can provide supplementary information regarding channel stability, in-stream habitat, water quality, and riparian conditions. Such assessments would also provide insights into stresses and adjustments of the watercourse at that time with regards to both sediment transport and flow regime (*Padovan, 2016*). Furthermore, as was done in *Papangelakis et al. (2022[a])*, the results from the SPIN tool could be overlayed onto a provincial geology map to better understand the control of the underlying geology on urban river responses.

As far as expanding the scope, though flow discharge has been extensively researched for Southern Ontario, adding a component where that is also measured and analyzed against the more sediment-focused parameters would add additional context for the watershed conditions. As well, echoing the suggestion of *Padovan (2016)*, analyzing other restoration performance variables such as individual riffle/cascade transport and unit-scale aggradation and degradation rates may prove beneficial in furthering our understanding of restoration performance. Furthermore, looking at fractional transport rates may also be an interesting component to consider, as they are "the product of spatial grain entrainment, displacement length, and displacement frequency" (*Wilcock & McArdell, 1997*). Therefore, they could add additional context to the sediment transport aspect of each watershed characterization.

Additionally, developing regional curves for the areas in this thesis would be a valuable research addition as, according to *Chandler & Amirault (2018)*, they have the potential to indicate appropriate bankfull dimensions for impaired watercourses with unreliable bankfull features. This would have particular application for stream designers and design reviewers in reviewing drainage area against width, depth, and cross-sectional area. With respect to the portion of the statistical analysis conducted in R Studio, additional parameters could be added such as D_{50} and measured width and depth as previous literature supports a theory of coarseness (e.g., *Papangelakis et al., 2022[a]*) which the addition of these parameters could assist in describing for the intended study sites.

Finally, this research framework could be scaled up to be utilized on a provincial basis instead of such a localized context to provide an even wider range of applicability for its results.

CHAPTER 5: Conclusions

Due to resource constraints, the effects of urbanization on the specifics of adjustment pathways and timelines of change of river systems for all urbanizing watersheds are not well understood as appropriate field parameters for representing such changes require years of consistent data for an accurate comparison. Most of the previous literature related to fluvial geomorphology in urban watersheds has focused on individual river systems (e.g., *Ashmore et al., 2023*), which left the question of whether results were universal among watersheds with varying degrees of urbanization and in different stages in their evolutionary trajectory an open problem. Due to their heterogeneous land use, consistent and predictable responses are difficult to identify, complicating the establishment of representative sites. The prediction of the effects of urbanization on river systems therefore remains challenging, a difficulty this study aimed to remedy through the expansion of approaches conducted by *Wood-Smith & Buffington (1996)* for watersheds impacted by logging.

The aim of this research was to better understand the trajectories of fluvial responses to urbanization in the GTA, and to assess whether universal parameters that could act as indicators of fluvial disturbance across watersheds could be identified. To achieve this, three objectives were set:

1. Provide a baseline historical geomorphic analysis of urbanizing watersheds in the GTA
2. Present a current geomorphic condition snapshot of watersheds to assess fluvial responses to urbanization in the GTA
3. Identify the most sensitive geomorphic indicators of urbanization that can be used as predictive tools to guide watershed monitoring and management priorities

The objectives were met through a literature review, aerial imagery analysis, field analysis, and statistical analysis, culminating in an outline of the management implications of the results.

Results were able to confirm channel enlargement, coarsening, and steepening is occurring in the study watersheds, as there was a statistically reliable difference between "urban" and "rural" sites. Through the ~50-year comparative aerial imagery analysis, sinuosity was found to have increased from the initial comparison year (1973, 1977, or 1978) to 2021, directly contradicting the pre-study prediction based on previous literature such as *Chin (2006)*. Of course, significant alterations have been made to the waterways in lieu of complete removal such as artificial hardening. This is evident in photographs obtained through the field analysis conducted in 2023 as well as the aftereffects of such activities such as relatively large bankfull width and shallow depth measurements.

The results from the t-tests between sites of ≤30% imperviousness ("rural") and >30% imperviousness ("urban") revealed that when a control is placed on drainage area, specific stream power is higher, the is D_{50} larger, bankfull width is wider, and bankfull depth is deeper in "urban" areas. As well, slope was found to be steeper in "urban" streams, displaying a p-value of 0.00629, supporting a statistical difference between "urban" and "rural" streams at 95% confidence. Unfortunately, the other parameters of W_{bf}/h_{bf}, entrenchment, and D_{50}/h_{bf} ratios were not statistically different with enough confidence to be applicable. The comparison for the τ_{c50}/τ_{bf} ratio was found to be on the cut off for applicability and it is believed that with a larger sample size and/or more testing, a definitive level of applicability would be able to be determined.

The results from this work advise that some parameters can be utilized across different watersheds as consistent indicators of geomorphic adjustment (specific stream power, D_{50}, normalized bankfull width and bankfull depth, and slope) while others can not (W_{bf}/h_{bf}, entrenchment, and D_{50}/h_{bf} ratios). Unfortunately, the attempt to identify robust watershed and flow parameters that can predict these geomorphic responses did produce any statistically reliable relationships across the studied watersheds. The lack of consistent correlations and a reliable relationship between the watershed and reach parameters suggests that there is no universal geomorphic response to urbanization in the studied watersheds.

The overarching goal of this research was that it may be utilized for education and decision-making purposes on a municipal and provincial level with respect to watershed management and development. This research has demonstrated that each watershed responds to urbanization differently, which makes comparing between them utilizing the same metrics challenging. Though the tools and methods used in this study prove the potential for such applications to refine future monitoring and management efforts, it is strongly recommended that a comprehensive assessment still be conducted comprising of historically significant measures as rivers do not fit into a standard set of parameters for classification. With future research and documented practical applications, the applied methods such as the SPIN tool and the refined Pearson correlation analysis and stepwise regression in this study will further prove their suitability for broad applications.

REFERENCES

Afzalimehr, H., Singh, V. P., & Abdolhosseini, M. (2009). Effect of nonuniformity of flow on hydraulic geometry relations. *Journal of Hydrologic Engineering, 14*(9). https://doi.org/10.1061/(ASCE)HE.1943-5584.0000095

Annable, W. K., Watson, C. C., & Thompson, P. J. (2012). Quasi-Equilibrium Conditions of Urban Gravel-Bed Stream Channels in Southern Ontario, Canada. *River Research and Applications*, *28*, 302-325. https://doi.org/10.1002/rra.1457

Aquafor Beech Limited. (2006). *Stormwater management and watercourse impacts: the need for a water balance approach*. Sustainable Technologies Evaluation Program.

Arnold Jr, C. L., & Gibbons, C. J. (1996). Impervious surface coverage: the emergence of a key environmental indicator. *Journal of the American Planning Association, 62*(2), 243-258. https://doi.org/10.1080/01944369608975688

Ashmore, P. (2015). Towards a sociogeomorphology of rivers. *Geomorphology, 251*, 149-156. https://doi.org/10.1016/j.geomorph.2015.02.020

Ashmore, P. (2018). Transforming Toronto's Rivers: A Socio-Geomorphic Perspective. In R. Lave, C. Biermann, & S. Lane (Eds.), *The Palgrave Handbook of Critical Physical Geography* (pp. 485–511). Springer International Publishing. https://doi.org/10.1007/978-3-319-71461-5_23

Ashmore, P., McDonald, J., & Barlow, V. (2023). Multi-decadal changes in river morphology in an urbanizing watershed: Highland Creek, Toronto, Canada. *Geomorphology, 433*. https://doi.org/10.1016/j.geomorph.2023.108710

Bagnold, R. A. (1966). An approach to the sediment transport problem from general physics. United States Geological Survey. https://pubs.usgs.gov/publication/pp422I

Beechie, T. J., Sear, D. A., Olden, J. D., Pess, G. R., Buffington, J. M., Moir, H., Roni, P., & Pollock, M. M. (2010). Process-Based Principles for Restoring River Ecosystems. *BioScience, 60*(3), 209–222. https://doi.org/10.1525/bio.2010.60.3.7

Bertalan, L., Rodrigo-Comino, J., Surian, N., Šulc Michalková, M., Kovács, Z., Szabó, S., Szabó, G., & Hooke, J. (2019). Detailed assessment of spatial and temporal variations in river channel changes and meander evolution as a preliminary work for effective floodplain management. The example of Sajó River, Hungary. *Journal of Environmental Management*, *248*. https://doi.org/10.1016/j.jenvman.2019.109277

Bevan, V., MacVicar, B., Chapuis, M., Ghunowa, K., Papangelakis, E., Parish, J., & Snodgrass, W. (2018). Enlargement and evolution of a semi-alluvial creek in response to urbanization. *Earth Surface Processes and Landforms, 43*(11), 2295-2312. https://doi.org/10.1002/esp.4391

Bizzi, S., & Lerner, D. N. (2015). The use of stream power as an indicator of channel sensitivity to erosion and deposition processes. *River Research and Applications*, *31*(1), 16–27. https://doi.org/10.1002/rra.2717

Bledsoe, B. P. (2002). Stream erosion potential and stormwater management strategies. *Journal of Water Resources Planning and Management, 128*(6), 451–455. https://doi.org/10.1061/(ASCE)0733-9496(2002)128:6(451)

Bledsoe, B. P., & Watson, C. C. (2001). Effects of urbanization on channel instability. *Journal of the American Water Resources Association, 37*(2), 255–270. https://doi.org/10.1111/j.1752-1688.2001.tb00966.x

Boggs, J. L., & Sun, G. (2011). Urbanization alters watershed hydrology in the Piedmont of North Carolina. *Ecohydrology, 4*(2), 256-264. https://doi.org/10.1002/eco.198

Booth, D. B., & Fischenich, C. J. (2015). A channel evolution model to guide sustainable urban stream restoration. *Area, 47*(4), 408–421. https://doi.org/10.1111/area.12180

Booth, D. B., & Jackson, C. R. (1997). Urbanization of Aquatic Systems: Degradation Thresholds, Stormwater Detection, and the Limits of Mitigation. *Journal of the American Water Resources Association, 33*(5), 1077-1090. https://doi.org/10.1111/j.1752-1688.1997.tb04126.x

Booth, D. B., Roy, A. H., Smith, B., & Capps, K. A. (2016). Global perspectives on the urban stream syndrome. *Freshwater Science, 35*(1), 412–420. https://doi.org/10.1086/684940

Boothroyd, R. J., Williams, R. D., Hoey, T. B., Barrett, B., & Prasojo, O. A. (2020). Applications of Google Earth Engine in fluvial geomorphology for detecting river channel change. *WIREs Water, 8*(1). https://doi.org/10.1002/wat2.1496

Bowman, D. (2019). Fan Entrenchment. In *Principles of Alluvial Fan Morphology* (pp. 61-67). Springer Nature. https://doi.org/10.1007/978-94-024-1558-2_8

Bravard, J. P., & Petit, F. (2009). Geomorphology of Streams and Rivers. In G.E. Likens (Ed.), *Encyclopedia of Inland Water* (pp. 387-395). Academic Press. https://doi.org/10.1016/B978-012370626-3.00043-0

Bunte, K., & Abt, S. R. (2001). *Sampling surface and subsurface particle-size distributions in wadable gravel-and cobble-bed streams for analyses in sediment transport, hydraulics, and streambed monitoring*. United States Department of Agriculture. https://research.fs.usda.gov/treesearch/4580

Candel, J., Kleinhans, M., Makaske, B., & Wallinga, J. (2021). Predicting river channel pattern based on stream power, bed material and bank strength. *Progress in Physical Geography: Earth and Environment, 45*(2), 253-278. https://doi.org/10.1177/0309133320948831

Cao, Z., Pender, G., & Meng, J. (2006). Explicit Formulation of the Shields Diagram for Incipient Motion of Sediment. *Journal of Hydraulic Engineering, 132*(10). https://doi.org/10.1061/(ASCE)0733-9429(2006)132:10(1097)

Careless, J. M. S. (2022, March 11). *Toronto*. The Canadian Encyclopedia. https://www.thecanadianencyclopedia.ca/en/article/toronto

Chandler, T., & Amirault, H. (2018). Regional curves to support stream restoration initiatives in Southern Ontario. *Canadian Water Resources Journal, 44*(1), 65-78. https://doi.org/10.1080/07011784.2018.1503067

Chen, W., & Wei, X. (2008). Assessing the Relations Between Aquatic Habitat Indicators and Forest Harvesting at Watershed Scale in the Interior of British Columbia. *Forest Ecology and Management, 256*, 152-160. https://doi.org/10.1016/j.foreco.2008.04.019

Chin, A. (2006). Urban transformation of river landscapes in a global context. *Geomorphology, 79*(3-4), 460-487. https://doi.org/10.1016/j.geomorph.2006.06.033

City of Pickering. (2008, August). *Master Environmental Servicing Plan Seaton Community Existing Conditions*.

City of Pickering. (n.d.). *Seaton Community*. https://www.pickering.ca/en/city-hall/seatoncommunity.aspx#Seaton-FAQ-the-who-what-where

City of Toronto. (n.d.[a]). *Highland Creek Rehabilitation Project -Markham Branch*. https://epe.lac-bac.gc.ca/100/205/301/ic/cdc/streams/projects/Metro/project64.html

City of Toronto. (n.d.[b]). *Toronto at a Glance*. https://www.toronto.ca/city-government/data-research-maps/toronto-at-a-glance/

Clerici, A., & Perego, S. (2016). A Set of GRASS GIS-Based Shell Scripts for the Calculation and Graphical Display of the Main Morphometric Parameters of a River Channel. *International Journal of Geosciences, 7*(2), 135-143. https://doi.org/10.4236/ijg.2016.72011

Conservation Ontario. (2010). *Overview of Integrated Watershed Management in Ontario*.

Cyples, N., & Wojda, M. (2020). Preliminary fluvial geomorphology assessment of Little Etobicoke Creek Dixie-Dundas flood mitigation. Matrix Solutions Inc.

De Rosa, P., Cencetti, C., & Fredduzzi, A. (2017). An automated method for river sinuosity calculation using QGIS. *Geoingegneria Ambientale e Mineraria, 151*(2), 81-84.

Ferguson, R. I. (2005). Estimating critical stream power for bedload transport calculations in gravel-bed rivers. *Geomorphology, 70*(1-2), 33–41. https://doi.org/10.1016/j.geomorph.2005.03.009

Finkenbine, J. K., Atwater, J. W., & Mavinic, D. S. (2000). Stream Health After Urbanization. *Journal of the American Water Resources Association, 36*(5), 1149-1160. https://doi.org/10.1111/j.1752-1688.2000.tb05717.x

Fletcher, T. D., Shuster, W., Hunt, W. F., Ashley, R., Butler, D., Arthur, S., Trowsdale, S., Barraud, S., Semadeni-Davies, A., Bertrand-Krajewski, J., Mikkelsen, P. S., Rivard, G., Uhl, M., Dagenais, D., & Viklander, M. (2015). SUDS, LID, BMPs, WSUD and more – The evolution and application of terminology surrounding urban drainage. *Urban Water Journal, 12*(7), 525–542. https://doi.org/10.1080/1573062X.2014.916314

Florsheim, J. L., Mount, J. F., & Chin, A. (2008). Bank erosion as a desirable attribute of rivers. *BioScience, 58*(6), 519-529. https://doi.org/10.1641/B580608

Fryirs, K. A., Brierley, G. J., & Dixon, T. (2019). Engaging with research impact assessment for an environmental science case study. *Nature Communications, 10*(4542). https://doi.org/10.1038/s41467-019-12020-z

Fuller, I. C., Death, R. G., Garcia, J. H., Trenc, N., Pratt, R., Pitiot, C., Matos, B., Ollero, A., Neverman, A., & Death, A. (2021). An index to assess the extent and success of river and floodplain restoration: Recognising dynamic response trajectories and applying a process-based approach to managing river recovery. *River Research and Applications, 37*(2), 163-175. https://doi.org/10.1002/rra.3672

Gazendam, E., Gharabaghi, B., Ackerman, J. D., & Whiteley, H. (2016). Integrative neural networks models for stream assessment in restoration projects. *Journal of Hydrology, 536*, 339-350. https://doi.org/10.1016/j.jhydrol.2016.02.057

Ghunowa, K., MacVicar, B. J., & Ashmore, P. (2021). Stream power index for networks (SPIN) tool for decision support in urbanizing watersheds. *Environmental Modelling & Software, 144*. https://doi.org/10.1016/j.envsoft.2021.105185

Government of Ontario. (2008, May 28). *Lake Ontario Atlantic salmon Restoration Program*. https://news.ontario.ca/en/backgrounder/178/lake-ontario-atlantic-salmon-restoration-program

Gregory, K. J. (2011). Wolman MG (1967) A cycle of sedimentation and erosion in urban river channels. Geografiska Annaler 49A: 385–395. *Progress in Physical Geography: Earth and Environment, 35*(6), 831-841. https://doi.org/10.1177/0309133311414527

Habberfield, M. W., Blersch, S. S., Bennett, S. J., & Atkinson, J. F. (2014). Rapid geomorphic and habitat stream assessment techniques inform restoration differently based on levels of stream disturbance. *Journal of the American Water Resources Association, 50*(4), 1051-1062. https://doi.org/10.1111/jawr.12156

Hawley, R. J., MacMannis, K. R., & Wooten, M. S. (2013). Bed Coarsening, Riffle Shortening, and Channel Enlargement in Urbanizing Watersheds, Northern Kentucky, USA. *Geomorphology, 201*, 111-126. https://doi.org/10.1016/j.geomorph.2013.06.013

Hayes, A. (2022, January 10). *Stepwise Regression: Definition, Uses, Example, and Limitations*. Investopedia. https://www.investopedia.com/terms/s/stepwise-regression.asp

Hazbavi, Z. (2018). Importance of geology and geomorphology in watershed health assessment. *Agriculture and Forestry, 64*(4), 277-287. https://doi.org/10.17707/AgricultForest.64.4.27

Houshmand, A., Vietz, G., & Hatt, B. (2014, July). Improving Urban Stream Condition by Redirecting Sediments: A Review of Associated Contaminants. In *Proceedings of the 7th Australian Stream Management Conference*. Townsville, Queensland, Australia. https://doi.org/10.13140/2.1.1228.6080

Howett, J. (2017). *Meander belt delineation: Developing a predictive model for meander belt width* [Master's Thesis, Western University]. Electronic Thesis and Dissertation Repository.

Hung, C. L. J., James, L. A., & Carbone, G. J. (2018). impacts of urbanization on stormflow magnitudes in small catchments in the Sandhills of South Carolina, USA. *Anthropocene, 23*, 17-28. https://doi.org/10.1016/j.ancene.2018.08.001

Jang, S., Hyunseo, J., Choi, J., Suh, K., & Kim, H. (2021). Investigation of correlation between surface runoff rate and stream water quality. *Water Supply, 21*(4), 1495-1505. https://doi.org/10.2166/ws.2021.023

Kleinhans, M. G., & van den Berg, J. H. (2011). River channel and bar patterns explained and predicted by an empirical and a physics-based method. *Earth Surface Processes and Landforms*, *36*(6), 711-852. https://doi.org/10.1002/esp.2090

Kusratmoko, E., Wibowo, A., & Ahmad Kurnia, A. (2019). Changes in the Value of Sinuosity Index in Komering River Channel, Province South Sumatera Years 1990 - 2016. *IOP Conference Series: Earth and Environmental Science*, *338*. https://doi.org/10.1088/1755-1315/338/1/012024

Levine, J. (2004). *Adaptive Management in River Restoration: Theory vs. Practice in Western North America* [LA 227 Term Project, University of California]. UC Riverside: Water Resources Collections and Archives.

Library of Parliament. (2020, January 31). *Climate Change: Its Impact and Policy Implications*. https://lop.parl.ca/sites/PublicWebsite/default/en_CA/ResearchPublications/201946E

Limaye, A. B., Lazarus, E. D., Li, Y., & Schwenk, J. (2021). River sinuosity describes a continuum between randomness and ordered growth. *Geology, 49*(12), 1506-1510. https://doi.org/10.1130/G49153.1

Lisle, T. E., Buffington, J. M., Wilcock, P. R., & Bunte, K. (2015). Can Rapid Assessment Protocols Be Used to Judge Sediment Impairment in Gravel-Bed Streams? A Commentary. *Journal of the American Water Resources Association*, *51*(2), 373-387. https://doi.org/10.1111/jawr.12255

Lisle, T. E., & Hilton, S. (1992). The volume of fine sediment in pools: an index of sediment supply in gravel-bed streams. *Journal of the American Water Resources Association, 28*(2), 251-423. https://doi.org/10.1111/j.1752-1688.1992.tb04003.x

Mackenzie, K. M., Gharabaghi, B., Binns, A. D., & Whiteley, H. R. (2022[a]). Early detection model for the urban stream syndrome using specific stream power and regime theory. *Journal of Hydrology, 604*. https://doi.org/10.1016/j.jhydrol.2021.127167

Mackenzie, K. M., Singh, K., Binns, A. D., Whiteley, H. R., & Gharabaghi, B. (2022[b]). Effects of urbanization on stream flow, sediment, and phosphorous regime. *Journal of Hydrology, 612*(Part C). https://doi.org/10.1016/j.jhydrol.2022.128283

Maestas, J. D., Conner, S., Zeedyk, B., Neely, B., Rondeau, R., Seward, N., Chapman, T., With, L., & Murph, R. (2018). Hand-built structures for restoring degraded meadows in sagebrush rangelands: Examples and lessons learned from the Upper Gunnison River Basin, Colorado. United States Department of Agriculture. https://doi.org/10.13140/RG.2.2.33628.08321

Meyer, J. L., Paul, M. J., & Taulbee, W. K. (2005). Stream ecosystem function in urbanizing landscapes. *Journal of the North American Benthologica9l Society, 24*(3), 602-612. https://doi.org/10.1899/04-021.1

Minnesota Department of Natural Resources (DNR). (2006). *The Shape of Healthy Streams: Characteristics of Natural Watercourses*.

Montgomery, D. R., & MacDonald, L. H. (2002). Diagnostic Approach to Stream Channel Assessment and Monitoring. *Journal of The American Water Resources Association, 38*(1). https://doi.org/10.1111/j.1752-1688.2002.tb01530.x

Mörtl, C. & De Cesare, G. (2021). Sediment Augmentation for River Rehabilitation and Management—A Review. *Land*, *10*(12), 1309. https://doi.org/10.3390/land10121309

Natural Resources Conservation Service (NRCS) (2007). Chapter 11: Rosgen Geomorphic Channel Design. In *Part 654 National Engineering Handbook*. United States Department of Agriculture.

Nehrke, S. M., & Roesner, L. A. (2004). Effects of design practice for flood control and best management practices on the flow-frequency curve. *Journal of Water Resources Planning and Management*, *130*(2), 131–139. https://doi.org/10.1061/(ASCE)0733-9496(2004)130:2(131)

Obach, L. M. (2011). *The Hydrodynamics of Pool-Riffle Sequences with Changing Bedform Length* [Master's Thesis, University of Waterloo]. Theses in UWSpace.

Ock, G., Sumi, T., & Takemon, Y. (2013). Sediment replenishment to downstream reaches below dams: implementation perspectives. *Hydrological Research Letters*, *7*(3), 54–59. https://doi.org/10.3178/hrl.7.54

O'Neill, M. P., & Abrahams, A. D. (1984). Objective Identification of Pools and Riffles. *Water Resources Research, 20*(7), 1003-1002. https://doi.org/10.1029/WR020i007p00921

Ontario Ministry of Transportation (MTO). (1997, October). Part 3. In *MTO Drainage Management Manual*. Ontario Ministry of Transportation.

Padovan, P. (2016). *Hydrogeomorphic Adjustments in Urban Channel Restoration Projects* [Master's Thesis, University of Guelph]. Theses & Dissertations (2011 - present).

Palmer, M., Allan, J. D., Meyer, J., & Bernhardt, E. S. (2007). River Restoration in the Twenty-First Century: Data and Experiential Knowledge to Inform Future Efforts. *Restoration Ecology, 15*(3), 472-481. https://doi.org/10.1111/j.1526-100X.2007.00243.x

Papangelakis, E., MacVicar, B., & Ashmore, P. (2019). Bedload Sediment Transport Regimes of Semi-alluvial Rivers Conditioned by Urbanization and Stormwater Management. *Water Resources Research, 55*(12), 10565-10587, https://doi.org/10.1029/2019WR025126

Papangelakis, E., MacVicar, B., Ashmore, P., Gingerich, D., & Bright, C. (2022[a]). Testing a Watershed-Scale Stream Power Index Tool for Erosion Risk Assessment in an Urban River. *Journal of Sustainable Water in the Built Environment*, *8*(13). https://doi.org/10.1061/JSWBAY.000098

Papangelakis, E., MacVicar, B., Montakhab, A. F., & Ashmore, P. (2022[b]). Flow Strength and Bedload Sediment Travel Distance in Gravel Bed Rivers. *Water Resources Research, 58*(7). https://doi.org/10.1029/2022WR032296

Papangelakis, E., Hassan, M. A., Luzi, D., Burge, L. M., & Pierce, S. (2023). Measuring geomorphology in river assessment procedures 1: A global overview of current practices. *Journal of the American Water Resources Association*, *59*(6), 1342-1359. https://doi.org/10.1111/1752-1688.13146

Parish Geomorphic. (2004). *Belt Width Delineation Procedures*.

Parker, C., Clifford, N. J., & Thorne, C. R. (2011). Understanding the influence of slope on the threshold of coarse grain motion: Revisiting critical stream power. *Geomorphology, 126*(1-2), 51–65. https://doi.org/10.1016/j.geomorph.2010.10.027

Phillips, J. (2015). Hydrologic and Geomorphic Flow Thresholds in the Lower Brazos River, Texas. *Hydrological Sciences Journal*, *60*(9), 1631-1648. https://doi.org/10.1080/02626667.2014.943670

Phillips, R. T. J., & Desloges, J. R. (2014). Glacially conditioned specific stream powers in low-relief river catchments of the southern Laurentian Great Lakes. *Geomorphology*, *206*, 271–287. https://doi.org/10.1016/j.geomorph.2013.09.030

Phillips, R. T. J., & Desloges, J. R. (2015). Alluvial floodplain classification by multivariate clustering and discriminant analysis for low-relief glacially conditioned river catchments. *Earth Surface Processes and Landforms*, *40*(6), 756-770. https://doi.org/10.1002/esp.3681

Ratnasari, D., Nazir, F., Toresano, L. O. H. Z., Pawiro, S. A., & Soejoko, D. S. (2016). The correlation between effective renal plasma flow (ERPF) and glomerular filtration rate (GFR) with renal scintigraphy ^{99m}Tc-DTPA study. *Journal of Physics: Conference Series, 694*. https://doi.org/10.1088/1742-6596/694/1/012062

Richards, K. S. (1976). The morphology of riffle-pool sequences. *Earth Surface Processes and Landforms*, *1*(1), 71-88. https://doi.org/10.1002/esp.3290010108

Robinson, A. M. (1976). The effects of urbanization on stream channel morphology. In *National Symposium on Urban Hydrology, Hydraulics, and Sediment Control* (pp. 115-127). University of Kentucky.

Rohrer, C. A., Roesner, L. A., & Bledsoe, B. P. (2004, March 10). *The Effect of Stormwater Controls on Sediment Transport in Urban Streams* [Presentation]. Hydrology Days, Colorado, U.S. https://api.mountainscholar.org/server/api/core/bitstreams/d15f8f69-ea4d-4e29-b9c3-10995879500e/content

Rohrer, C. A., & Roesner, L. A. (2006). Matching the critical portion of the flow duration curve to minimise changes in modelled excess shear. *Water Science and Technology, 54*(6-7), 347–354. http://doi.org/10.2166/wst.2006.590

Rosgen, D. L. (1994). A classification of natural rivers. *Catena*, *22*(3), 169-199. https://doi.org/10.1016/0341-8162(94)90001-9

Rosgen, D. L. (2001). *A stream channel stability assessment methodology*. Proceedings of the Seventh Federal Interagency Sedimentation Conference.

Russell, K. L., Geoff, J. V., & Fletcher, T. D. (2017). Global Sediment Yields from Urban and Urbanizing Watersheds. *Earth-Science Reviews, 168*, 73-80. https://doi.org/10.1016/j.earscirev.2017.04.001

Schiff, R., MacBroom, J. G., & Bonin, J. A. (2007). *Guidelines for naturalized river channel design and bank stabilization*. Milone & MacBroom, Inc.

Schumm, S. A., Harvey, M. D., & Watson, C. C. (1984). *Incised Channels: Morphology, Dynamics, and Control*. Water Resources Publications.

Sen, D, Tauriac, A., Tarabetz, R., & Vandenberg, R. (2008). Development Of Simple Stream Rehabilitation Techniques for Urban Watersheds. *Proceedings of the Water Environment Federation 2008*(16), 915-934. https://doi.org/10.2175/193864708788735060

Sharpe, D. R., & Russell, H. A. J. (2023). Sedimentary architecture and glacial hydrodynamic significance of the stratified Oak Ridges Moraine, southern Ontario, Canada. *Boreas, 52*, 341-380. https://doi.org/10.1111/bor.12612

Simic, A., Fernandes, R., & Wang, S. (2014). Assessing the Impact of Leaf Area Index on Evapotranspiration and Groundwater Recharge across a Shallow Water Region for Diverse Land Cover and Soil Properties. *Journal of Water Resource and Hydraulic Engineering*, *3*(4), 60-73.

Simon, A., & Rinaldi, M. (2006). Disturbance, stream incision, and channel evolution: The roles of excess transport capacity and boundary materials in controlling channel response. *Geomorphology, 79*(3), 361-383. https://doi.org/10.1016/j.geomorph.2006.06.037

Smith, S., & Wilcock, P. (2015). Upland sediment supply and its relation to watershed sediment delivery in the contemporary mid-Atlantic Piedmont (USA). *Geomorphology 232*, 33-46. https://doi.org/10.1016/j.geomorph.2014.12.036

Statistics Canada. (2009, August 7). *Population of greater cities, 1941 compared with 1931*. Government of Canada. https://www65.statcan.gc.ca/acyb02/1947/acyb02_19470103003-eng.htm

Statistics Canada. (2023, February 1). Census Profile, 2021 Census of Population (Toronto) [Dataset]. Government of Canada. https://www12.statcan.gc.ca/census-recensement/2021/dp-pd/prof/details/page.cfm?Lang=E&GENDERlist=1,2,3&STATISTIClist=1,4&HEADERlist=0&DGUIDlist=2021A00053520005&SearchText=toronto

Sumi, T., Kantoush, S., Esmaeili, T., & Ock, G. (2017). Reservoir Sediment Flushing and Replenishment Below Dams. In D. Tsutsumi & J. B. Laronne (Eds.), *Gravel-Bed Rivers: Processes and Disasters* (pp. 385-414). John Wiley & Sons Ltd. https://doi.org/10.1002/9781118971437.ch14

Sustainable Technologies Evaluation Program (STEP). (n.d.). *Addressing the Stormwater Management Crisis in Urban Ontario: Aggregated Private-Public Land Green Infrastructure Retrofits*.

Talpur, M. A., & Bishop, B. (2022, March 1). *Mimico Creek Stabilization - Project File Report*. Wood Environment & Infrastructure Solutions, a Division of Wood Canada Limited.

Tam, J. (2023, June 12). *Watersheds TRCA* [Map]. Conservation Ontario. https://trca-camaps.opendata.arcgis.com/datasets/camaps::watersheds-trca/about

The World Bank. (2023, April 3). *Urban Development*. https://www.worldbank.org/en/topic/urbandevelopment/overview

Thompson, A. (1986). Secondary flows and the pool-riffle unit: a case study of the processes of meander development. *Earth Surface Processes and Landforms, 11*(6), 581-696. https://doi.org/10.1002/esp.3290110606

Tillekeratne, K. (2024). *Review of Toronto's Water Policy Design for the Greater Toronto Area*. https://www.researchgate.net/publication/379900532_Toronto's_Water_Policy_Design_for_the_Greater_Toronto_Area

Toronto and Region Conservation Authority (TRCA). (2013[a]). *Duffins Creek Watershed Report Card 2013*. https://reportcard.trca.ca/library/

Toronto and Region Conservation Authority (TRCA). (2018[a]). *Duffins Creek Watershed Report Card 2018*. https://reportcard.trca.ca/library/

Toronto and Region Conservation Authority (TRCA). (2018[b]). *Etobicoke Creek Watershed Report Card 2018.* https://reportcard.trca.ca/library/

Toronto and Region Conservation Authority (TRCA). (2021, June). *Etobicoke Creek Watershed Characterization Report*. https://trca.ca/conservation/watershed-management/etobicoke-creek-watershed-plan/

Toronto and Region Conservation Authority (TRCA). (2018[c]). *Highland Creek Watershed Report Card 2018*. https://reportcard.trca.ca/library/

Toronto and Region Conservation Authority (TRCA). (2013[d]). *Mimico Creek Watershed Report Card 2013*. https://reportcard.trca.ca/library/

Toronto and Region Conservation Authority (TRCA). (2018[d]). *Mimico Creek Watershed Report Card 2018*. https://reportcard.trca.ca/library/

Toronto and Region Conservation Authority (TRCA). (n.d.[a]). *About TRCA*. https://trca.ca/about/

Toronto and Region Conservation Authority (TRCA). (n.d.[b]). *Duffins Creek*. https://trca.ca/conservation/watershed-management/duffins-creek/

Toronto and Region Conservation Authority (TRCA). (n.d.[c]). *Flood Risk Management*. https://trca.ca/conservation/flood-risk-management/

Trudeau, M. P., & Richardson, M. (2016). Empirical assessment of effects of urbanization on event flow hydrology in watersheds of Canada's Great Lakes-St Lawrence basin. *Journal of Hydrology, 541*, 1456–1474. https://doi.org/10.1016/j.jhydrol.2016.08.051

U.S. Army Corps of Engineers (USACE). (2013, June). *Galveston District Stream Condition Assessment*.

U.S. Environmental Protection Agency (EPA). (n.d.). *Fundamentals of Rosgen Stream Classification System*. https://cfpub.epa.gov/watertrain/moduleFrame.cfm?parent_object_id=1262

Vocal Ferencevic, M., & Ashmore, P. (2011). Creating and evaluating model-based stream-power map as a stream assessment tool. *River Research and Applications, 28*(9), 1394–1416. https://doi.org/10.1002/rra.1523

Wade, R. J., Rhoads, B. L., Rodriguez, J., Daniels, M., Wilson, D., Herricks, E. E., Bombardelli, F., Garcia, M., & Schwartz, J. (2002). Integrating science and technology to support stream naturalization near Chicago, Illinois. *Journal of the American Water Resources Association, 38*(4), 895-1155. https://doi.org/10.1111/j.1752-1688.2002.tb05535.x

Walker, D. R., Millar, R. G., & Newbury, R. W. (2004). Energy Profiles Across Constructed Riffles. *Journal of Hydraulic Engineering, 130*(3). https://doi.org/10.1061/(ASCE)0733-9429(2004)130:3(199)

Wang, F., Wang, S., Yao, W., Li, X., Meng, F., & Xia, K. (2023). Effect of roughness on the shear behavior of rock joints subjected to impact loading. *Journal of Rock Mechanics and Geotechnical Engineering, 15*(2), 339-349. https://doi.org/10.1016/j.jrmge.2022.04.011

Wilcock, P. R., & McArdell, B. W. (1997). Surface-Based Fractional Transport Rates: Mobilization Thresholds and Partial Transport of a Sand-Gravel Sediment. *Water Resources Research, 29*(4), 1297-1312. https://doi.org/10.1029/96WR02672

Wilzbach, M. A., & Cummins, K. W. (2018). Rivers and Streams: Physical Setting and Adapted Biota. In B. Fath (Ed.), *Encyclopedia of Ecology* (2nd ed) (pp. 594-606). Elsevier. https://doi.org/10.1016/B978-0-12-409548-9.11093-0

Wohl, E., Lane, S. N., & Wilcox, A. C. (2015). The science and practice of river restoration. *Water Resources Research, 51*(8), 5974–5997. https://doi.org/10.1002/2014WR016874

Wohl, E., & Merritts, D. J. (2007). What is a natural river? *Geography Compass, 1*(4), 871-900. https://doi.org/10.1111/j.1749-8198.2007.00049.x

Wolman, M. G. (1967). A Cycle of Sedimentation and Erosion in Urban River Channels. *Geografiska Annaler: Series A, Physical Geography, 49*(2-4), 385-395. https://doi.org/10.1080/04353676.1967.11879766

Wolman, M. G., & Leopold, L. B. (1957). *River Flood Plains: Some Observations on their Formation*. U.S. Geological Survey Professional Paper 282-C, Washington, D.C. https://doi.org/10.3133/pp282C

Wood-Smith, R. D., & Buffington, J. M. (1996). Multivariate Geomorphic Analysis of Forest Streams: Implications for Assessment of Land Use Impacts on Channel Condition. *Earth Surface Processes and Landforms, 21*, 377-393. https://doi.org/10.1002/(SICI)1096-9837(199604)21:4<377::AID-ESP546>3.0.CO;2-2

Yochum, S. E., Sholtes, J. S., Scott, J. A., & Bledsoe, B. P. (2017). Stream power framework for predicting geomorphic change: The 2013 Colorado front range flood. *Geomorphology, 292*, 178–192. https://doi.org/10.1016/j.geomorph.2017.03.004

Zeug, S., Sellheim, K., Watry, C., Rook, B., Hannon, J., Zimmerman, J., Cox, D., & Merz, J. (2013). Gravel augmentation increases spawning utilization by anadromous salmonids: a case study from California, USA. *River Research and Applications, 30*(6), 707–718.

APPENDIX A: Site Maps

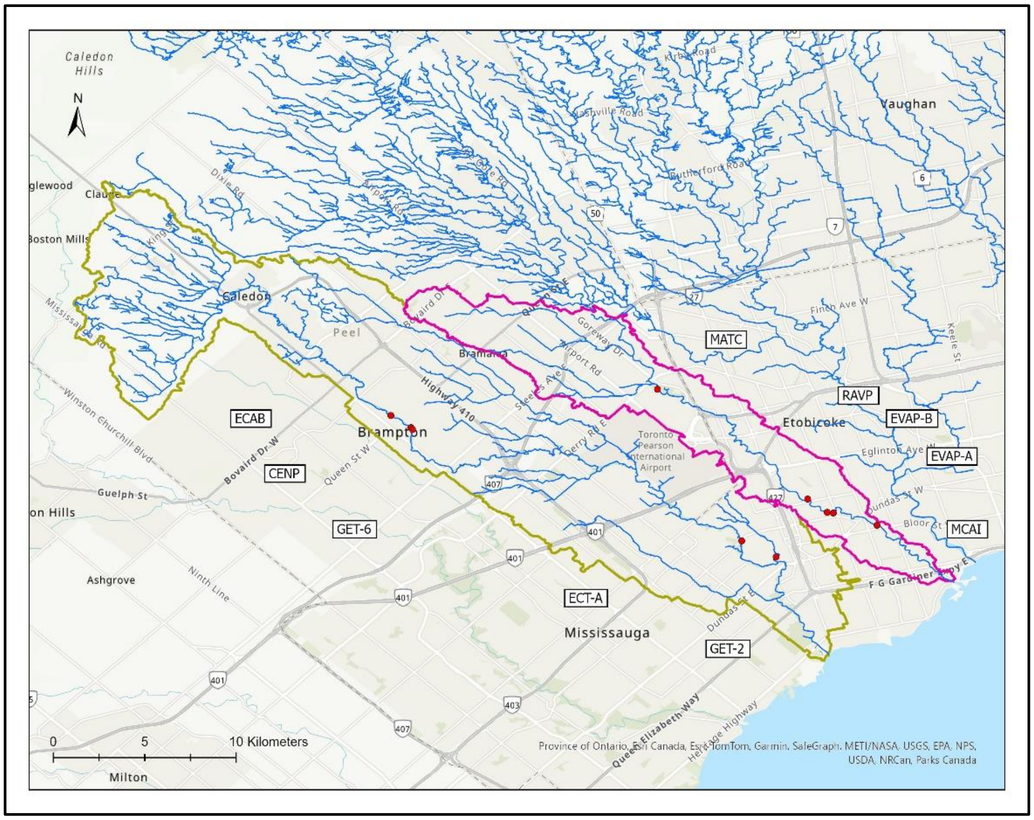

Figure A1. Etobicoke Creek (left/yellow) and Mimico Creek (right/pink) Study Sites Map

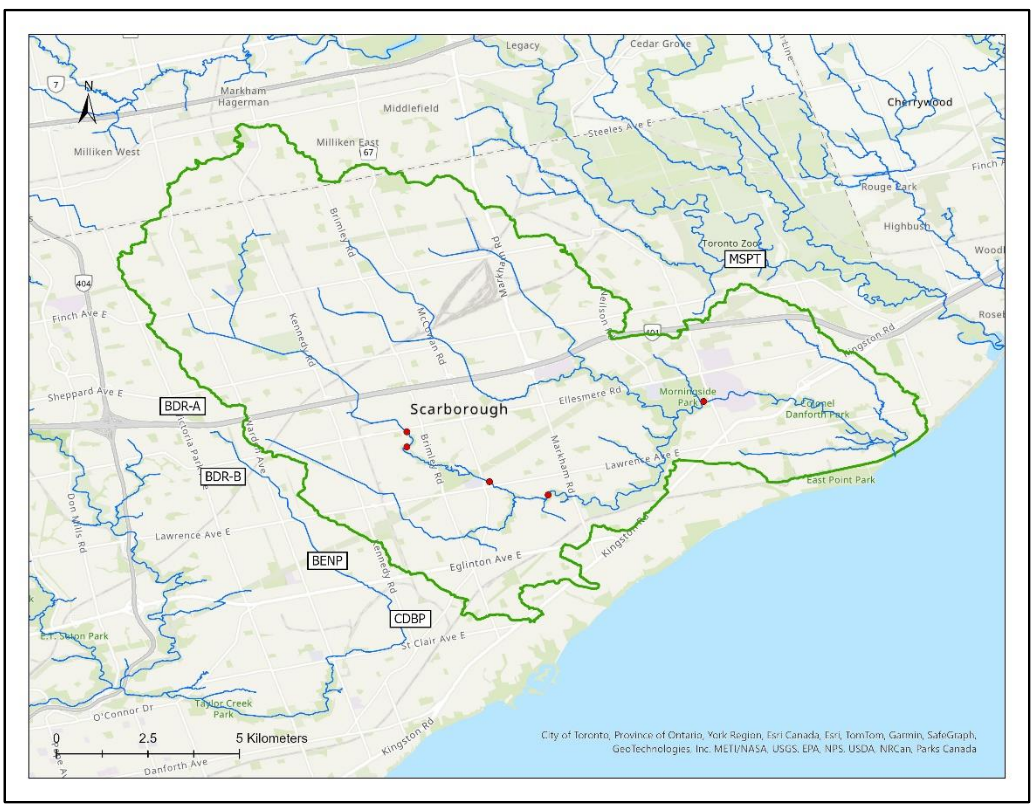

Figure A2. Highland Creek Study Sites Map

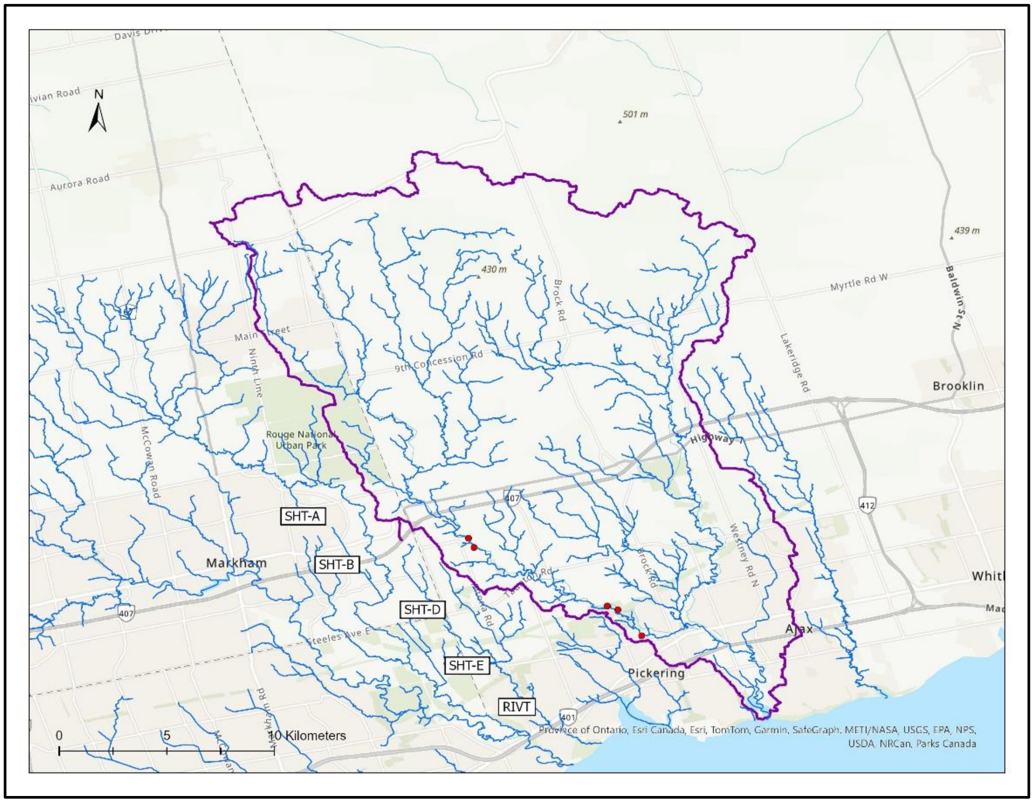

Figure A3. Duffins Creek Study Sites Map

APPENDIX B: Site Photos

Mimico Creek (B1-B25)
Etobicoke Creek (B26-B50)
Highland Creek (B51-B75)
Duffins Creek (B76-B100)

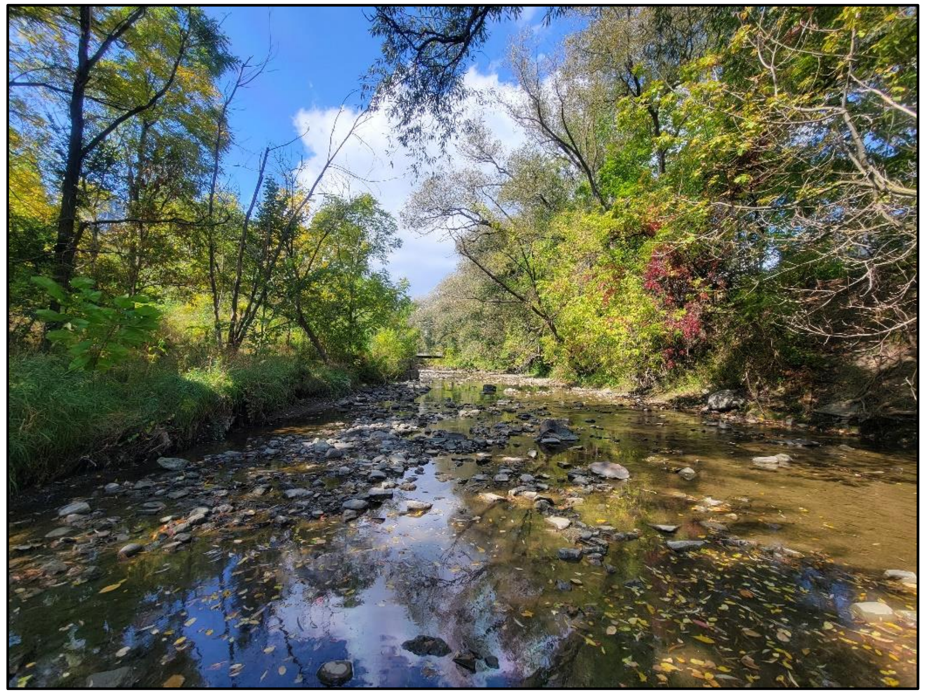

Figure B1. MCAI, Upstream

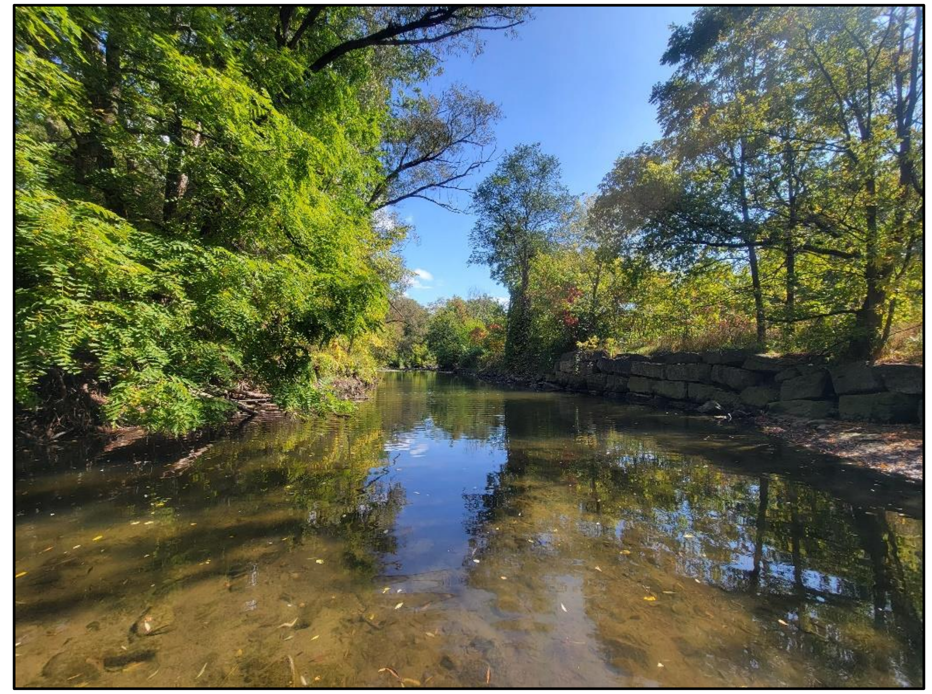

Figure B2. MCAI, Downstream

Figure B3. MCAI, Left Bank

Figure B4. MCAI, Right Bank

Figure B5. MCAI, Bed

Figure B6. RAVP, Upstream

Figure B7. RAVP, Downstream

Figure B8. RAVP, Left Bank

Figure B9. RAVP, Right Bank

Figure B10. RAVP, Bed

Figure B11. MATC, Upstream

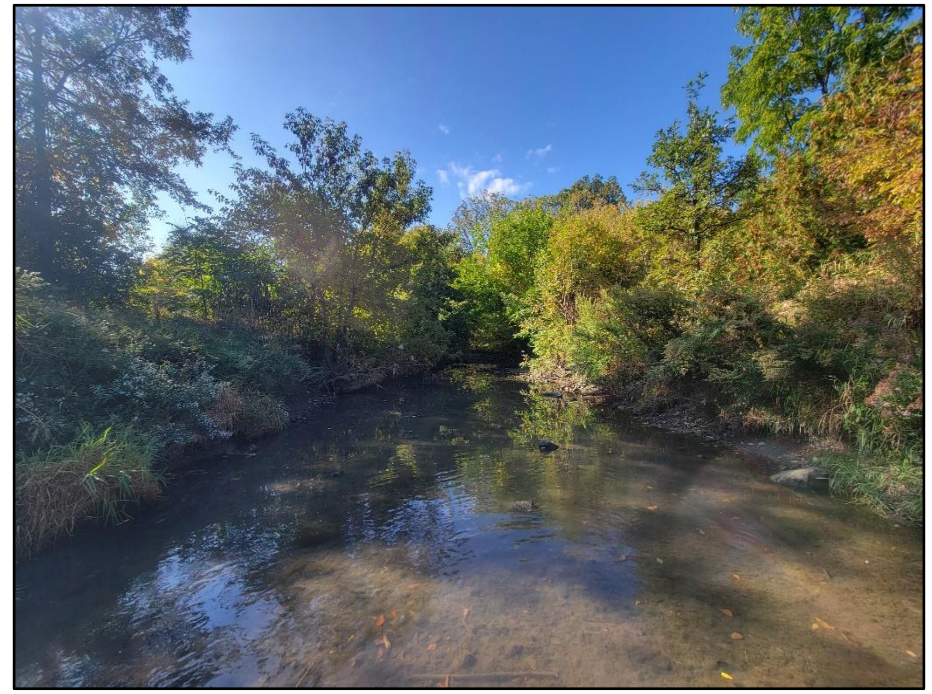

Figure B12. MATC, Downstream

Figure B13. MATC, Left Bank

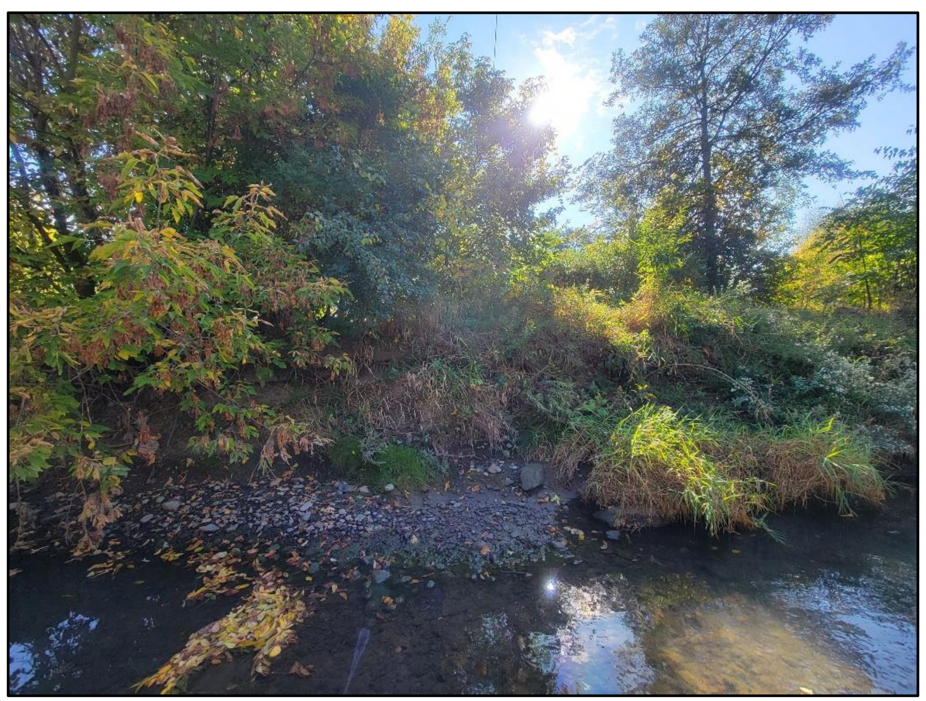

Figure B14. MATC, Right Bank

Figure B15. MATC, Bed

Figure B16. EVAP-A, Upstream

Figure B17. EVAP-A, Downstream

Figure B18. EVAP-A, Left Bank

Figure B19. EVAP-A, Right Bank

Figure B20. EVAP-A, Bed

Figure B21. EVAP-B, Upstream

Figure B22. EVAP-B, Downstream

Figure B23. EVAP-B, Left Bank

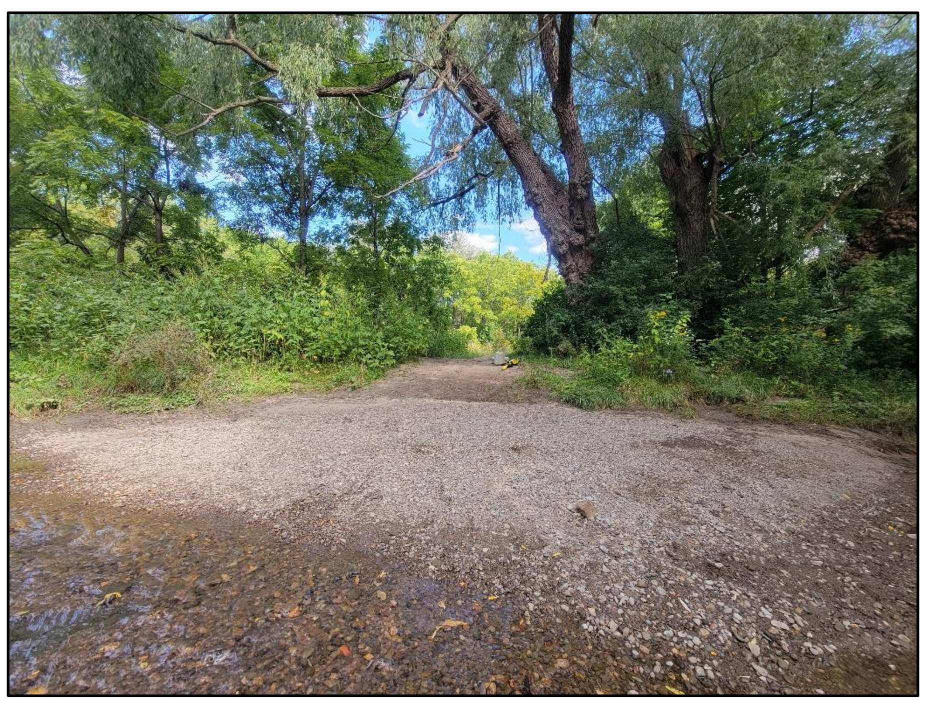

Figure B24. EVAP-B, Right Bank

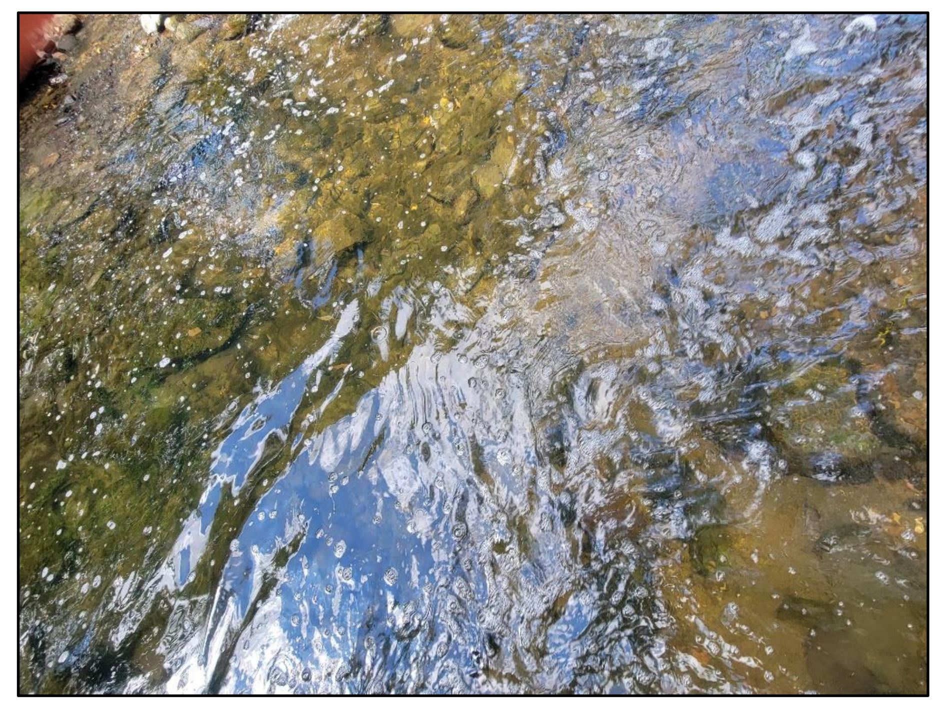

Figure B25. EVAP-B, Bed

Figure B26. ECT-A, Upstream

Figure B27. ECT-A, Downstream

Figure B28. ECT-A, Left Bank

Figure B29. ECT-A, Right Bank

Figure B30. ECT-A, Bed

Figure B31. GET-6, Upstream

Figure B32. GET-6, Downstream

Figure B33. GET-6, Left Bank

Figure B34. GET-6, Right Bank

Figure B35. GET-6, Bed

Figure B36. CENP, Upstream

Figure B37. CENP, Downstream

Figure B38. CENP, Left Bank

Figure B39. CENP, Right Bank

Figure B40. CENP, Bed

Figure B41. ECAB, Upstream

Figure B42. ECAB, Downstream

Figure B43. ECAB, Left Bank

Figure B44. ECAB, Right Bank

Figure B45. ECAB, Bed

Figure B46. GET-2, Upstream

Figure B47. GET-2, Downstream

Figure B48. GET-2, Left Bank

Figure B49. GET-2, Right Bank

Figure B50. GET-2, Bed

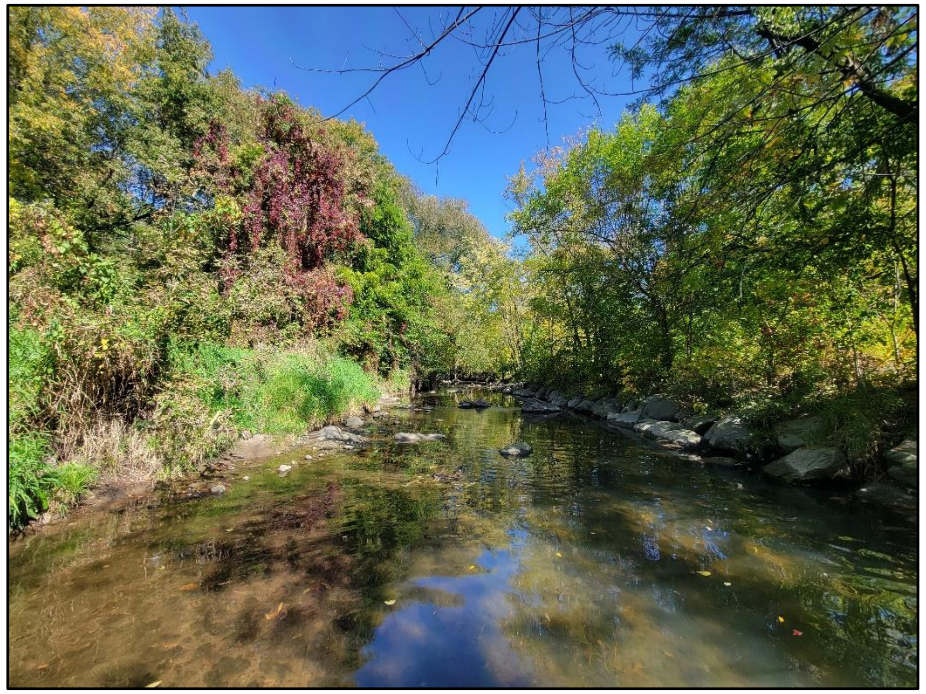

Figure B51. BDR-B, Upstream

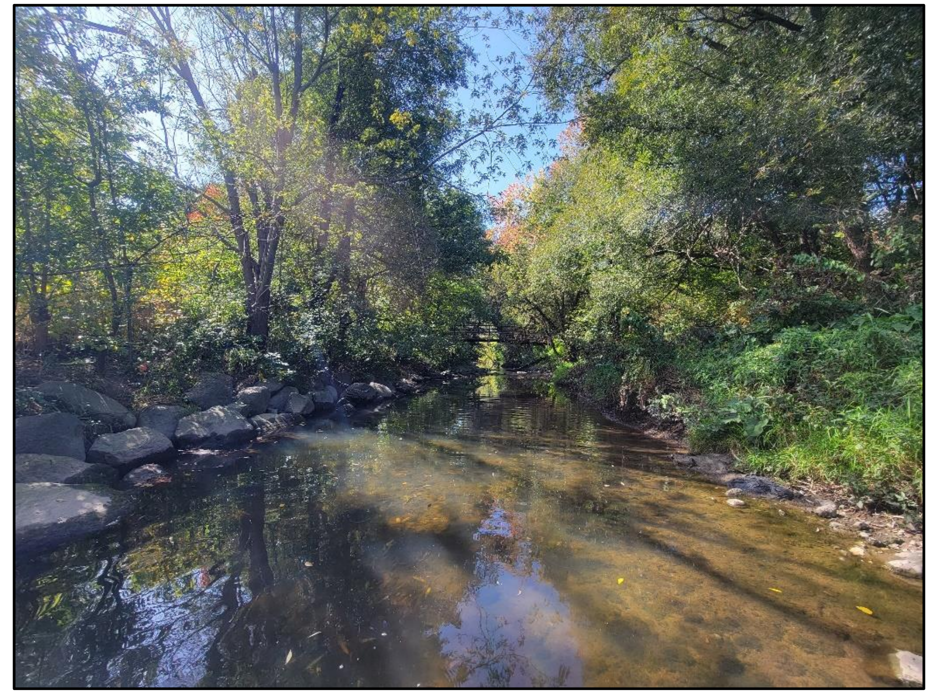

Figure B52. BDR-B, Downstream

Figure B53. BDR-B, Left Bank

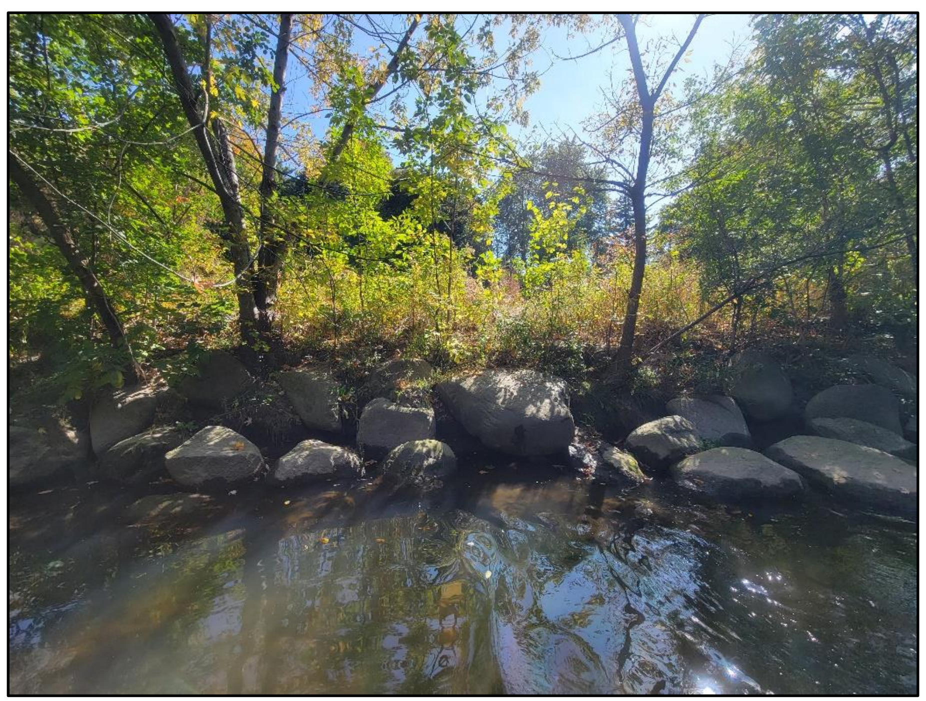

Figure B54. BDR-B, Right Bank

Figure B55. BDR-B, Bed

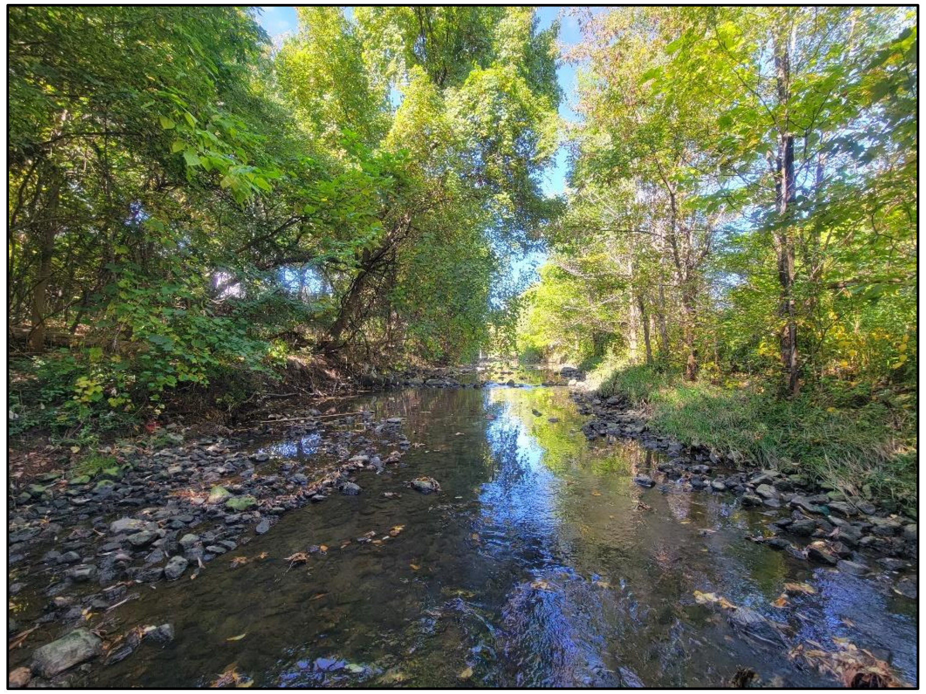

Figure B56. BDR-A, Upstream

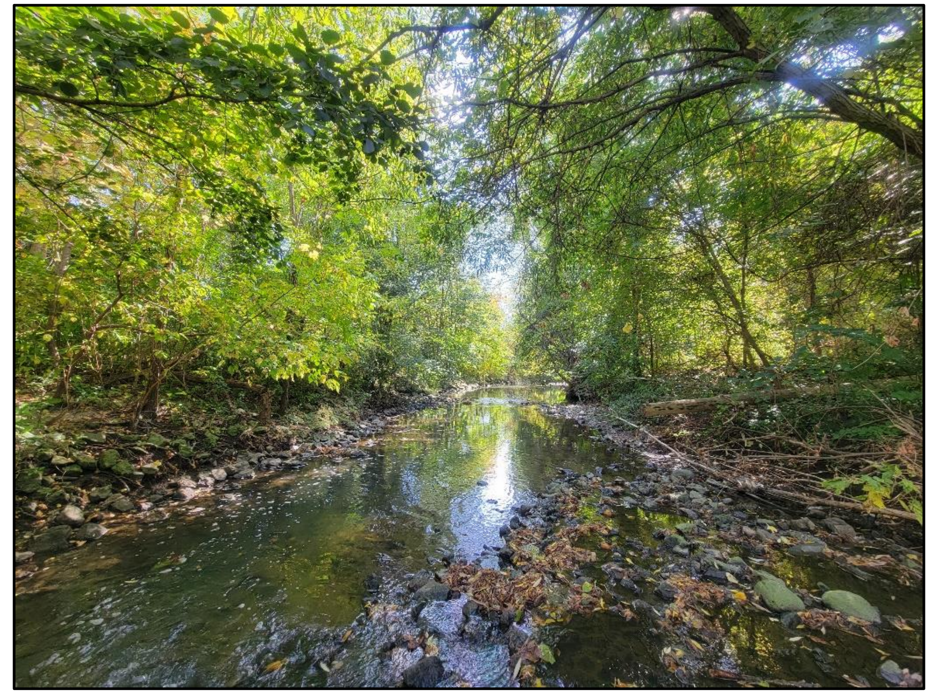

Figure B57. BDR-A, Downstream

Figure B58. BDR-A, Left Bank

Figure B59. BDR-A, Right Bank

Figure B60. BDR-A, Bed

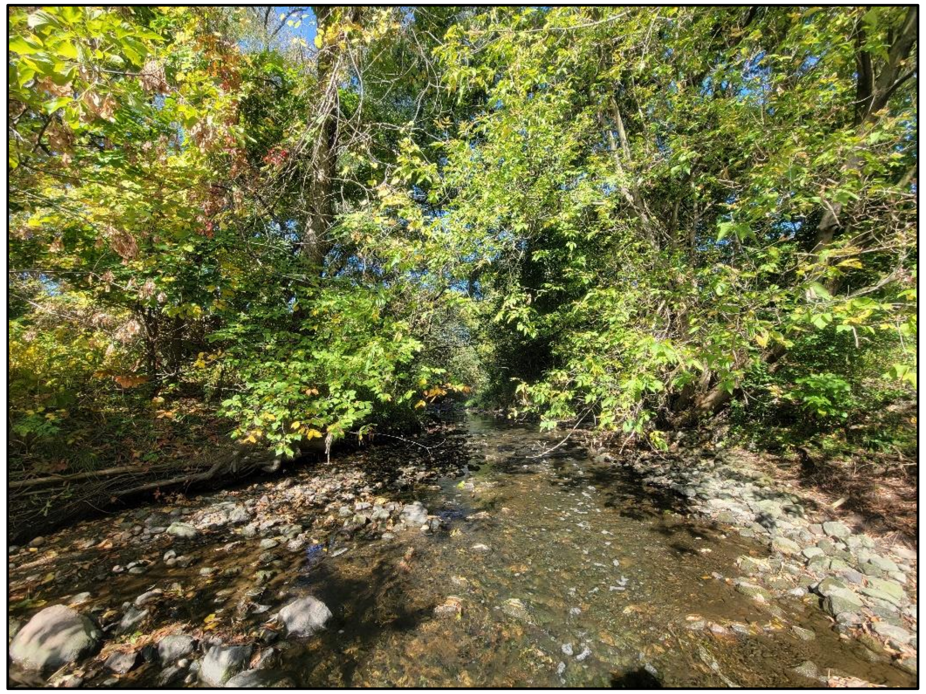

Figure B61. BENP, Upstream

Figure B62. BENP, Downstream

Figure B63. BENP, Left Bank

Figure B64. BENP, Right Bank

Figure B65. BENP, Bed

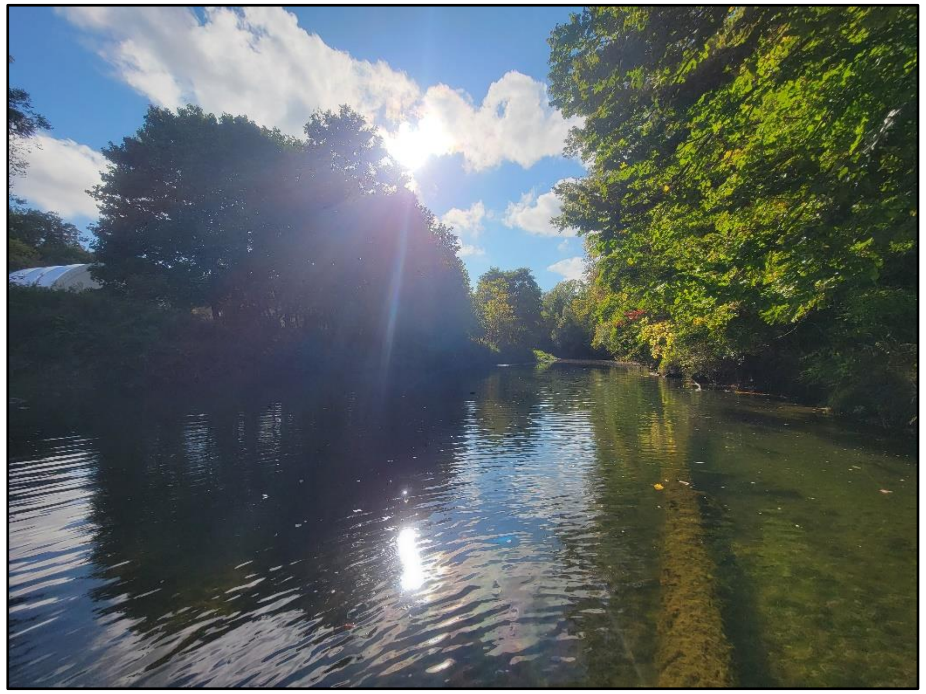

Figure B66. MSPT, Upstream

Figure B67. MSPT, Downstream

Figure B68. MSPT, Left Bank

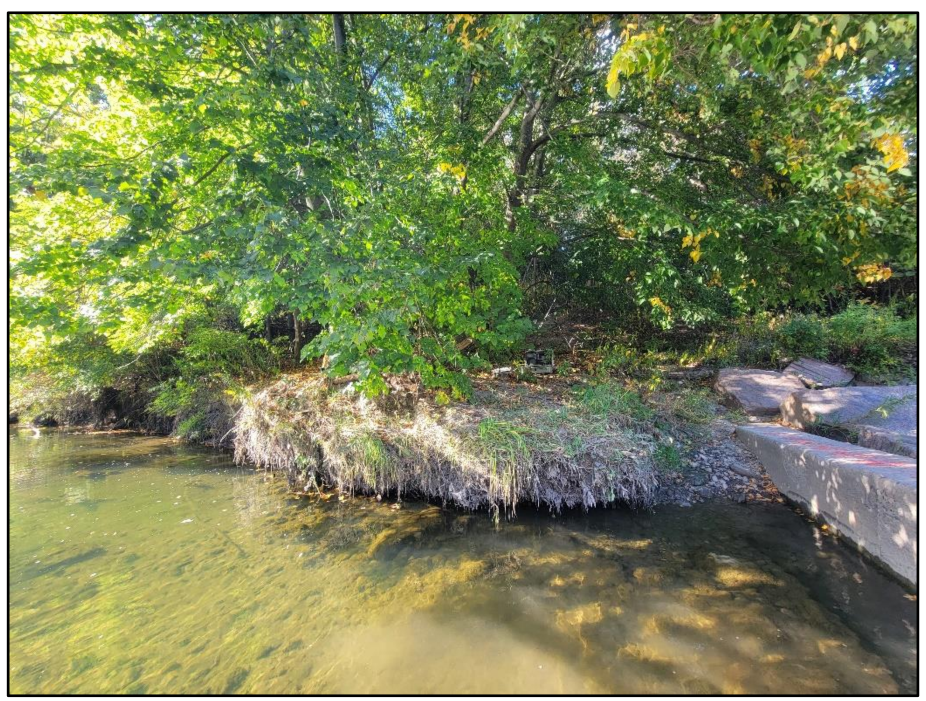

Figure B69. MSPT, Right Bank

Figure B70. MSPT, Bed

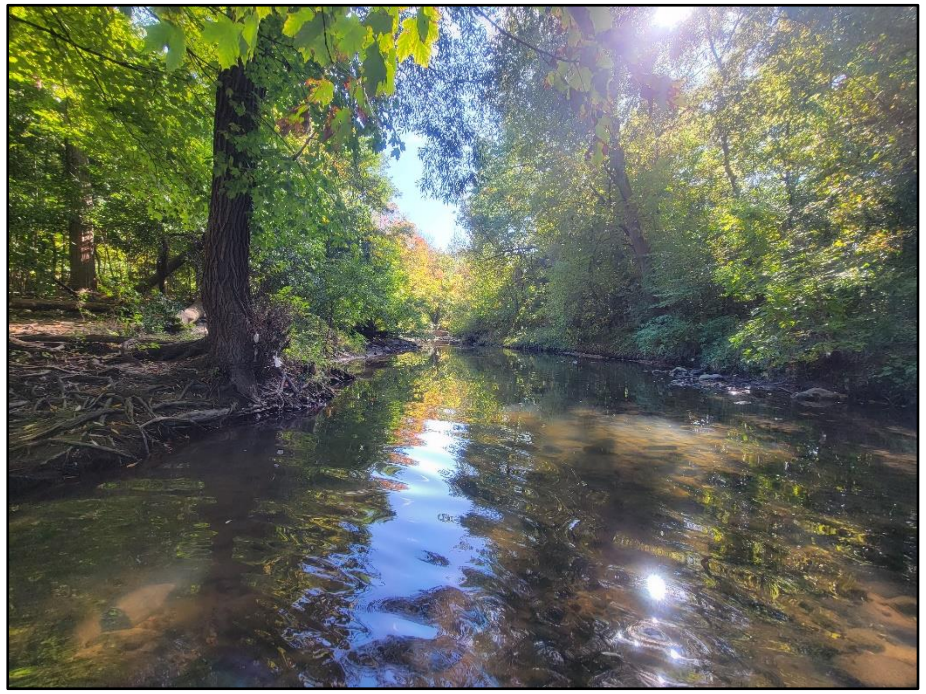

Figure B71. CDBP, Upstream

Figure B72. CDBP, Downstream

Figure B73. CDBP, Left Bank

Figure B74. CDBP, Right Bank

Figure B75. CDBP, Bed

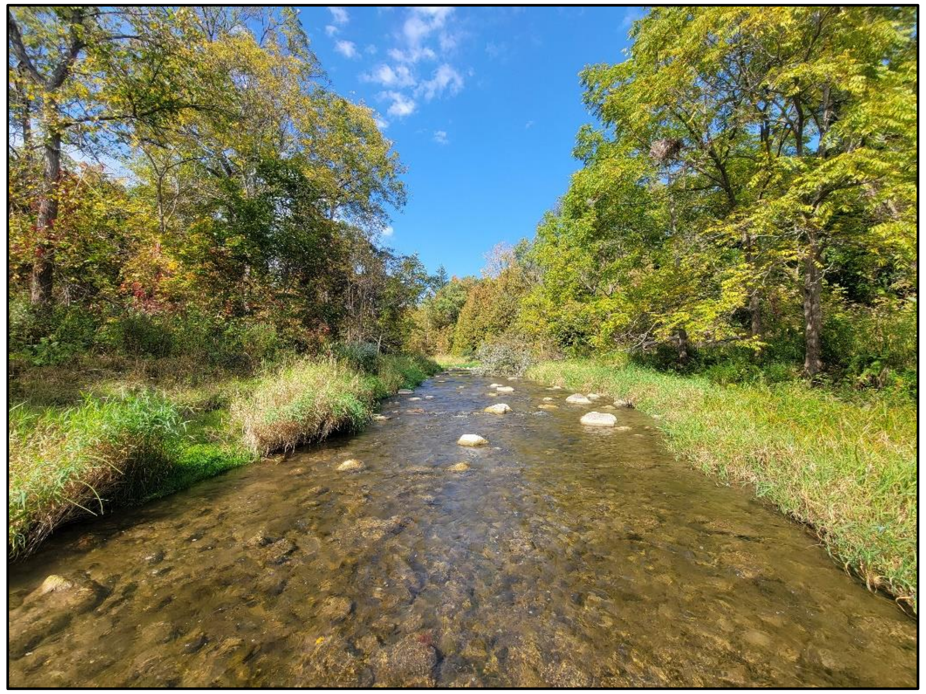

Figure B76. SHT-A, Upstream

Figure B77. SHT-A, Downstream

Figure B78. SHT-A, Left Bank

Figure B79. SHT-A, Right Bank

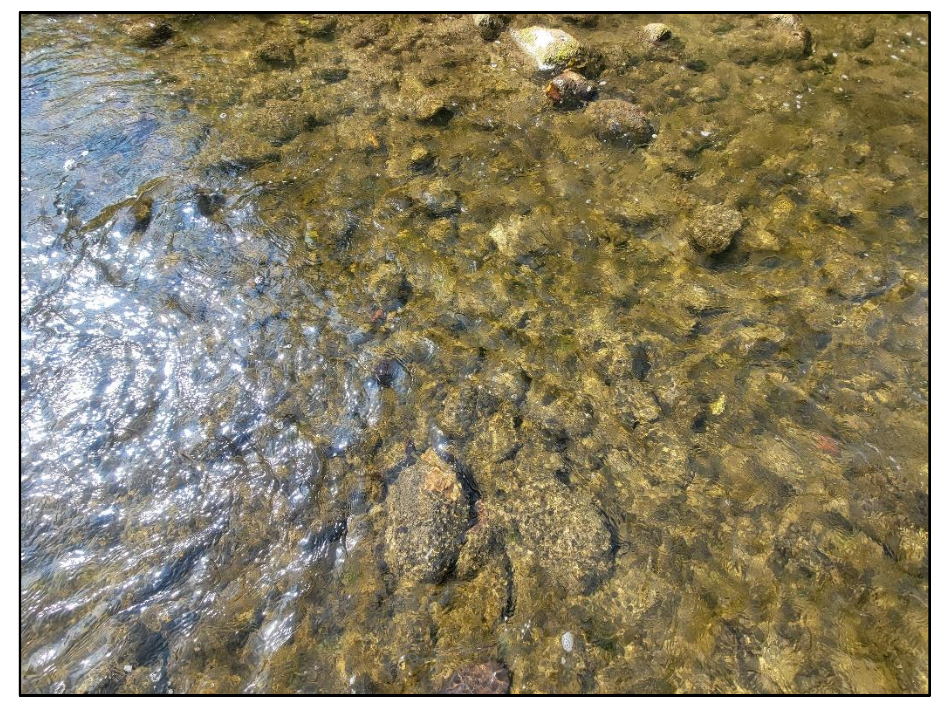

Figure B80. SHT-A, Bed

Figure B81. SHT-B, Upstream

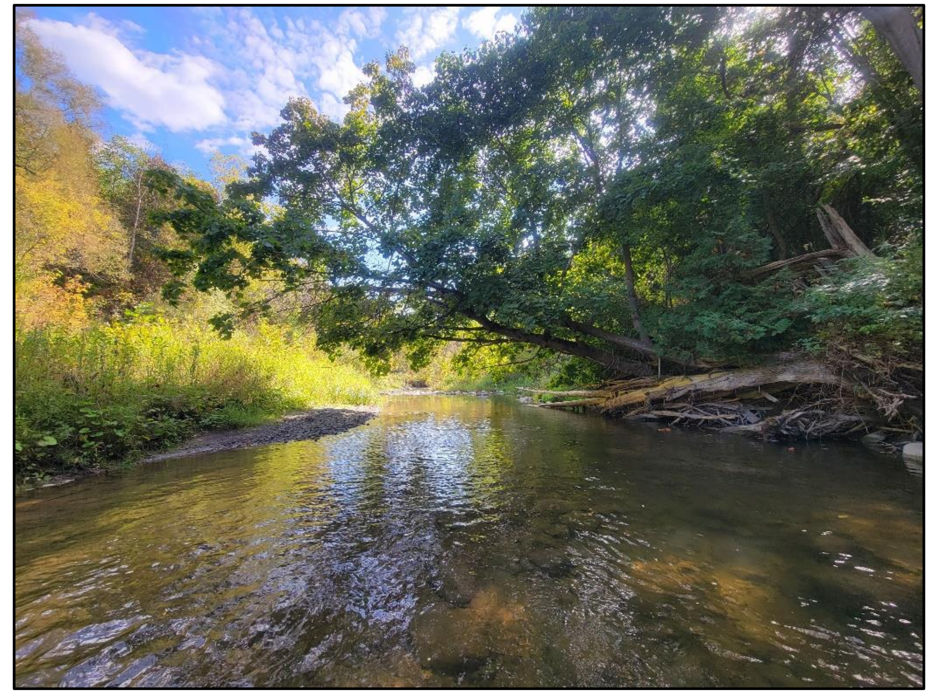

Figure B82. SHT-B, Downstream

Figure B83. SHT-B, Left Bank

Figure B84. SHT-B, Right Bank

Figure B85. SHT-B, Bed

Figure B86. SHT-E, Upstream

Figure B87. SHT-E, Downstream

Figure B88. SHT-E, Left Bank

Figure B89. SHT-E, Right Bank

Figure B90. SHT-E, Bed

Figure B91. SHT-D, Upstream

Figure B92. SHT-D, Downstream

Figure B93. SHT-D, Left Bank

Figure B94. SHT-D, Right Bank

Figure B95. SHT-D, Bed

Figure B96. RIVT, Upstream

Figure B97. RIVT, Downstream

Figure B98. RIVT, Left Bank

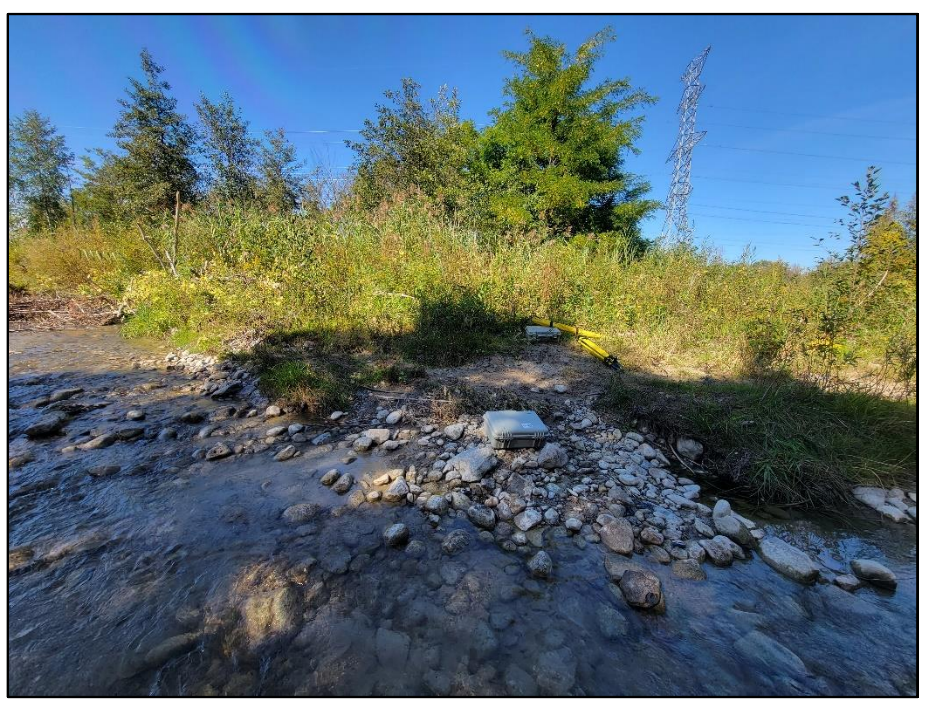

Figure B99. RIVT, Right Bank

Figure B100. RIVT, Bed

APPENDIX C: Aerial Imagery Linework

Mimico Creek (C1-C10)
Etobicoke Creek (C11-C20)
Highland Creek (C21-C30)
Duffins Creek (C31-C40)

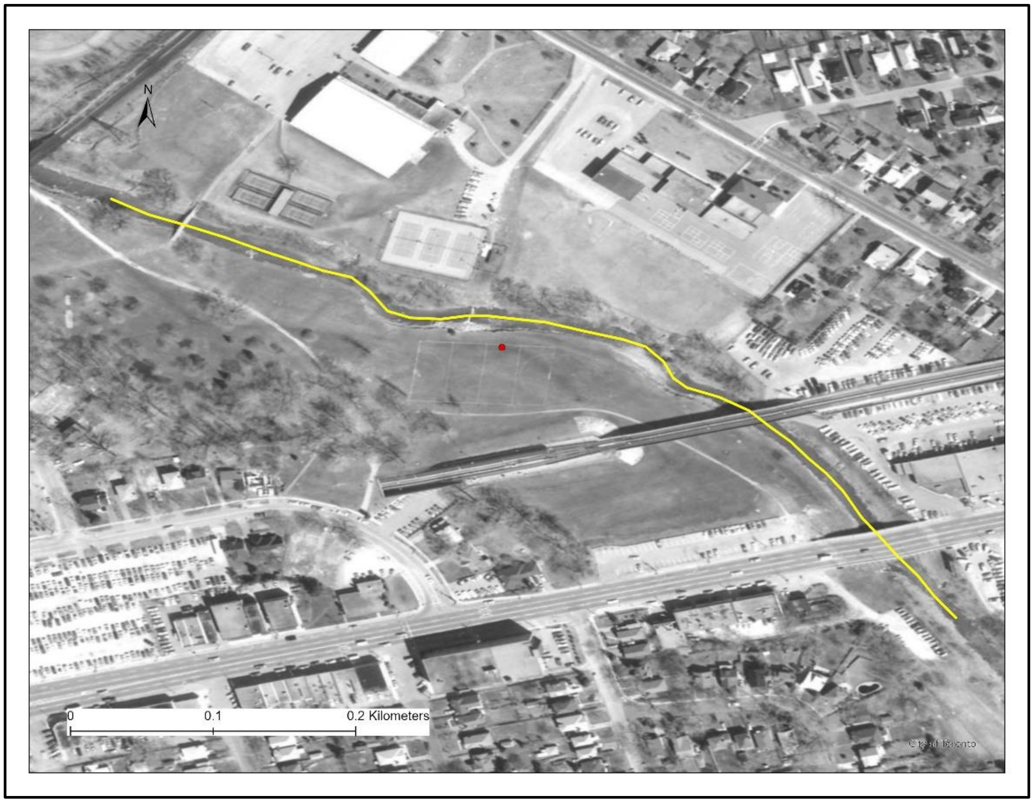

Figure C1. MCAI 1978 Thalweg Linework

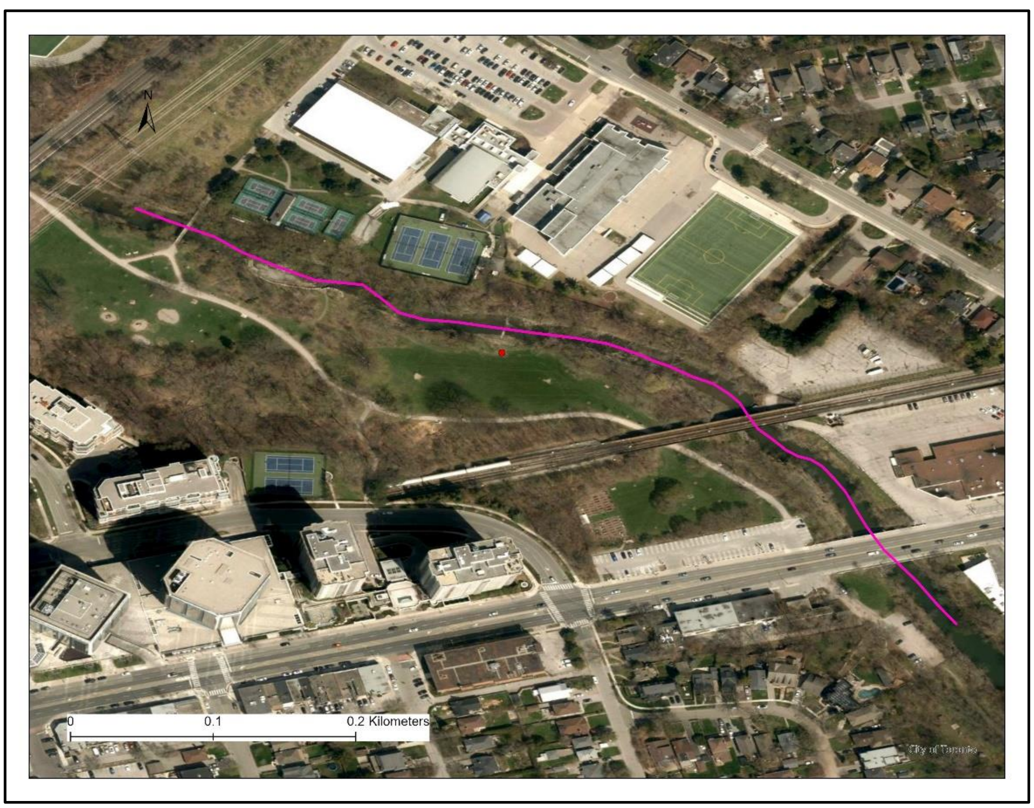

Figure C2. MCAI 2021 Thalweg Linework

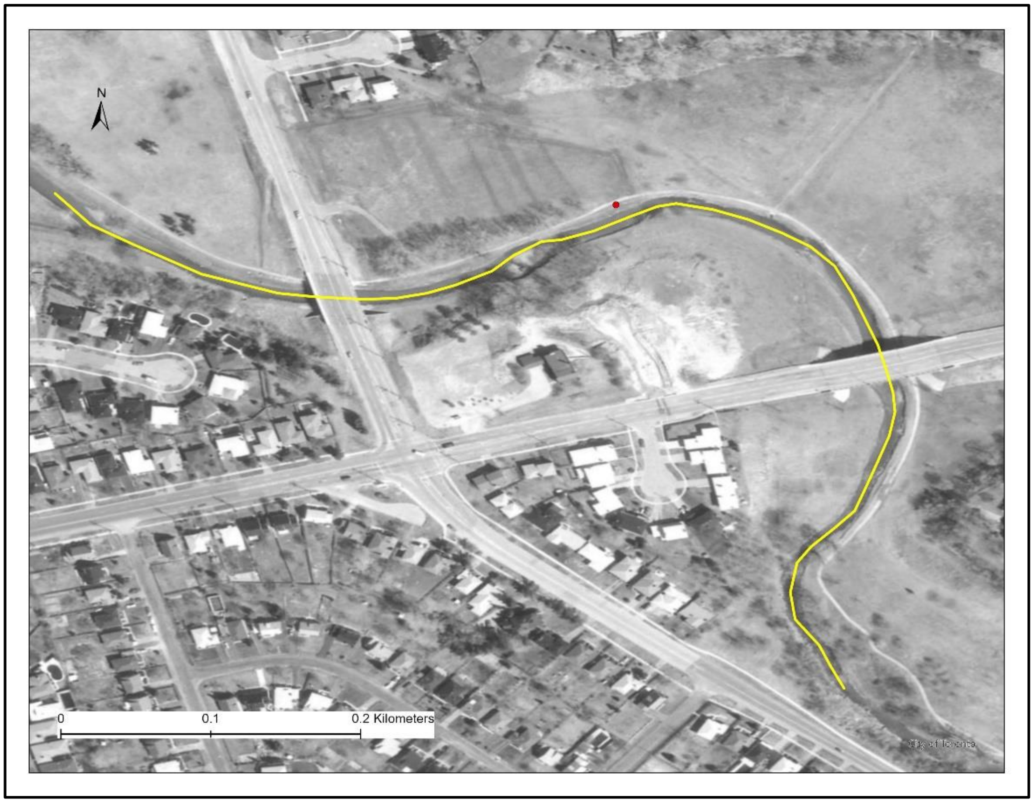

Figure C3. RAVP 1978 Thalweg Linework

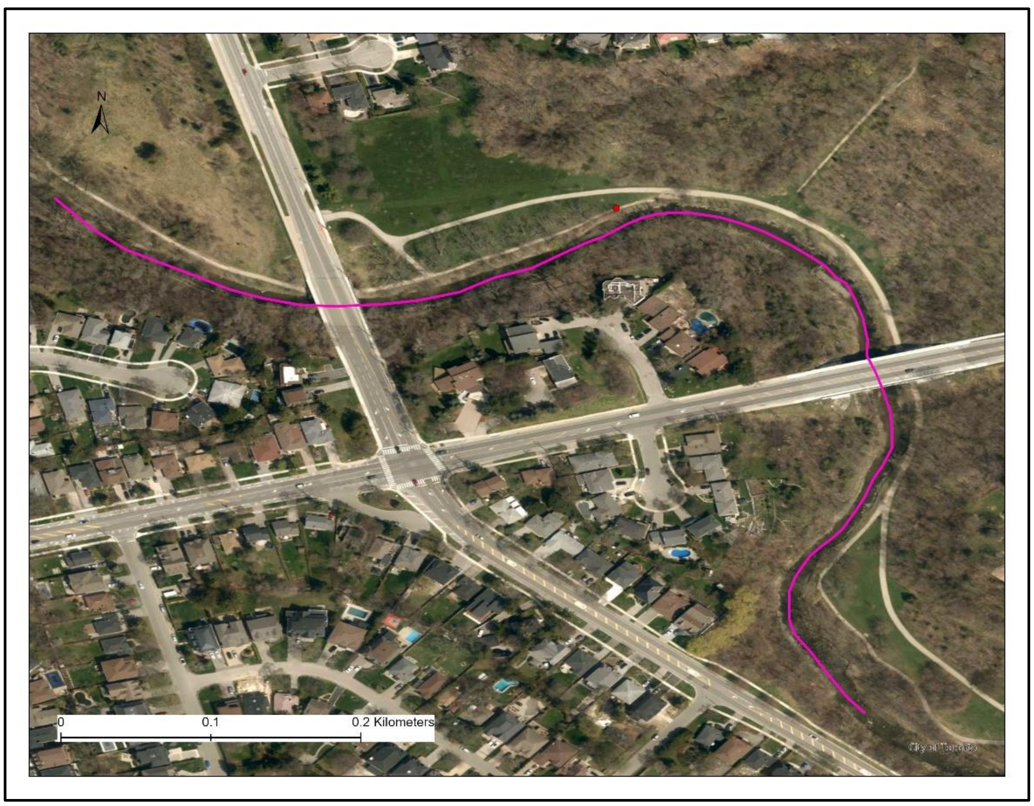

Figure C4. RAVP 2021 Thalweg Linework

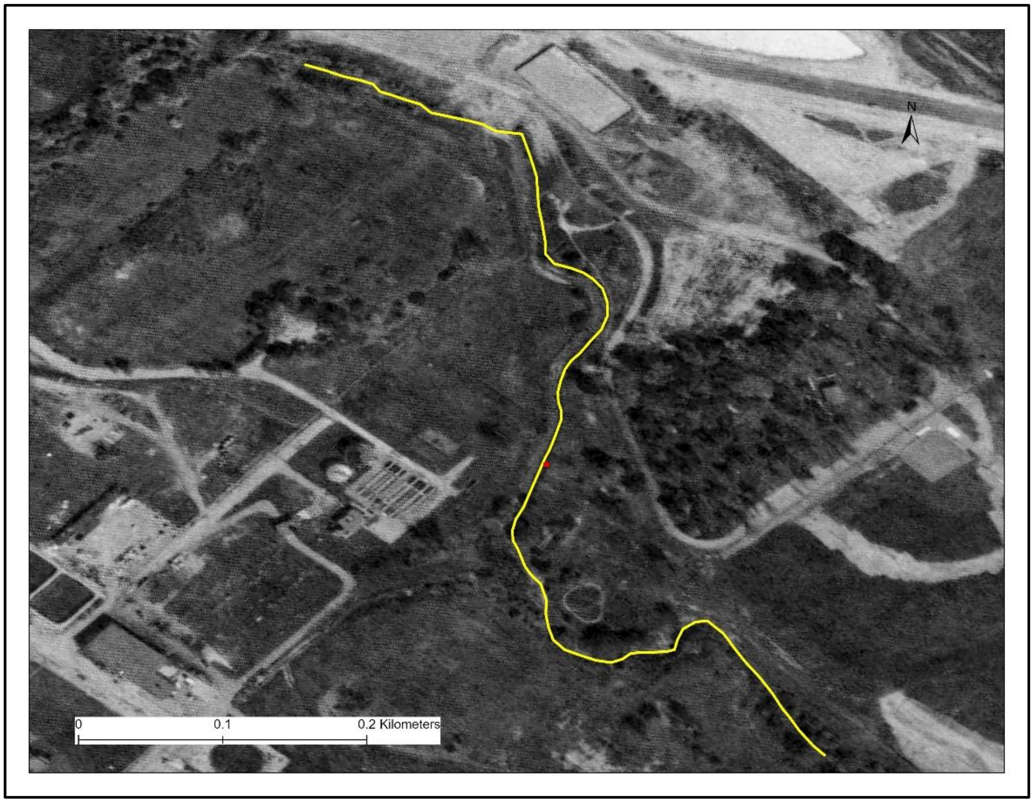

Figure C5. MATC 1973 Thalweg Linework

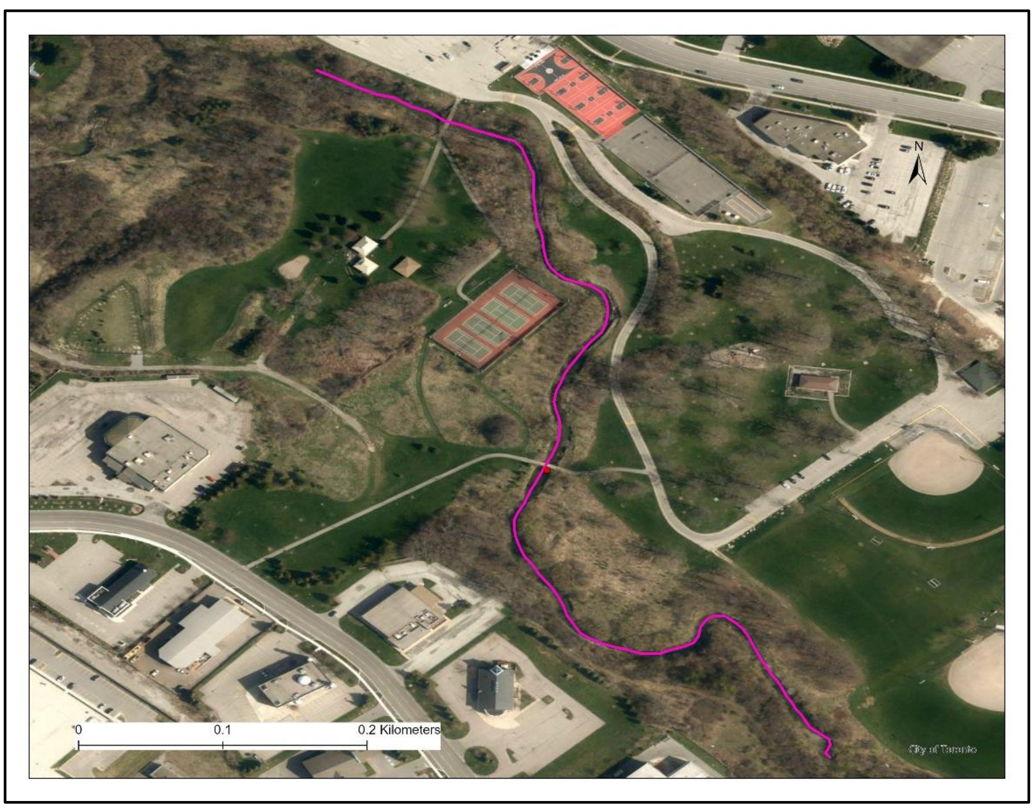

Figure C6. MATC 2021 Thalweg Linework

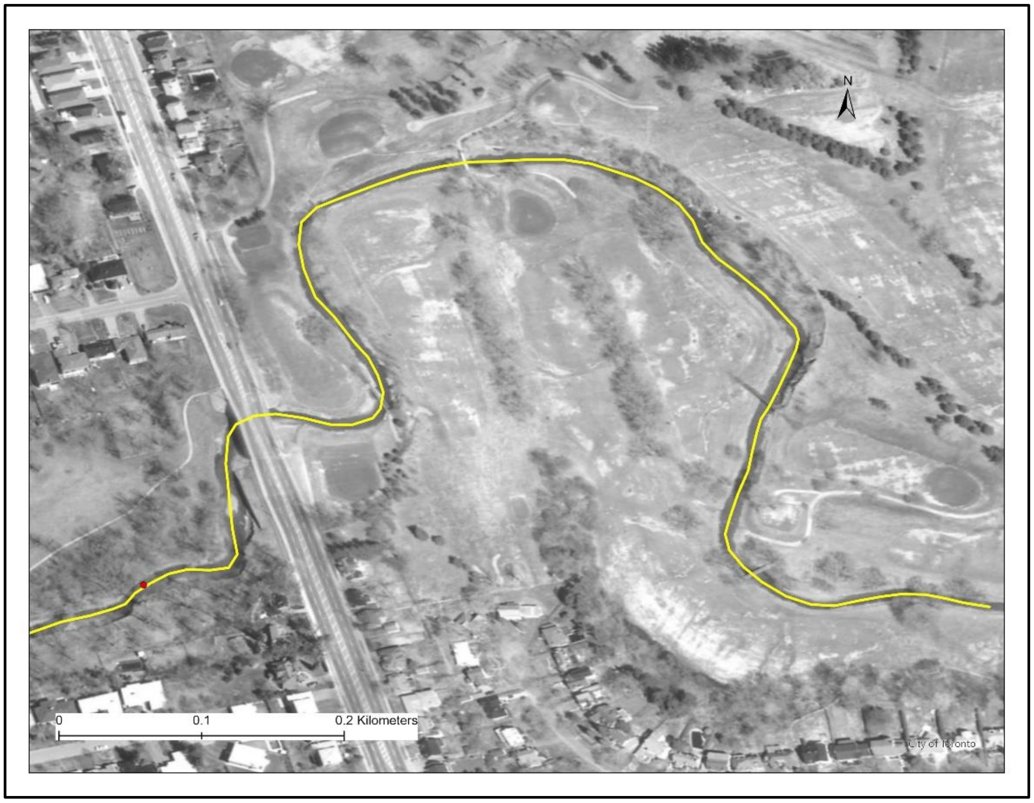

Figure C7. EVAP-A 1978 Thalweg Linework

Figure C8. EVAP-A 2021 Thalweg Linework

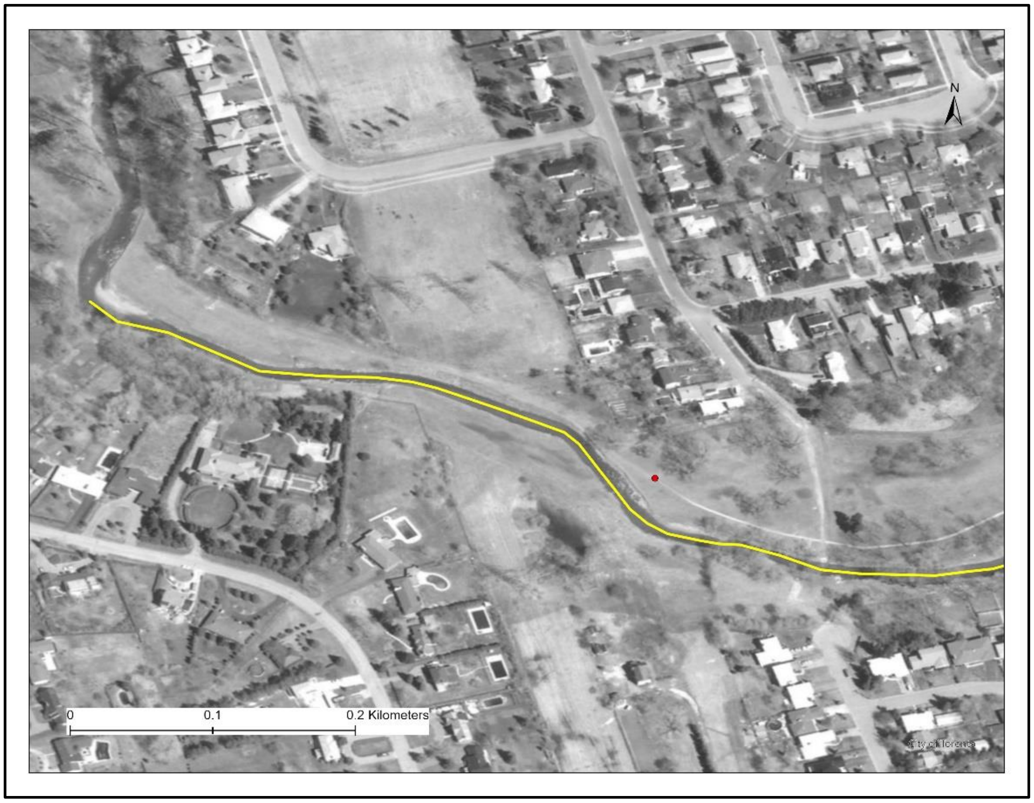

Figure C9. EVAP-B 1978 Thalweg Linework

Figure C10. EVAP-B 2021 Thalweg Linework

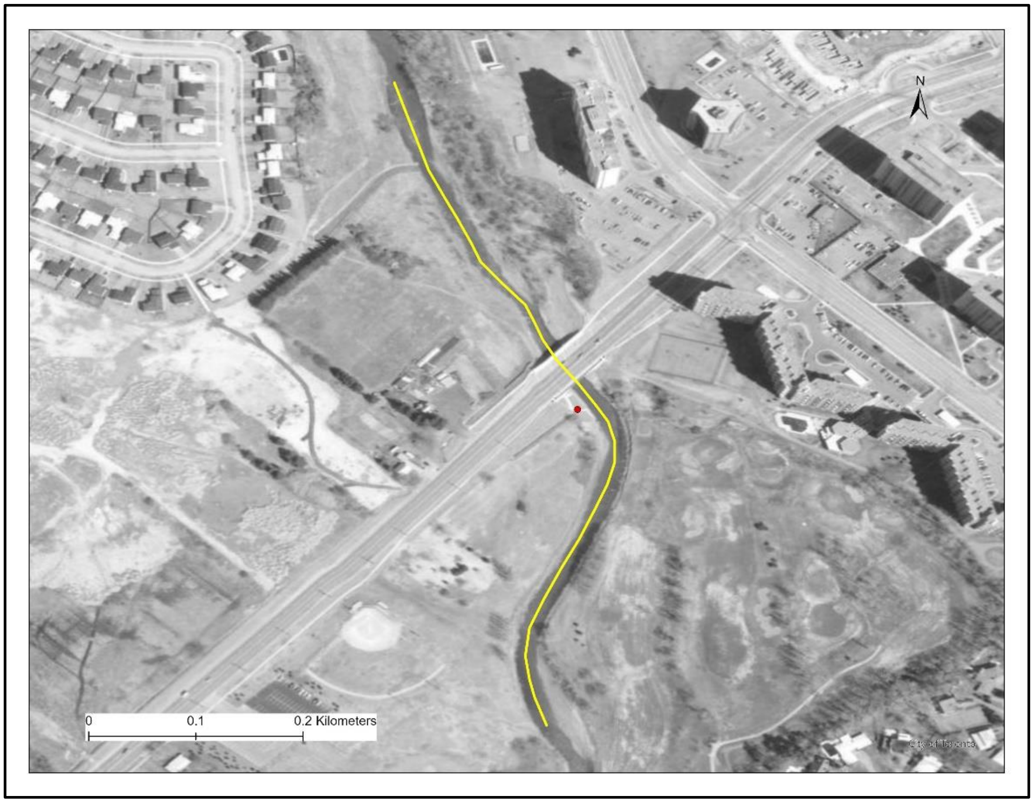

Figure C11. ECT-A 1978 Thalweg Linework

Figure C12. ECT-A 2021 Thalweg Linework

Figure C13. GET-6 1973 Thalweg Linework

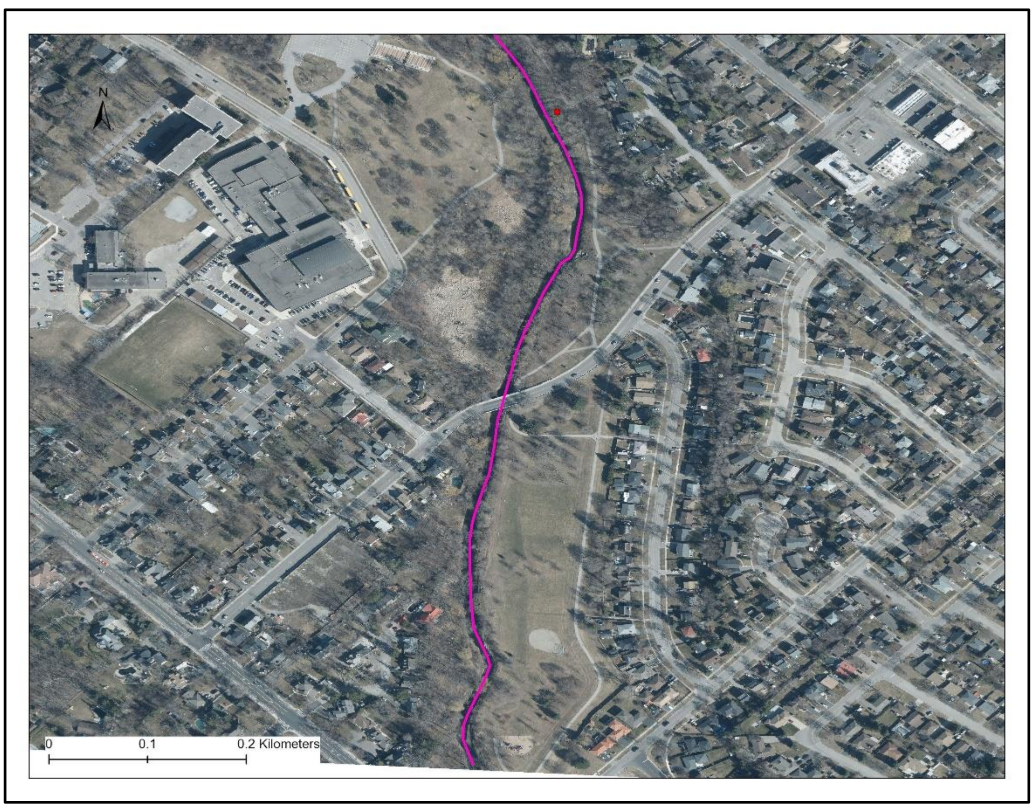

Figure C14. GET-6 2021 Thalweg Linework

Figure C15. CENP 1973 Thalweg Linework

Figure C16. CENP 2021 Thalweg Linework

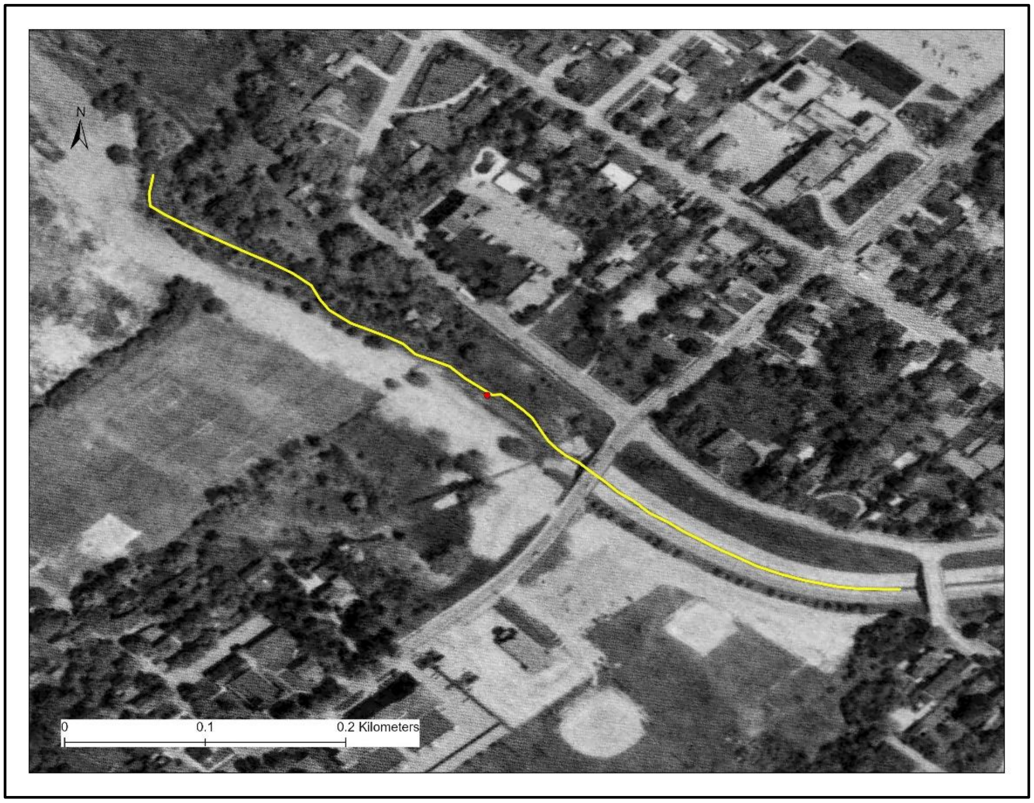

Figure C17. ECAB 1973 Thalweg Linework

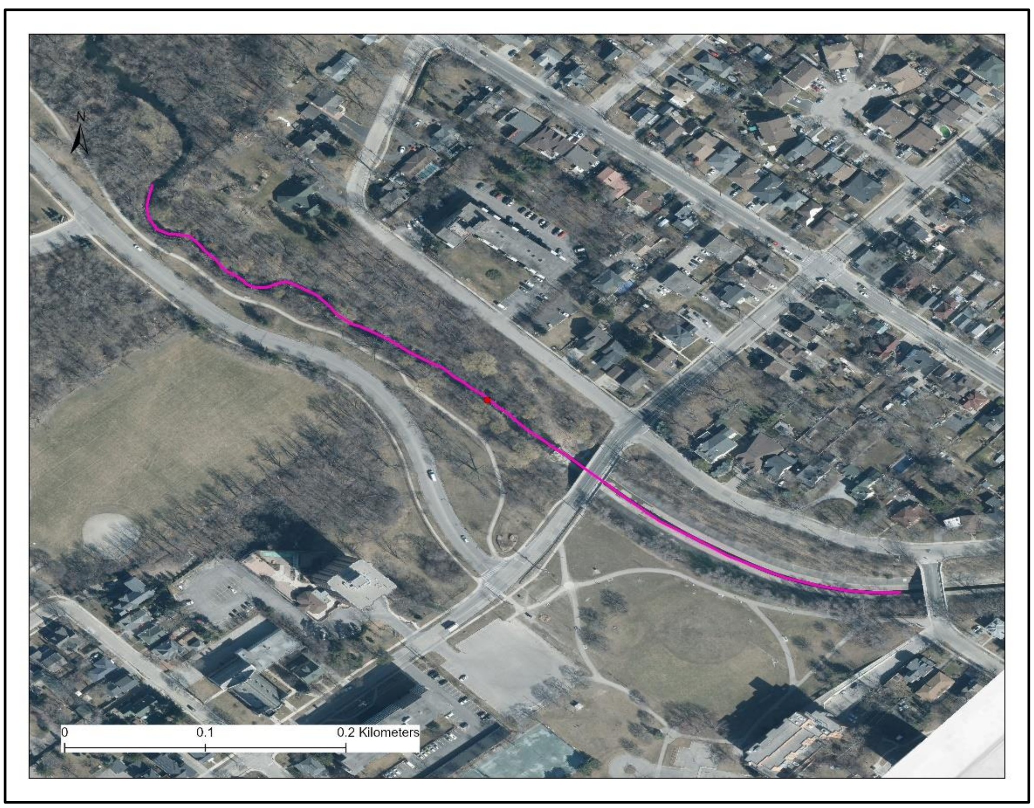

Figure C18. ECAB 2021 Thalweg Linework

Figure C19. GET-2 1978 Thalweg Linework

Figure C20. GET-2 2021 Thalweg Linework

Figure C21. BDR-B 1978 Thalweg Linework

Figure C22. BDR-B 2021 Thalweg Linework

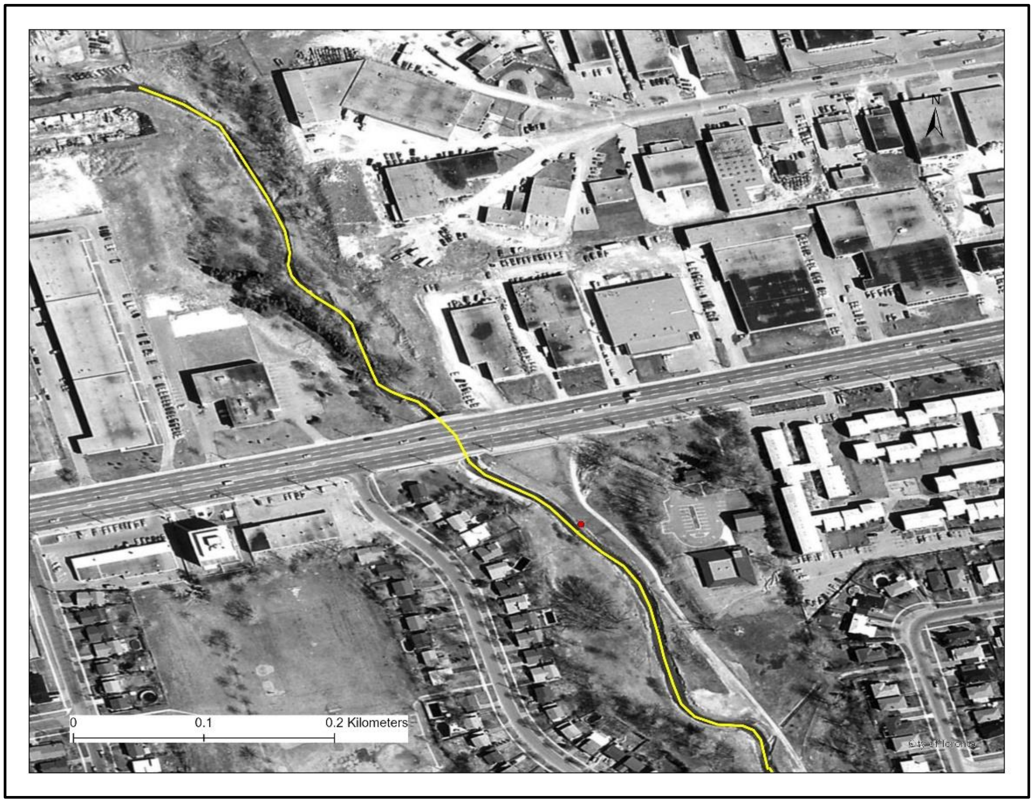

Figure C23. BDR-A 1978 Thalweg Linework

Figure C24. BDR-A 2021 Thalweg Linework

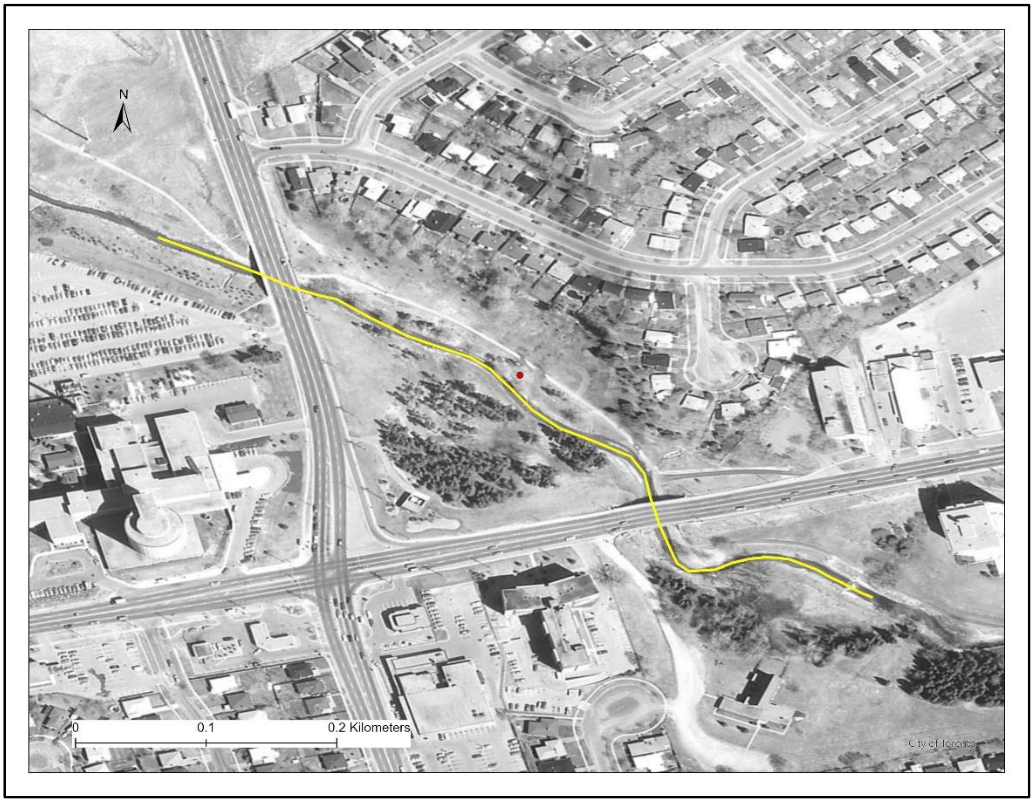

Figure C25. BENP 1978 Thalweg Linework

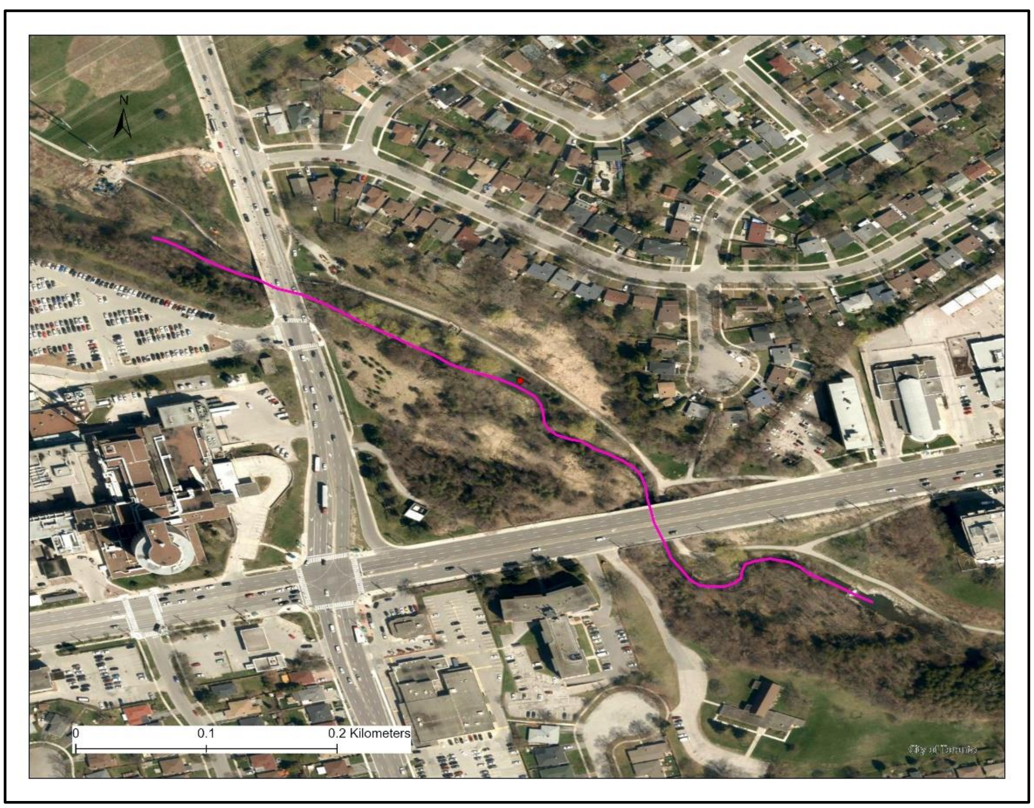

Figure C26. BENP 2021 Thalweg Linework

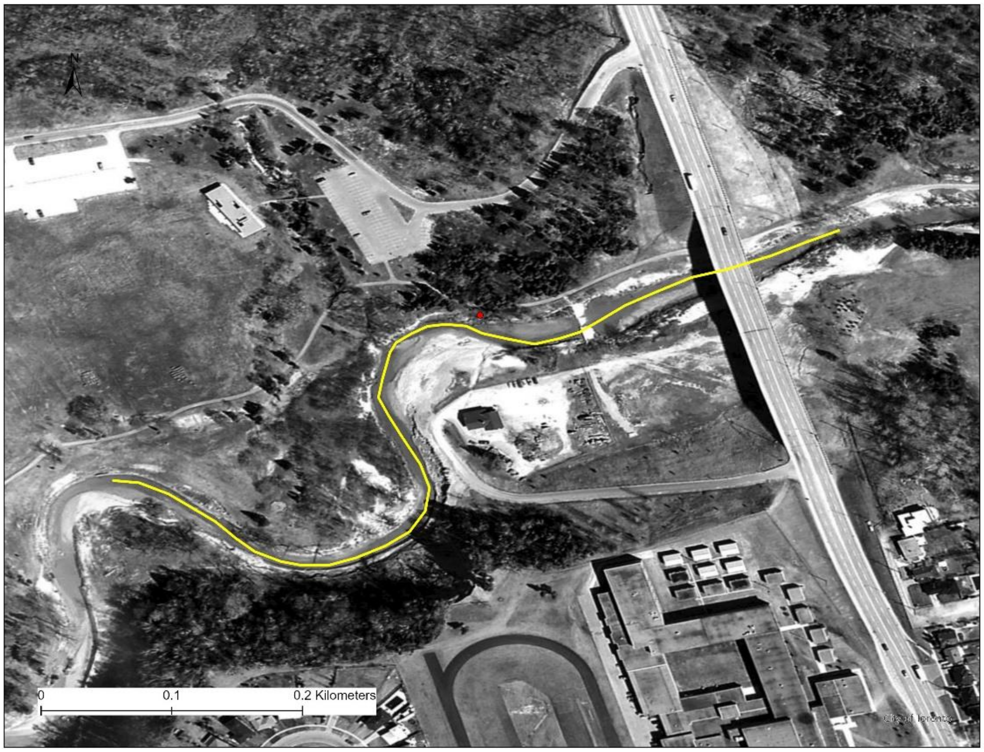

Figure C27. MSPT 1978 Thalweg Linework

Figure C28. MSPT 2021 Thalweg Linework

Figure C29. CDBP 1978 Thalweg Linework

Figure C30. CDBP 2021 Thalweg Linework

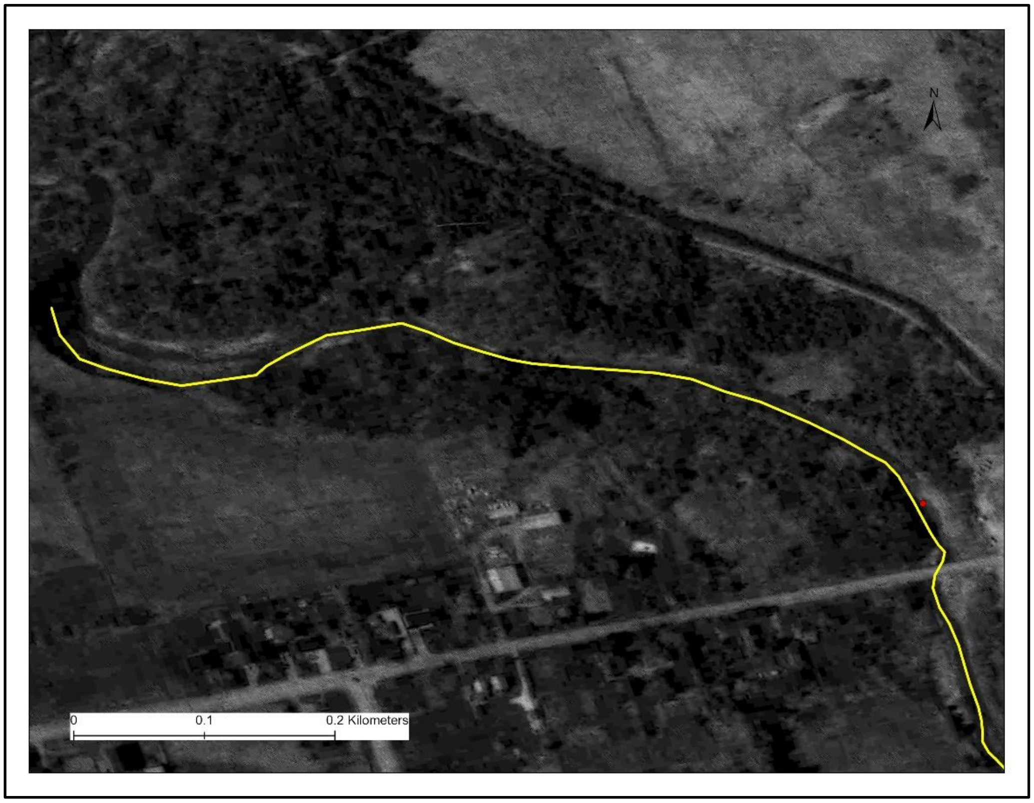

Figure C31. SHT-A 1977 Thalweg Linework

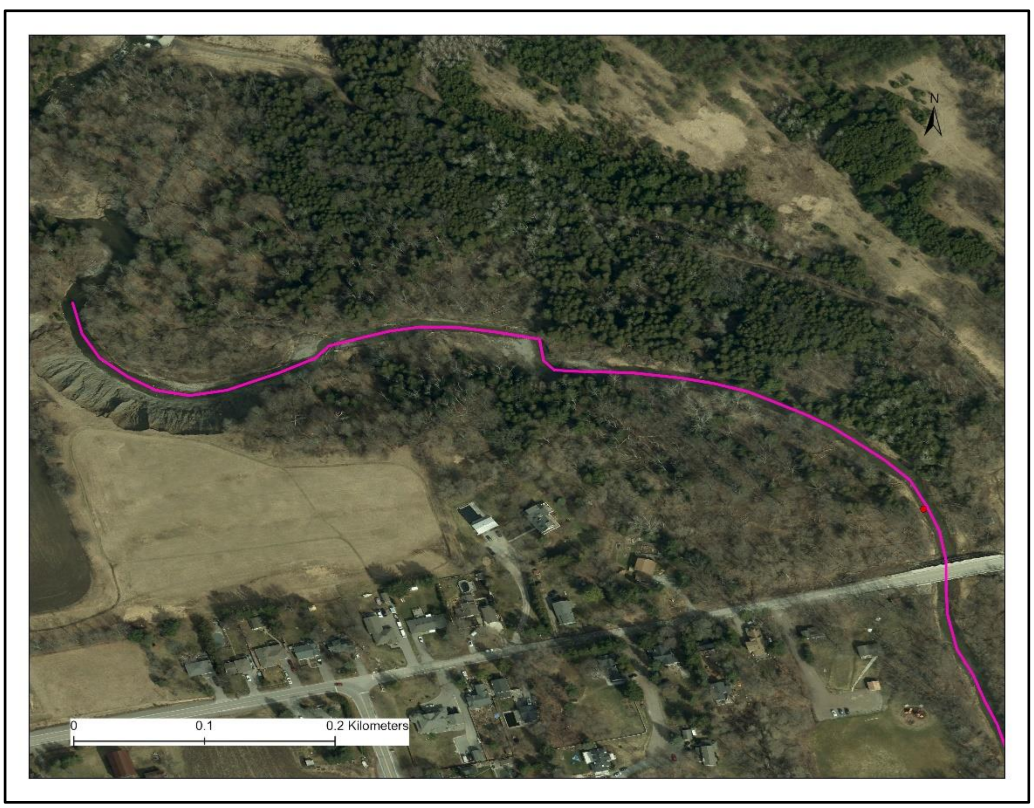

Figure C32. SHT-A 2021 Thalweg Linework

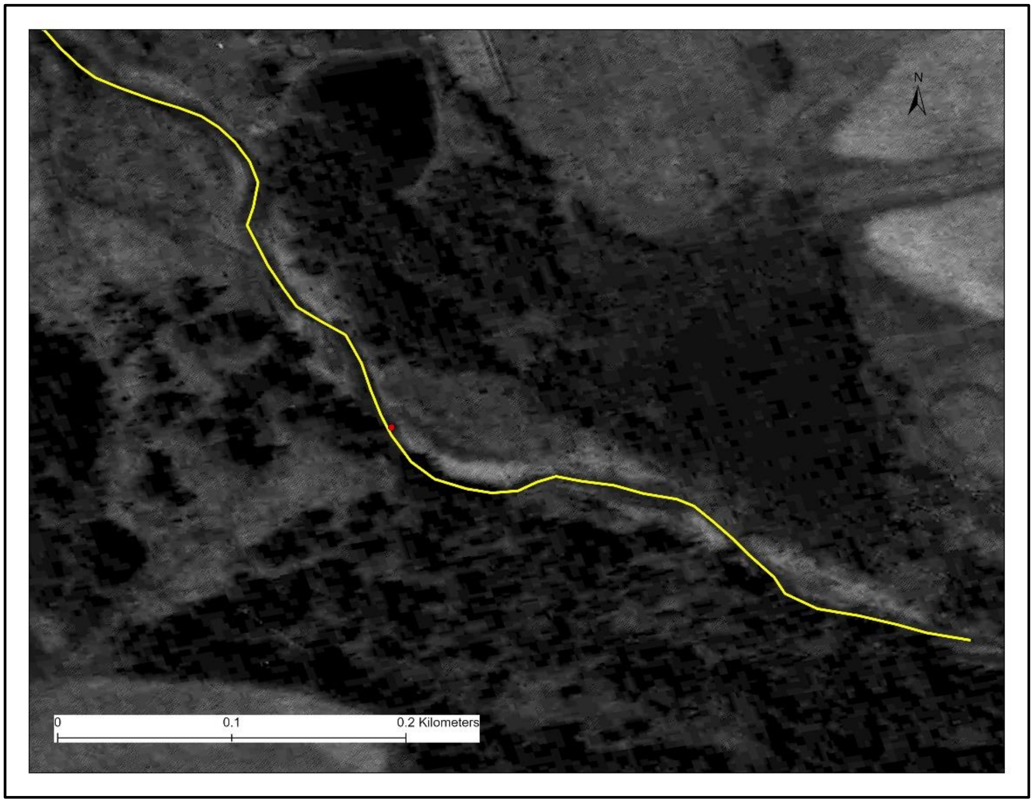

Figure C33. SHT-B 1977 Thalweg Linework

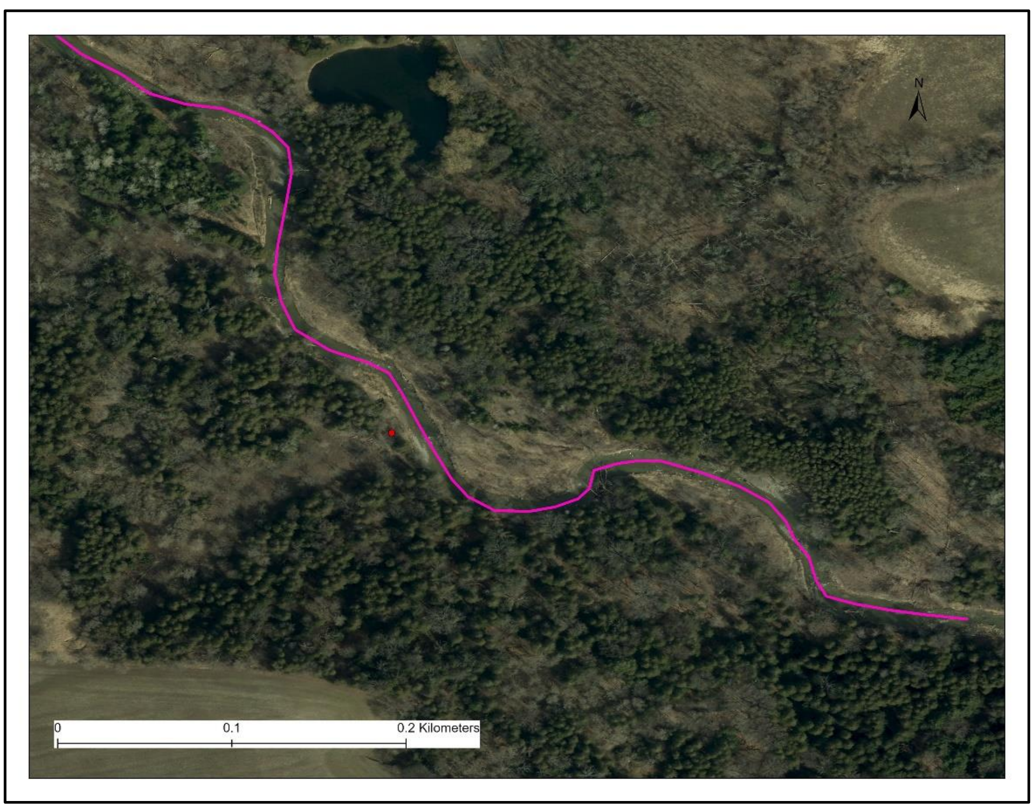

Figure C34. SHT-B 2021 Thalweg Linework

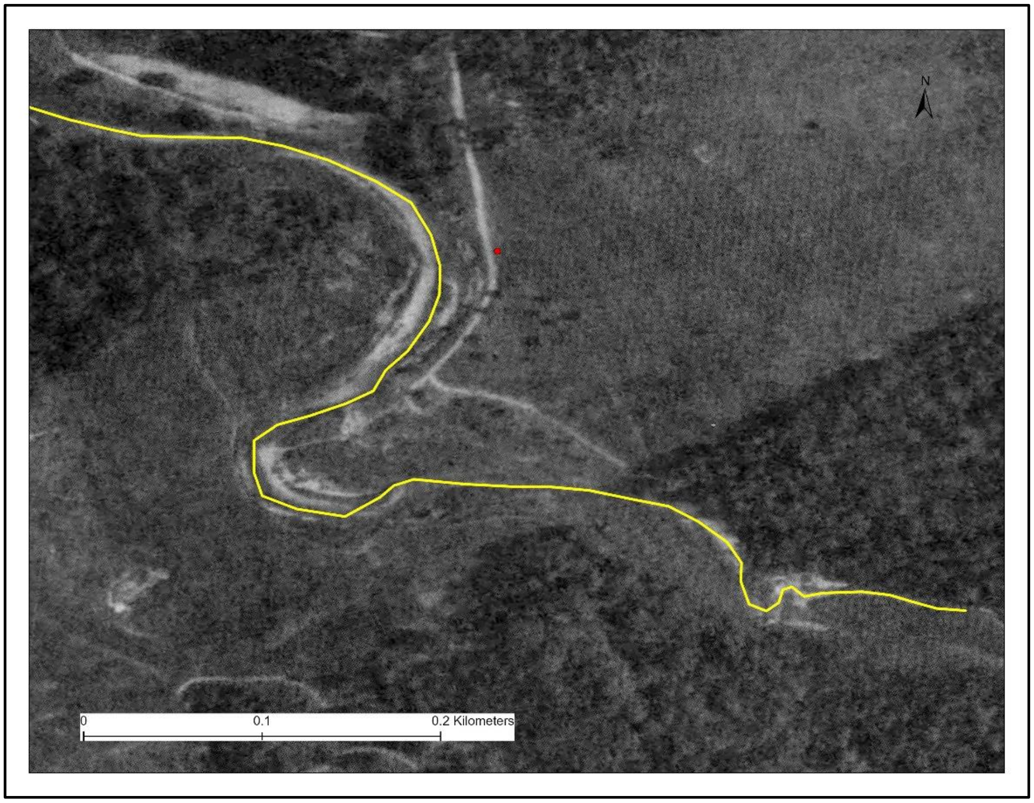

Figure C35. SHT-E 1973 Thalweg Linework

Figure C36. SHT-E 2021 Thalweg Linework

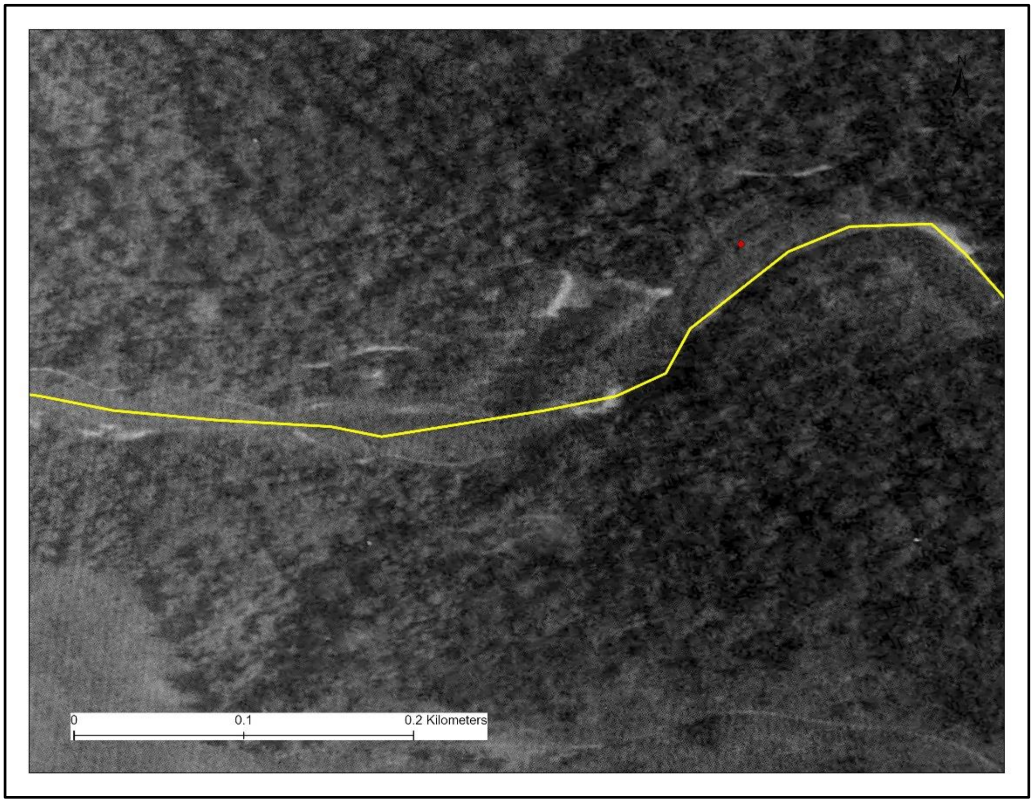

Figure C37. SHT-D 1973 Thalweg Linework

Figure C38. SHT-D 2021 Thalweg Linework

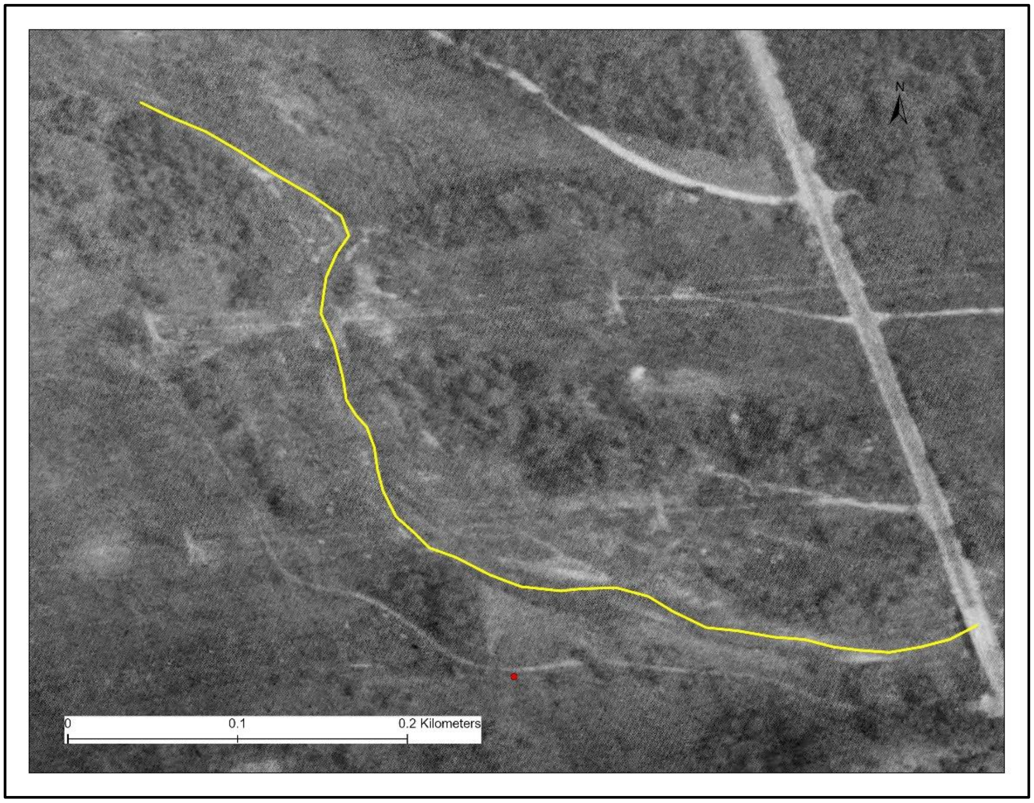

Figure C39. RIVT 1973 Thalweg Linework

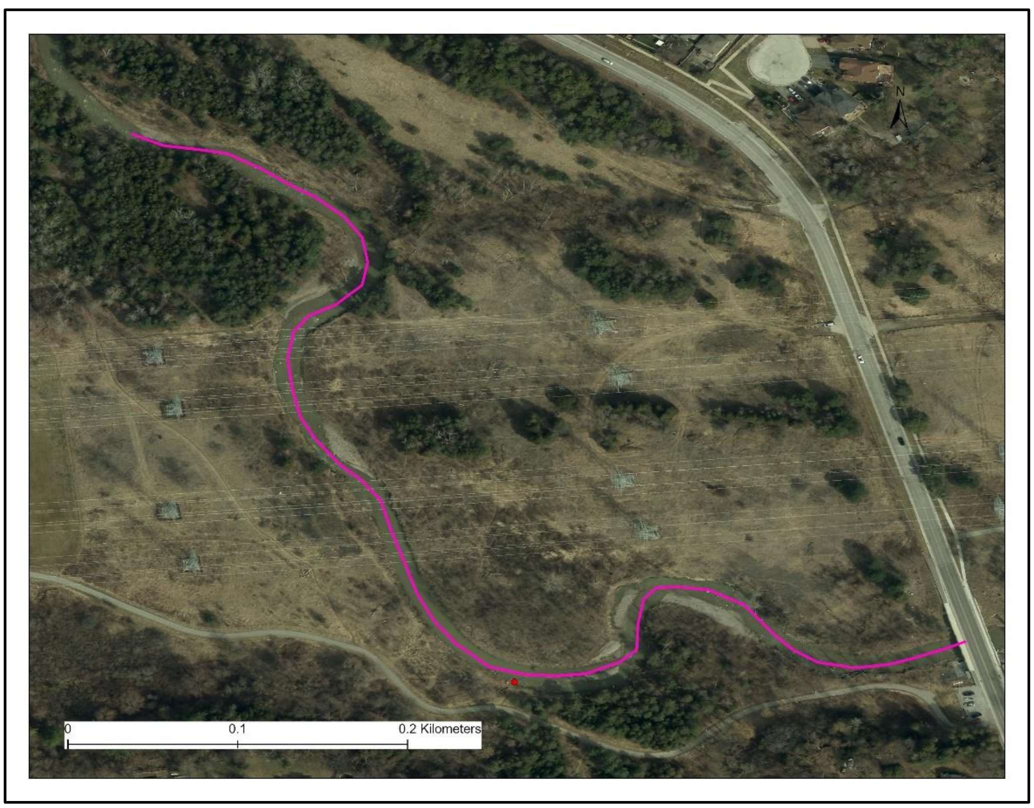

Figure C40. RIVT 2021 Thalweg Linework

APPENDIX D: Sinuosity Index Results

Site	Valley Length (m)	Channel Length (m)	Sinuosity (1970s)	Channel Length (m)	Sinuosity (2021)	Change
Mimico						
MCAI	500	532.91	1.065	519.13	1.038	*0.027*
RAVP	500	749.79	1.499	765.29	1.530	*0.031*
MATC	500	725.98	1.451	709.87	1.419	*0.032*
EVAP-A	500	1064.32	2.128	1084.94	2.169	*0.031*
EVAP-B	500	507.34	1.014	502.05	1.004	*0.010*
Etobicoke						
ECT-A	500	660.68	1.321	664.37	1.328	*0.007*
GET-6	500	805.74	1.611	797.26	1.594	*0.017*
CENP	500	543.01	1.086	550.09	1.100	*0.014*
ECAB	500	505.07	1.010	508.04	1.016	*0.006*
GET-2	500	927.21	1.854	929.97	1.859	*0.005*
Highland						
BDR-B	500	844.31	1.688	836.14	1.672	*0.016*
BDR-A	500	656.64	1.313	676.72	1.353	*0.040*
BENP	500	518.02	1.036	540.32	1.080	*0.044*
MSPT	500	622.67	1.245	595.52	1.191	*0.054*
CDBP	500	758.1	1.516	698.17	1.396	*0.120*
Duffins						
SHT-A	500	780.14	1.560	844.84	1.689	*0.129*
SHT-B	500	578.07	1.156	561.88	1.123	*0.033*
SHT-E	500	681.01	1.362	773.74	1.547	*0.185*
SHT-D	500	643.63	1.287	792.83	1.585	*0.298*
RIVT	500	551.4	1.102	649.44	1.298	*0.196*
Average		**682.802**	**1.365**	**700.031**	**1.400**	***0.065***

APPENDIX E: Cross-Sectional Profile Graphs

Mimico Creek (E1-E5)
Etobicoke Creek (E6-E10)
Highland Creek (E11-E15)
Duffins Creek (E16-E20)

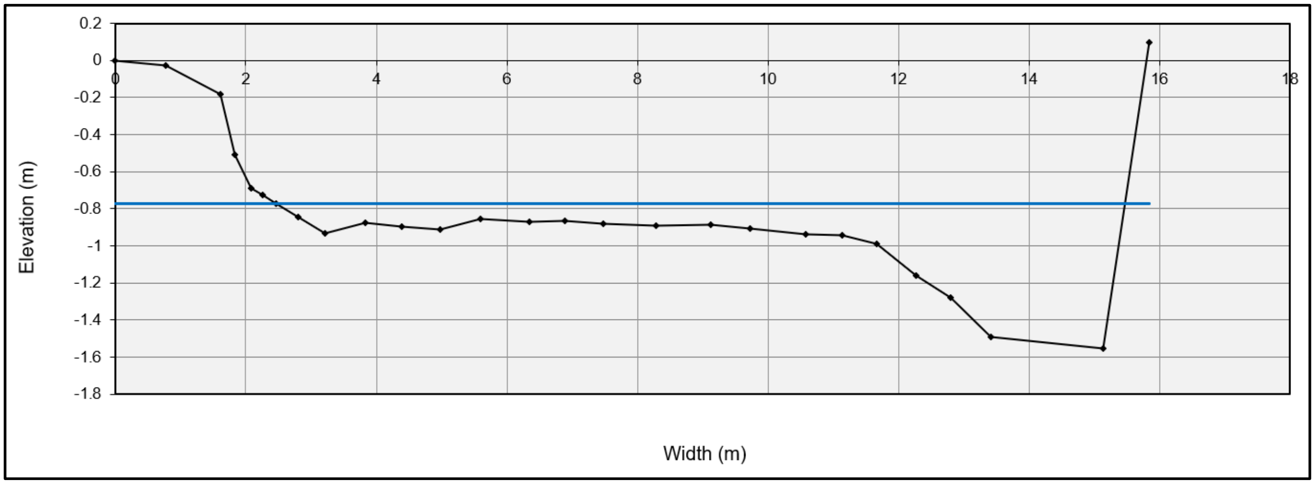

Figure E1. MCAI Cross-Section Profile

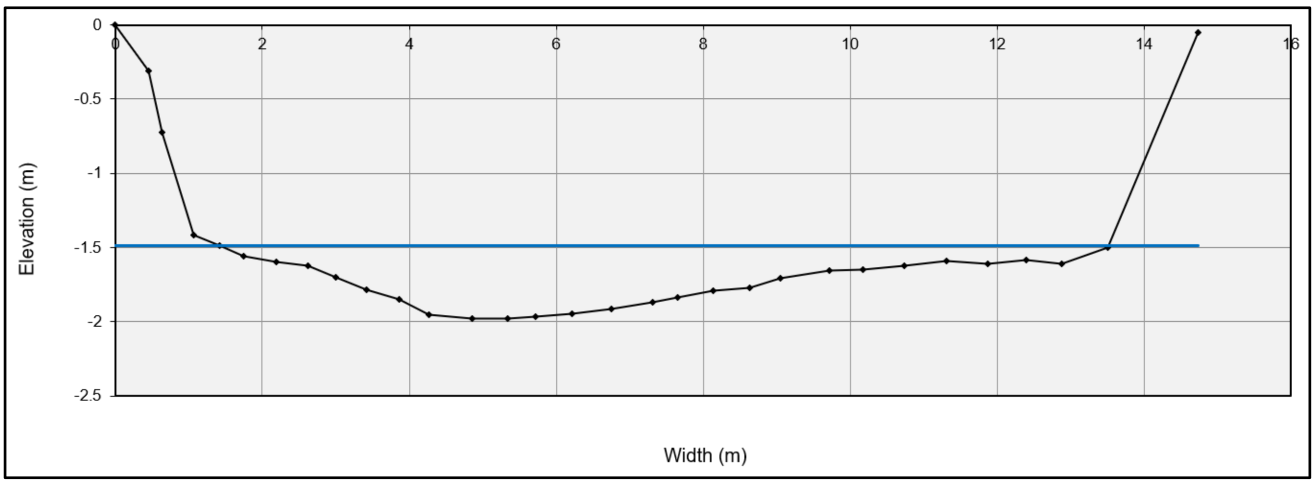

Figure E2. RAVP Cross-Section Profile

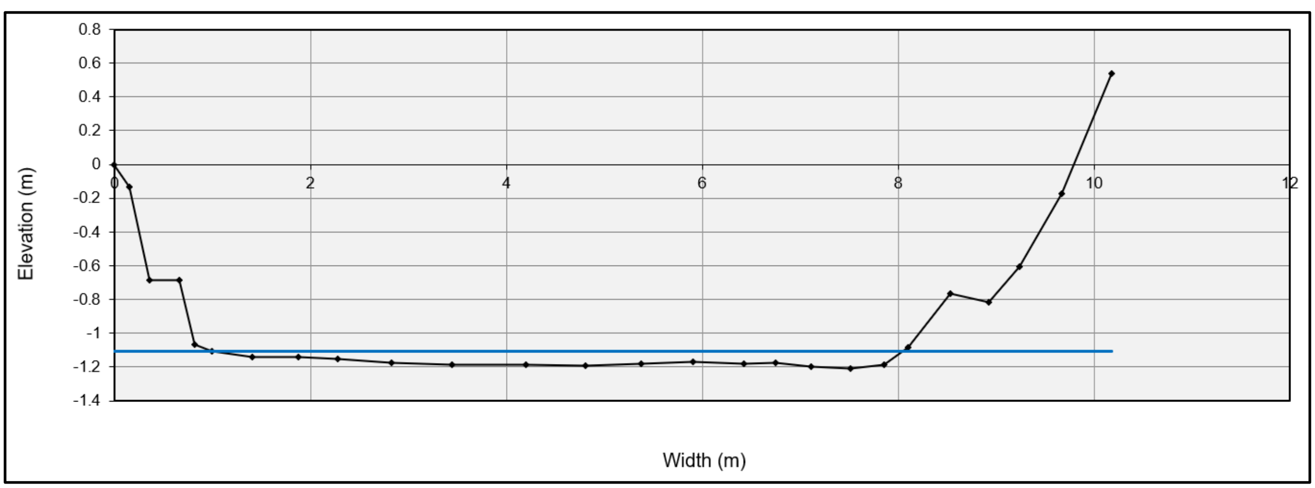

Figure E3. MATC Cross-Section Profile

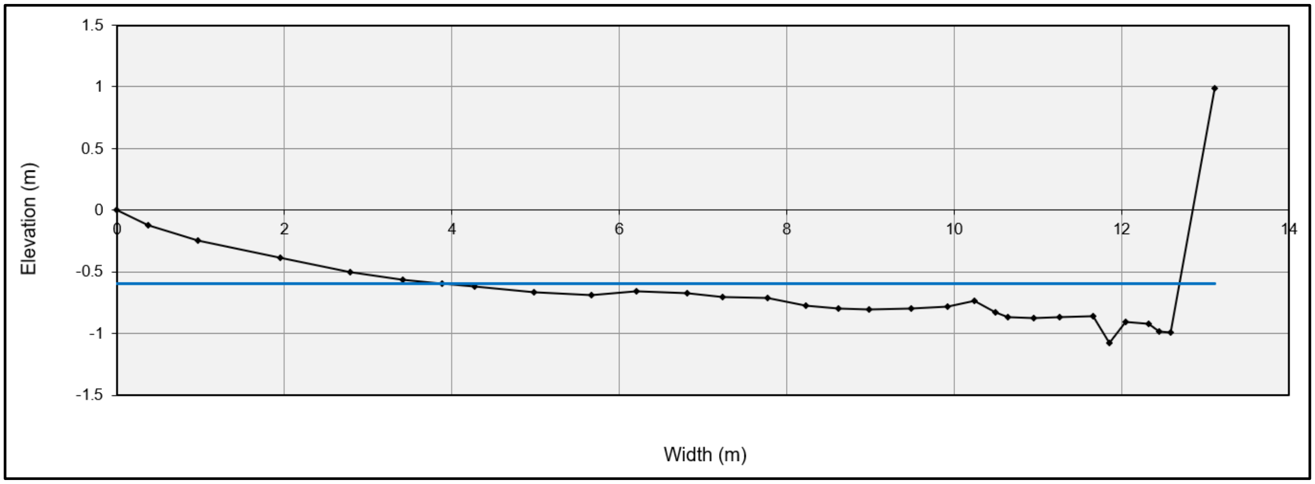

Figure E4. EVAP-A Cross-Section Profile

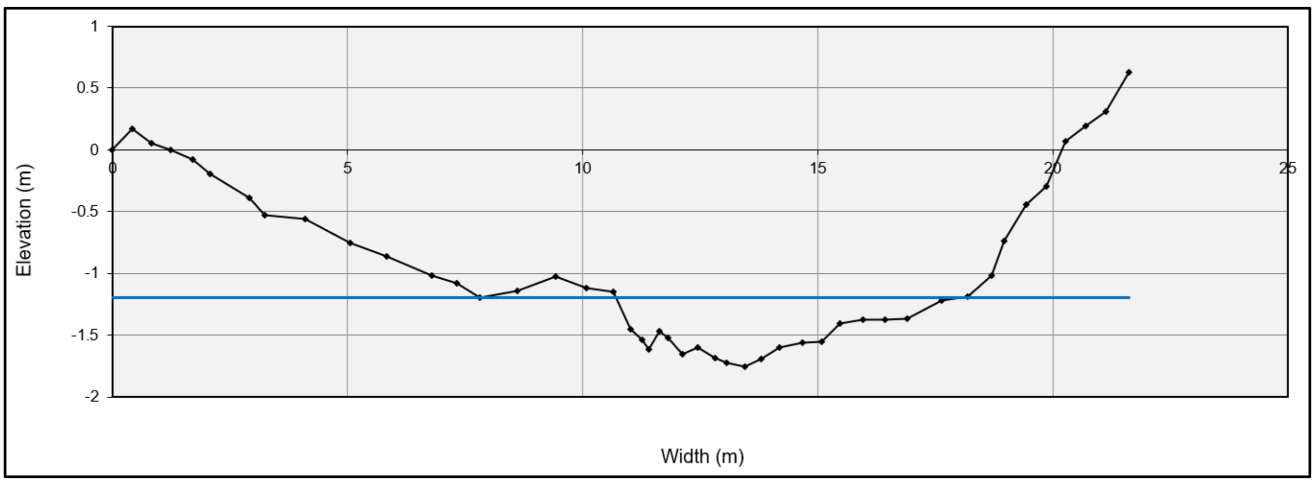

Figure E5. EVAP-B Cross-Section Profile

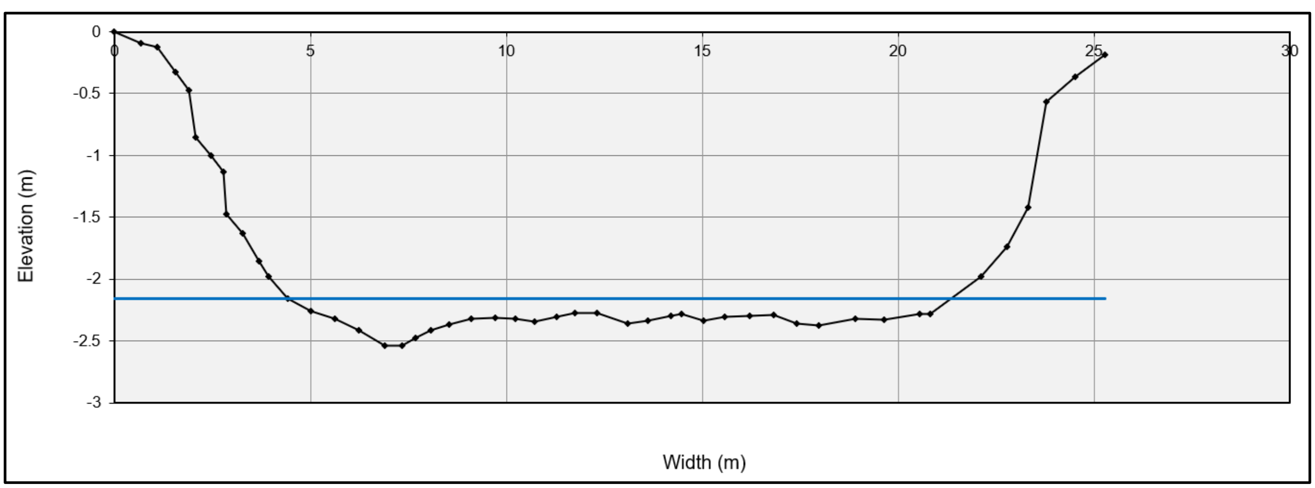

Figure E6. ECT-A Cross-Section Profile

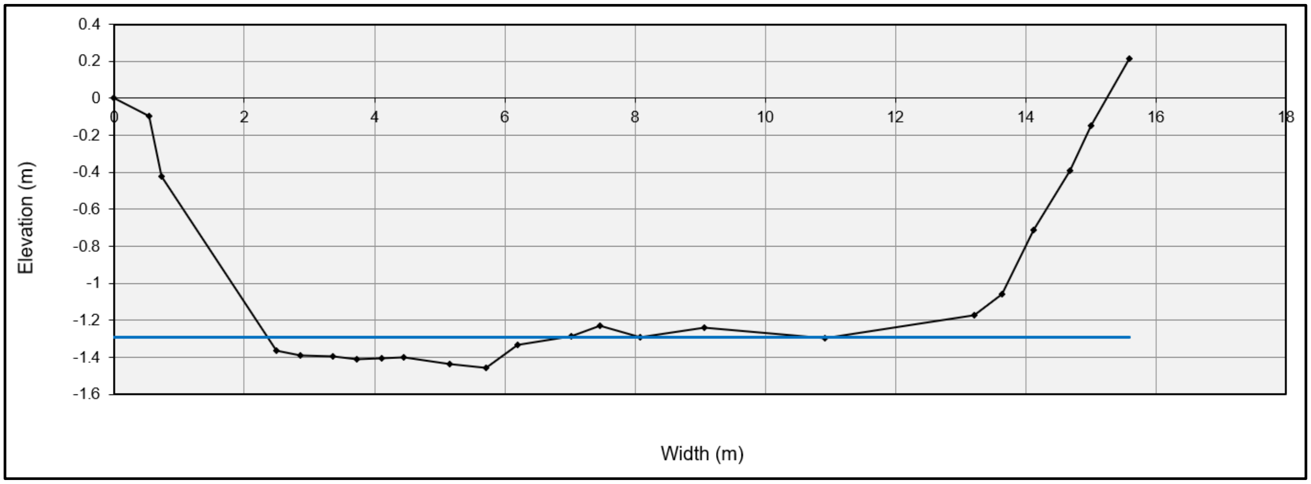

Figure E7. GET-6 Cross-Section Profile

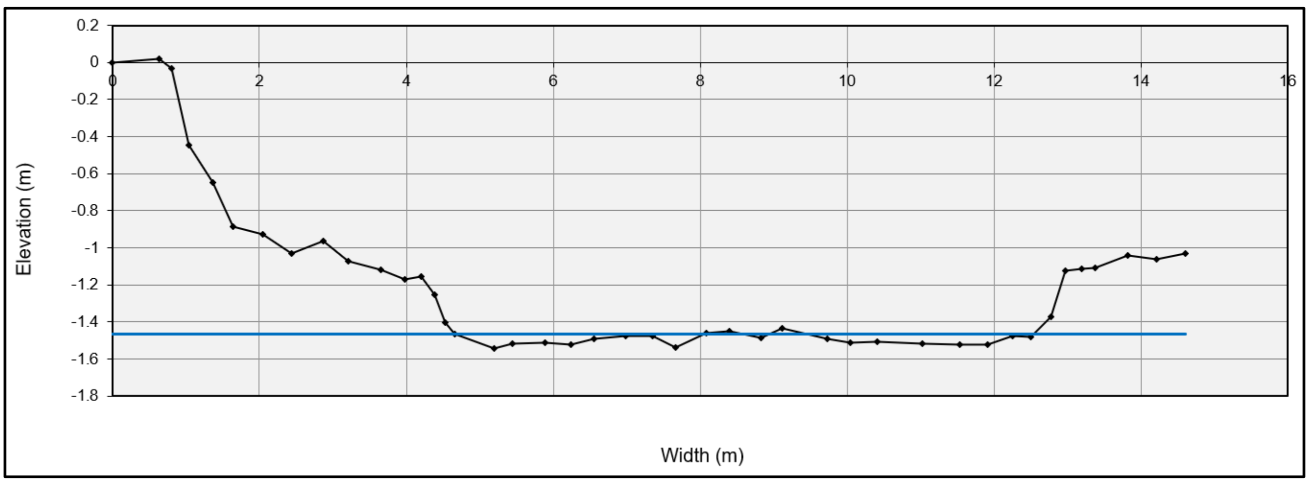

Figure E8. CENP Cross-Section Profile

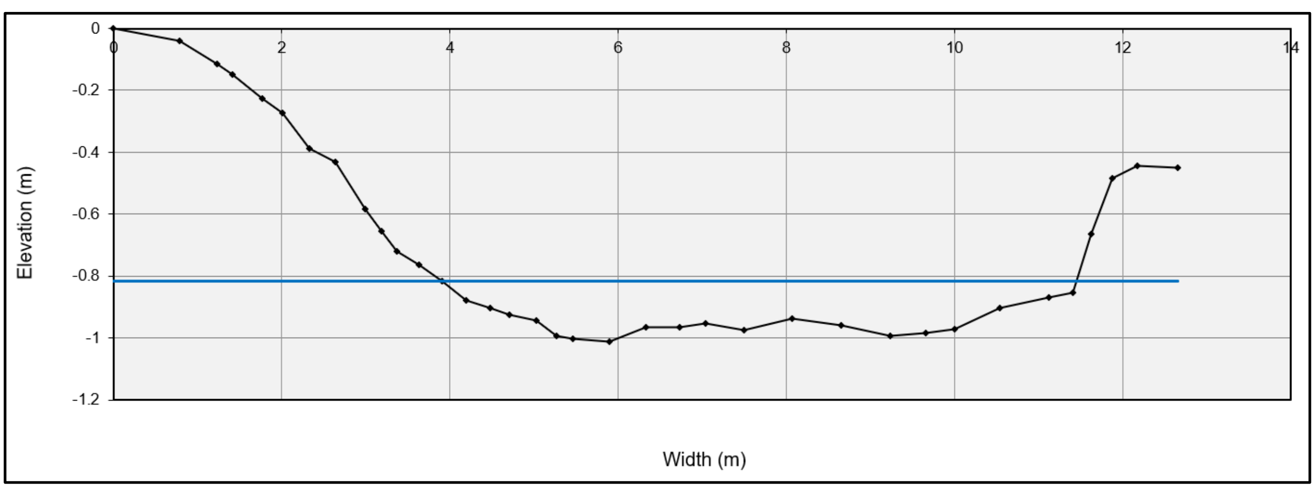

Figure E9. ECAB Cross-Section Profile

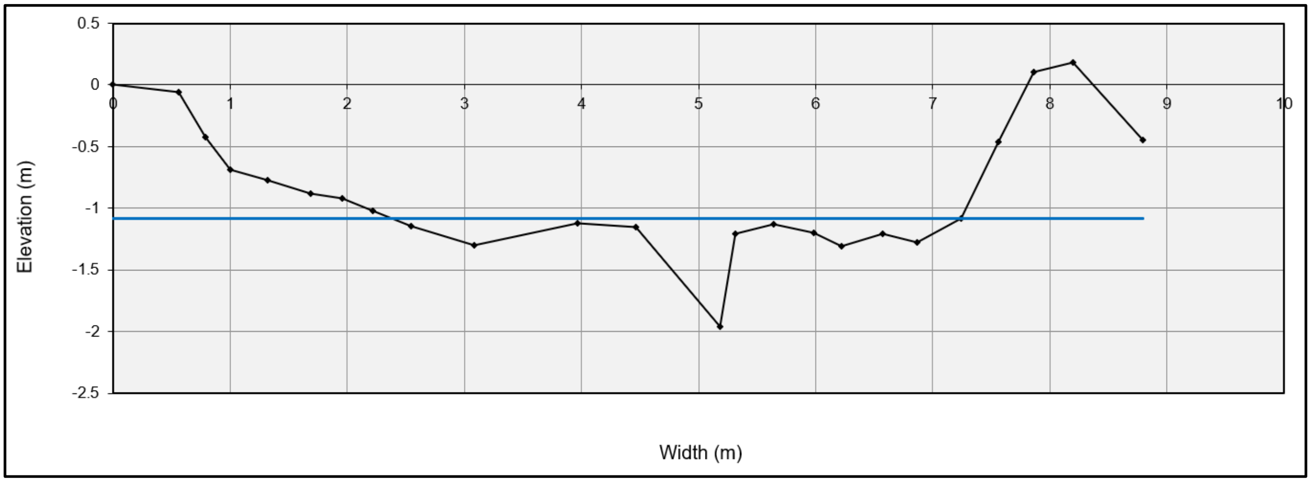

Figure E10. GET-2 Cross-Section Profile

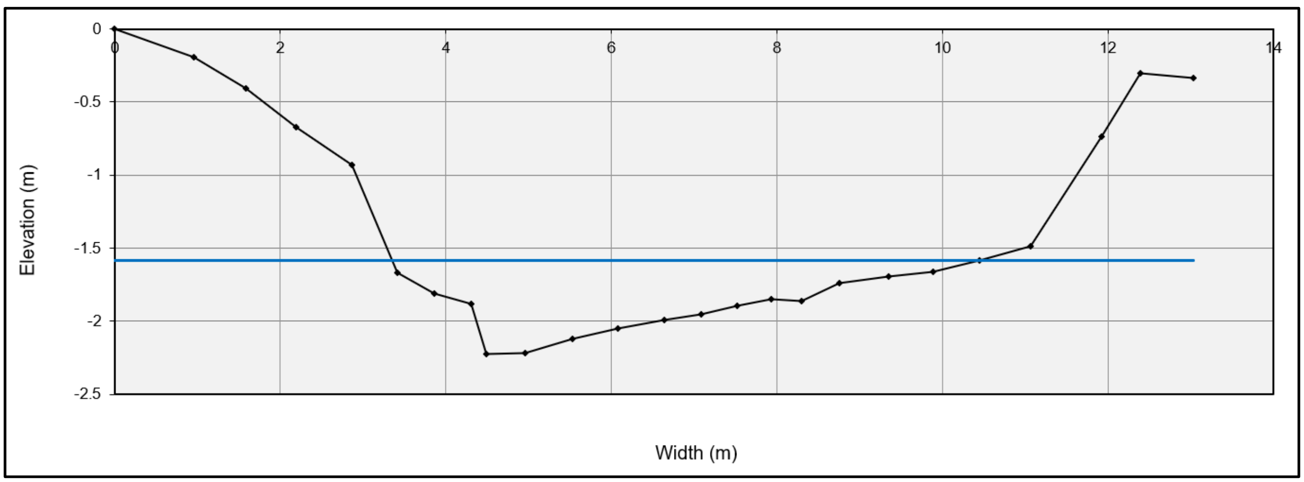

Figure E11. BDR-B Cross-Section Profile

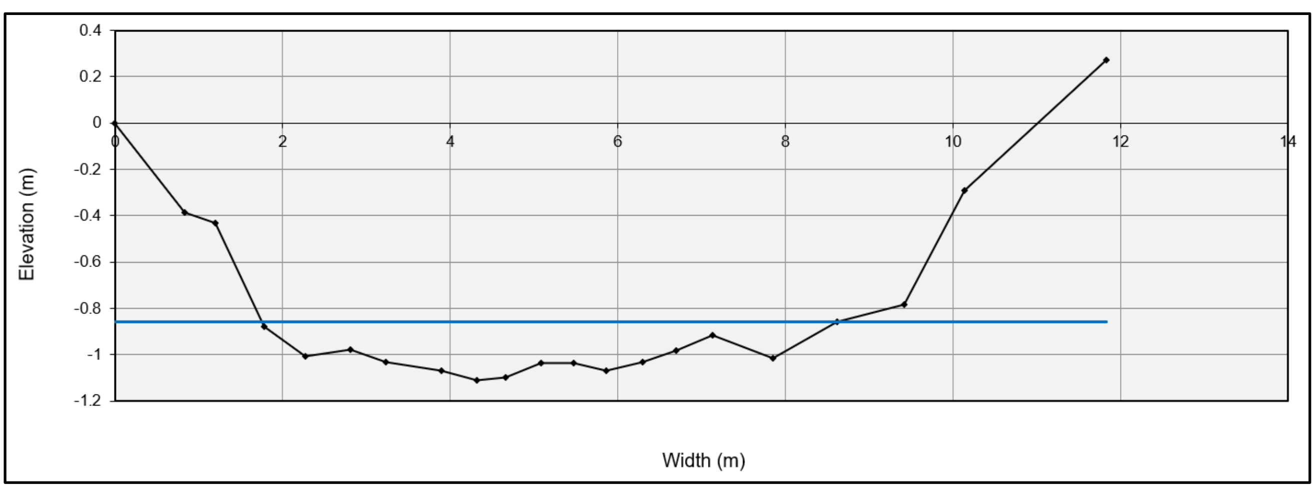

Figure E12. BDR-A Cross-Section Profile

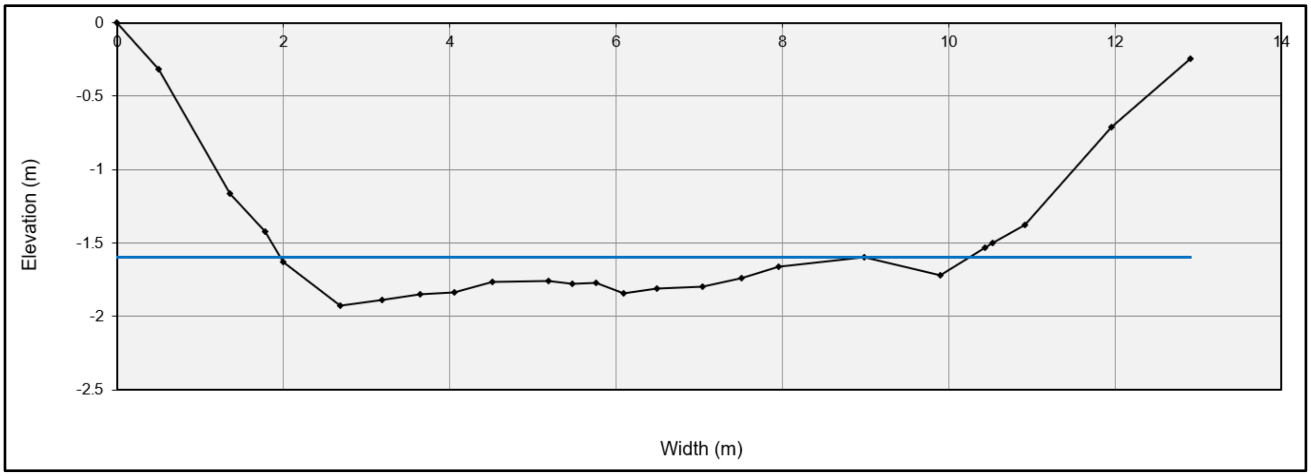

Figure E13. BENP Cross-Section Profile

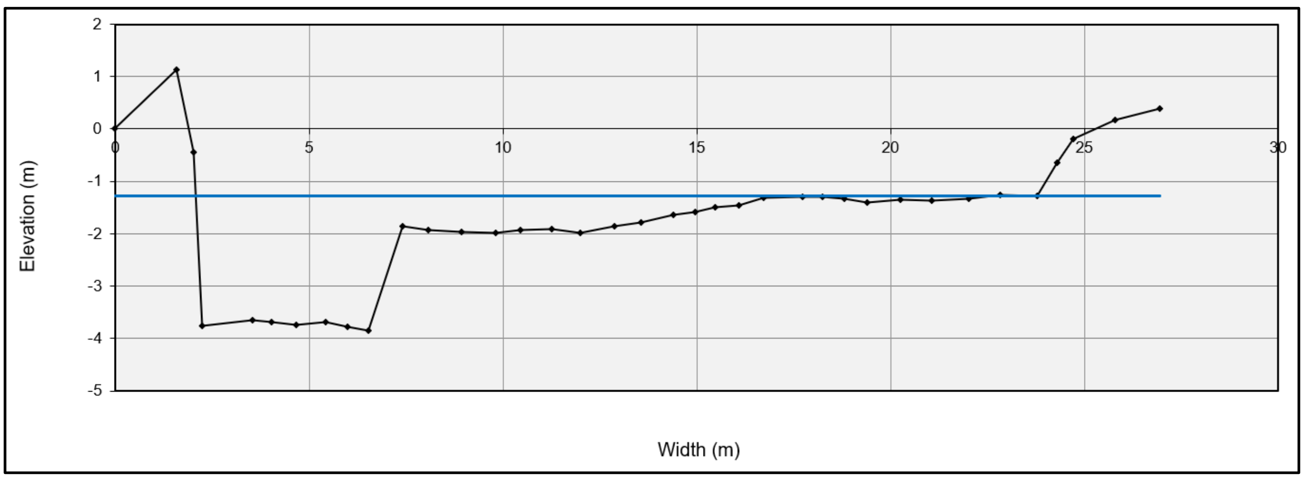

Figure E14. MSPT Cross-Section Profile

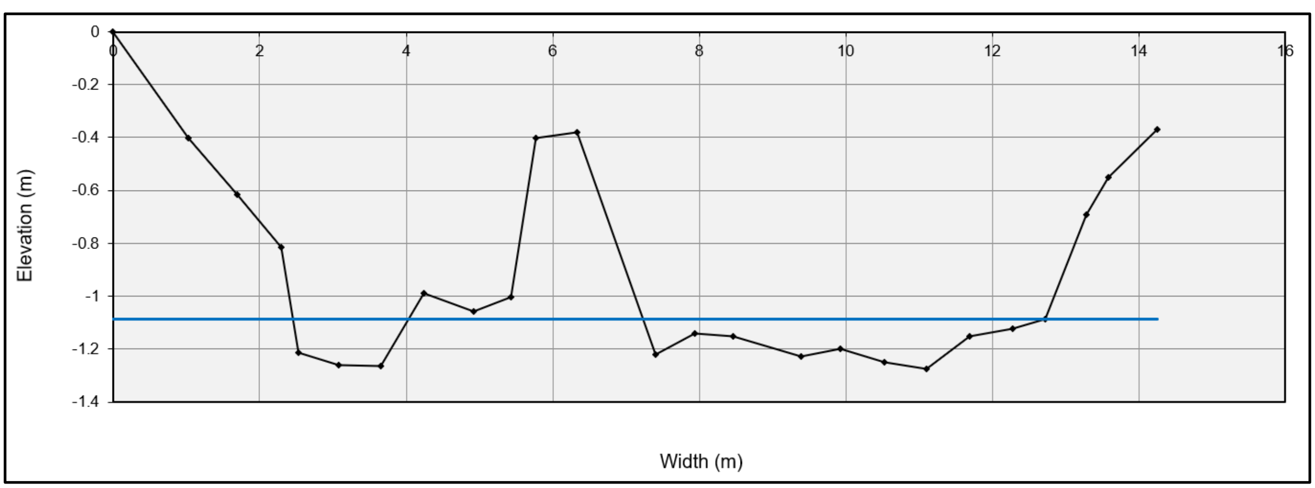

Figure E15. CDBP Cross-Section Profile

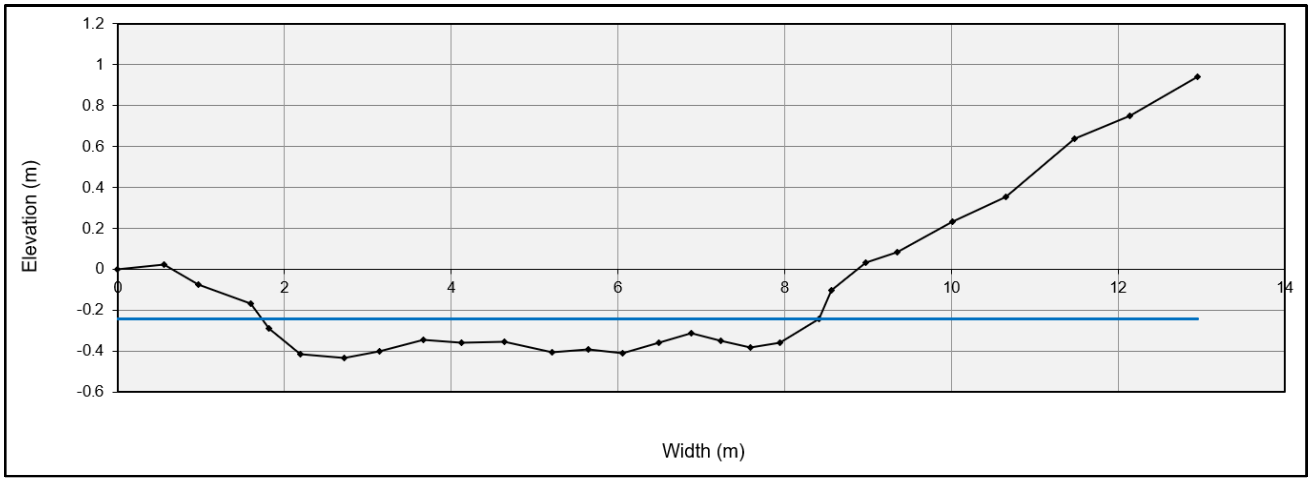

Figure E16. SHT-A Cross-Section Profile

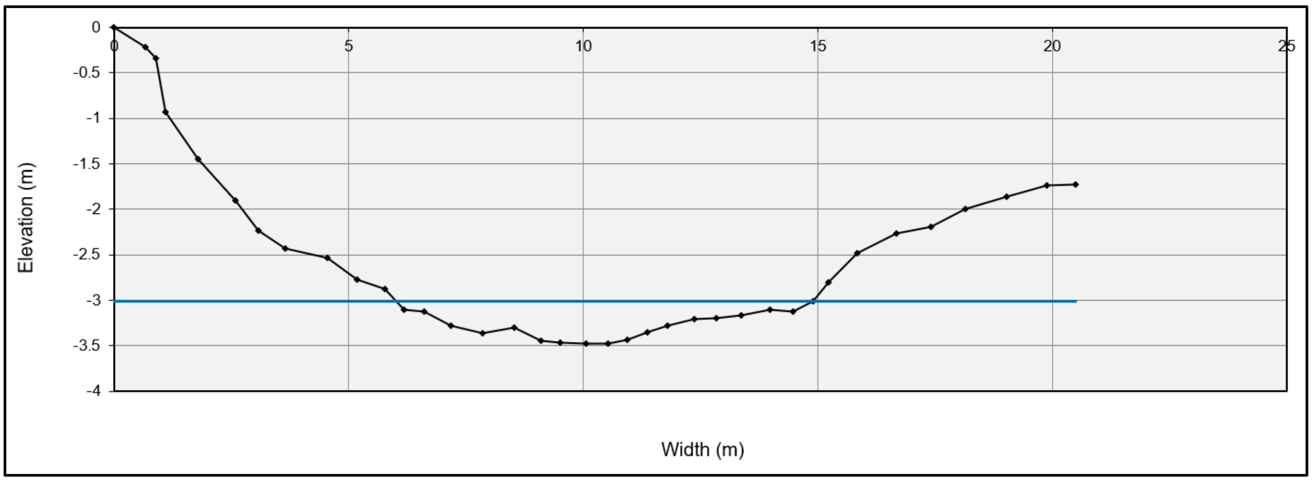

Figure E17. SHT-B Cross-Section Profile

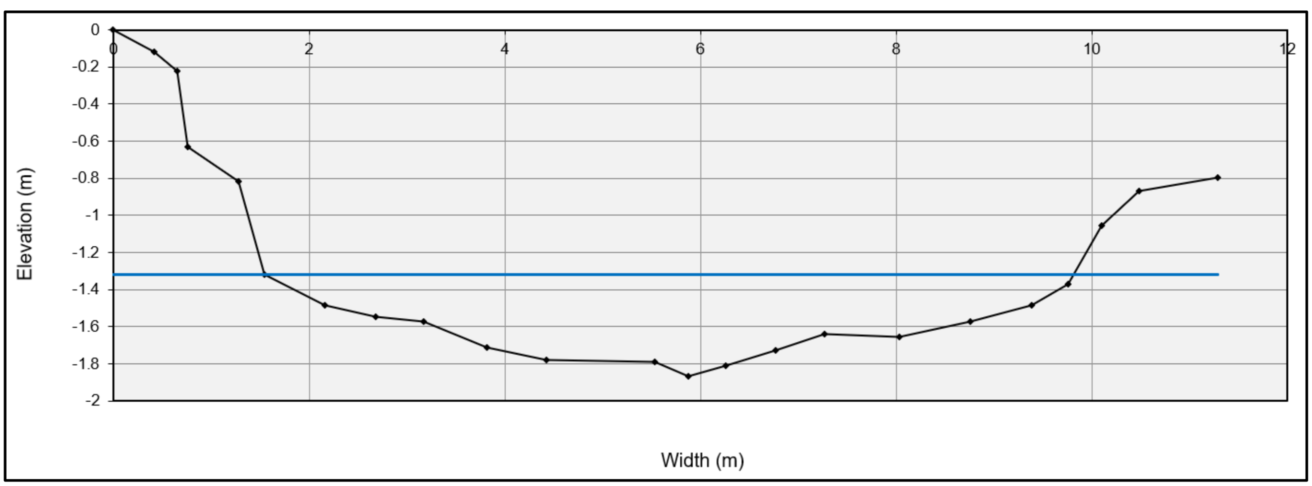

Figure E18. SHT-E Cross-Section Profile

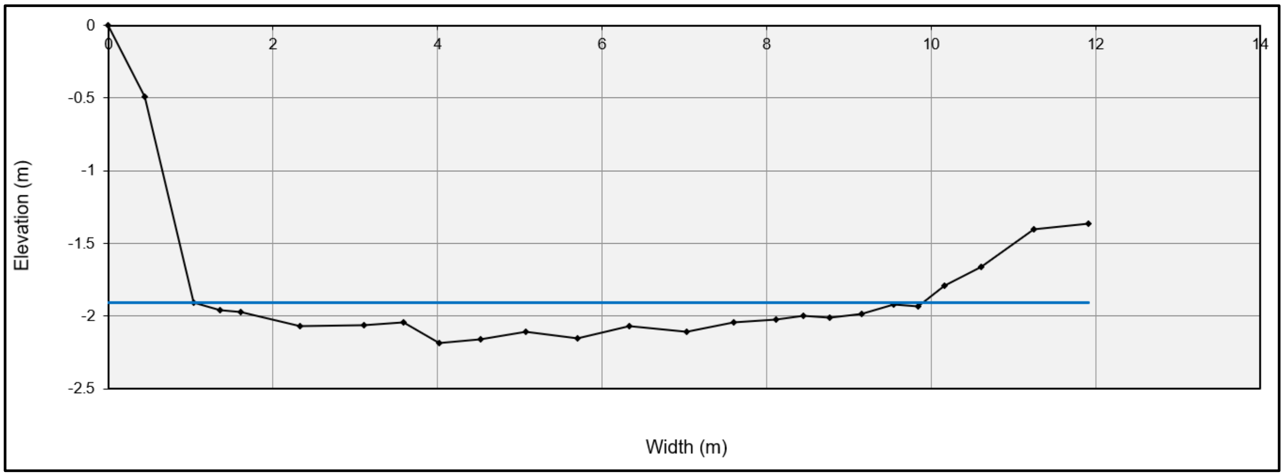

Figure E19. SHT-D Cross-Section Profile

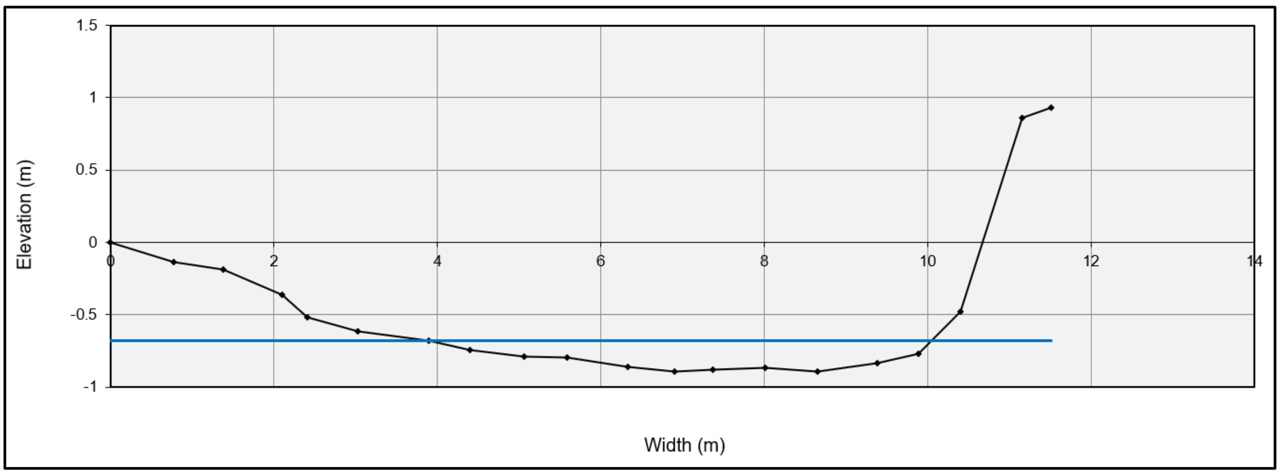

Figure E20. RIVT Cross-Section Profile

APPENDIX F: Sediment Distribution Graphs

Mimico Creek (F1-F10)
Etobicoke Creek (F11-F20)
Highland Creek (F21-F30)
Duffins Creek (F31-F40)

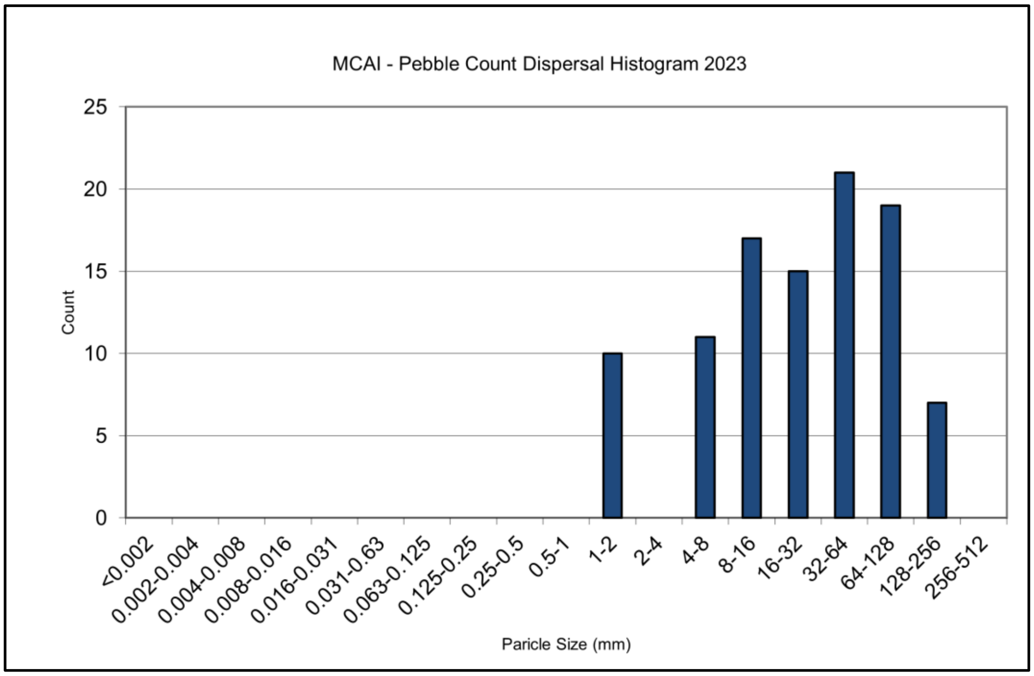

Figure F1. MCAI Pebble Count Dispersal Histogram 2023

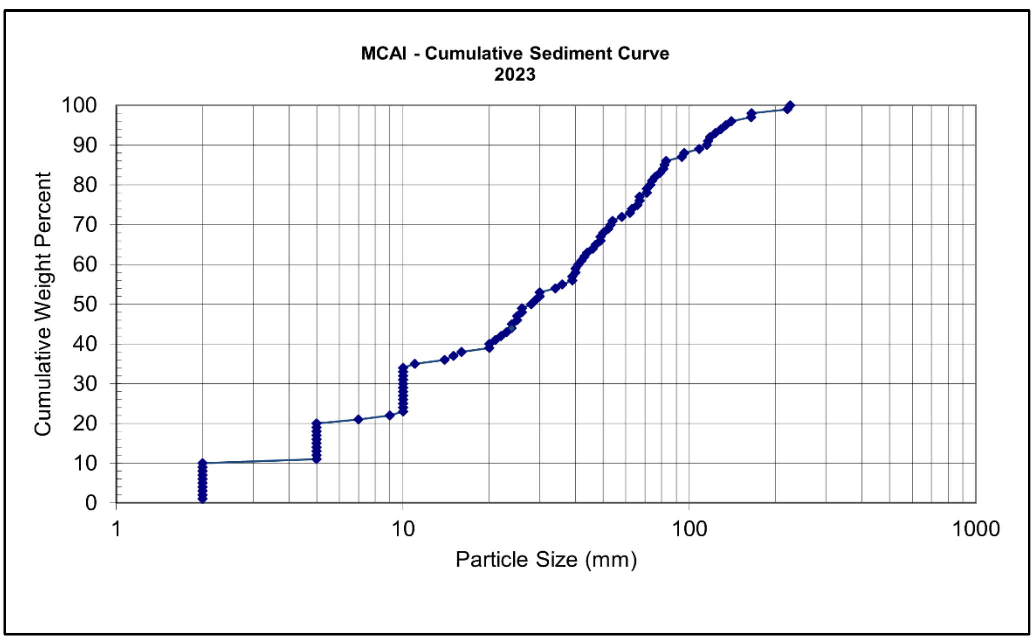

Figure F2. MCAI Cumulative Sediment Curve 2023

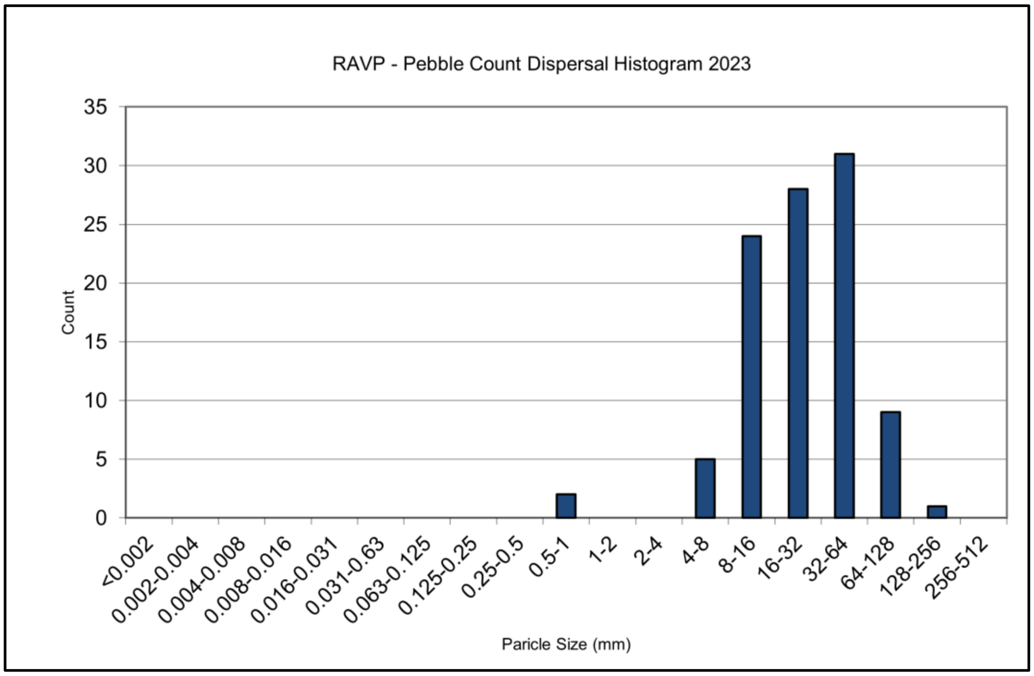

Figure F3. RAVP Pebble Count Dispersal Histogram 2023

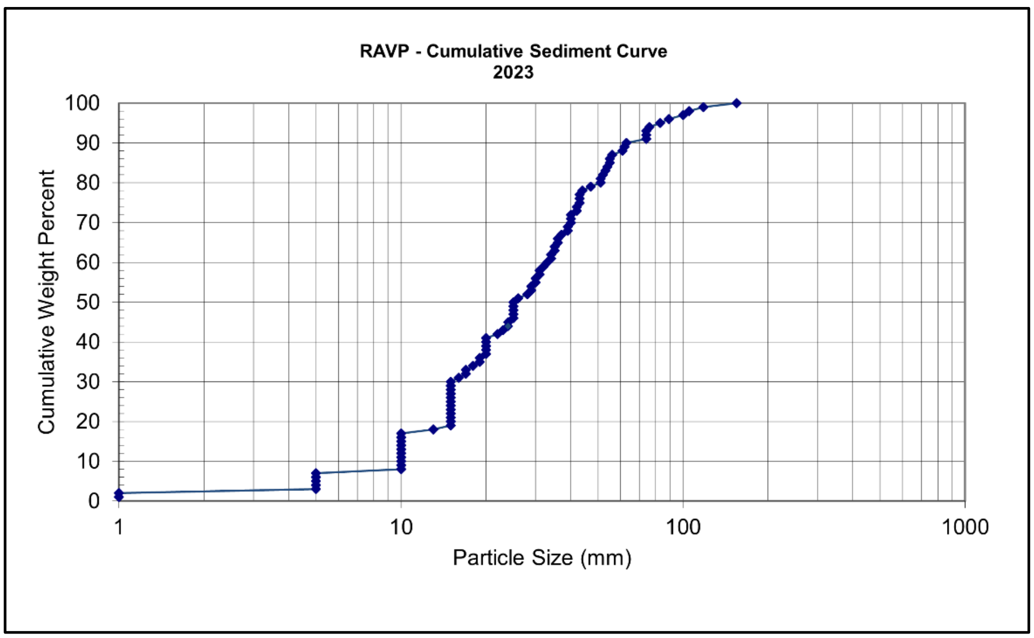

Figure F4. RAVP Cumulative Sediment Curve 2023

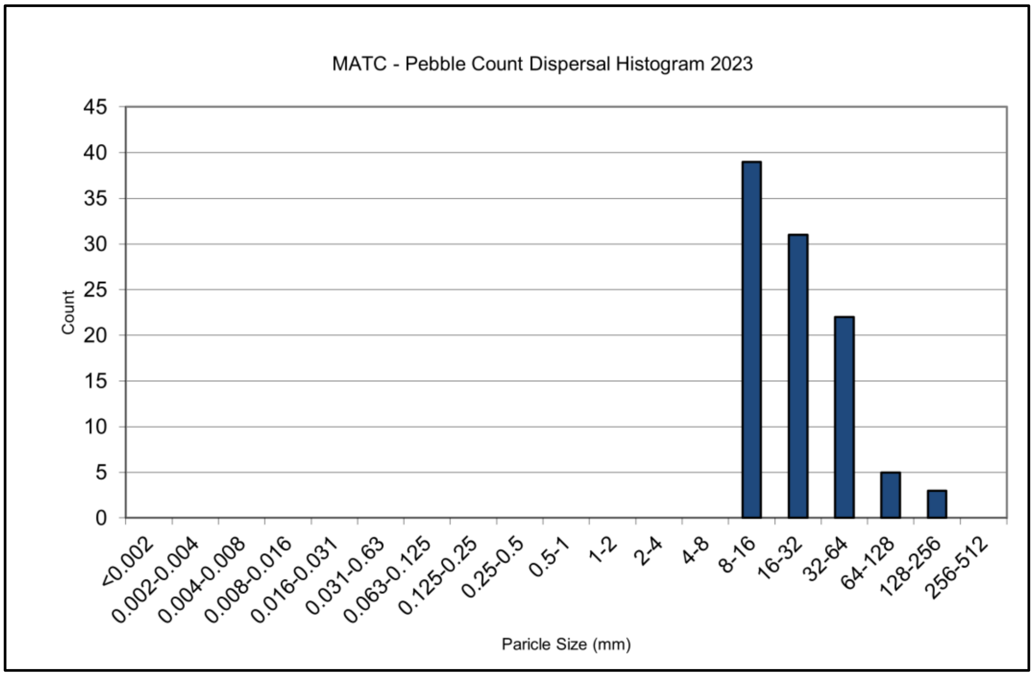

Figure F5. MATC Pebble Count Dispersal Histogram 2023

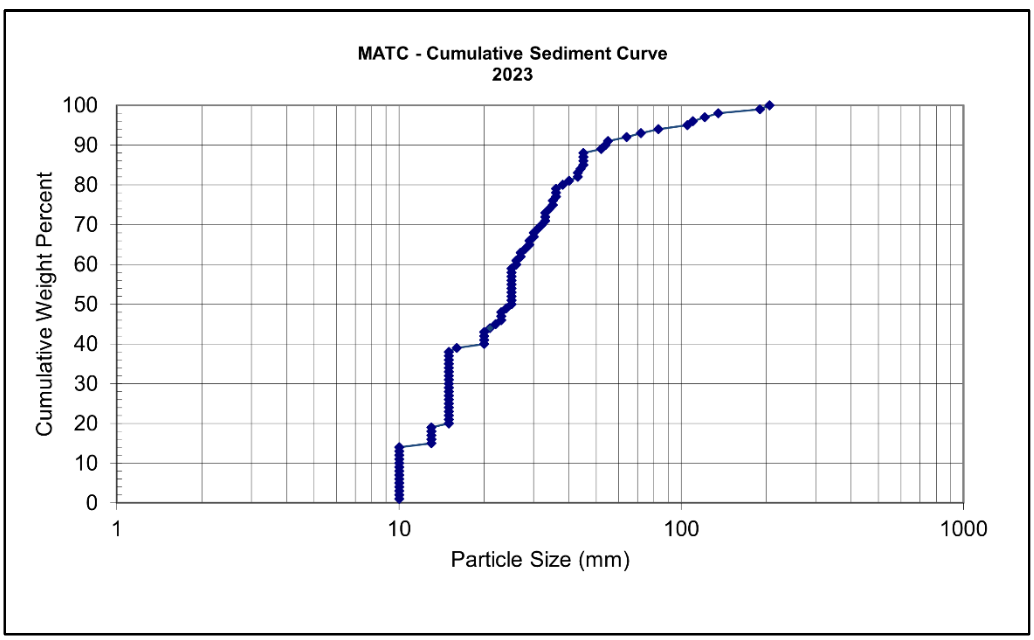

Figure F6. MATC Cumulative Sediment Curve 2023

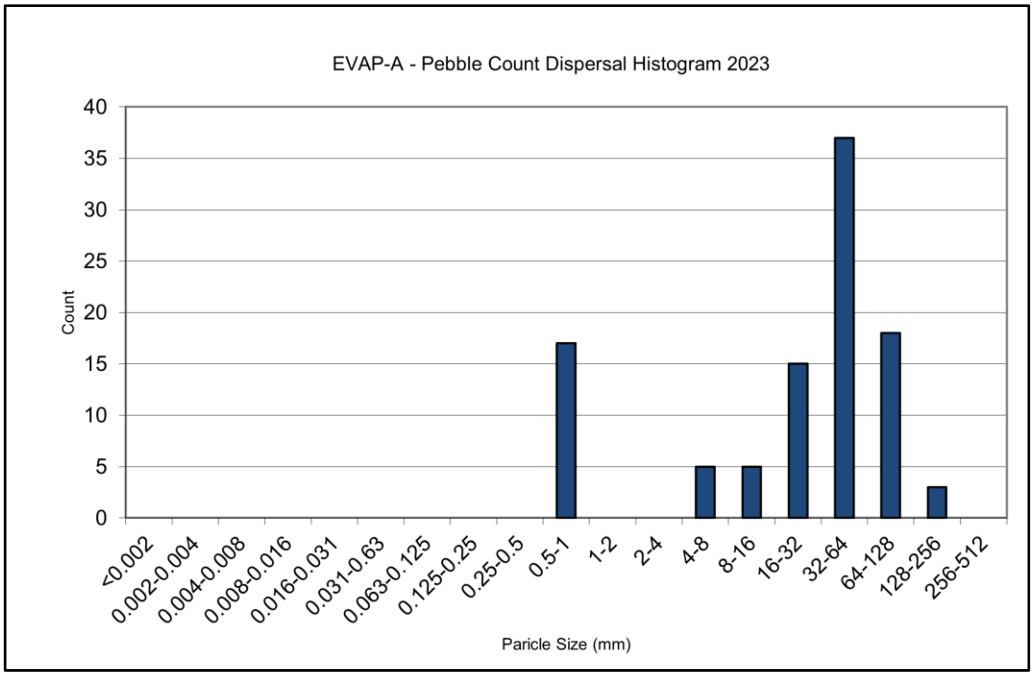

Figure F7. EVAP-A Pebble Count Dispersal Histogram 2023

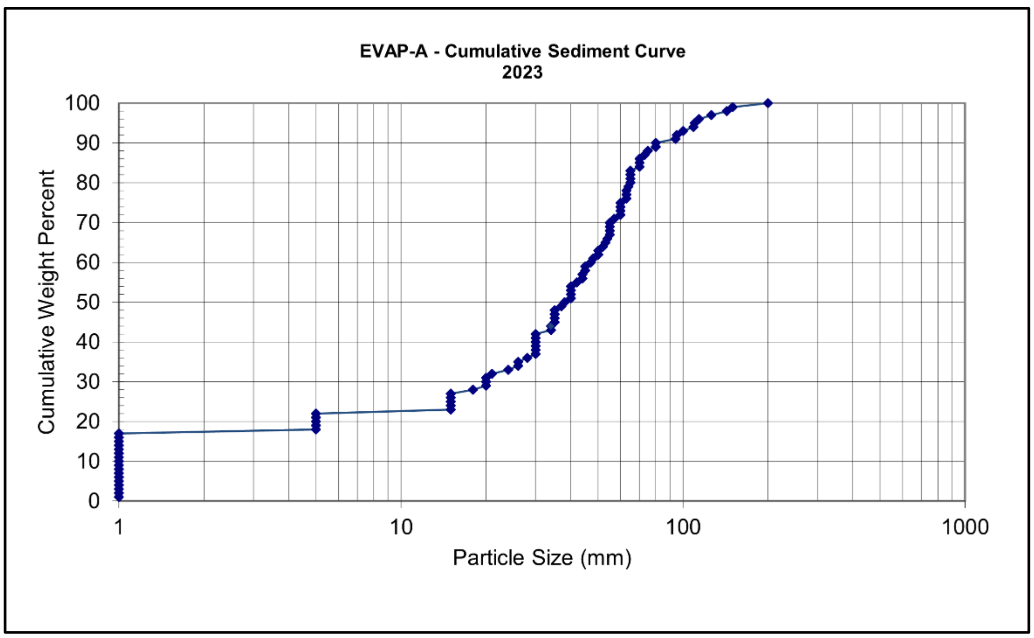

Figure F8. EVAP-A Cumulative Sediment Curve 2023

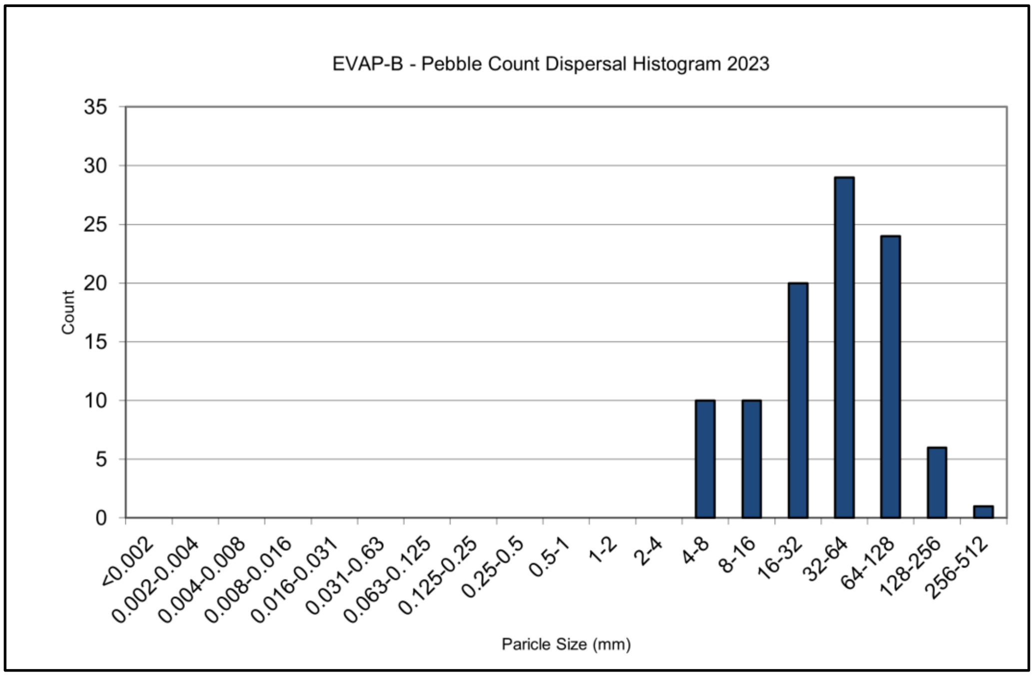

Figure F9. EVAP-B Pebble Count Dispersal Histogram 2023

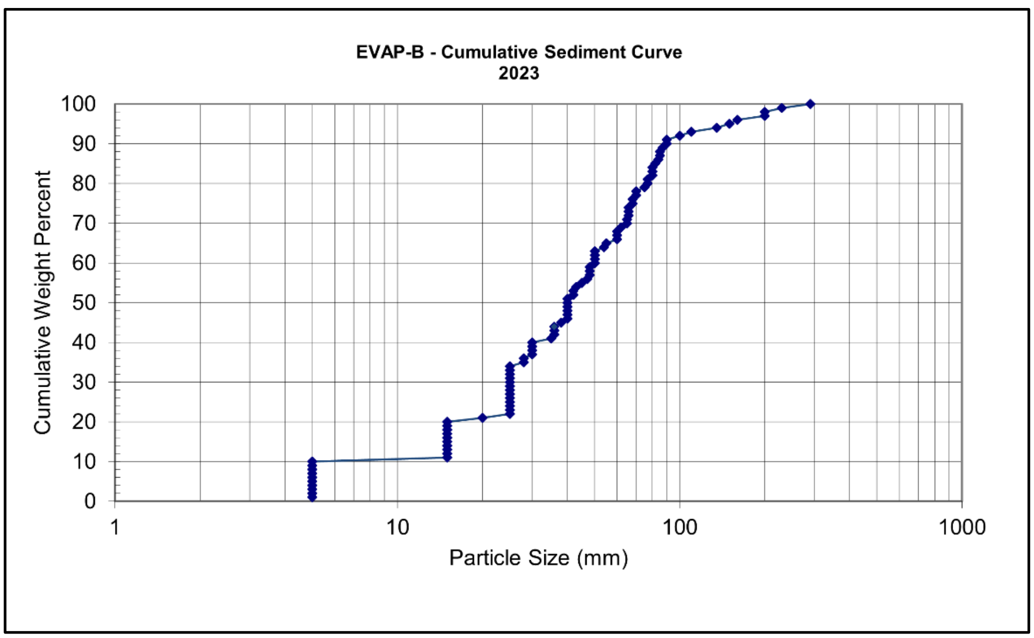

Figure F10. EVAP-B Cumulative Sediment Curve 2023

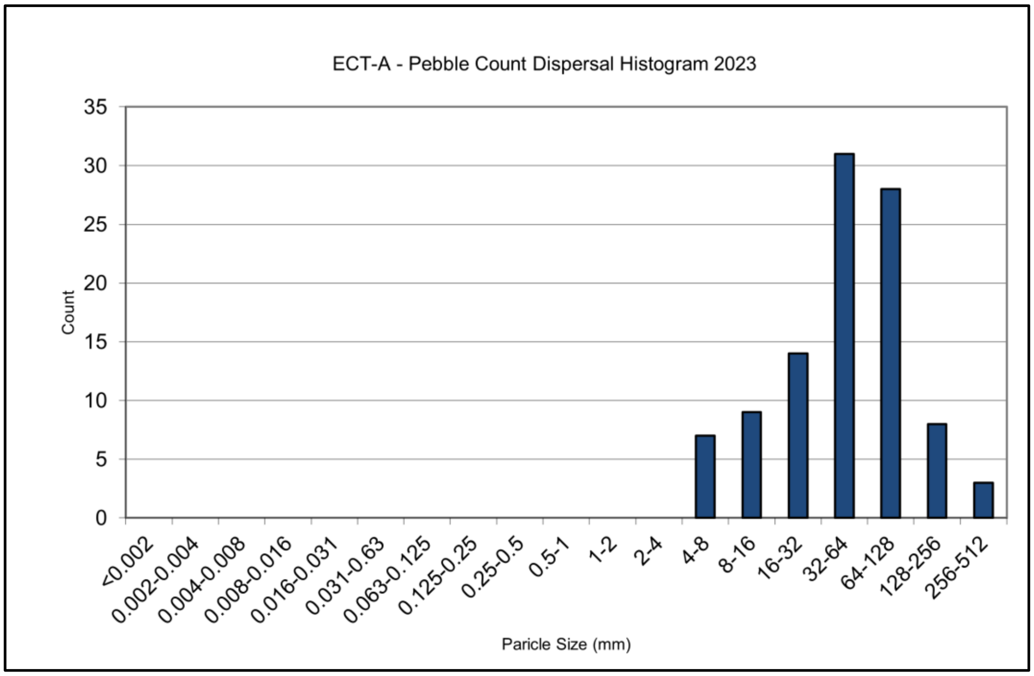

Figure F11. ECT-A Pebble Count Dispersal Histogram 2023

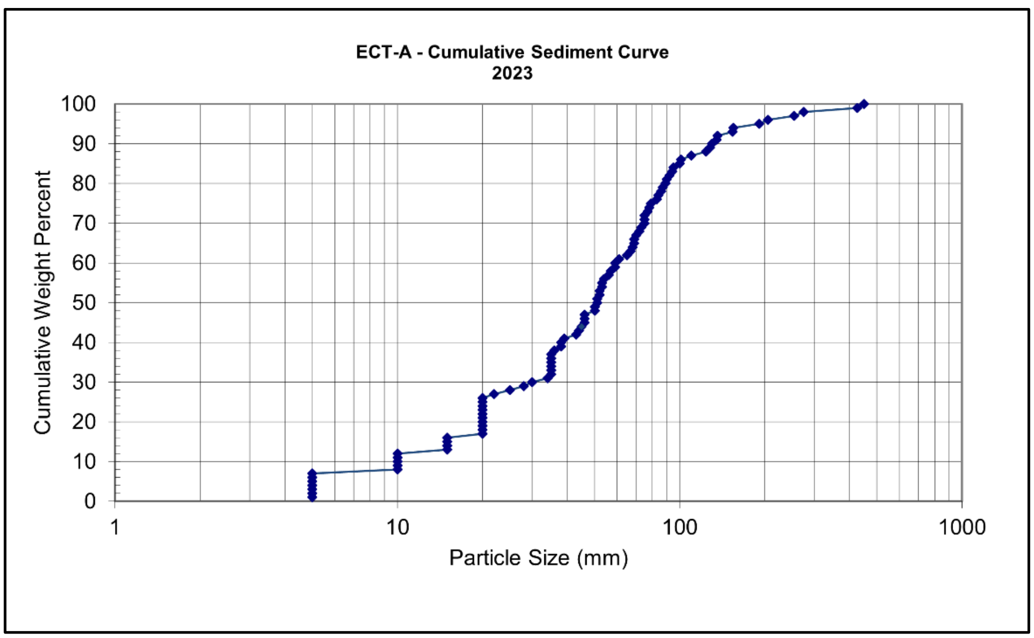

Figure F12. ECT-A Cumulative Sediment Curve 2023

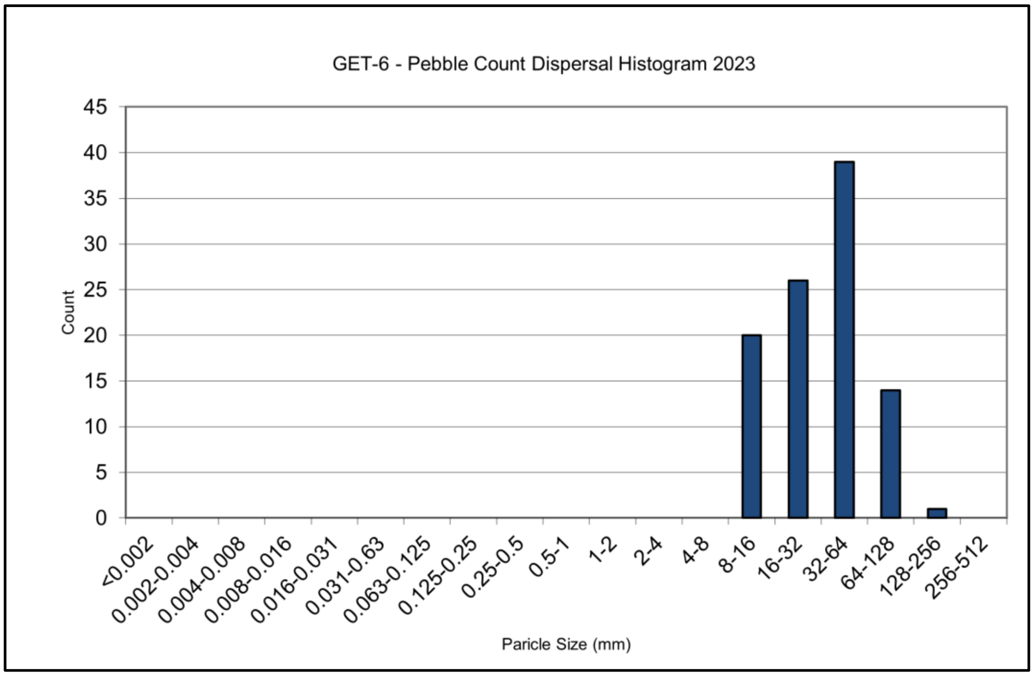

Figure F13. GET-6 Pebble Count Dispersal Histogram 2023

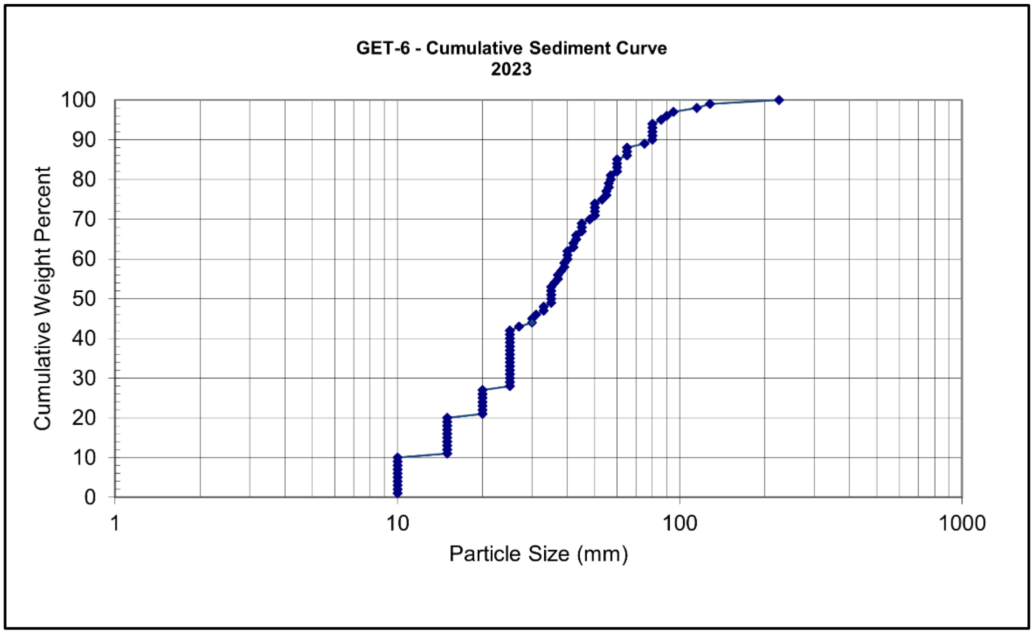

Figure F14. GET-6 Cumulative Sediment Curve 2023

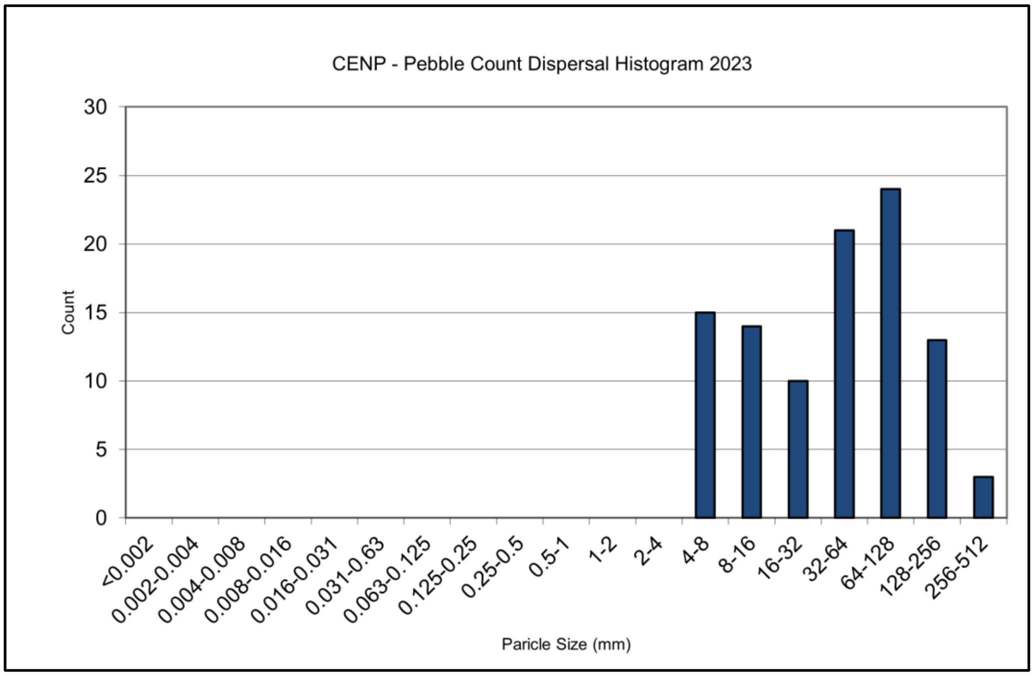

Figure F15. CENP Pebble Count Dispersal Histogram 2023

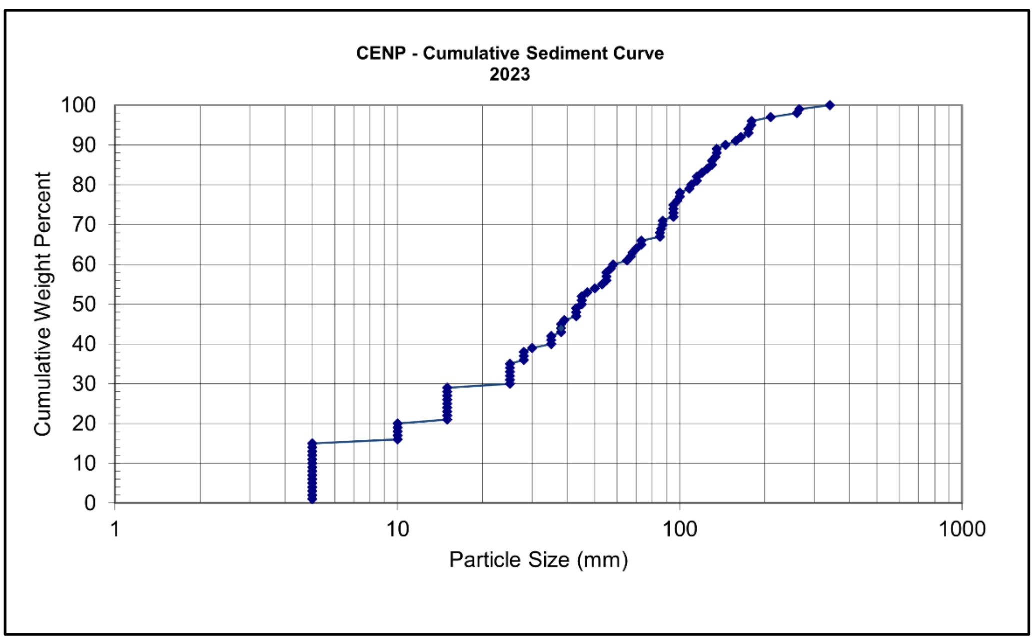

Figure F16. CENP Cumulative Sediment Curve 2023

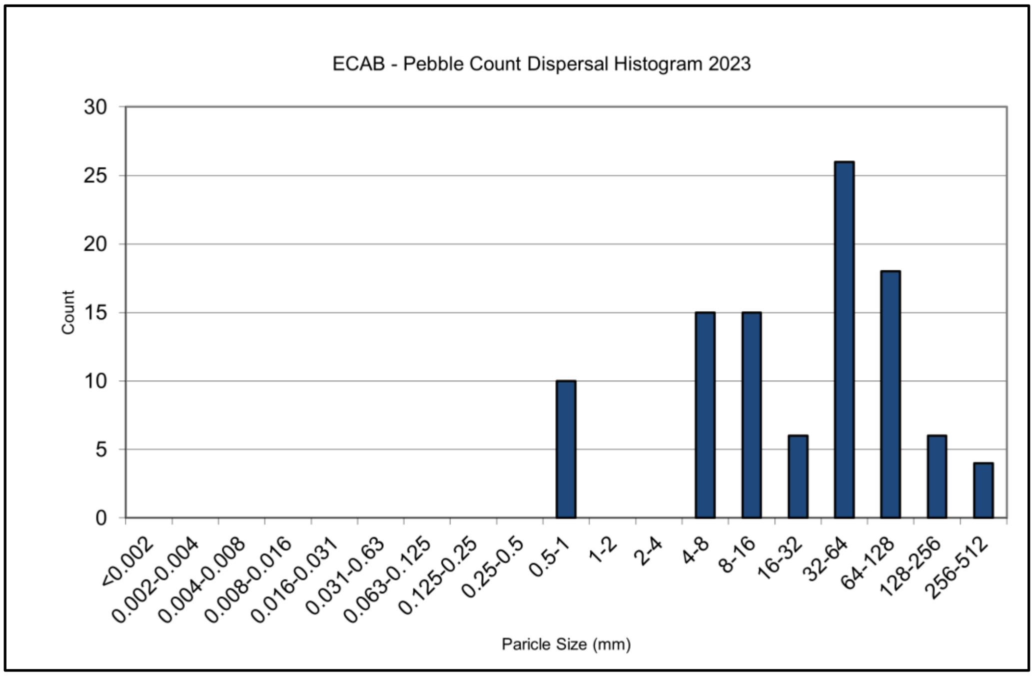

Figure F17. ECAB Pebble Count Dispersal Histogram 2023

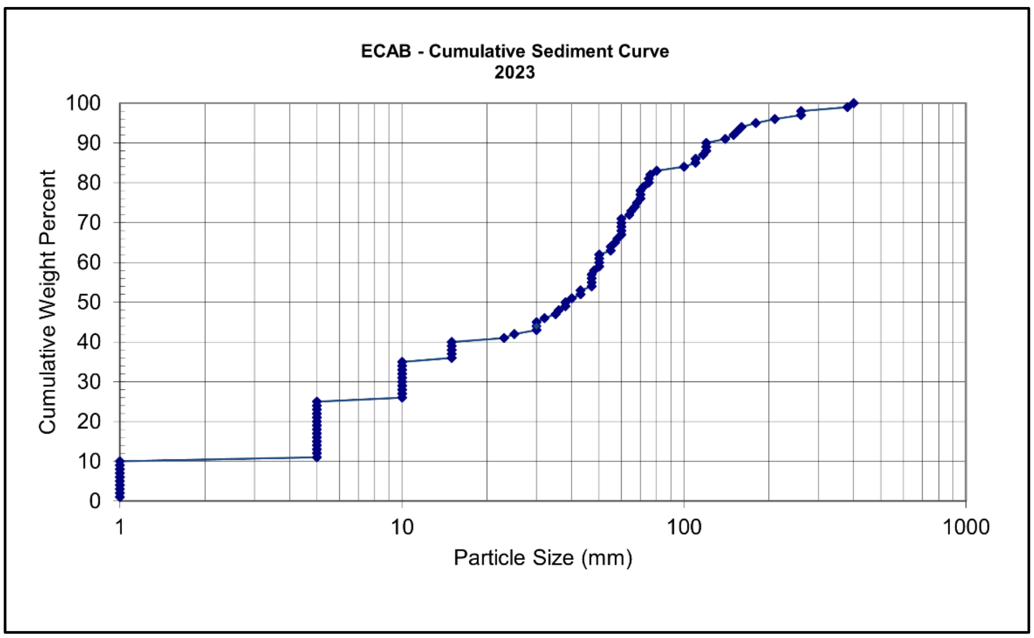

Figure F18. ECAB Cumulative Sediment Curve 2023

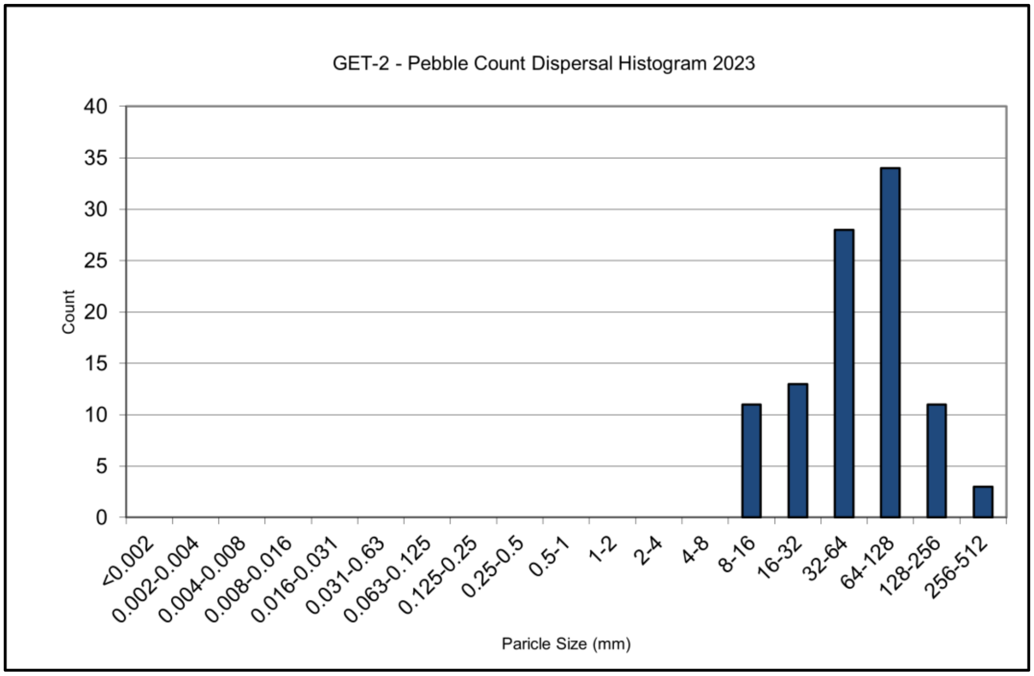

Figure F19. GET-2 Pebble Count Dispersal Histogram 2023

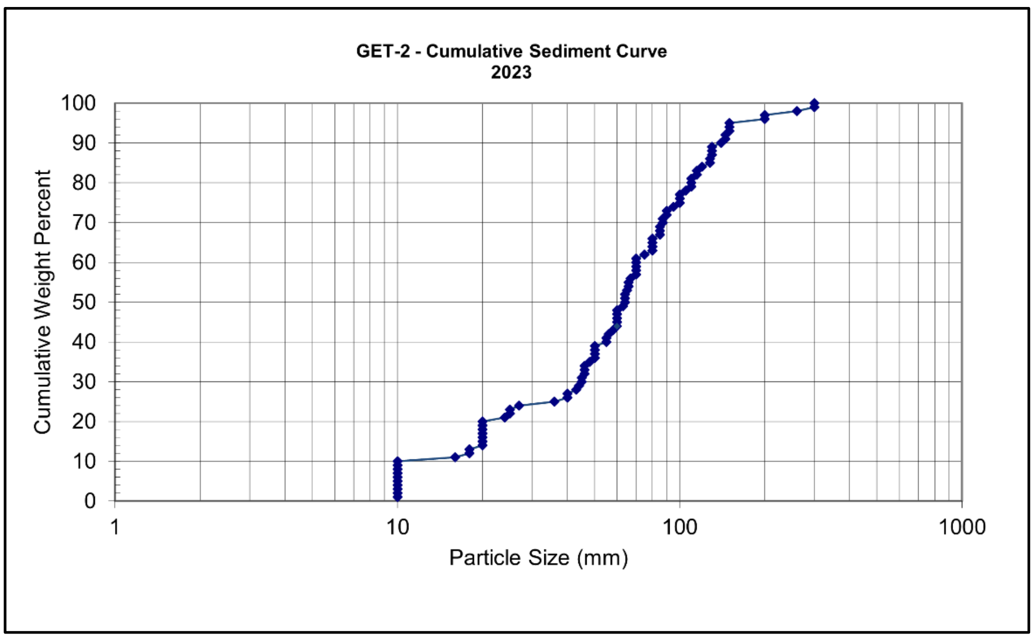

Figure F20. GET-2 Cumulative Sediment Curve 2023

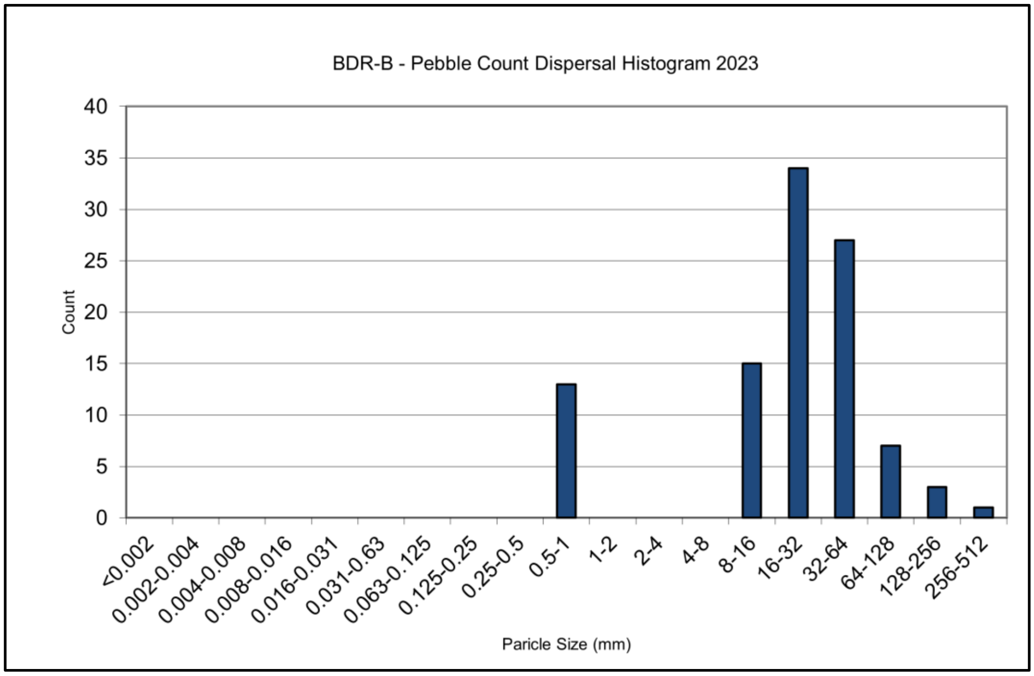

Figure F21. BDR-B Pebble Count Dispersal Histogram 2023

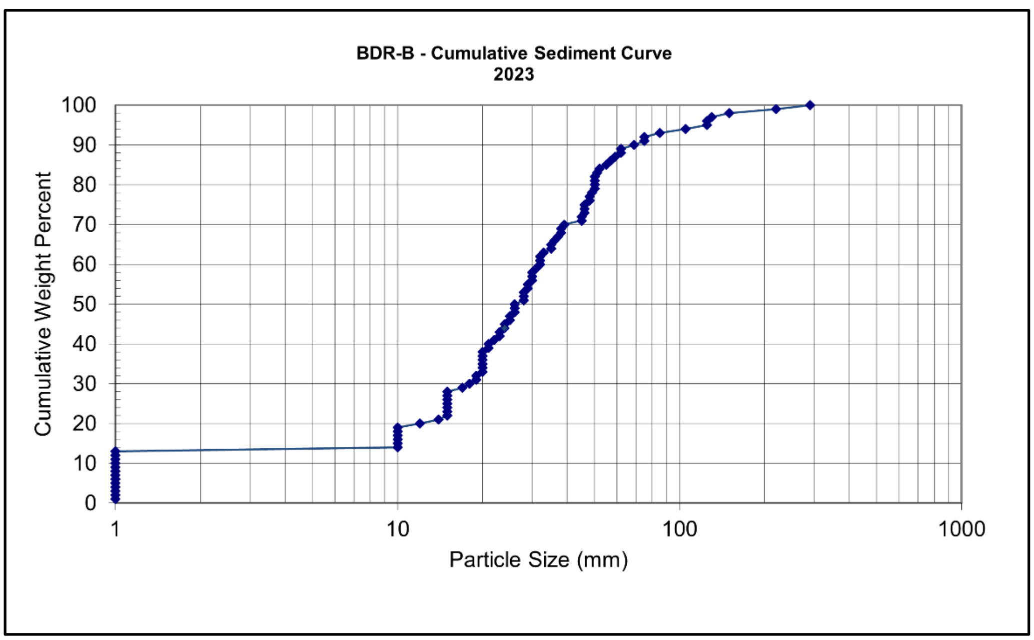

Figure F22. BDR-B Cumulative Sediment Curve 2023

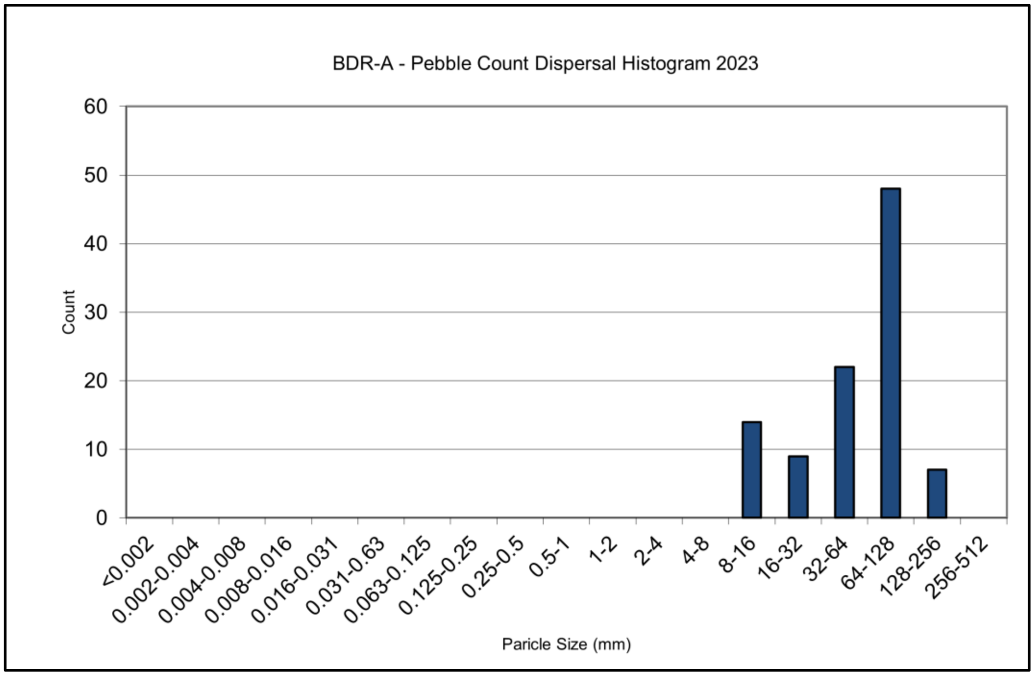

Figure F23. BDR-A Pebble Count Dispersal Histogram 2023

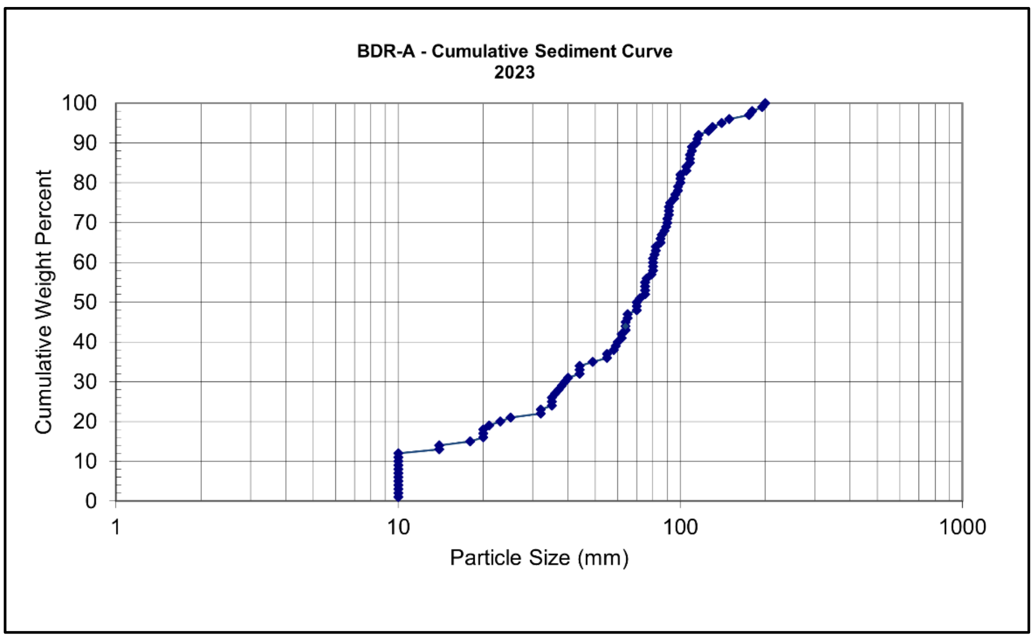

Figure F24. BDR-A Cumulative Sediment Curve 2023

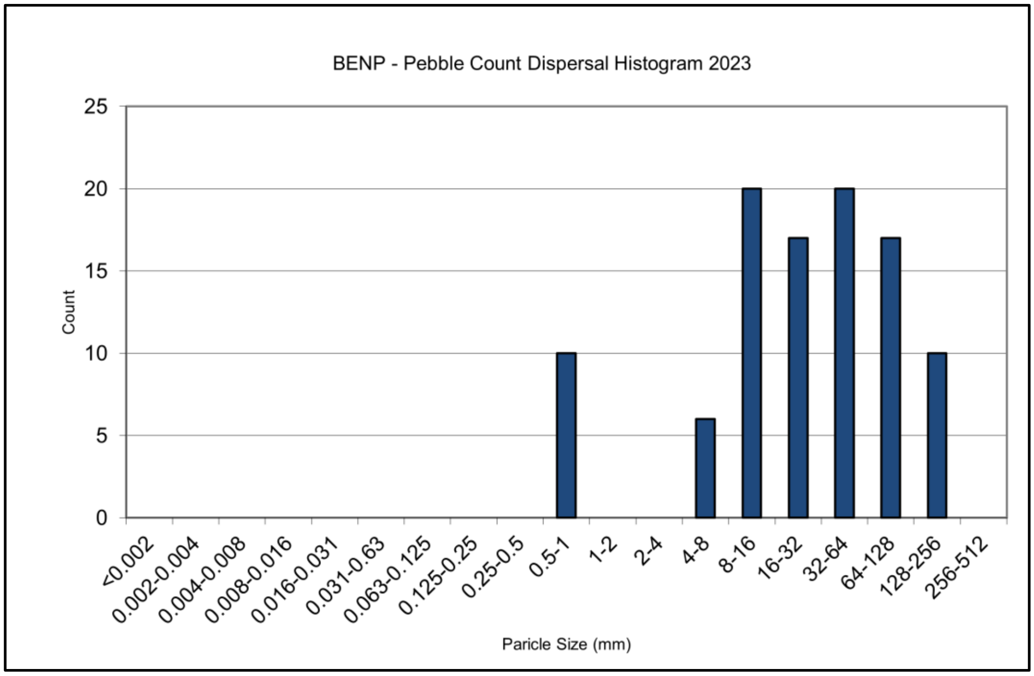

Figure F25. BENP Pebble Count Dispersal Histogram 2023

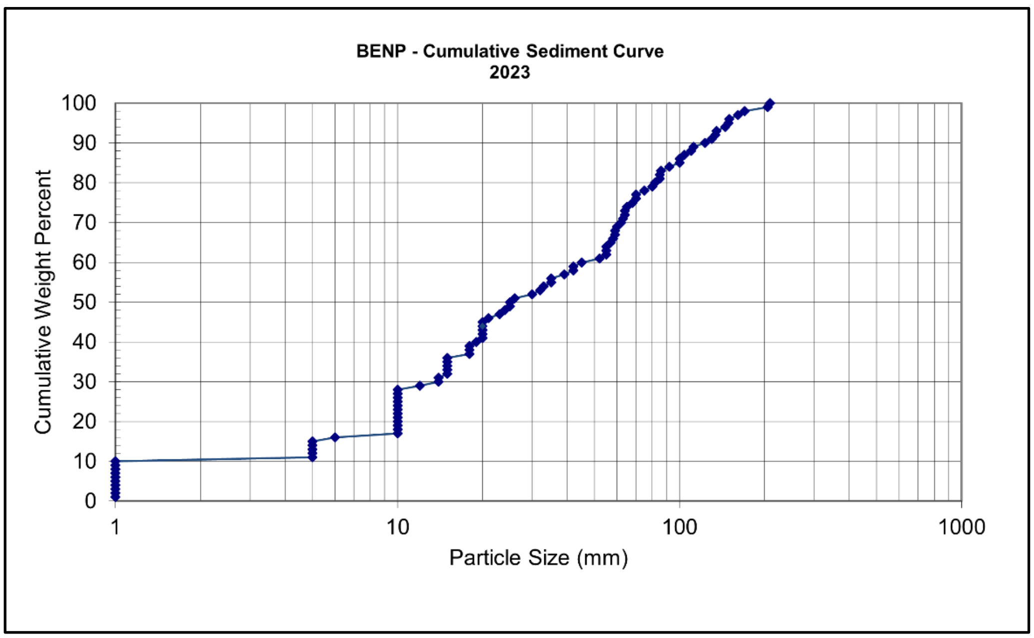

Figure F26. BENP Cumulative Sediment Curve 2023

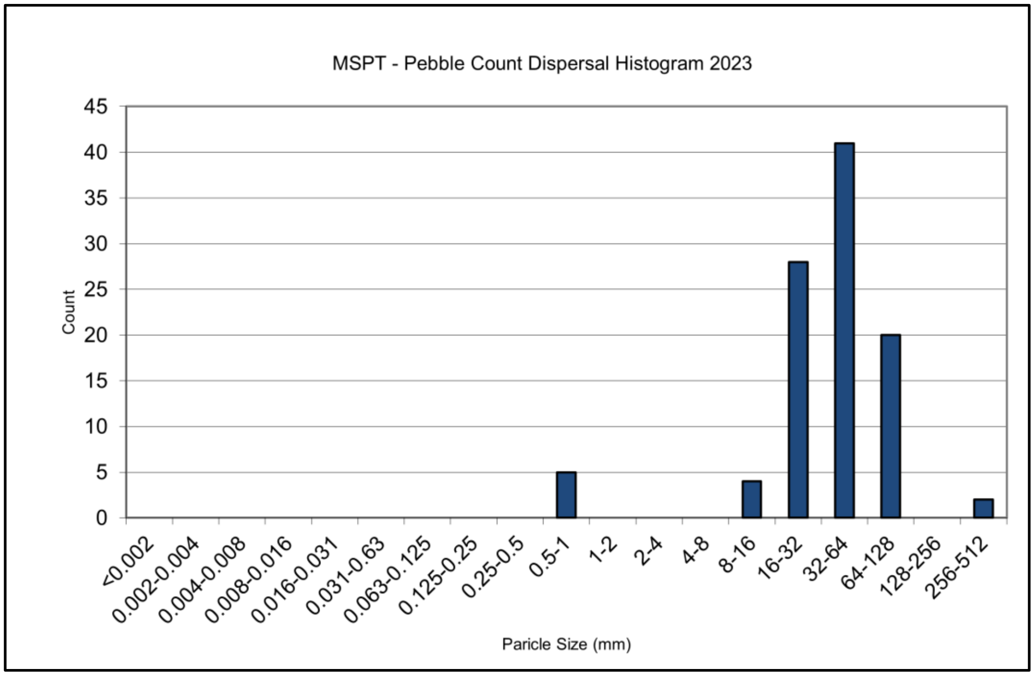

Figure F27. MSPT Pebble Count Dispersal Histogram 2023

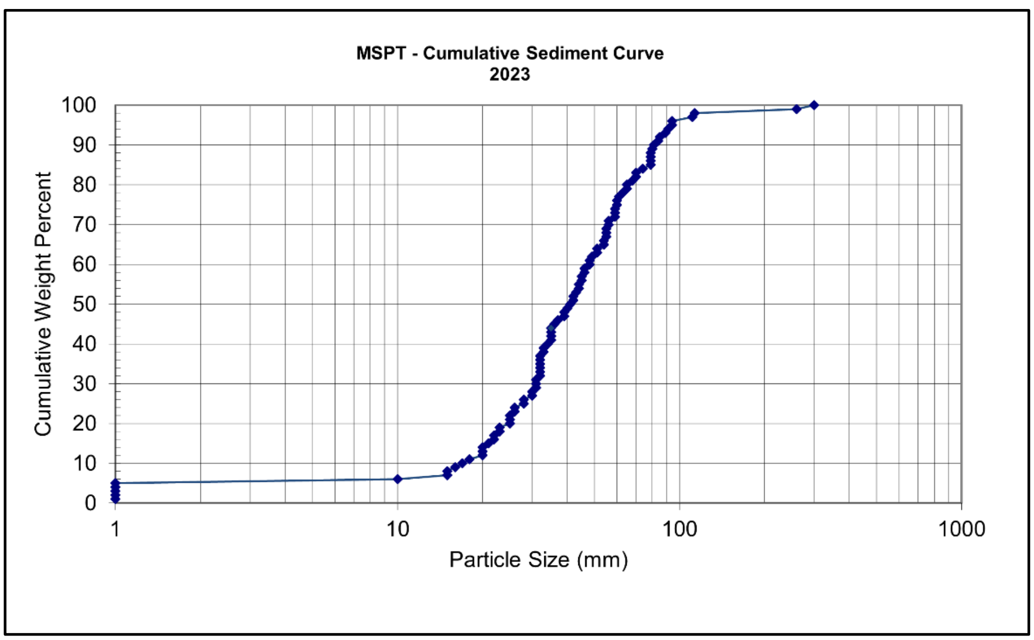

Figure F28. MSPT Cumulative Sediment Curve 2023

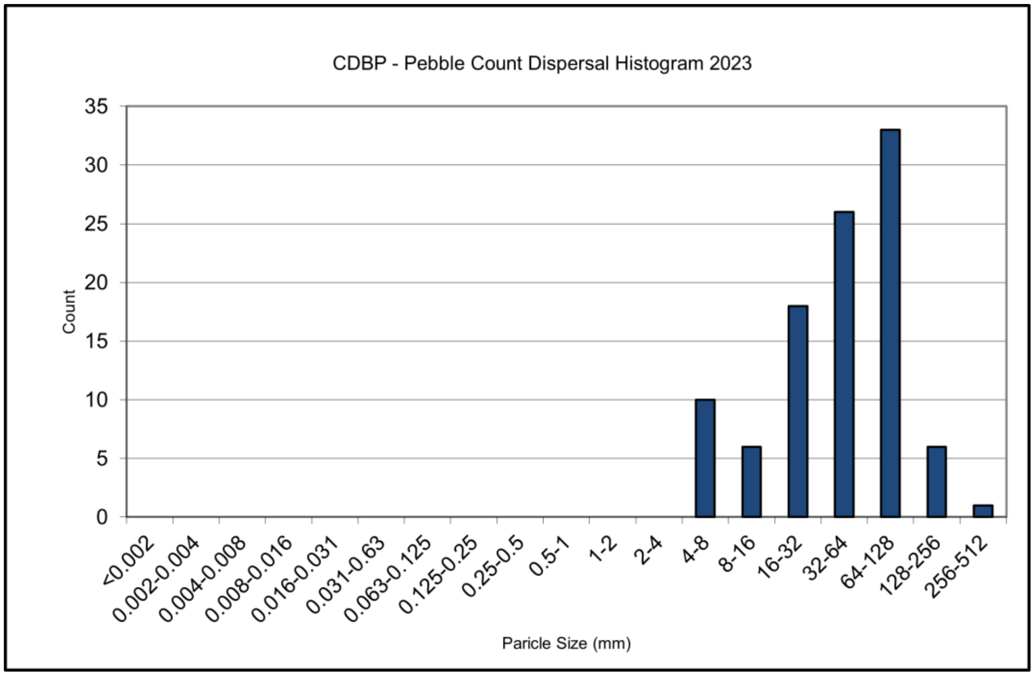

Figure F29. CDBP Pebble Count Dispersal Histogram 2023

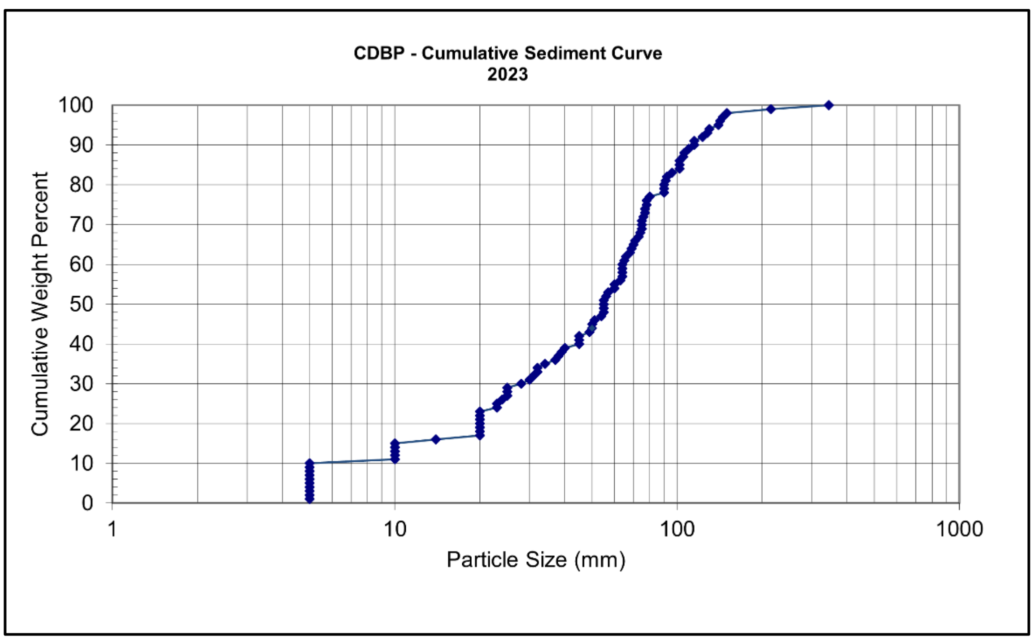

Figure F30. CDBP Cumulative Sediment Curve 2023

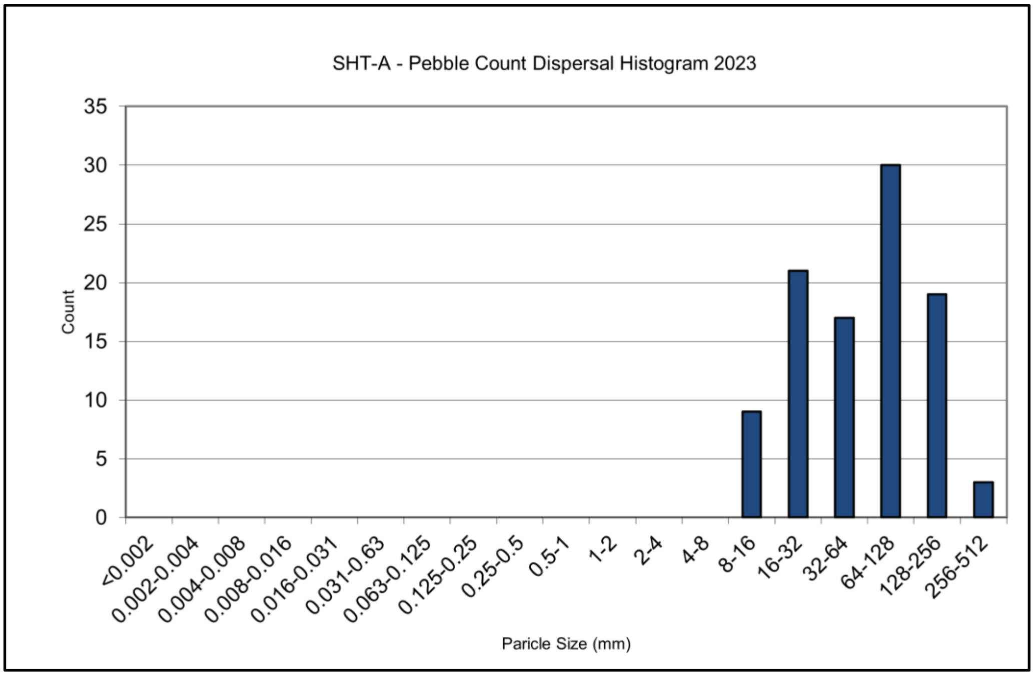

Figure F31. SHT-A Pebble Count Dispersal Histogram 2023

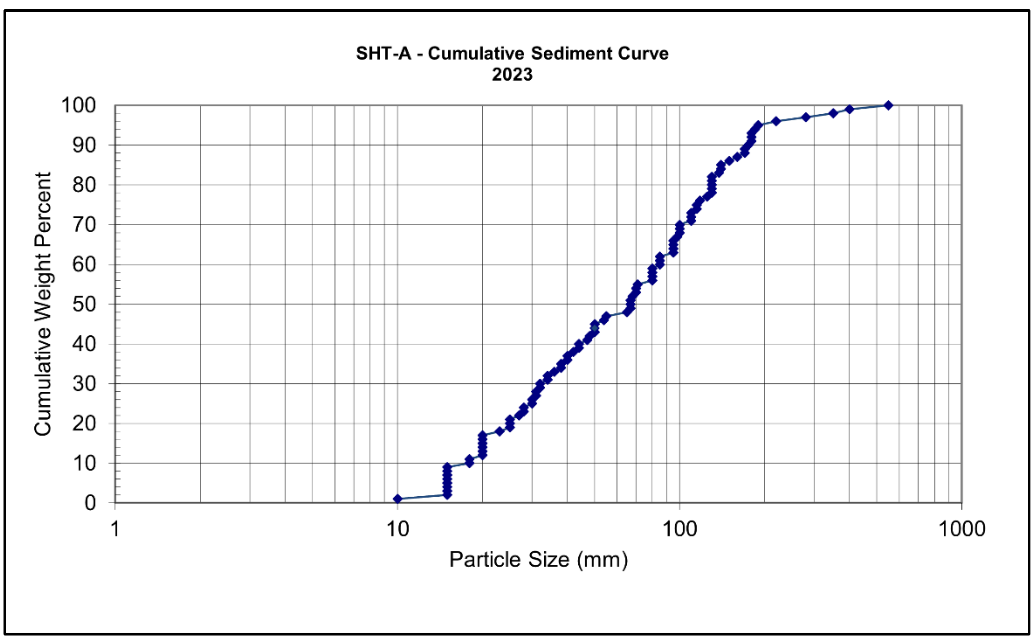

Figure F32. SHT-A Cumulative Sediment Curve 2023

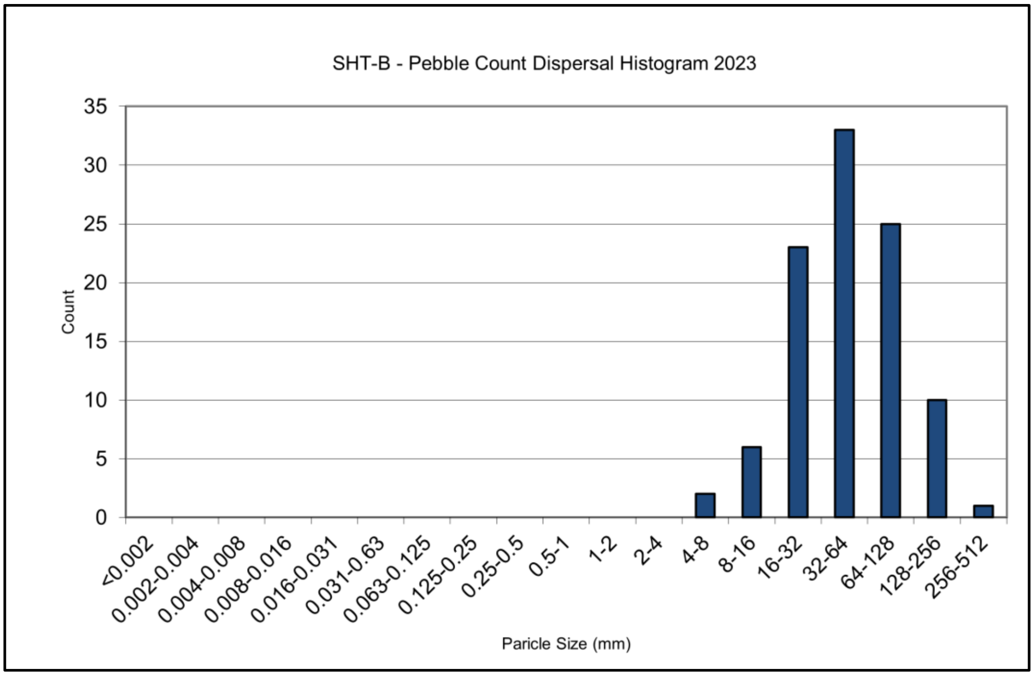

Figure F33. SHT-B Pebble Count Dispersal Histogram 2023

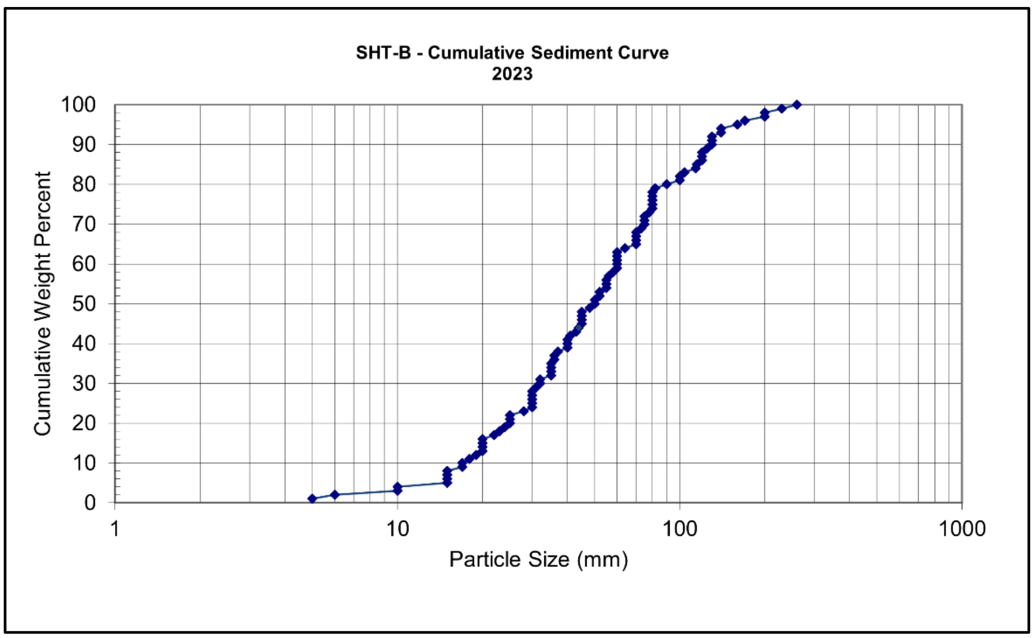

Figure F34. SHT-B Cumulative Sediment Curve 2023

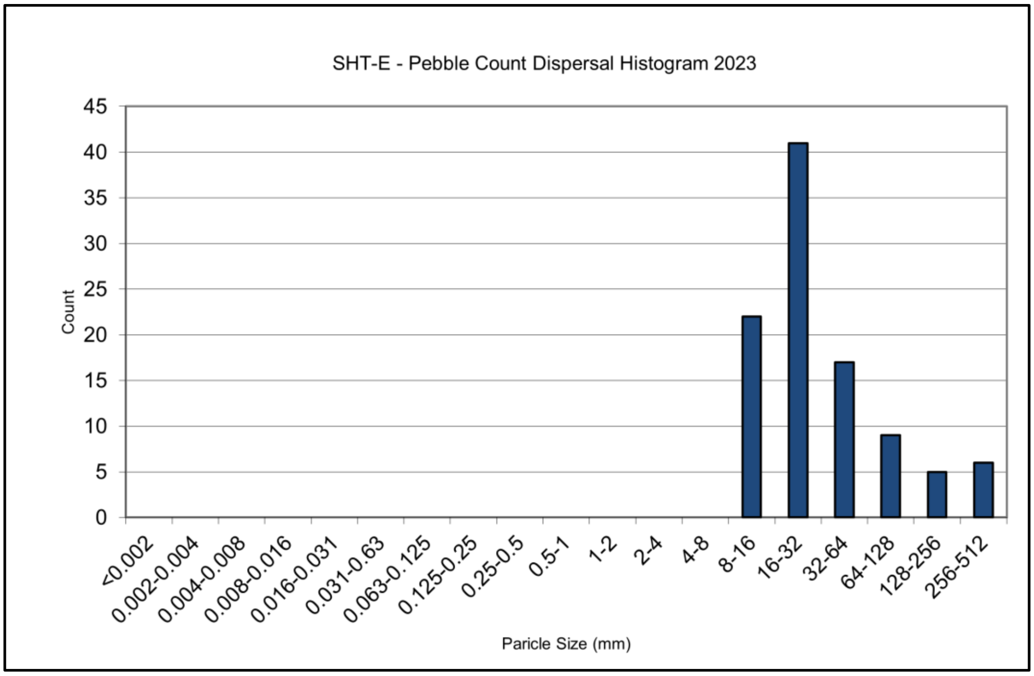

Figure F35. SHT-E Pebble Count Dispersal Histogram 2023

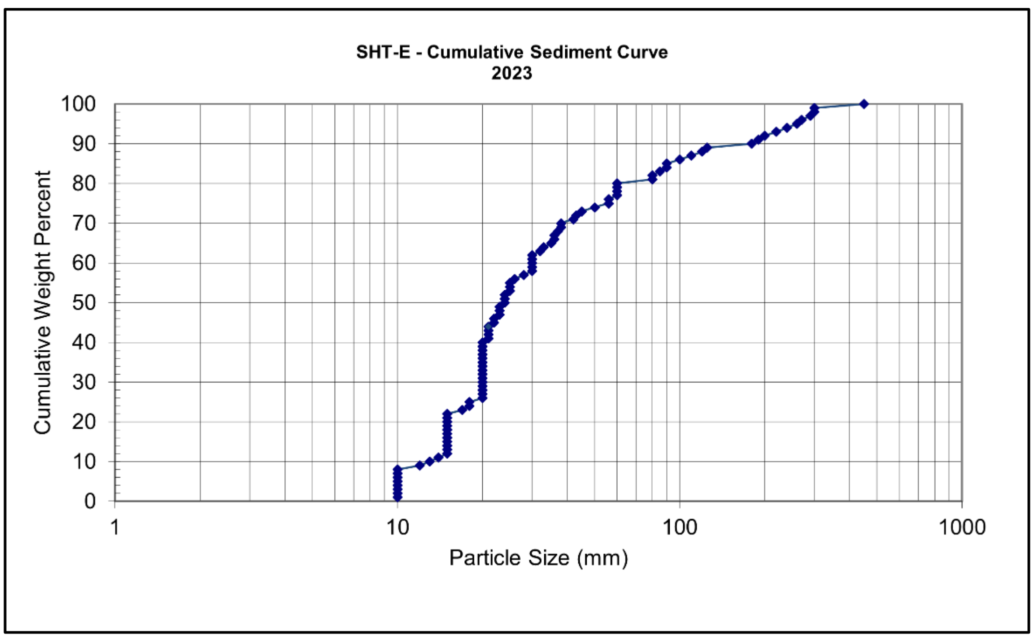

Figure F36. SHT-E Cumulative Sediment Curve 2023

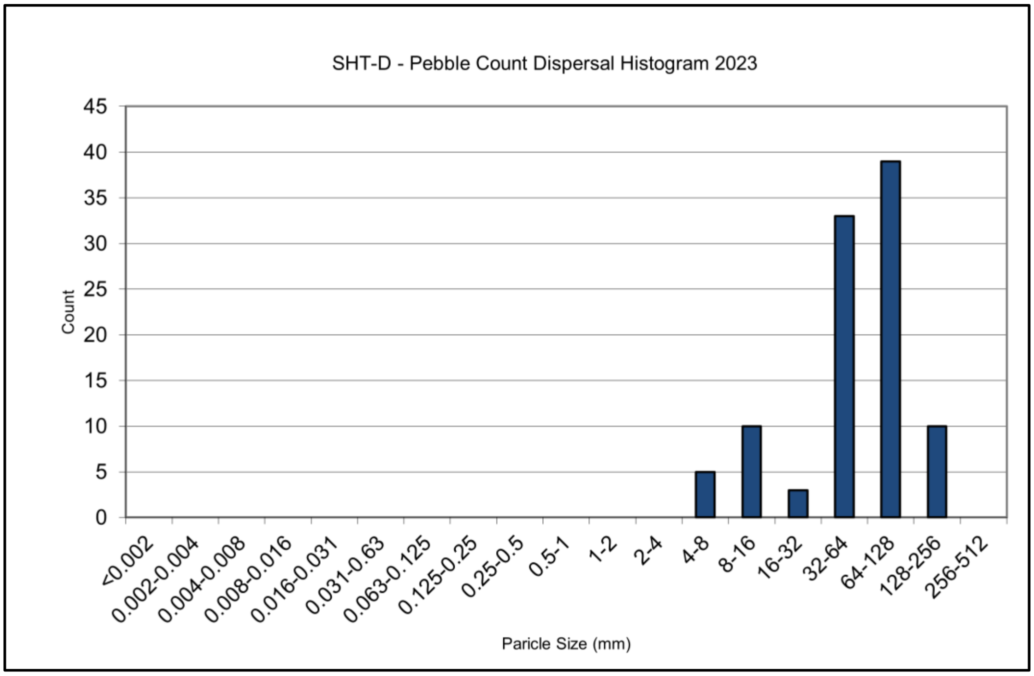

Figure F37. SHT-D Pebble Count Dispersal Histogram 2023

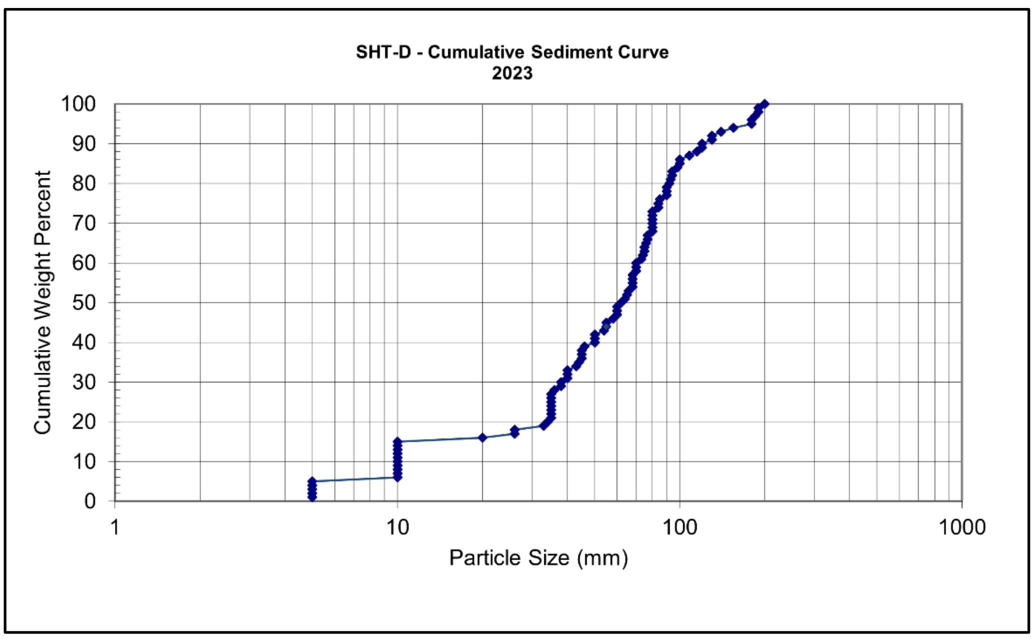

Figure F38. SHT-D Cumulative Sediment Curve 2023

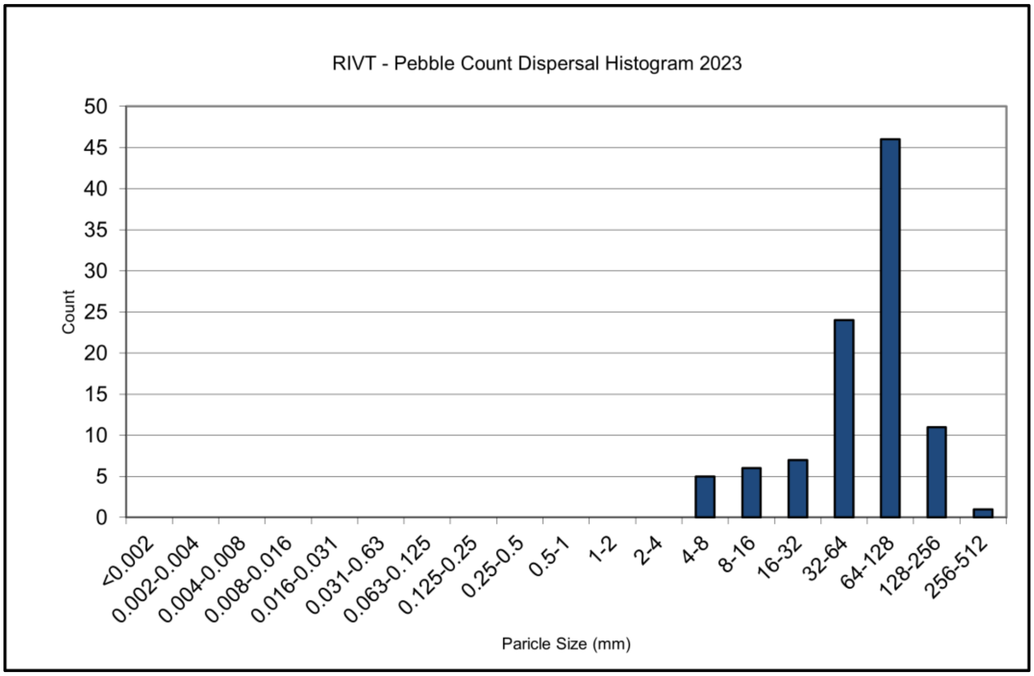

Figure F39. RIVT Pebble Count Dispersal Histogram 2023

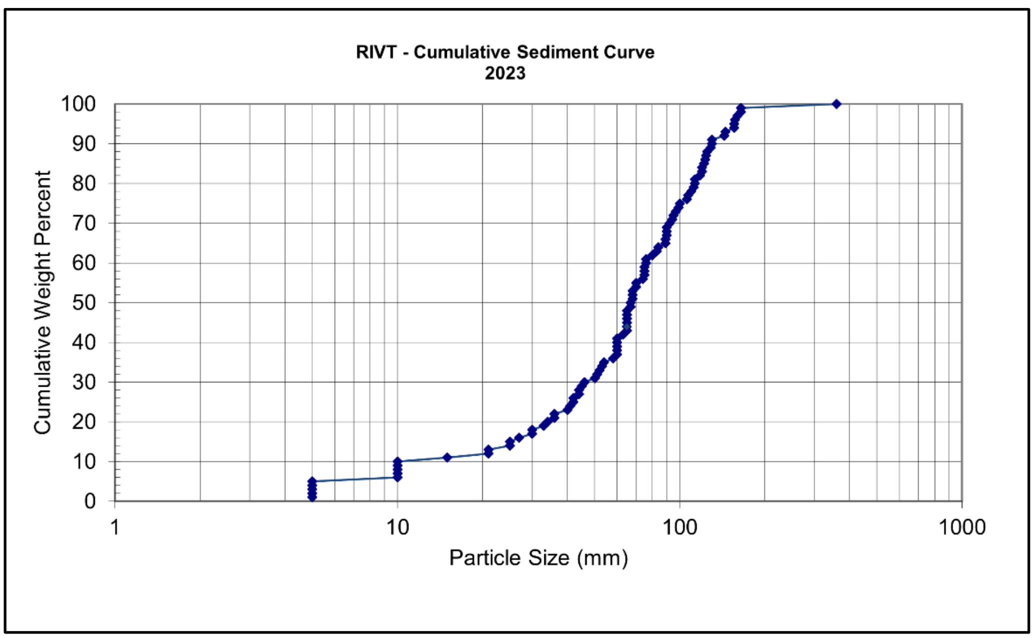

Figure F40. RIVT Cumulative Sediment Curve 2023

APPENDIX G: Pearson Correlation Results

Combination	All Watersheds	Mimico	Etobicoke	Highland	Duffins
DA + Imp	moderately negative	strongly negative	no association	moderately positive	strongly negative
SP + Imp	moderately negative	weakly negative	weakly positive	no association	weakly negative
SP + DA	moderately positive	no association	strongly positive	moderately negative	weakly positive
W/D + Imp	weakly negative	no association	moderately negative	weakly positive	moderately positive
W/D + DA	weakly positive	weakly positive	moderately positive	no association	moderately negative
W/D + SP	no association	weakly negative	no association	moderately positive	no association
E + Imp	no association	weakly positive	moderately positive	weakly negative	weakly negative
E + DA	no association	weakly negative	moderately negative	no association	weakly positive
E + SP	no association	weakly positive	weakly negative	moderately negative	weakly positive
E + W/D	strongly negative	strongly negative	strongly negative	strongly negative	strongly negative
Rough + Imp	weakly negative	no association	weakly negative	weakly positive	weakly positive
Rough + DA	no association	no association	moderately negative	weakly negative	weakly negative
Rough + SP	weakly positive	weakly negative	strongly negative	strongly positive	weakly negative
Rough + W/D	strongly positive	moderately positive	no association	strongly positive	strongly positive
Rough + E	moderately negative	moderately negative	weakly positive	strongly negative	strongly negative
tau ratio + Imp	weakly negative	weakly positive	weakly negative	no association	no association
tau ratio + DA	no association	no association	no association	weakly negative	no association
tau ratio + SP	no association	moderately negative	moderately negative	strongly positive	weakly negative
tau ratio + W/D	weakly positive	moderately positive	moderately positive	moderately positive	strongly positive
tau ratio + E	weakly negative	moderately negative	weakly negative	moderately negative	strongly negative
tau ratio + Rough	weakly positive	strongly positive	moderately positive	strongly positive	strongly positive